

CHAPTER I

Introduction

1.1 Historical background

The study of fluid mechanics dates back to the time of ancient Greece. The first major investigation on fluid statics and buoyancy force was carried out by Greek mathematician and physicist Archimedes (287 B.C. – 212 B.C.) and results are written in the treatise *On Floating Bodies*. The laws of buoyancy given by Archimedes are popularly known as Archimedes Principle. From that onwards, applications and inventions of fluid mechanics flourish through numerous trial and error methods. Different mathematical theories regarding fluid mechanics have immensely contributed to the development of the subject. But advancement in the field of fluid mechanics was scarcely explored till the Middle Ages. In 16th century prominent Italian artist Leonardo da Vinci (1452-1519) and Dutch scientist Simon Stevin (1548-1617) conducted some simple experiments. Based on the contraction and expansion of air, Italian astronomer and physicist Galileo Galilei (1564-1642) made a simple thermometer.

Advancement in fluid mechanics accelerated in the 17th century with Italian physicist Evangelista Torricelli (1608-1647) developed a relationship between the pressure and velocity of a fluid. French physicist Blaise Pascal (1623-1662) established laws of equilibrium of liquids in a most simple manner. Irish chemist Robert Boyle (1627-1691) presented his law regarding pressure and volume of gas which is known as Boyle's law. French physicist Edme Mariotte (1620-1684) and Italian chemist Domenico Guglielmini (1655-1710) observed the velocity of fluid in a glass pipe and river respectively. English physicist Sir Isaac Newton (1643-1727) analyzed viscosity, fluid inertia, and resistance using his laws of fluids.

In the 18th century, the most notable work on fluid mechanics was done by Swiss mathematician and physicist Daniel Bernoulli (1700-1782) and French physicist Jean le Rond d'Alembert. In his classic *Hydrodynamica*, Bernoulli discussed the pressure and velocity of fluids. D'Alembert applied the principle of equilibrium to the motion of fluids. In 1786, based on experiments, Pierre Louis Georges Dubuat (1734-1809) published his book *Principles d'hydraulique* which contains a gratifying theory related to fluid motion.

Rapid progress in fluid mechanics was observed in the 19th century. German civil engineer Gotthilf Heinrich Ludwig Hagen (1797-1884) and French physicist Jean Leonard Marie Poiseuille (1797-1869) both researched laminar flow properties. In 1850, German

physicist Rudolph Clausius (1822-1888) brought a new revolution by giving the kinetic theory of gases. In 1877, French mathematician and physicist Joseph Boussinesq (1842-1929) described eddy viscosities in a turbulent flow. Irish scientist Osborne Reynolds (1842-1912) characterized between laminar and turbulent pipe flow while Irish hydraulic engineer Robert Manning (1816-1897) researched on open channel flow.

The first decade of the 20th century added a new dimension to the field of fluid mechanics with the invention of boundary layer theory. On 8th August, 1904 German fluid dynamicist and aerospace scientist Ludwig Prandtl (1875-1953) presented a revolutionary paper titled *On the Motion of Fluids in Very Little Friction* at the Third International Mathematics Congress at Heidelberg, Germany. This paper is about the boundary layer and its importance in streamlining and drag. Prandtl also developed a solution to Navier- Stokes equation. German physicist Paul Richard Heinrich Blasius (1883-1970) investigated the solution of the boundary layer equation for flow past a flat plate. German engineer Johann Nikuradse (1894-1979) and American professor Lewis Ferry Moody (1880-1953) researched the relationship between pipe flow, friction factor, and Reynolds number.

1.2 General description of fluid

Application of external force deforms all materials. However, fluid is such a substance that deforms limitlessly under the action of shearing stress. Fluids are categorized into liquids and gases. The volume of fluid is reduced under compression. The contraction of volume in liquid is much less than that of gas. This is because intermolecular forces in the fluid particle are significantly stronger than in gaseous particles. As a result, liquid maintains its shape or volume. Gaseous particles move freely in air colliding with each other. Consequently, gas has no definite size and shape. So, for practical problems, liquids and gases are treated to be incompressible and compressible fluids respectively.

Fluid mechanics is concerned with the conditions under which a fluid is at rest or enduring in motion. Fluid mechanics can be subdivided into three main parts- fluid statics, fluid kinematics, and fluid dynamics. Fluid statics is associated with the conditions under which a fluid is at rest. The study of fluid in motion without considering the effect of external pressure is defined as fluid kinematics. It is only involved with the rotation, deformation, and translation of fluid elements. Fluid dynamics is concerned with the velocity, acceleration, and different forces including external pressure exerted by a fluid in motion. The two main

categories of fluid dynamics associated with the motion of liquids are hydrodynamics concerned with the movement of gases.

Fluid dynamics has comprehensive applications in various branches of science and engineering. The studies of large-scale flow on earth's atmosphere, oceanic waves and currents, turbulence, etc. are some geophysical applications of fluid dynamics. Technological and engineering applications include heat engine design, hydroelectric power plants, grinding and screwing of heavy machinery parts, design of canals and dams, different types of brakes (like hydraulic brake, anti-lock braking system (ABS), disc brake) rocket engines, oil pipelines, design of flood control system, design of wind turbine, hydraulic machines, design of flood control system, air conditioning and refrigeration system, etc. Applications of fluid dynamics in the human body are so huge that it is studied under a new branch called biofluid mechanics. It is concerned with the blood circulation in the human body, interaction between blood cells and vessel walls, blood pumps, heart valve prostheses, magnetic drug targeting, heat transfer and diffusion in tissues, etc.

Considering the importance of fluid dynamics in day- today life, researchers are now studying it as a multidisciplinary subject with other classical branches of science. For example, Electrohydrodynamics (EHD) deals with the motion of electrically charged fluids. Magnetohydrodynamics (MHD) is based on fluid dynamics and electromagnetic theory. Hydrology is associated with the movement, management, and distribution of water on earth and other planets.

1.3 Basic Terminologies

1.3.1 Fluid Pressure:

When a fluid is kept in a container, it exerts a force at both normal and tangential directions at each point of the inner side of the container. The normal force acting on the inner side of the container is termed pressure. Simply, normal force per unit area exerted by the fluid at each point of the surface of contact is defined as fluid pressure. There are two main circumstances for the existence of fluid pressure- one is the open condition or open channel flow (for example, river, atmosphere) and the other is the closed condition or closed conduit (for example, gas pipelines, water pipelines). Mathematically pressure p at any point on the fluid is defined as

$$p = \lim_{\delta A \rightarrow 0} \frac{\delta p}{\delta A} = \frac{dp}{dA}$$

where δA and δp are the surface area and normal force acting on a fluid element respectively.

The S.I. unit of pressure is Pascal (Pa) or Newton/m².

1.3.2 Fluid Density

Fluid density, denoted by the symbol ρ is defined as mass per unit volume of the fluid. Mathematically, fluid density at any point of the fluid is defined as

$$\rho = \lim_{\delta V \rightarrow 0} \frac{\delta m}{\delta V}$$

where δV is the volume around the fluid element and δm is the mass of the element.

The S.I. unit of density is Kg/m³

1.3.3 Fluid Temperature

The physical quantity that distinguishes a hot body from a cold body is termed temperature. It is proportional to the kinetic energy of molecules stored in a body. In a fluid, temperature suggests the random motion of the molecules. With decreasing temperature, the volume of most of the liquids and all the gases reduces. The temperature at which gas will not occupy any volume is called absolute zero temperature. At this temperature, the kinetic energy of gas molecules vanishes and hence no molecular movement is observed.

The S.I. unit of temperature is Kelvin (K).

1.3.4 Fluid Viscosity

The resistive force that opposes the motion of the fluid is termed viscosity. This arises due to the shearing resistance in a fluid caused by inter-molecular friction exerted when one layer of fluid attempts to slide over another adjacent layer. As strong intermolecular forces produce a huge amount of friction, a fluid with high viscosity struggles to flow. Honey, Mercury, Glue, etc. are some common examples of this type of fluid. On the other hand, a fluid having low viscosity can easily flow. Water, air, milk, vegetable oil, etc. are fluids having low viscosity.

Newton's law of viscosity states that the shear stress between two adjacent fluid layers is proportional to the velocity gradient between the two layers. Mathematically, it can be written as

$$\tau = \mu \frac{du}{dy}$$

where τ is the shear (tangential) stress, μ is a proportionality constant called the coefficient of viscosity or dynamic viscosity, and $\frac{du}{dy}$ is the velocity gradient.

Therefore, the dynamic viscosity μ of a fluid can be defined as the tangential force required per unit area to overcome its internal molecular friction and maintain unit relative velocity between two fluid layers at a unit distance apart. However, in many practical and industrial applications, viscosity on the movement of flow is described by the ratio of dynamic viscosity μ to fluid density ρ rather than μ alone. This ratio is called kinematic viscosity and it is denoted by ν . Thus, mathematically,

$$\nu = \frac{\mu}{\rho}$$

Kinematic viscosity is utilized when both inertia and viscous forces are dominant whereas dynamic viscosity is utilized when only viscous force is dominant. Pressure has almost no effect on the dynamic viscosity of fluids unless an extreme case occurs. However, for gases, kinematic viscosity varies with pressure. Like dynamic viscosity, kinematic viscosity is independent of pressure for liquids. Ascending temperature diminishes dynamic viscosity for gases. However, dynamic viscosity for gases hikes with sing temperature.

The S.I. unit of dynamic viscosity is Pascal seconds (Pa.s) or $\text{Kg.m}^{-1}.\text{s}^{-1}$ and that of kinematic viscosity is m^2/s .

1.3.5 Compressible and Incompressible Fluids

A fluid is called compressible if it shows a considerable amount of change in density when pressure is applied. Gases exhibit variation in volume and density in presence of even small variations in temperature or pressure. This is because the volume of the gas is composed of a large amount of free space between the particles. When external pressure is

applied, the particles move close to one another and hence volume declines. So, gases are treated as compressible fluids.

On the other hand, the volume and density of fluid do not vary easily if external pressure is applied to it. The molecules or atoms of the liquids are more closely packed than that of gases. When the pressure is applied to liquid its density does not change to a substantial degree. As a result volume of liquids does not vary considerably when external pressure is applied to them. So, liquids are treated as incompressible fluids.

To distinguish a compressible fluid from an incompressible fluid analytically, the concept of Mach number is required. Mach number is the ratio of the velocity of fluid flow to the velocity of sound in that fluid. For compressible fluids, the Mach number is greater than 0.3 and for an incompressible fluid, it is less than 0.3.

1.3.6 Ideal and Real Fluids

An ideal fluid is inviscid and incompressible. This kind of fluid is only imaginary and has no existence in nature. Ideal fluids do not offer any shear resistance, i.e., they can flow smoothly. Real or practical fluids are those fluids that are compressible, viscous, and have surface tension. This type of fluid offers shear resistance.

1.3.7 Newtonian and Non- Newtonian Fluids

Newtonian fluids obey Newton's law of viscosity. They possess constant viscosity and a zero shear rate at zero shear stress i.e., the shear rate is directly proportional to shear stress. This means the quotient of the shear stress and the shear rate is constant throughout the fluid. Water, air, gasoline, and alcohol are some common examples of Newtonian fluids.

Non- Newtonian fluids do not obey Newton's law of viscosity. They exhibit variable viscosity i.e., the viscosity of these fluids can change under the action of a force. They do not follow a linear relationship between shear stress and the rate of angular deformation. Glue, paint, and cosmetics are some well-known examples of Non- Newtonian fluids.

1.3.8 Laminar and Turbulent Flow

The movement of fluid particles along distinct paths or streamlines where no two paths intersect each other is called laminar flow. In this type of flow, the fluid particles flow in layers or laminae gliding smoothly over the adjacent layers. The flow of a highly viscous fluid through a pipe with a small diameter with low velocity is a good example of laminar flow. Laminar flow is also termed as viscous flow or streamline flow.

The movement of fluid particles in a zigzag way, i.e., the fluid particles do not follow non-intersecting paths is termed turbulent flow. The movement of fluid particles causes high energy loss in a turbulent flow. The speed of the fluid at a point continuously changes in both magnitude and direction. The flow of a fluid through a pipe with a large diameter with high velocity is a perfect example of turbulent flow.

1.3.9 Steady and Unsteady Flow

In steady flow, the fluid properties like density, velocity, pressure, acceleration, etc. independent of time. In steady flow, the properties are functions of position only and they do not depend on time. If P denotes all the fluid properties, then for a steady flow,

$$\frac{\partial P}{\partial t} = 0$$

On the other hand, if the fluid properties depend on time, i.e., if they vary from time to time, then the flow is termed unsteady. For unsteady flow,

$$\frac{\partial P}{\partial t} \neq 0$$

When water flows out of a tap that has just been opened, the flow is unsteady initially, but with time the flow becomes steady.

1.3.10 Uniform and Non- Uniform Flow

A flow is called uniform if the velocity at a given instant of time is the same in both magnitude and direction at all points in the flow.

On the contrary, if the velocity changes from point to point in a flow at any given instant of time, the flow is termed as non-uniform.

1.3.11 One, Two, and Three Dimensional Flow

A flow is termed as one dimensional if different flow parameters like velocity, temperature, pressure, etc. are functions of time and one space co-ordinate only. Assuming variation of velocity and pressure along the cross section to be negligible, a flow through a pipe is a good example of a one- dimensional flow.

If all the flow parameters are functions of time and two space co-ordinates, then the flow is said to be two-dimensional. The flow between two infinite plates is a common example of two-dimensional flow.

A flow is labelled as three-dimensional if all the flow parameters are functions of time and all three space co- ordinates. An example of such kind is a flow in an open channel in which the width and the water depth are of the same order of magnitude.

1.4 Heat Transfer

As a consequence of the second law of thermodynamics, heat will flow spontaneously from a hotter region to a cooler region without any external help. Thus, heat is a vector quantity and its flow is directed towards decreasing temperature, with a negative temperature gradient. In general, the transmission of heat or thermal energy from one region to another due to temperature differences is termed heat transfer. This process is spontaneous and irreversible until thermal equilibrium is reached.

There are numerous examples of heat transfer in the universe. The human body continuously ejects heat to its surroundings. The flow of air, the process of cooking, food processing, etc. are some common examples of heat transfer. The process of heat transfer plays a pivotal role in many technological and industrial practices. Some of them are processing of oil and gas, temperature control in die casting, design of I.C. engines, steam generators, molding of plastic, etc.

There are three modes of heat transfer, namely conduction, convection, and radiation. It should be noted that more than one mode of heat transfer can occur simultaneously.

1.4.1 Conduction

The conduction process, also termed thermal conduction, is the method of transfer of heat within parts of a material or between two substances that are in physical contact. This process occurs in solids as well as fluids. Conduction can occur in two ways-

By exchange of thermal energy from molecules at relatively higher temperatures to neighbouring molecules with lower temperatures due to the kinetic motion or direct impact of molecules.

By the movement of free (valance) electrons, occurring due to variance in concentrations of free electrons as in the case of liquid metals, electrolytes, and metallic liquids. The ability of metallic alloys to conduct varies directly with the concentration of free electrons within them.

As temperature difference is the driving potential for heat transfer, a linear relationship between the flow of heat and the temperature difference exists. In 1822, renowned French physicist and mathematician Jean- Baptiste Joseph Fourier (1768-1830), in his monumental work *Theorie Analytique de la Chaleur (The Analytic Theory of Heat)*, proposed an experimental law. This law is termed Fourier's law of heat conduction and it states that the rate of heat conduction through a plane layer is directly proportional to the temperature gradient across the layer and the area of heat transfer but it is inversely proportional to the thickness of the layer. In mathematical form, this law can be expressed as

$$Q = -K_T A \frac{dT}{dx}$$

In the above equation, K_T is a proportionality constant known as the thermal conductivity, A is the area of heat transfer which is perpendicular to the direction of flow of heat, $\frac{dT}{dx}$ is the temperature gradient. The negative sign indicates the flow of heat is along the positive direction of the X -axis and hence heat transfer is a positive quantity. Q is defined as the heat flow per unit area per unit time across any surface (through which heat propagates) and is termed heat flux. Fourier's law of heat conduction is similar to Newton's law of viscosity for laminar flow.

Thermal conductivity is a physical property of a material and is defined as the capacity of the material to conduct heat. Its S.I. unit is Watts per meter Kelvin ($Wm^{-1}K^{-1}$).

1.4.2 Convection

The process of energy transfer between a bounding solid surface and the adjacent fluid (liquid or gas) when they are at different temperatures and there exists relative motion between them is termed convection. It is the mode of heat transfer by the bulk movement of fluid molecules. Initially, heat transfer between the object and the fluid takes place through conduction, but bulk heat transfer happens due to the motion of the fluid. Convective heat transfer depends on fluid motion. The faster the fluid movement, the greater is the heat transfer by convection. When bulk movement is absent, heat transfer between a solid surface and the adjacent fluid is by conduction (random molecular motion of surface molecules) only. There are three types of convection - free, forced, and mixed.

When temperature difference occurs, thermal expansion takes place. The hotter layers of fluid become less dense and the colder layers are denser. This generates buoyancy force and it propels hotter i.e., less dense parts away. Consequently, the cooler, i.e., the less dense part rushes to replace it. This induces the movement of fluid. The process of heat transfer in this manner is called free or natural convection. Sea breezes, oceanic breezes, and land breezes are perfect examples of free convection. Applications of free convection can be observed in the cooling of electrical equipment, solar collectors, nuclear reactors thermal hydraulics, etc.

When fluid flow is induced by some external agencies like pumps, fans, etc., forced convection takes place. In forced convective flow, the driving force is external to the fluid and the flow velocities are high. The cooling systems of a car, water geysers, electric fans, etc., are some common examples of forced convection. Forced convection is used in many technological phenomena such as the flow within a shell and tube heat exchanger, the flow of fluids over flat surfaces, the flow of water through nuclear heating elements, the flow of a cryogenic liquid coolant in certain digital computers, etc.

When free and forced convection are both of the same orders of magnitude, the convection is called mixed. For instance, if air flows over a vertical surface at a relatively low velocity but the surface is heated at a considerably high rate, both free and forced convection

are expected to occur. Mixed convection takes place in various industrial and technological applications such as electronic devices cooled by fans, cooling of nuclear reactors heat exchangers placed in a low-velocity environment, etc.

In 1701, noted scientist Sir Isaac Newton observed that the rate of heat loss from a body is directly proportional to the temperature between the body and the surroundings. This law is known as Newton's law of cooling. Mathematically, this law can be stated as

$$Q = hA_s (T_s - T_\infty)$$

where A_s is the surface area through which convection takes place, Here h is the convective heat transfer coefficient, A_s is the surface area through which convection takes place, T_s is the surface temperature, T_∞ is the temperature of the fluid far away from the surface, and Q is the convective heat flux.

The S.I. unit of convective heat transfer coefficient is $Wm^{-2}K^{-1}$.

1.4.3 Radiation

The process of emission or transmission of energy by matter in the form of electromagnetic waves or photons is termed as radiation. Conduction or convection requires a material medium for the energy to transmit. However, radiation does not necessarily require a material medium to transport energy. Hence, radiation is the most powerful mode of heat transfer. Heating up of the earth's surface by the rays of the sun is a perfect example of radiation.

The two main theories that explain the heat transfer process by radiation are- wave theory and quantum theory.

1.4.3.1 Wave Theory

In his treatise *A Dynamical Theory of the Electromagnetic Field*, Scottish scientist James Clerk Maxwell (1831-1879) first proposed that if an electrically charged particle moves under acceleration, alternating electrical and magnetic fields are produced and transmitted. These fields are transmitted in the form of waves. These waves are called electromagnetic waves or

electromagnetic radiation. The radiation in form of electromagnetic waves declines the internal energy of the emitting body unless the heat is generated within that body equivalent to the decrease in internal energy. However, this theory does not explain the photoelectric effect and blackbody radiation.

1.4.3.2 Quantum Theory

Renowned German physicist Max Planck (1858-1947) postulated quantum theory. According to this theory, molecules and atoms emit or absorb energy only in discrete quantities. The smallest amount of energy that can be emitted or absorbed in the form of electromagnetic radiation is called a quantum. The energy of the radiation absorbed or emitted is directly proportional to the frequency of the radiation. Mathematically, it can be written as

$$E = h\nu$$

where E is the energy of radiation, ν is the frequency of the radiation and h is a proportionality constant known as Planck's constant. The experimental value of Planck's constant is $6.626 \times 10^{-34} \text{ J}\cdot\text{s}$

The form of radiation emitted by bodies due to their temperature is termed thermal radiation. It is different from other types of electromagnetic radiation such as x-rays, microwaves, gamma rays, radio waves, etc. as these are not related to temperature. Thermal radiation depends on various factors like surface area, spectral emissivity, surface reflexivity, temperature, geometrical configuration, etc. All materials which are at a temperature above absolute zero naturally emit thermal radiation at various intensities. Hence every solid and fluid emits, absorbs or transmits radiation spontaneously to varying degrees. Radiation is considered to be a surface phenomenon for solids whereas it is considered to be a volumetric phenomenon for fluids.

The highest rate of radiation that can be emitted from a surface is given by Stephen-Boltzmann law-

$$Q_{\max} = \sigma A_s T_s^4$$

where A_s is the surface area, T_s is the temperature, and σ is the Stephen- Boltzmann constant whose value is $5.67 \times 10^{-8} Wm^{-2} K^{-4}$. The body that emits radiation at the rate Q_{max} known as a blackbody and radiation emitted by such a body is called blackbody radiation. However, radiation emitted by all real bodies is less than blackbodies at the same temperature. The amount of radiation emitted by real bodies is defined as

$$Q_{emit} = \varepsilon \sigma A_s T_s^4$$

here ε is the emissivity of the surface. ($0 \leq \varepsilon \leq 1$)

Similarly, radiation absorbed on a real surface is defined as

$$Q_{absorbed} = \alpha \sigma A_s T_s^4$$

here α is the absorptivity of the surface. ($0 \leq \alpha \leq 1$)

For blackbody, both emissivity and absorptivity are of magnitude unity. Hence a blackbody is a perfect emitter as well as a perfect absorber. The quantity $Q_{net} = Q_{emit} - Q_{absorbed}$ gives the net radiative heat transfer of the surface. The surface loses energy if $Q_{net} > 0$ and gains energy if $Q_{net} < 0$. Radiative heat transfer between a surface and its surroundings occurs simultaneously with conduction or convection. Though radiation is considered to be insignificant relative to forced convection, it is very significant relative to conduction and free convection.

1.5 Mass Transfer

The movement of a species from a higher concentration region to a lower concentration region is called mass transfer. The process of mass transfer requires two regions at distinct species concentrations and the process continues until an equilibrium state is established. Mass transfer occurs in solids, liquids as well as in gases. Unlike heat transfer, the mass transfer phenomenon has several driving forces like concentration difference (for liquids), mole difference (for gases and liquids), pressure difference (for gases), etc. Evaporation of water from river to the atmosphere, distillation of alcohol, purification of

blood in the kidneys and liver, etc. are some common examples of mass transfer. Many industrial and engineering activities like adsorption such as scrubbers or stripping, separation of chemical components in distillation columns, absorbing activated carbon beds, absorption, liquid extraction, drying, leaching, etc. encounter mass transfer. There are two main modes of mass transfer- mass diffusion and mass convection.

1.5.1 Mass Diffusion

Mass diffusion occurs due to macroscopic random molecular motion or the laminar flow of fluids. Like the conduction process of heat transfer, diffusive mass transfer originates from molecular activity. Mass diffusion can be observed in solids, liquids, and gases. However, mass transfer is strongly influenced by molecular spacing diffusion and as a result, it occurs more expeditiously in gases than in liquids and solids and more rapidly in liquids than in solids. In 1855, renowned German scientist Adolf Eugen Fick (1829-1901) put forward a rate equation for mass diffusion stating that the mass flux of the diffused substance and the concentration gradient are responsible for mass transfer. This law is known as Fick's law of diffusion. Suppose, in a binary mixture of two species A and B, in which composition varies in the X direction and molecular diffusion occurs within the fluid due to the non-uniformity of composition until equilibrium is established. According to Fick's law of diffusion, the mass flux of an element per unit area is proportional to the concentration gradient. Mathematically, it can be written as,

$$J_{A_x} = -D_{AB} \frac{dC_A}{dx}$$

where J_{A_x} , is the molal flux of species A in x direction, $\frac{dC_A}{dx}$ is the molal concentration gradient of component A in the x-direction, D_{AB} is a constant of proportionality known as mass diffusivity (or the diffusion coefficient) of component A diffusing through component B. The molal concentration of component A is expressed by the quantity C_A and is defined as the number of molecules of component A per unit volume of the mixture. The negative sign in Fick's law indicates that mass diffusion takes place in the direction of decreasing concentration. Similarly, we can find the rate equation for the molal flux of species B. It should be noted that for a binary mixture of species A and B, the mass diffusivity of A with respect to B is equal to the mass diffusivity of B with respect to A i.e., $D_{AB} = D_{BA}$.

The SI unit of mass diffusivity is m^2/s .

1.5.2 Mass Convection

Mass transfer by convection takes place due to the bulk movement of fluid. It is concerned with the transfer of mass between two relatively immiscible moving fluids or between a moving fluid and a surface. Convective mass transfer arises if the bulk velocity is appreciable or the constituents in a binary mixture are moving with significant relative velocities. Likewise to convective heat transfer, mass transfer by convection can be subdivided into free or natural and forced mass convection. The convective mass transfer phenomenon is analogous to the convective heat transfer process.

The difference in species concentration causes variation in densities in a fluid mixture. This variation produces a buoyancy force. The movement of mass due to buoyancy force is termed free convective mass transfer. The evaporation of alcohol is a perfect example of free convective mass transfer.

The process of movement of mass developing with the help of external sources is called forced convective mass transfer. An example of forced convective mass transfer is the evaporation of water from an ocean when air blows over it.

1.6 Chemical Reaction

A chemical reaction is a process in which a substance is transformed chemically under the influence of some energy such as light, heat, electricity, etc. This process can be spontaneous or non-spontaneous. It involves the exchange of electrons in the breaking and formation of chemical bonds, and consequently, chemical substances change, and some energy is absorbed or released in the process. A chemical reaction can be segregated as homogeneous and heterogeneous. If the chemical reaction appears evenly in a single phase i.e., either gas, solid, or liquids, or is entirely dependent on the nature of the interactions of the reacting substances, then it is termed as homogeneous chemical reaction. An example of such kind of reaction is a mixture of oxygen and common LPG gas that produces flame under heat energy. On the other hand, in a heterogeneous chemical reaction, one or more chemical reactants experience chemical change at an interface. Some common examples of such kind of reaction include corrosion of iron, the reaction of solid metals with acids, etc.

The concentration of the reactants plays a pivotal role in a chemical reaction. The rate of a chemical reaction is defined as the variation in concentration over time. The number that characterizes the relationship between the rate of a chemical reaction and the concentrations of the reactants is termed as the order of that chemical reaction. The chemical reactions where the rate is independent of the concentration of reactant, i.e., the change in concentration of reactant does not affect the speed of the reaction is called a zeroth-order chemical reaction. The rate equation of zeroth order chemical reaction can be written as $rate = K_0 [A]^0 = K_0$, where K_0 is the zeroth order homogeneous rate constant and $[A]$ is the concentration of one of the reactants. If the rate depends linearly on the concentration of only one reactant, then it is known as a first-order chemical reaction. The rate equation of first-order chemical reaction can be stated as $rate = K_1 [A]^1 = K_1 [A]$ where K_1 is the first-order homogeneous rate constant. Similarly, if in a reaction whose rate depends on the concentration of one reactant raised to the second power or on the concentration of two different reactants, each raised to the first power is called second – order reaction chemical reaction. Mathematically, the rate equation for second-order chemical reaction can be written as $rate = K_2 [A]^2$ or $rate = K_2 [A][B]$ where K_2 is the second-order rate constant and $[A]$ and $[B]$ are the concentration of the reactants.

1.7 Gray and Non-Gray Gases

The optimal thickness of a material is defined mathematically as

$$\tau = \log_e \left(\frac{I_0}{\bar{I}} \right),$$

where I_0 denotes the original intensity of the beam of light and \bar{I} denotes the intensity of light after passing through the material. A gas is termed as optically thin if $\tau \ll 1$ and it is called optically thick if $\tau \gg 1$. Optical thickness is a dimensionless quantity and it measures the capacity of a particular material.

Also, a gas is said to be gray if its optical thickness τ does not depend on the wave number of electromagnetic radiation. Otherwise, the gas is said to be non-gray. All commonly found atmospheric gases are non-gray in general. For optically thick non- gray gas, the Rosseland approximation method is used to describe the heat flux due to radiation

that appears in the energy equation whereas, in the case of optically thin non-gray gas, Cogley's model is used for the same.

1.8 Porous Medium

A medium or material that contains holes or voids through which fluids can easily flow is termed as a porous medium. The skeletal part of the material is called pore space or frame or matrix. Generally, pore space is constituted of solids. Many natural substances such as rocks, soils, zeolites, biological tissues (such as wood, cork, bones, etc.), and artificial materials such as foams, cement, ceramics, etc. are some examples of porous medium. Numerous scientists and researchers work extensively in the fields involving porous medium due to their diverse practical applications. Some of these fields are soil mechanics, rock mechanics, petroleum engineering, geo-mechanics, bioremediation, hydrogeology, filtration, geoscience, acoustics, constructing engineering, material sciences, physical sciences, life sciences, etc. In his book *Ankituing Zun Naturlehre*, Leonhard Euler was the first to introduce the concept of a porous medium.

However, the basic law governing fluid flow through porous media was given by French civil engineer Henry Philibert Gaspard Darcy (1803-1858) in the year 1856. This law is known as Darcy's law. He formulated this law based on an experiment with natural sand, the proportion of water volume flowing through the sand, and the loss of pressure. This law is valid only for laminar flow through fine-grained sediments. To formulate the law, Darcy used Navier- Stokes equation. The law is analogous to Ohm's law of electrical networks, Fick's law of mass diffusion, and Fourier's law of heat conduction. Though porous media is non-homogeneous, for experimental analysis, Darcy considered it to be homogeneous. Hence, this law is valid for a situation where the porous material is already homogeneous and already saturated with the fluid. Mathematically, this can be expressed as-

$$\vec{q} = -\frac{k}{\mu} \vec{\nabla} p$$

where, \vec{q} is the filter velocity or volume flow rate or filter velocity, μ is the coefficient of viscosity, p is the pressure, and k is in general a second-order tensor called the permeability of the porous media. Permeability characterizes fluid motion through a porous medium.

To elucidate the transitional flow between the boundaries, noted researcher H.C. Brickman extended Darcy's law by adding a term known as Brickman's term. However, this correction term is only applicable for those flows where the medium is highly porous. Due to its complexity in use, such a term is generally omitted. Including the Brickman term, mathematically Brickman equation can be expressed as-

$$\vec{q} = -\frac{k}{\mu}(\vec{\nabla}p - \bar{\lambda}_1 \nabla^2 \vec{q})$$

where $\bar{\lambda}_1$ is called as effective dynamic viscosity for the Brickman model and it is defined as

$\bar{\lambda}_1 = \frac{\mu}{porosity}$. In the case of laminar viscous flow, a first approximation gives result as

$\bar{\lambda}_1 \cong \mu$ Incorporating with the above two equations, the Navier-Stokes equation for the flow of an incompressible viscous fluid through a porous medium can be stated as-

$$\rho \left[\frac{\partial \vec{q}}{\partial t} + (\vec{q} \cdot \vec{\nabla}) \vec{q} \right] = -\vec{\nabla}p - \frac{\mu}{k} \vec{q} + \mu \nabla^2 \vec{q} + \rho \vec{F}$$

where \vec{F} is the external force acting on the fluid per unit mass.

1.9 Thermal Diffusion Effect or Soret Effect

When both thermal and solutal convection occurs simultaneously in a fluid mixture, then the relation between driving potential and flux becomes more complicated. The mass flux is generated by both the temperature gradient and concentration gradient. The effect of mass flux under temperature gradient is termed as the Soret effect or thermal diffusion effect. This effect was first observed by German physician Carl Ludwig in 1859. But, the first experimental work was done by Swiss chemist Charles Soret in 1879. He conducted the experiment using solutions containing Sodium Chloride (*NaCl*) and Potassium Nitrate (*KNO₃*) in pipes with heated or cooled ends. He observed that when two parts of a liquid are maintained at different temperatures, then the solute of the liquid has a tendency to move from a warmer region to colder region. Consequently, the smaller light molecules get separated from large heavy molecules under a temperature gradient. In Soret effect, there exists a difference in concentration of components in the region of high and low temperatures. This concentration difference in turn contributes in the occurrence of diffusion.

The aspect of mass flux under a large temperature gradient fascinates several theoretical and experimental researchers. Renowned Dutch physical chemist Jacobus Henricus van't Hoff (1852-1911) was the first to publish theoretical work on Soret effect in 1887. He developed an interrelationship between gases and dilutes solutions and predicted that the solute would distribute itself so that its osmotic pressure remains constant throughout the system. Later, this effect was elaborated by British mathematician and geophysicist Sydney Chapman (1888-1970). This effect has many applications in different chemical and physical processes, isotope separation, etc.

1.10 Diffusion Thermo Effect or Dufour Effect

If two non-reacting and chemically different fluids are allowed to diffuse into each other, initially at the same temperature, then the system produces a heat flux. The effect of heat flux owing to a significant composition gradient is termed as the Dufour effect or diffusion thermo effect. It is the inverse phenomenon of the thermal diffusion effect. Renowned Swiss scientist L. Dufour discovered this effect in 1873. The Dufour effect is typically disregarded in heat and mass transport processes as they are of a lower order of magnitude compared to the effects described by Fick's or Fourier's laws. This effect is usually negligible for binary liquid mixtures. However, the diffusion thermo effect is found to be of considerable magnitude in the case of medium molecular weight (like N_2 , air) so it cannot be neglected as emphasized by Eckert and Drake (1972). Application of diffusion thermo effect can be found in many areas, especially in chemical reactors and CVD problems.

1.11 Magnetohydrodynamics (MHD)

The branch of physics that deals with the interaction of a magnetic field with electrically conducting fluid is termed as Magnetohydrodynamics (MHD). “*Magneto*” means electromagnetic fields, “*hydro*” means fluids and “*dynamics*” denotes the forces and the laws of motion. So basically, MHD is the mathematical model for low-frequency interaction between electrically conducting fluids and electromagnetic fields. Saltwater, liquid metals, electrolytes, and plasma are some common examples of electrically conducting fluids. *(A gas is electrically insulating at ordinary temperature. However, at a very high temperature (6000 K-10000 K), almost every element of the gas gets ionized and it becomes highly electrically conducting. Such state of a gas is known as plasma)*. Both fluid Mechanics and MHD are part of continuum mechanics, and often they produce closely related results. Both of them are

fundamental to many spellbinding areas of astrophysics and geophysics. They have a wide variety of applications in the human body, many engineering and technological problems as well as numerous cosmic events. Magnetohydrodynamics is also called Magneto gas dynamics and Magneto-fluid mechanics. It is the only dynamics related to electrically conducting fluids. With the introduction of the Lorentz force, the governing laws of MHD become different from conventional laws of hydrodynamics. Due to its complexity, many researchers devoted themselves to studying different consequences of MHD. The principle of MHD is based on the following two phenomenons-

- i. An induced magnetic field associated with the current which perturbs the original magnetic field.
- ii. An electromagnetic force originating from the interaction of current and field which perturbs the original fluid motion.

Thus, MHD appears from one of the mutual interactions between the electromagnetic field and fluid velocity field. The motion affects the magnetic field by carrying the magnetic field lines partially (depending upon the electrical conductivity of the fluid) along with it and the magnetic field affects the motion by producing a mechanical force namely the Lorentz force.

The equations which describe MHD flow are a combination of Maxwell's equations of electromagnetism and Navier-Stokes equations of fluid dynamics. As MHD is a continuum theory, it cannot be treated like a kinetic phenomenon, i.e. those in which the existence of discrete particles or of non-thermal velocity distribution is important. Maxwell's equations describe the properties of electric and magnetic fields and connect them to their sources, charge density, and current density. There are four equations of electromagnetism emphasized by Maxwell and they are as follows:

- i. $\vec{\nabla} \cdot \vec{E} = \frac{\rho}{\epsilon_0}$ (Gauss's law of electrostatics)
- ii. $\vec{\nabla} \cdot \vec{B} = 0$ (Gauss's law of magnetism)
- iii. $\vec{\nabla} \times \vec{E} = -\frac{\partial \vec{B}}{\partial t}$ (Faraday's law of electromagnetic induction)

$$\text{iv.} \quad \vec{\nabla} \times \vec{B} = \mu_0 \vec{J} + \mu_0 \varepsilon_0 \frac{\partial \vec{E}}{\partial t} \text{ (Ampere's law with Maxwell's correction)}$$

where \vec{B} , \vec{E} , \vec{J} , μ_0 , ρ , t , ε_0 denote the magnetic induction vector, electric field density vector, current density vector, magnetic permeability of the medium, density, time and permittivity of the medium respectively.

It is assumed that the medium is not significantly polarisable or magnetisable, which is pertinent for a highly conducting medium where currents are produced due to the movement of free electrons. Gauss's law of electrostatics relates the total electric charge contained within a closed surface (called Gaussian surface) to the surrounding electric field. Mathematically, this law depicts how charges affect the divergence of an electrical field (electric field lines diverge from positive charges toward negative charges). It also states that the total electric flux through a Gaussian surface is independent of the shape and size of that surface. Gauss's law of magnetism states that the total magnetic flux through a Gaussian Surface is zero. This is due to the fact that in the real world, magnetic charges exist in pairs (referred to as dipoles) and they create opposite magnetic field divergences which cancel out each other. In theory, a single magnetic charge is termed as a magnetic monopole. As a consequence of Gauss's law for magnetism, it is clear that magnetic monopoles (i.e. free magnetic charges) do not exist in nature. Faraday's law of electromagnetic induction interprets the reason behind the electric field being produced by a varying magnetic field. The principles of several electric generators are based on this law. For instance, the force of water falling from a hydroelectric dam spins a huge magnet, and the varying magnetic field induces an electric field that drives electricity through the power grid. Based on a series of experiments, noted British scientist Michael Faraday (1791-1867) formulated this law in 1831. Ampere's law with Maxwell's correction states that magnetic fields can be generated in two ways- one by electrical current (this was the original law given by French physicist Andre Ampere (1775-1836)) and the other by time-varying electric fields. The phenomenon of changing electric field induce magnetic field can be described from the modern concept of displacement current $\varepsilon_0 \frac{\partial \vec{E}}{\partial t}$ which was introduced to maintain the solenoid nature of Ampere's law in a vacuum capacitor circuit. Here, ε_0 denotes the permittivity of free space. This modern displacement current concept has the same mathematical form as Maxwell's

original displacement current $\varepsilon \frac{\partial \vec{E}}{\partial t}$. Maxwell's original displacement current applies to polarization current in a dielectric medium and it sits adjacent to the modern displacement current in Ampere's law. The modern extension to displacement current applies in the pure vacuum. This asserts that a changing electric field can induce a magnetic field, and vice-versa. From this modern interpretation, it is understood that, even if no electric charges or currents are present, it is possible to have stable, self-perpetuating waves of oscillating electric and magnetic fields, with each field driving the other. Ampere's law emphasizes the fact that a changing electric field induces a magnetic field. Maxwell's equations are generally applied to macroscopic averages of the fields, and it is only in this averaged sense that one can define quantities such as the permittivity and permeability of a material/medium. The fields in Maxwell's equations are generated by charges and currents.

There are two types of MHD- ideal and resistive. The simplest form of magnetohydrodynamics is termed as ideal MHD. In an ideal MHD, resistivity is assumed to be very little and hence it is a perfect conductor. In an ideal MHD, magnetic field lines surround or bounds the fluid as stated in Lenz's law. The equation of the ideal MHD consists of the continuity equation, the Cauchy momentum equation, Ampere's law avoiding current displacement and a temperature evolution equation. Fine-scale magnetic turbulence or current sheets introduce small spatial scales into the system over which ideal MHD demolishes. This causes magnetic diffusion to occur very rapidly and resistive MHD takes place.

In an MHD heat transfer problem, the term containing Joule heating turns up in the energy equation and the Lorentz force comes into action as stated earlier. In a system with forced convection, the energy equation is detached from Navier-Stokes equation and Maxwell's equations electromagnetic equations. However, in a natural convection system, the Navier-Stokes equation breaches the energy equation. To efficiently design a magnetohydrodynamic device, it is important to study thoroughly information regarding electromagnetic, velocity and temperature fields.

There are several applications of the MHD principle in various branches of science and technology such as in engineering, geophysics, astrophysics, aeronautics, medical science, etc. Engineering applications include electromagnetic casting, liquid metal cooling of nuclear fission reactors, creation of MHD propulsion force, welding, design of heat exchangers, magnetic filtration and separation, refining and solidification, design of

laboratory devices, brakes, dispersion and granulation of metals, metallurgy, etc. Scientists use MHD to study numerous geophysical phenomena out of which earthquakes and the earth's magnetic field are preeminent. MHD is used to describe different astrophysical events such as solar wind, solar flares, astrophysical plasma, etc. The method of magnetic drug targeting which is generally used in cancer treatment is based on the MHD principle.

1.12 Boundary Layer Theory

In 1903, American aviation scientist brothers Orville Wright and Wilbur Wright invented and flew the first practical airplane. However, with the passing of time, it became more and more arduous in determining the lift and drag forces on airplanes. Aviation scientists need to calculate both pressure and shear-stress distributions and integrate them over the surface of the airfoil to measure these forces. With the help of various approximations, the distribution of pressure can be appraised. But, the calculation of the shear-stress distribution requires the inclusion of internal friction and the consideration of viscous flow and is thus needed to tackle the Navier-Stokes equations for viscous flow. Navier-Stokes equations become weak nonlinear due to the presence of the convective term “ $\vec{q} \cdot \vec{\nabla}$ ” (\vec{q} and $\vec{\nabla}$ are velocity of fluid and gradient operator respectively). To date, it is not possible to obtain a complete analytical solution of Navier-Stokes equations. For very small Reynolds number i.e., for high viscous fluid flow, where inertial forces can be neglected completely, some exact solutions of the Navier-Stokes equations can be calculated. However, if the fluid flow is characterized by a large Reynolds number, i.e., when either viscosity is small or when viscous forces and inertia forces are of the same order of magnitude in a significant portion of the flow system, the effect of viscosity of the fluid cannot be neglected. It is therefore required to retain both inertial and viscous terms in Navier-Stokes equations and consequently, the theory of non-viscous fluid dynamics fails to explain the flow of such fluids neighboring a solid boundary placed in the fluid itself. To overcome these limitations, German scientist Ludwig Prandtl proposed boundary layer theory for a fluid flow concerning small viscosity or large Reynolds number. His approximations for boundary layer simplify Navier Stokes equations so that it becomes solvable keeping both inertial and viscous forces. Brief discussions on various types of boundary layers involved with real fluid flow are given below:

1.12.1 Velocity Boundary Layer

Let us consider a two-dimensional laminar flow of a viscous, incompressible, and electrically conducting Newtonian fluid past a semi-infinite vertical flat plate at zero incidences. We also assume that this fluid possesses a very small viscosity, i.e., the Reynolds number of the fluid is large. As the fluid is real and Newtonian, so it does not slip or slide over the plate, but sticks to it and as a result, the adherent fluid particles will attain zero velocity on the plate, ($u = 0$, at the plate). The flow configuration is given below

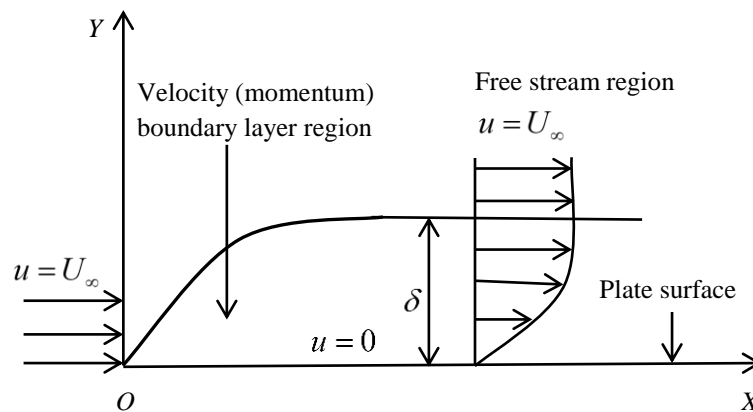


Figure 1.1: Velocity boundary layer

The velocity of the fluid increases gradually and attains the free stream (or full stream) velocity asymptotically at a sizable distance from the plate. The transition from zero velocity at the plate surface to the free stream velocity U_∞ generates a velocity gradient within a very thin fluid layer in contact with the plate and this layer is termed as the velocity boundary layer. The velocity boundary layer is also called the momentum boundary layer as it changes in momentum within the layer. Practically, the velocity boundary layer is considered to be the region where the fluid velocity is parallel to the surface of the plate and it is less than 99% of the free stream velocity. The quantity δ is referred as the thickness of the velocity boundary layer. As the distance from the surface increases, the boundary layer thickness δ hikes. Although there is no such physical delimitation between the boundary layer and the mainstream, a fictional line having almost zero velocity gradients separates the mainstream from the boundary layer. This imaginary line is termed as the edge of the boundary layer. Ludwig Prandtl first proposed the idea of dividing the fluid into two regions. For the convenience of mathematical analysis, the flow region is divided into two sub-regions-

- A very slim layer (called boundary layer) contiguous to the plate surface in which the effect of fluid viscosity is prominent and the viscous and the inertial forces have magnitudes of the same order. A velocity gradient with a very large value near the wall exists in presence of viscous drag as $\tau \frac{\partial u}{\partial y}$ (as emphasized by Newton) even when fluid viscosity is quite small.
- In the region outside of the boundary layer, the velocity gradient $\frac{\partial u}{\partial y}$ is so small that it can be neglected and accordingly viscous forces may be ignored completely. The inertial forces dominate this region and here the theory of ideal fluid offers a very good approximation.

Whenever there is fluid flow over a surface, the velocity boundary layer develops and it acts as a basic concept behind convective transport problems. In some situations where the fluid passes the leading edge of the plate, both viscous forces and velocity gradients are of higher order in magnitude. Then the fluid moves in the laminar regime and the boundary layer thus developed is very thin. This type of boundary layer is termed as the laminar boundary layer. However, as the fluid travels further downstream along the plate, the flow of the fluid gets retarded under the influence of viscous shear and accordingly, the boundary layer becomes thick. This results in a gradual decrease of the velocity gradient. The thickness of the boundary layer forces the particles to move out of the smooth layers and thus the laminar motion becomes unstable. As a result, the flow becomes turbulent. This type of boundary layer is labelled as a turbulent boundary layer.

1.12.2 Thermal Boundary Layer

When there is a difference between solid surface temperature and free stream temperature exists, the thermal boundary layer develops. Let us consider a non-conducting isothermal flat plate placed horizontally along X –axis. The plate temperature is kept uniform at value T_w except the leading edge, where the temperature is equal to the outside free temperature and is measured as T_∞ . Let us consider $T_w > T_\infty$, i.e., the plate is ‘hot’. At the plate's surface temperature, the fluid particles coming into contact with the plate surface achieve thermal equilibrium. Subsequently, these particles swap energy with those in the adjacent fluid layers, and hence thermal gradients establish in the fluid. The region of the

fluid in which temperature gradients take place is termed as the thermal boundary layer. The thickness of this layer is denoted by and its thickness δ_t . With increasing Y - distance from the plate surface, the fluid temperature inside the boundary layer tends to the free stream temperature, i.e., $T(x, y, t) \rightarrow T_\infty$. As the distance from the leading edge increases (i.e, with increasing values of x), the effects of heat transfer permeate further into the free stream and in the expansion of thermal boundary layer thickness δ_t can be defined as the value of y for which $\frac{T_w - T}{T_w - T_\infty} = 0.99$.

The thickness of the velocity boundary layer δ and the thickness of the thermal boundary layer δ_t are connected by Prandtl number of the fluid. For fluids having $Pr = 1$, it is noticed that $\delta = \delta_t$. For those fluids having $Pr \gg 1$, it is observed that $\delta_t \ll \delta$ and on the other hand, for fluids having $Pr \ll 1$, it is noticed that $\delta_t \gg \delta$.

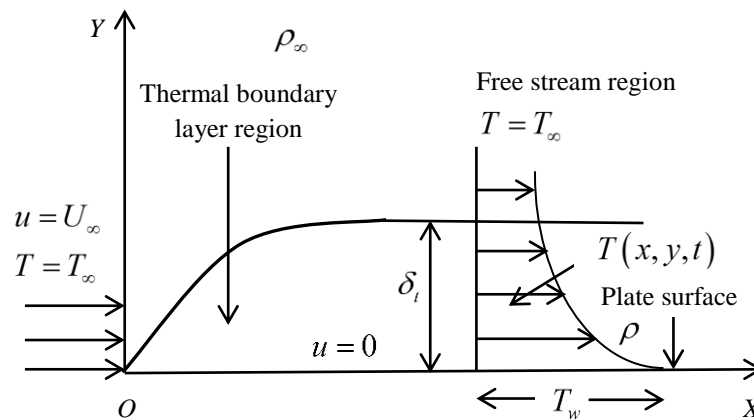


Figure 1.2: Thermal boundary layer

Due to the existence of temperature gradient in the fluid, variation in fluid density take place. Let ρ and ρ_∞ be the densities of fluid in the thermal boundary layer and in free-stream respectively. The fluid particles in the immediate vicinity of the hot plate become warmer (and hence lighter) than the surrounding colder (and hence heavier) fluid particles and this result in a local change of density. Under the assumption of no-slip conditions, heat transfer takes place only by heat conduction. Heat flux q^* at any distance x from the leading edge may be determined by applying Fourier's law of heat conduction to the fluid at the plate (i.e., at $y=0$) as

$$q^* = \kappa \left. \frac{\partial T}{\partial y} \right]_{y=0}$$

where κ is the thermal conductivity of the fluid medium. Also from Newton's law of cooling, we get $q^* = h_T (T_w - T_\infty)$, where h_T is the local heat transfer coefficient. Combining Fourier's law with Newton's law of cooling, we obtain

$$h_T = \frac{-\kappa \left. \frac{\partial T}{\partial y} \right]_{y=0}}{T_w - T_\infty}$$

It should be noted that both T_w and T_∞ are taken to be constant, and hence $T_w - T_\infty$ is also a constant. Also thickness of thermal boundary layer δ_t hikes with increasing x , and hence the magnitude of the temperature gradient $\left(\frac{\partial T}{\partial y} \right)_{y=0}$ must decrease with increasing x .

1.12.3 Concentration Boundary Layer

When there is exists a difference between the surface concentration and free stream concentration of the species, a concentration boundary layer establishes. The concept of concentration boundary layer is analogous to that of thermal boundary layer.

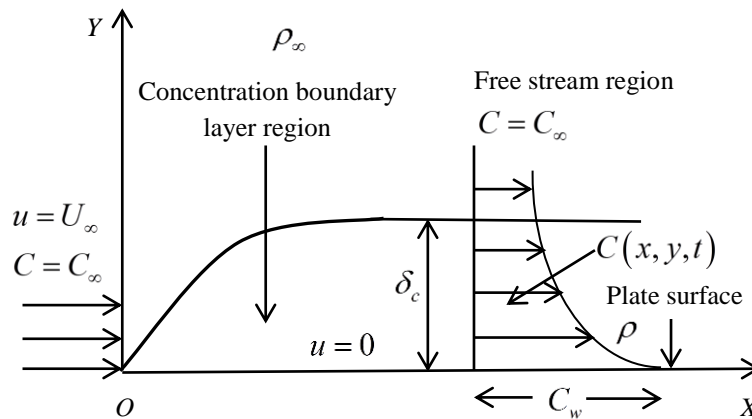


Figure 1.3: Concentration boundary layer

Let us consider a flat plate lying along the X-axis and the fluid is viscous Newtonian, incompressible, electrically conducting and it flows over the plate. It is also assumed that the fluid medium composed of a single chemical species. Let concentration of species in the fluid

at the surface is uniform and equal to C_w and that in the free-stream is also uniform and equal to C_∞ . For $C_w > C_\infty$, the chemical species present in the fluid diffuses from the surface of the plate into the fluid and a concentration boundary layer will be formed. This diffusion is based on the fact that mass flows from a region of higher concentration to a region of lower concentration. The effects of mass transfer penetrate further into the free-stream resulting in the growth of concentration boundary layer thickness δ_c which is defined as the value of y

$$\text{for which } \frac{C_w - C}{C_w - C_\infty} = 0.99$$

Due to the difference of species concentration in the fluid, variation in fluid density take place. Let ρ and ρ_∞ be the densities of fluid in the concentration boundary layer and in the free-stream respectively. Under the assumption of no-slip conditions, there is no fluid motion at the plate surface. Consequently, the mass transfer takes place only by diffusion. Mass flux M_w at any distance x from the leading edge, may be determined by applying Fick's law of mass diffusion to the fluid at the plate (i.e., at $y=0$) as

$$M_w = -D_M \left. \frac{\partial C}{\partial y} \right]_{y=0}$$

where D_M is the mass diffusivity of the fluid medium. Again as analogy to Newton's law of cooling, we get $D_M = h_M (T_w - T_\infty)$, where h_M is the local mass transfer coefficient. Combining both, we obtain

$$h_M = \frac{-D_M \left. \frac{\partial C}{\partial y} \right]_{y=0}}{C_w - C_\infty}$$

1.13 Basic Equations

Fundamental equations that govern the convective flow of an electrically conducting, incompressible, viscous, chemically reacting and radiating fluid in a porous medium in presence of a magnetic field having constant mass diffusivity and thermal diffusivity taking account of both thermal diffusion and diffusion thermo effects are

Continuity equation:

$$\vec{\nabla} \cdot \vec{q} = 0$$

Gauss law of magnetism:

$$\vec{\nabla} \cdot \vec{B} = 0$$

Ohm's law for moving conductor:

$$\vec{J} = \sigma (\vec{E} + \vec{q} \times \vec{B})$$

Faraday's law of electromagnetic induction:

$$\vec{\nabla} \times \vec{E} = -\frac{\partial \vec{B}}{\partial t}$$

Kirchhoff's first law:

$$\vec{\nabla} \cdot \vec{J} = 0$$

Ampere's law:

$$\vec{\nabla} \times \vec{B} = \mu_e \vec{J}$$

Magnetic induction equation:

$$\frac{\partial \vec{B}}{\partial t} = \eta \nabla^2 \vec{B} + \nabla \times (\vec{q} \times \vec{B})$$

Momentum equation:

$$\rho \left[\frac{\partial \vec{q}}{\partial t} + (\vec{q} \cdot \vec{\nabla}) \vec{q} \right] = \vec{F} - \vec{\nabla} p + \vec{J} \times \vec{B} + \mu \nabla^2 \vec{q} - \frac{\mu \vec{q}}{K^*}$$

Energy equation:

$$\rho C_p \left[\frac{\partial T}{\partial t} + (\vec{q} \cdot \vec{\nabla}) T \right] = \kappa \nabla^2 T + \frac{\vec{J}^2}{\sigma} + \bar{\phi} + Q - \vec{\nabla} \cdot \vec{q}_r + \frac{\rho D_M K_T}{C_s} \nabla^2 C$$

Species continuity equation:

$$\frac{\partial C}{\partial t} + (\vec{q} \cdot \vec{\nabla}) C = D_M \nabla^2 C + \frac{D_M K_T}{T_M} \nabla^2 T + R_c$$

Equation of state as per Boussinesq approximation:

$$\rho_\infty = \rho \left[1 + \beta (T - T_\infty) + \bar{\beta} (C - C_\infty) \right]$$

where

\vec{q} denotes fluid velocity vector

\vec{B} denotes the magnetic flux density

σ denotes electrical conductivity

\vec{E} denotes electrical field

\vec{J} denotes the current density

μ_e denotes magnetic permeability

η denotes magnetic diffusivity

ρ denotes fluid density

\vec{F} denotes external force per unit volume

p denotes pressure

μ denotes coefficient of viscosity

K^* denotes permeability of the medium

C_p denotes specific heat at constant pressure

T denotes fluid temperature

κ denotes thermal conductivity

$\bar{\phi}$ denotes viscous dissipation of energy per unit volume

Q denotes heat source/sink

\vec{q}_r denotes radiation heat flux vector

D_M denotes mass diffusivity

C_s denotes concentration susceptibility

C denotes molar species concentration

T_M denotes mean fluid temperature

R_C denotes rate of molar production of species per unit mass by chemical reaction

β denotes volumetric coefficient of thermal expansion

$\bar{\beta}$ denotes volumetric coefficient of solutal expansion

1.14 Boundary Conditions

The boundary conditions of a flow of an incompressible viscous electrically conducting fluid through a porous medium in the presence of a transverse magnetic field are:

- i. The fluid does not slip at the boundary.
- ii. $T = 0$ or $T = T_w$ or $\left(\frac{\partial T}{\partial y}\right)_{y=0}$ is constant.
- iii. $C = 0$ or $C = C_w$ or $\left(\frac{\partial C}{\partial y}\right)_{y=0}$ is constant.
- iv. $T \rightarrow T_\infty$ at a large distance from the boundary (i.e., far away from the plate).
- v. $C \rightarrow C_\infty$ at a large distance from the boundary (i.e., far away from the plate).

1.15 Dimensions of some some important physical quantities

<u>Fundamental Quantity</u>	<u>Dimension</u>
Mass	M
Length	L
Time	T
Temperature	K
Electric current	A
Amount of substance	mol

<u>Derived Quantity</u>	<u>Dimension</u>
Magnetic flux density	$\mathbf{M^1L^0T^{-2}A^{-1}}$
Specific heat at constant pressure	$\mathbf{M^0L^2T^{-2}K^{-1}}$
Chemical molecular mass diffusivity	$\mathbf{M^0L^2T^{-1}}$
Pressure	$\mathbf{M^1L^{-1}T^{-2}}$
Permeability	$\mathbf{M^0L^2T^0}$
Molar species concentration	$\mathbf{M^0L^{-3}T^0mol^1}$
Acceleration due to gravity	$\mathbf{M^0L^1T^{-2}}$
Velocity	$\mathbf{M^0L^1T^{-1}}$
Convective rate of mass transfer per unit area (Mass flux)	$\mathbf{M^0L^{-2}T^{-1}mol^1}$
Convective rate of heat transfer per unit area (Heat flux)	$\mathbf{M^1L^0T^{-3}K^0}$
Viscosity	$\mathbf{M^1L^{-1}T^{-1}}$

Kinematic Viscosity	$M^0 L^2 T^{-1}$
Volumetric coefficient of thermal expansion	$M^0 L^0 T^0 K^{-1}$
Volumetric coefficient of thermal expansion	$M^0 L^3 T^0 \text{mol}^{-1}$
Thermal diffusivity	$M^0 L^2 T^{-1} K^0$
Density	$M^1 L^{-3} T^0$
Shear stress	$M^1 L^{-1} T^{-2}$
Thermal conductivity	$M^1 L^1 T^{-3} K^{-1}$
Electrical conductivity	$M^1 L^{-3} T^3 A^2$

1.16 Dimensional Analysis and Non- Dimensional Quantities

A physical equation is nothing but the relationship between more than one physical quantity. For any equation expressing a physical relationship between quantities to be correct, it must be dimensionally homogeneous and numerically equivalent. By dimensional homogeneity, we mean that every term in an equation when reduced to fundamental dimensions must contain identical powers of each dimension. A dimensionally homogeneous equation can be applied to all systems of units. Dimensional analysis is the mathematical technique of obtaining the equations that govern certain natural or physical unknown phenomenon by balancing the fundamental dimensions such as, mass, length, time and temperature. Every physical phenomenon can be expressed by equations giving a relationship between dimensional and non – dimensional quantities. By incorporating dimensional variables to non – dimensional parameters, dimensional analysis helps us to determine a systematic arrangement of the variables present in the physical relationship. This analysis uses the dimensions of pertinent variables affecting the phenomenon and it is based on the principle of dimensional homogeneity. Dimensional analysis has the utmost importance in analyzing fluid flow problems. This method can be applied to all types of heat and mass flow problems as well as to many other problems of thermodynamics and fluid mechanics.

The equation produced by dimensional analysis also contains some non – dimensional numbers. Using this method, the dimensionless parameters are found without knowing the governing equations. Instead, the pertinent variables are collected and combined to get the maximum number of independent non – dimensional parameters. The complete set of pertinent variables must be known and no irrelevant variables can be introduced, else ways, the determinative set of dimensionless parameters may be meaningless. These non – dimensional numbers are very significant in numerous engineering phenomenons, as it empowers the researchers to analyze the behaviour of problems of the same type provided the linear dimensions are geometrically similar. There are many non – dimensional parameters associated with different flow configurations. Some of them are discussed below:

1.16.1 Reynolds Number

Reynolds number (Re) is a non- dimensional quantity that is used to predict similar flow patterns in different-size fluid flow situations. The concept of this number was initiated by Irish physicist George Gabriel Stokes (1819-1903) in 1851. However, this number was popularized by another Irish fluid dynamist Osborne Reynolds (1842-1912) by examining its behavior. Thus in his honor, the number is named after him. Reynolds number is the ratio of inertia force to viscous force. Mathematically, it is defined as-

$$Re = \frac{\rho UL}{\mu} = \frac{UL}{\nu}$$

where ρ, μ and ν are the density , dynamic viscosity and kinematic viscosity of the fluid respectively and U is the characteristic velocity and L is the characteristic length.

From the definition, it is observed that for large Reynolds numbers, inertia forces are dominant while viscous forces are more significant in the case of small Reynolds numbers. That is, the higher value of Re , the greater will be the relative contribution of the inertia effect; and the smaller value of Re , the greater will be the relative magnitude of the viscous stresses. Reynolds number is also used to predict the changeover from laminar flow to turbulent flow. In the case of laminar flow, the Reynolds number is less than 2300, whereas, for turbulent flow, the Reynolds number exceeds 4000. Reynolds number lying between 2300 and 4000 indicates a transition of fluid flow from laminar to turbulent. Reynolds number is also used as an important criterion of kinematic and dynamic similarities in forced convection heat transfer.

1.16.2 Prandtl Number

For a given fluid flow, the Prandtl number (Pr) is the measure of the relative effectiveness of momentum and thermal energy by diffusion. This number is used to control the relationship between the velocity and temperature distribution of the fluid. It is named after German physicist Ludwig Prandtl. Mathematically, it can be written as

$$Pr = \frac{\mu C_p}{\kappa} = \frac{\nu}{\alpha}$$

where μ is the dynamic viscosity, ν is the kinematic viscosity, κ is the thermal conductivity, C_p is the specific heat at constant pressure, and α is the thermal diffusivity of the medium. Thermal diffusivity estimates the rate of propagation of heat through the medium.

Hence for gases with $Pr \approx 1$, the transfer of momentum and energy by the diffusion process are comparable. For oils with $Pr \gg 1$, the momentum diffusion is much greater than the energy diffusion; whereas in liquids with $Pr \ll 1$ and it indicates that the momentum diffusion rate is very slow than that of energy diffusion. Thus, the Prandtl number is a connecting link between the velocity field and temperature field and its value strongly influences the relative growth of velocity and thermal boundary layers.

1.16.3 Magnetic Prandtl Number

The ratio of momentum diffusivity to magnetic diffusivity in a fluid flow is termed as the Magnetic Prandtl number (Pm). This dimensionless number has the utmost importance when we consider the effect of the induced magnetic field in a hydromagnetic flow. Mathematically, it is defined as

$$Pm = \frac{\nu}{\eta}$$

where ν is the kinematic viscosity and η is the magnetic diffusivity.

1.16.4 Schmidt Number

The ratio of momentum diffusivity to mass diffusivity in a fluid flow is termed as Schmidt number (Sc). It was named after German engineer Ernst Heinrich Wilhelm Schmidt (1892-1975). Mathematically it is defined as

$$Sc = \frac{\nu}{D_M}$$

where D_M is the mass diffusivity of the fluid and ν is the kinematic viscosity of the fluid.

Thus Schmidt number is used to measure the relative effectiveness of momentum and mass transport by diffusion in a fluid medium, for a given fluid flow consisting of convective mass transfer. Apparently, Schmidt number manages the relationship between the velocity and the molar species concentration profile for the fluid flow. It distinguishes convective mass transfer in the same manner as the Prandtl number characterizes convective heat transfer.

1.16.5 Thermal Grashof Number

The ratio of thermal buoyancy force to the viscous force acting on a fluid flow is termed as Thermal Grashof number (Gr). It was named after German engineer Franz Grashof (1826 - 1893). Mathematically, the thermal Grashof number is defined as

$$Gr = \frac{\beta g L^3 (\Delta T)}{\nu}$$

where β is the volumetric coefficient of thermal expansion, g is the acceleration due to gravity, L is the characteristic length, ν is the kinematic viscosity and ΔT is some suitable reference temperature difference .

Thermal Grashof number bears great importance in heat transfer by natural convection where buoyancy force is the only driving force. In free convection, a transition from laminar to turbulent flow can be indicated by assigning critical values to the thermal Grashof number together with the Reynolds number (Re) as follows-

- The combined effects of free and forced convection must be considered if $\frac{Gr}{Re^2} \approx 1$.
- Forced convection is negligible if $\frac{Gr}{Re^2} \gg 1$.
- Free convection is negligible if $\frac{Gr}{Re^2} \ll 1$.

Here, volumetric coefficient of thermal expansion (β) is a thermodynamic property of the fluid that provides a measure of the amount by which the density changes in response to a

change in temperature at constant pressure. Density gradients originating from these temperature differences are solely responsible for free convective heat transfer.

1.16.6 Solutal Grashof Number

The ratio of solutal buoyancy force to the viscous force acting on a fluid flow is termed as the Solutal Grashof number (Gm). Mathematically, it is defined as-

$$Gm = \frac{\bar{\beta} g L^3 (\Delta C)}{\nu}$$

where $\bar{\beta}$ is the volumetric coefficient for solutal expansion, g is the acceleration due to gravity, L is the characteristic length, ν is the kinematic viscosity and ΔC is some suitable reference molar species concentration difference.

Solutal Grashof number bears great importance in free convection flows involving mass transfer where buoyancy force is the only driving force. Here, the volumetric coefficient of solutal expansion ($\bar{\beta}$) is a thermodynamic property of the fluid that provides a measure of the amount by which the density changes due to a variation of species concentration at constant pressure. Density gradients occurring from these concentration differences initiate free convective heat transfer.

1.16.7 Magnetic Parameter

The ratio of electromagnetic forces to inertial forces is termed as the magnetic parameter. This number is also called the Stuart number or magnetic interaction parameter. Mathematically, it is defined as

$$M = \frac{\sigma B_0^2 L}{\rho U}$$

where σ is the electrical conductivity of the fluid medium, B_0 is an applied magnetic field component, ρ is the fluid density, L is the characteristic length and U is the characteristic velocity. Depending on the particular flow problem and other dimensionless substitutions, the choice of M may be made conveniently.

In some hydromagnetic flow problems, we encounter another non-dimensional quantity called the Hartmann number (Ha). It is nothing but the square root of the product of the magnetic parameter with Reynolds number (Re). Mathematically, it is defined as-

$$Ha = \sqrt{M \cdot Re} = B_0 L \sqrt{\frac{\sigma}{\nu \rho}}$$

1.16.8 Soret Number

Soret number (Sr) is a non-dimensional number which is proportional to the quotient of the temperature gradient to the concentration gradient. Mathematically, it is defined as-

$$Sr = \frac{D_T (\Delta T)}{\nu \Delta C}$$

where ν is kinematic viscosity, D_T is molar thermal diffusivity and ΔT and ΔC are some suitable reference temperature gradient and concentration gradient respectively.

1.16.9 Dufour Number

Dufour number (Sr) is a dimensionless number that is proportional to the quotient of the concentration gradient to the temperature gradient. Mathematically, it is defined as-

$$Du = \frac{D_M K_T (\Delta C)}{C_s C_p \nu (\Delta T)}$$

where ν is kinematic viscosity, D_M is molar mass diffusivity, C_s denotes concentration susceptibility, C_p denotes specific heat at constant pressure and ΔT and ΔC are some suitable reference temperature gradient and concentration gradient respectively.

1.17 Laplace Transform Technique

Laplace transform technique is a special type of integral transform technique. French Mathematician Marquis Pierre-Simon Laplace (1749-1827) initiated this technique. However, this technique was methodically extended by the British mathematician and physicist Oliver Heaviside (1850-1925), to simplify the solution of various types of differential equations that govern physical phenomena. This method is frequently used by electric engineers to attain solutions to various electronic circuit problems. Applications of this technique can be

observed in fields related to flow and transport phenomena (Fluid Mechanics, Thermodynamics, etc.), wave propagation and acoustics, Geophysics, Celestial Mechanics etc. This transform technique is widely used in problems dealing with impulsively started flow. This method is also applicable for flow problems consisting of small Reynolds number, (i.e., for slow motion or creeping motion). The solutions obtained by using the Laplace transform technique are generally exact or of closed form. Therefore it does not require stability analysis for checking of validation.

1.17.1 Definition of Laplace Transform:

Suppose, $F(t)$ is a function of t for $t > 0$. Then, the Laplace transformation of $F(t)$, denoted by $L\{F(t)\}$ or $f(s)$ is defined as

$$L\{F(t)\} = f(s) = \int_0^{\infty} e^{-st} F(t) dt$$

1.17.2 Some Important Properties of Laplace Transform

- i. First shifting or translation property

$$\text{If } L\{F(t)\} = f(s), \text{ then } L\{e^{at} F(t)\} = f(s-a)$$

- ii. Second shifting or translation property

$$\text{If } L\{F(t)\} = f(s) \text{ and } G(t) = \begin{cases} F(t-a), & t > a \\ 0, & t < a \end{cases}, \text{ then } L\{G(t)\} = e^{-as} f(s)$$

- iii. Change of scale property

$$\text{If } L\{F(t)\} = f(s), \text{ then } L\{F(at)\} = \frac{1}{a} f\left(\frac{s}{a}\right)$$

- iv. Laplace transform of derivatives

$$\text{If } L\{F(t)\} = f(s), \text{ then}$$

$$L\{F'(t)\} = sf(s) - F(0) \text{ and } L\{F''(t)\} = s^2 f(s) - sF(0) - F'(0)$$

- v. Division by t

$$\text{If } L\{F(t)\} = f(s), \text{ then } L\left\{\frac{F(t)}{t}\right\} = \int_0^{\infty} f(u) du$$

1.17.3 Definition of inverse Laplace transform:

If the Laplace transform of a function $L\{F(t)\}$ is $f(s)$, i.e., $L\{F(t)\} = f(s)$, then $F(t)$ is called the inverse Laplace transform of $f(s)$ and symbolically, it is written as $F(t) = L^{-1}\{f(s)\}$. Here, L^{-1} is called the inverse Laplace transform operator.

1.17.4 Some Important Properties of Inverse Laplace Transform

i. First shifting or translation property

$$\text{If } L^{-1}\{f(s)\} = F(t), \text{ then } L^{-1}\{f(s-a)\} = e^{at}F(t)$$

ii. Second shifting or translation property

$$\text{If } L^{-1}\{f(s)\} = F(t), \text{ then } L^{-1}\{e^{-as}f(s)\} = \begin{cases} F(t-a), t > a \\ 0, t < a \end{cases}$$

iii. Change of scale property

$$\text{If } L^{-1}\{f(s)\} = F(t), \text{ then } L^{-1}\{f(as)\} = \frac{1}{a}F\left(\frac{t}{a}\right)$$

iv. Division by s

$$\text{If } L^{-1}\{f(s)\} = F(t), \text{ then } L^{-1}\left\{\frac{f(s)}{s}\right\} = \int_0^t F(u)du$$

v. Inverse Laplace transform of derivatives

$$\text{If } L^{-1}\{f(s)\} = F(t), \text{ then } L^{-1}\{f^{(n)}(s)\} = L^{-1}\left\{\frac{d^n}{ds^n}f(s)\right\} = (-1)^n t^n F(t)$$

vi. The convolution property

$$\text{If } L^{-1}\{f(s)\} = F(t) \text{ and } L^{-1}\{g(s)\} = G(t), \text{ then}$$

$$L^{-1}\{f(s)g(s)\} = \int_0^t F(u)G(t-u)du$$

1.17.5 Heaviside's Unit Step Function, Error Function, and Complementary Error Function

Heaviside's unit step function is defined by

$$H(t-t_1) = \begin{cases} 1, t > t_1 \\ 0, t < t_1 \end{cases}.$$

The error function is defined as

$$\operatorname{erf}(t) = \frac{2}{\sqrt{\pi}} \int_0^t e^{-u^2} du .$$

The complementary error function is defined as

$$\operatorname{erfc}(t) = 1 - \operatorname{erf}(t) = 1 - \frac{2}{\sqrt{\pi}} \int_0^t e^{-u^2} du = \frac{2}{\sqrt{\pi}} \int_t^{\infty} e^{-u^2} du .$$

1.17.6 Some Properties of Error Function and Complementary Error Function

- i. $\operatorname{erf}'(0) = \frac{2}{\sqrt{\pi}}$
- ii. $\operatorname{erfc}'(0) = -\frac{2}{\sqrt{\pi}}$
- iii. $\operatorname{erf}(0) = 0$
- iv. $\operatorname{erfc}(0) = 1$
- v. $\operatorname{erf}(x) + \operatorname{erf}(-x) = 0$
- vi. $\operatorname{erfc}(x) + \operatorname{erfc}(-x) = 2$
- vii. $\operatorname{erfc}(x) - \operatorname{erfc}(-x) = -2\operatorname{erf}(x)$
- viii. $\operatorname{erfc}'(z) = -\frac{2e^{-z^2}}{\sqrt{\pi}}$
- ix. $\operatorname{erf}'(z) = \frac{2e^{-z^2}}{\sqrt{\pi}}$
- x. $\operatorname{erfc}'(z) + \operatorname{erfc}'(-z) = -4\sqrt{\frac{1}{\pi}}e^{-z^2}$

1.17.7 Bar Function

Let $f(x_1, x_2, x_3, \dots, x_k, y, t)$ be an arbitrary real-valued function of the variables

$x_1, x_2, x_3, \dots, x_k, y, t$. Then, the bar function of $f(x_1, x_2, x_3, \dots, x_k, y, t)$ is denoted by

$\bar{f}(x_1, x_2, x_3, \dots, x_k, y, t)$ and is defined as

$$\bar{f}(x_1, x_2, x_3, \dots, x_k, y, t) = f(x_1, x_2, x_3, \dots, x_k, y, t - t_1)H(t - t_1)$$

where $H(t-t_1)$ is the Heaviside's unit step function defined earlier.

1.17.8 Properties of Bar Function

- i. $\Delta f = f - \bar{f}$
- ii. $\Delta(\lambda f + \mu g) = \lambda \Delta f + \mu \Delta g$, where λ, μ are constants and f, g are arbitrary real-valued functions.

1.18 Review of Relevant Literature

(a) MHD Convective Flows Past Flat Plates and Boundary Layer Theory:

The introductory work in the field of magnetohydrodynamics (MHD) was made by Faraday (1832), Maxwell (1864), Hertz (1884, 1888, 1962), Ampere, Coulomb, Gauss and Lorentz (1952). But it was Hannes Alfvén (1942), whose pioneering contribution to the field of MHD earned him Nobel Prize for physics in 1970. MHD is in present form due to remarkable contributions by many researchers like Cowling (1976), Shercliff (1965), Roberts (1967), Pai (1962), Hughes and Young (1966), Sutton and Sherman (1965), Ferraro and Plumpton (1966), Lehnert (1952), Creamer and Pai (1973), etc.

The study of convective magnetohydrodynamic flow over or cooled or heated plates become one of the fundamental problems of research owing to its enormous practical applications. Several researchers have investigated MHD free convective flows of viscous incompressible fluids past a flat plate under different physical and geometrical conditions. Several authors contributed to it out of which Glauert (1956), Greenspan and Carrier (1959), Meksyn (1962), Davies (1963), Tan and Wang (1968), Pop (1967, 1969), Sattar and Alam (1994), Das (1970), Gulab and Mishra (1977), Afzal (1972), Soundalgekar (1969, 1970, 1973, 1975, 1979), Revankar (1983), Devi and Nagaraj (1984), Devi et al. (1988), Elbashleshy (1997), Raptis and Perdikis (2006), Raptis and Singh (1983), Singh and Chand (2000), Acharya et al. (2000), Alam et al. (2006), Das et al. (2008), Afify (2009), Ahmed and Sarmah (2009), Ahmed and Dutta (2014), Gundagani et al. (2013), etc. are worth mentioning.

Famous mathematician and aerodynamicist James Lighthill (1950, 1954) initiated the studies related to the effects of external unsteady fluctuations for two-dimensional time dependent flows. It should be noted that the flow along a very thin flat plate is the simplest example of application of the boundary layer equations. After the initiation of Boundary layer

theory by Prandtl (1904), his doctoral scholar Blasius (1908) extensively investigated about this theory. After that several researchers made significant contributions to this field. Some of them are Lighthill (1963), Langlois (1964), Schlichting (1968), Sherman (1990), Young (1989), Veldman (1976), Wiedemann and Gersten (1984), Schlichting and Gersten (2004), Ingham(1978) etc.

(b) MHD Heat and Mass Transfer Flow with or without Radiation, Chemical Reaction, Heat Absorption/ Generation and Induced Magnetic Field

The study of incompressible and convective flows involving heat and mass transfer have become subject of great enthusiasm to many researchers due to their applications in many branches of physical science, chemical science, engineering and technology, Geophysics, Astrophysics etc. Fourier (1822) formulated the law of heat conduction while the law of mass diffusion was given by Fick (1855). Significant works in the field of heat and mass transfer were done by Nusselt (1915,1931), Glasstone et al. (1941), Brinkman (1947a,1947b), Jakob (1949), de Groot (1951), McAdams (1954), Hirschfelder et al. (1954), Crank (1957), Knudsen and Katz (1958), Bird (1960), Rohsenow and Choi (1961), Romig (1961), Grober et al. (1961), Spalding (1963), Boelter et al. (1965), Luikov and Mikhailov (1965), Bird et al. (1966), Reid and Sherwood (1966), Treybal (1968), Welty et al. (1969), Patankar and Spalding (1970), Gebhart (1971), Turner (1973), Welty (1974), Skelland (1974), Kays (1975), Sherwood et al. (1975), Ozisik (1977), Jaluria (1980), Thomas (1980), Vedhanayagam et al. (1980), Incropera and Dewitt (1981), Kaviany (1995), Kafoussias and Williams (1995), Camargo et al.(1996), Harries and Ingham (1997), Streeter et al. (1998), Baehr and Stephan (1998), Mills (1999),Wilkinson (2000), Schlichting and Gersten (2004), Choudhary and Jain (2007), Parida et al. (2011), Gurram et al. (2018), Poddar et al. (2021) etc.

Chemical reaction effect draws attention of numerous researchers to work in this field due to its enormous practical significance in many industrial, technological and natural processes. Some researchers who have considered the case chemical reaction in MHD flow problems are Devi and Kandaswamy (2000), Alam et al. (2006), Ibrahim et al. (2008), Swain et al. (2017), Aboeldahab and Azzam (2006), Seddeek et al. (2007), Rajaiah et al. (2015), Sehra et al. (2021), Nayak et al. (2014) etc.

Radiative convective flows can be observed in many environmental and industrial phenomenons. This type of flow takes pivotal role in space technology and high temperature processes. It is also used in polymer processing industry. Influencing by the importance of

applications, many researchers have carried out model research on free convection in many hydrodynamic and magnetohydrodynamic flow problems with thermal radiation effect under different physical and geometrical circumstances. Some of them are Muthucumaraswamy and Kumar (2004), Seth et al. (2011), Seth and Sarkar (2015), Raptis (2017), Das (2011), Manivannan et al. (2009), Eswaramoorthi et al. (2015), Ali et al. (2021), Choudhary et al. (2015), Kumar and Kumar (2017), Abdullah et al. (2019) etc.

Effects of heat absorption/ generation carry great importance in many chemical processes as well as in renewable energy systems. Chamka (2004), Seth et al. (2015), Olajuwon and Oahimire (2014), Turkyilmazoglu (2019), Reddy and Makinde (2022), Reddy et al. (2023) etc. are some authors who extensively studied heat absorption/ generation effect in different MHD flow models.

In order to simplify the mathematical analysis of a flow problem, many researchers neglect the effect of induced magnetic field. However, in various physical situations where the intensity of the imposed magnetic field is very high, it is necessary to consider this effect to validate the mathematical model. Some authors who studied this effect on different MHD flow models are Denno and Fouad (1972), Singh and Singh (2000), Ghosh et al. (2010), Jha and Aina (2018), Goud et al. (2021), Suneetha et al. (2021), Ahmed (2023) etc.

(c) Flows Through Porous Media:

The study of flow through porous media is a subject of great importance. Movement of water and oil inside the earth, filtering of water using sand or other porous material, movement of blood through cells etc. are some examples of this type of flow. Its applications can be observed in many processes related to chemistry and chemical engineering such as chromatography, adsorption, filtration, absorption, flow in packed columns, reactor engineering, ion exchange, and so on. The investigations of flow problems through porous media are based on Darcy's experimental law (1856). Later, this law was modified by Brinkman (1947a, 1947b) and Wooding (1957) and it is used by several investigators to study convective flows through porous media. Significant research regarding flows through porous media were also done by Terill and Shrestha (1965a,1965b), Pop and Ingham (1969a,1969b,1969c,1969d), Ahmadi and Manvi (1971), Bear (1972), Yamanoto and Iwamura (1976), Bejan (1978), Raptis et al. (1981a,1981b), Megahed (1984), Qin and Kaloni (1992), Singh et al. (1993), Tobbal and Bennacer(1998), Jain and Gupta (2005), Xu et

al.(2005), Zueco (2008), Xie et al.(2012), Nield and Bejan (2017), Wu and Xu (2022), Sahoo et al. (2022), Joshna et al. (2022) etc.

(d) Flows with Thermal Diffusion and Diffusion Thermo Effects:

In combined heat and mass transfer processes, density difference in the fluid mixture works as the driving force. However, this variation can occur due to both temperature gradient as well as concentration gradient. The mass flux initiated by a temperature gradient is called as Soret effect or thermal diffusion effect. Though this effect was theoretically investigated by C. Ludwing in 1859, the first experimental work on this effect was performed by Charles Soret in 1879. On the other hand, the energy flux caused by concentration differences is termed as Dufour effect or diffusion-thermo effect. L. Dufour was the first to observe this effect in 1873. These two effects have great application in many chemical and industrial processes. Eckert and Drake (1972) made significant investigation on these effects. Realizing the importance of these effects on fluid flows, comprehensive analysis was done by Alam and Rahman (2005), Sharma (2005), Ferdows et al. (2008), Ferdows and Chen (2009), Cheng C. Y. (2009,2011,2012a,2012b,2012c), Murthy and Narayana (2010), Olanrewaju and Makinde (2011), Makinde (2011), El-Kabeir (2011), El-Kabeir et al. (2011), Zaib and Shafie (2014), Vedavathi et al.(2015), Mahdy and Ahmed (2015), Sharma, P.K. (2015), Yabo et al. (2016), Khan et al. (2016), Zhao et al. (2016), Niranjana et al. (2017), Sarma and Ahmed (2022a, 2022b) etc.

1.19 Some Common Functions Often Used in the Thesis

- i.
$$\psi(\xi, \eta, y, t) = \frac{1}{2} \left[e^{\sqrt{\xi}\eta y} \operatorname{erfc} \left(\frac{y}{2} \sqrt{\frac{\xi}{t}} + \sqrt{\eta t} \right) + e^{-\sqrt{\xi}\eta y} \operatorname{erfc} \left(\frac{y}{2} \sqrt{\frac{\xi}{t}} - \sqrt{\eta t} \right) \right]$$
- ii.
$$\Psi(\xi, \eta, \zeta, y, t) = e^{\zeta t} \psi(\xi, \eta + \zeta, y, t)$$
- iii.
$$P(\eta, y, t) = \frac{\eta y}{2\sqrt{\pi t^3}} e^{-\frac{\eta^2 y^2}{4t}}$$
- iv.
$$K(\eta, y, t) = 2\sqrt{\frac{t}{\pi}} e^{-\frac{\eta^2 y^2}{4t}} - \eta y \operatorname{erfc} \left(\frac{\eta y}{2\sqrt{t}} \right)$$
- v.
$$\Omega(\xi, \eta, t) = - \left[\sqrt{\frac{\xi}{\pi t}} e^{-\eta t} + \sqrt{\xi \eta} \operatorname{erf}(\sqrt{\eta t}) \right]$$
- vi.
$$\Lambda(\xi, \eta, t) = -\eta \left[\sqrt{\frac{1}{\pi t}} e^{-\xi t} + \sqrt{\xi} \operatorname{erf}(\sqrt{\xi t}) \right]$$

- vii. $Z(\xi, \eta, \zeta, t) = e^{\zeta t} \Omega(\xi, \eta + \zeta, t)$
- viii. $\alpha(\xi) = -\frac{2\xi}{\sqrt{\pi}}$
- ix. $I(\eta, t) = \frac{\eta}{2\sqrt{\pi t^{\frac{3}{2}}}}$
- x. $G(y, t) = \frac{1}{24} \left[(y^4 + 12y^2t + 12t^2) \operatorname{erfc}\left(\frac{y}{2\sqrt{t}}\right) - 2y(y^2 + 10t) \sqrt{\frac{t}{\pi}} e^{-\frac{y^2}{4t}} \right]$
- xi. $\lambda(\xi, y, t) = t \left[\left(1 + \frac{y^2\xi}{2t}\right) \operatorname{erfc}\left(\frac{\sqrt{\xi}y}{2\sqrt{t}}\right) - y \sqrt{\frac{\xi}{\pi t}} e^{-\frac{\xi y^2}{4t}} \right]$
- xii. $f(\xi, \eta, y, t) = \left(\frac{t}{2} + \frac{y}{4} \sqrt{\frac{\xi}{\eta}}\right) e^{\sqrt{\xi\eta}y} \operatorname{erfc}\left(\frac{y}{2} \sqrt{\frac{\xi}{t}} + \sqrt{\eta t}\right) + \left(\frac{t}{2} - \frac{y}{4} \sqrt{\frac{\xi}{\eta}}\right) e^{-\sqrt{\xi\eta}y} \operatorname{erfc}\left(\frac{y}{2} \sqrt{\frac{\xi}{t}} - \sqrt{\eta t}\right)$
- xiii. $\varphi(\xi, \eta, y, t) = e^{\sqrt{\xi\eta}y} \operatorname{erfc}\left(\frac{y}{2} \sqrt{\frac{\xi}{t}} + \sqrt{\eta t}\right) - e^{-\sqrt{\xi\eta}y} \operatorname{erfc}\left(\frac{y}{2} \sqrt{\frac{\xi}{t}} - \sqrt{\eta t}\right)$
- xiv. $\Upsilon(\xi, \eta, y, t) = -\frac{y\sqrt{\xi t}}{4\eta\sqrt{\pi}} e^{-\left(\frac{\xi y^2}{4t} + \eta t\right)}$
- xv. $\omega(\xi, \eta, y, t) = \frac{\left(\frac{\xi y^2}{4t} + \eta t\right)t}{2\eta} \psi(\xi, \eta, y, t) + \frac{y(4\eta t - 1)\sqrt{\xi}}{16\eta\sqrt{\eta}} \varphi(\xi, \eta, y, t) + \Upsilon(\xi, \eta, y, t)$
- xvi. $\zeta(\eta, t) = -\frac{4\eta t\sqrt{t}}{3\sqrt{\pi}}$
- xvii. $\nu(\eta, t) = -2\sqrt{\frac{\eta t}{\pi}}$
- xviii. $\Phi(\xi, \eta, t) = -\left[\sqrt{\frac{\xi}{4\eta}} \operatorname{erf}\left(\sqrt{\eta t}\right) + t\sqrt{\xi\eta} \operatorname{erf}\left(\sqrt{\eta t}\right) + \sqrt{\frac{t\xi}{\pi}} e^{-\eta t} \right]$
- xix. $\Theta(\xi, \eta, t) = \frac{t^2}{2} \Omega(\xi, \eta, t) - \frac{(4\eta t - 1)\sqrt{\xi}}{8\eta\sqrt{\eta}} \operatorname{erf}\left(\sqrt{\eta t}\right) - \frac{\sqrt{\xi t}}{4\eta\sqrt{\pi}} e^{-\eta t}$
- xx. $m(y, t) = 2\sqrt{\frac{t}{\pi}} e^{-\frac{y^2}{4t}} - y \operatorname{erfc}\left(\frac{y}{2\sqrt{t}}\right)$

- xxi. $n(y, t) = \frac{\sqrt{t} e^{-\frac{y^2}{4t}(4t+y^2)}}{3\sqrt{\pi}} - \frac{1}{6} y(6t+y^2) \operatorname{erfc}\left(\frac{y}{2\sqrt{t}}\right)$
- xxii. $l(\xi, \eta, y, t) = \frac{\sqrt{\xi} y e^{-\eta - \frac{\xi y^2}{4t}}}{2\sqrt{\pi t}^{3/2}}$
- xxiii. $h(\xi, y, t) = \frac{1}{2} \left[e^{\sqrt{\xi} y} \operatorname{erfc}\left(\frac{y}{2\sqrt{t}} + \sqrt{\xi t}\right) + e^{-\sqrt{\xi} y} \operatorname{erfc}\left(\frac{y}{2\sqrt{t}} - \sqrt{\xi t}\right) \right]$
- xxiv. $r(\xi, y, t) = \frac{1}{2} \left[\left(t + \frac{y}{2\sqrt{\xi}} \right) e^{\sqrt{\xi} y} \operatorname{erfc}\left(\frac{y}{2\sqrt{t}} + \sqrt{\xi t}\right) + \left(t - \frac{y}{2\sqrt{\xi}} \right) e^{-\sqrt{\xi} y} \operatorname{erfc}\left(\frac{y}{2\sqrt{t}} - \sqrt{\xi t}\right) \right]$
- xxv. $q(\xi, y, t) = \frac{y e^{-\xi t - \frac{y^2}{4t}}}{2\sqrt{\pi t}^{3/2}}$
- xxvi. $T(\xi, \eta, t) = \frac{\sqrt{\xi} e^{-\eta}}{2\sqrt{\pi t}^{3/2}}$
- xxvii. $N(\xi, t) = - \left[\sqrt{\xi} \operatorname{erf}(\sqrt{\xi t}) + \frac{1}{\sqrt{\pi t}} e^{-\xi t} \right]$
- xxviii. $O(\xi, t) = - \left[\left(\frac{2}{\sqrt{\xi}} + \sqrt{\xi t} \right) \operatorname{erf}(\sqrt{\xi t}) + \sqrt{\frac{t}{\pi}} e^{-\xi t} \right]$
- xxix. $Y(\xi, t) = \frac{e^{-\xi t}}{2\sqrt{\pi t}^{3/2}}$
- xxx. $F(y, t) = t \left[\left(1 + \frac{y^2}{2t} \right) \operatorname{erfc}\left(\frac{y}{2\sqrt{t}}\right) - \frac{y}{\sqrt{\pi t}} e^{-\frac{y^2}{4t}} \right]$
- xxxi. $W(t) = t \left(1 - \frac{2}{\sqrt{\pi}} - \frac{1}{\sqrt{\pi t}} \right)$
- xxxii. $R(\xi, t) = 2\sqrt{\frac{t}{\pi}} - 1$

CHAPTER II

Thermal Diffusion and Thermal Radiation Effects on Free Convective MHD Radiating Flow Past an Impulsively Started Infinite Vertical Plate

(In Press for publication in Proceeding in Springer)

2.1 Introduction

MHD is a branch of physics, which is concerned with the motion of electrically conducting fluids in presence of magnetic field. The study of the interaction of magnetic field and the fluid velocity of conducting fluid falls under the purview of MHD. MHD principles find it's applications in Astrophysics, missile technology, space science cosmology, medical science etc. The scopes of applications of convection problems pertaining to electrically conducting fluid in presence of magnetic field have received much attention in recent years. Alfven (1942), Cowling (1957), Shercliff (1965), Ferraro and Plumpton (1966) and Crammer and Pai (1973) are the authors whose contributions lead MHD to take its present form.

The change in fluid temperature as well as species concentration results in a density variation in fluid mixture, which in turn produces buoyancy force that acts on the fluid. The flow caused merely due to buoyancy force is termed as natural or free convective flow. The process of heat transfer or mass transfer in this type of flow is called natural convection or free convection.

Radiation is also a mode of heat transfer through electromagnetic waves. Convective flows with thermal radiation occur in several industrial and environment processes. Due to importance of applications of thermal radiation in different heat and mass transfer problems, a large number of authors have carried out model studies on free convection in different hydrodynamic and hydro magnetic flows taking into account the thermal radiation effect, under various physical and geometrical conditions. Mbeledogu et al. (2007) studied unsteady free convection flow of a compressible fluid past a moving vertical plate considering the effect of radiation. Makinde (2005) and Samad and Rahman (2006) analysed free convection flow past a moving vertical porous plate taking thermal radiation and mass transfer into consideration. Orhan and Ahmet (2008) investigated radiation effect on MHD mixed convection flow about a permeable vertical plate. Prasad et al. (2006) discussed transient radiative hydro-magnetic free convection flow past an impulsively started vertical plate while Ahmed and Dutta (2014) extended this work considering ramped wall temperature effect. Seth et al. (2017) considered MHD double diffusive natural convection flow over exponentially accelerated inclined plate.

The relations connecting the fluxes and driving potentials are of a more intricate in nature, when both thermal and solutal convections appear simultaneously in fluid motion. It

is observed that, a mass flux can be caused not only by the composition gradient but by temperature gradient as well. The effect of mass flux under temperature gradient, or the flow characteristics is termed as thermal-diffusion effect or Soret effect. The experimental investigation of this effect was first carried out in laboratory by the renowned chemist Charles Soret in 1879. The Soret effect is relevant to isotope separation in mixtures of gases with a very light molecular weight like H_2 and He . Comprehensive literature on various aspects of Soret effect on different types of mass transfer problems can be found in the book of Eckert and Drake (1972). Kafoussias and Williams (1995) considered both Soret and Dufour effects on mixed convective boundary layer flow with temperature dependent viscosity while Postelnicu (2004) expanded this work in porous medium. Ahmed (2010) and Ahmed and Sengupta (2011) examined Soret and Dufour effects in a three dimensional MHD convective flow past an infinite vertical porous plate. Ahmed (2012) examined thermal diffusion and radiation effects on transient MHD free convection from an impulsively started infinite vertical plate.

In many works on MHD, a little attention is given to the effects caused by the induced magnetic field. In most of the cases, the induced magnetic field is neglected on assumption that, for most of the natural gases, the electrical conductivity is quite low and as a consequence the magnetic Reynolds number becomes very small. But when a high speed missile travels through the earth's atmosphere, a huge amount of heat is generated due to the friction of the gas molecules and this frictional heat may at times be so great as to ionize the gas in the surrounding air, near the stagnation point. The ionized gas in this stagnation region is electrically conducting. That is a magnetic field may be applied to it in order to induce an electromagnetic force in the air, which in turn affects the motion. Thus certain gases having low electrical conductivity may be good conductors under same physical conditions. It is recalled that the magnetic Reynolds number is the ratio of the induced magnetic field to the applied magnetic field. Thus, even though the magnetic Reynolds number is quite small, but the intensity of the imposed magnetic field is very high, the complete omission of the induced magnetic field is not fully justified. Realizing the importance of the induced hydro-magnetic effects on flows of electrically conducting fluids, several researchers have studied MHD flow problems under diverse physical and geometrical conditions. Singh and Singh (2000) analysed MHD effects on heat and mass transfer in flow of viscous fluid with induced magnetic field. Chaudhury and Sharma (2006) explored heat and mass transfer effects by

laminar mixed convection flow from a vertical surface with induced magnetic field while Hossain and Khatun (2012) extended this work taking Dufor effect into account.

Investigation on the effect of chemical reaction on heat and mass transfer in a flow is of great practical significance to the researchers owing to its nearly universal occurrence and wide scope of applications in many branches of engineering science. Many researchers have investigated the effect of chemical reaction on various mass transport flow problems. Apelblat (1982) studied combined effects of mass transfer, chemical reaction of first order and axial diffusion. Andersson et al. (1994) considered diffusion of a chemically reactive species from a stretching sheet. Muthucumaraswamy and Ganesar (2001) investigated the effect of chemical reaction and injection in an unsteady upward motion of an isothermal plate. Kandasamy et al. (2005) studied exclusively the effects of chemical reaction and heat and mass transfer along a wedge with heat source and concentration in the presence of suction or injection.

As the present authors are aware, no attempt has been made till date to study the problem of a free convective MHD radiating flow past an impulsively started infinite vertical plate taking into account the effects of thermal diffusion and induced magnetic field. Such an attempt has been in the present work.

2.2 Mathematical Analysis

The governing equations of the motion of an electrically conducting chemically reacting and radiating fluid in presence of a magnetic field having constant mass diffusivity and thermal diffusivity taking into account of diffusion- thermo effect are

Continuity equation (based on law of conservation of mass and Newton's 2nd law of motion)

$$\vec{\nabla} \cdot \vec{q} = 0 \quad (2.1)$$

Magnetic field continuity equation

$$\vec{\nabla} \cdot \vec{B} = 0 \quad (2.2)$$

Ampere's law

$$\vec{\nabla} \times \vec{B} = \mu_e \vec{J} \quad (2.3)$$

Momentum equation (based on law of conservation of linear momentum)

$$\rho \left[\frac{\partial \vec{q}}{\partial t} + (\vec{q} \cdot \nabla) \vec{q} \right] = -\nabla p + \rho \vec{g} + \vec{J} \times \vec{B} + \mu \nabla^2 \vec{q} \quad (2.4)$$

Energy equation (based on law of conservation of energy)

$$\rho C_p \left[\frac{\partial T}{\partial t} + (\vec{q} \cdot \nabla) T \right] = \kappa \nabla^2 T - \nabla \cdot \vec{q}_r + \alpha (T_\infty - T) \quad (2.5)$$

Species continuity equation (based on law of conservation of species)

$$\frac{\partial C}{\partial t} + (\vec{q} \cdot \nabla) C = D_M \nabla^2 C + D_T \nabla^2 T + \bar{K} (C_\infty - C) \quad (2.6)$$

Magnetic diffusion equation with small magnetic Reynolds number

$$\frac{\partial \vec{B}}{\partial t} = \eta \nabla^2 \vec{B} \quad (2.7)$$

Equation of state

$$\rho_\infty = \rho \left[1 + \beta (T - T_\infty) + \bar{\beta} (C - C_\infty) \right] \quad (2.8)$$

All the physical quantities are defined in the list of symbols.

Suppose we consider an unsteady free convective MHD mass transfer flow of a viscous incompressible electrically conducting optically thick non-Gray fluid past a suddenly started semi- infinite vertical plate in presence of a transverse magnetic field taking into account the diffusion- thermo effect.

In order to idealize the mathematical model, the present investigation is restricted to the following constraints-

- I. All the fluid properties are constants except the variation in density in the buoyancy force term.
- II. The viscous dissipations of energy are negligible.
- III. The magnetic Reynolds number is small.
- IV. The plate is electrically non- conducting.

- V. The radiation heat flux in the direction of the plate velocity is negligible in comparison to that in the normal direction.
- VI. The flow is parallel to the plate.
- VII. No external electric field is applied for which the polarization voltage is negligible.
- VIII. The chemical reaction is of first order and homogeneous.
- IX. The temperature and concentration fields are independent of the distance parallel to the surface.

Initially, the plate and the surrounding fluid were at the same temperature T_∞ with concentration level C_∞ at all points of the fluid. At time $\bar{t} > 0$, the plate is suddenly moved in its own plane with speed U_0 . The plate temperature and concentration are instantly raised to T_w ($T_w > T_\infty$) and C_w ($C_w > C_\infty$) which are thereafter maintained constant.

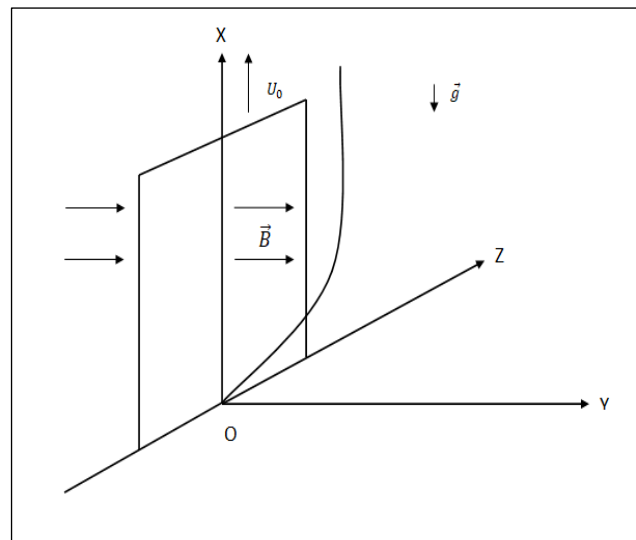


Figure 2.1: Flow Diagram

We introduce a rectangular Cartesian co- ordinate system $(\bar{x}, \bar{y}, \bar{z})$ with X - axis vertically upwards, Y - axis normal to the plate directed into the fluid region, Z - axis along the width of the plate. Let $\vec{q} = (u', 0, 0)$ be the fluid velocity, $\vec{B} = (B_x', B_0, 0)$ be the magnetic induction vector and $\vec{q}_r = (0, q_r, 0)$ be the radiation heat flux at the point $(\bar{x}, \bar{y}, \bar{z}, \bar{t})$ in the fluid.

Equation (2.1) gives

$$\frac{\partial u'}{\partial \bar{x}} = 0$$

$$\text{i.e., } u' = u'(\bar{y}, \bar{t}) \quad (2.9)$$

Equation (2.2) gives

$$\frac{\partial B'_x}{\partial \bar{x}} = 0$$

$$\text{i.e., } B'_x = B'_x(\bar{y}, \bar{t}) \quad (2.10)$$

Equation (2.4) reduces to

$$\rho \left[\frac{\partial u'}{\partial \bar{t}} + \left(u' \frac{\partial}{\partial \bar{x}} \right) u' \hat{i} \right] = -\hat{i} \frac{\partial p}{\partial \bar{x}} - \hat{j} \frac{\partial p}{\partial \bar{y}} - \rho g \hat{i} + B_0 \eta \sigma \frac{\partial B'_x}{\partial \bar{y}} \hat{i} + \mu (\nabla^2 u') \hat{i} \quad (2.11)$$

Equation (2.11) gives

$$\rho \frac{\partial u'}{\partial \bar{t}} = -\frac{\partial p}{\partial \bar{x}} - \rho g + B_0 \eta \sigma \frac{\partial B'_x}{\partial \bar{y}} + \mu \frac{\partial^2 u'}{\partial \bar{y}^2} \quad (2.12)$$

and

$$0 = -\frac{\partial p}{\partial \bar{y}} \quad (2.13)$$

Equation (2.13) shows that pressure near the plate and pressure far away from the plate is same along the normal to the plate.

For fluid region far away from the plate, equation (2.12) takes the form

$$0 = -\frac{\partial p}{\partial \bar{x}} - \rho_\infty g \quad (2.14)$$

Eliminating $\frac{\partial p}{\partial \bar{x}}$ from (2.12) and (2.14), we get

$$\rho \frac{\partial u'}{\partial \bar{t}} = (\rho_\infty - \rho) g + B_0 \eta \sigma \frac{\partial B'_x}{\partial \bar{y}} + \mu \frac{\partial^2 u'}{\partial \bar{y}^2} \quad (2.15)$$

Equation of state (2.8) gives

$$\rho_\infty - \rho = \rho \left[\beta(T - T_\infty) + \bar{\beta}(C - C_\infty) \right] \quad (2.16)$$

Putting value of (2.16) in (2.15)

$$\begin{aligned} \rho \frac{\partial u'}{\partial \bar{t}} &= \rho \left[\beta(T - T_\infty) + \bar{\beta}(C - C_\infty) \right] g + B_0 \eta \sigma \frac{\partial B'_x}{\partial \bar{y}} + \mu \frac{\partial^2 u'}{\partial \bar{y}^2} \\ \text{i.e., } \frac{\partial u'}{\partial \bar{t}} &= g \beta(T - T_\infty) + g \bar{\beta}(C - C_\infty) + \frac{B_0 \eta \sigma}{\rho} \frac{\partial B'_x}{\partial \bar{y}} + \nu \frac{\partial^2 u'}{\partial \bar{y}^2} \end{aligned}$$

The radiation heat flux as per Rosseland approximation is given by

$$\vec{q}_r = -\frac{4\sigma^*}{3\kappa^*} \nabla T^4 \quad (2.17)$$

Using (2.17), Energy equation (2.5) reduces to

$$\rho C_p \frac{\partial T}{\partial \bar{t}} = \kappa \frac{\partial^2 T}{\partial \bar{y}^2} + \frac{16\sigma^* T_\infty^3}{3\kappa^*} \frac{\partial^2 T}{\partial \bar{y}^2} + \alpha(T_\infty - T) \quad (2.18)$$

Species continuity equation (2.6) reduces to

$$\frac{\partial C}{\partial \bar{t}} = D_M \frac{\partial^2 C}{\partial \bar{y}^2} + D_T \frac{\partial^2 T}{\partial \bar{y}^2} + \bar{K}(C_\infty - C) \quad (2.19)$$

Magnetic diffusion equation (2.7) becomes

$$\frac{\partial B'_x}{\partial \bar{t}} = \eta \frac{\partial^2 B'_x}{\partial \bar{y}^2} \quad (2.20)$$

The appropriate initial and boundary conditions are

$$\left. \begin{aligned} \bar{y} \geq 0 : u' = 0, T = T_\infty, C = C_\infty, B'_x = 0; \bar{t} \leq 0 \\ \bar{y} = 0 : u' = U_0, T = T_w, C = C_w, B'_x = H_0; \bar{t} > 0 \\ \bar{y} \rightarrow \infty : u' = 0, T = T_\infty, C = C_\infty, B'_x = 0; \bar{t} > 0 \end{aligned} \right\} \quad (2.21)$$

For the sake of normalization of the mathematical model of the problem, we introduce the following non- dimensional quantities-

$$Sr = \frac{D_T(T_w - T_\infty)}{\nu(C_w - C_\infty)}, N = \frac{\kappa\kappa^*}{4\sigma^*T_\infty^3}, u = \frac{u'}{U_0}, y = \frac{\bar{y}U_0}{\nu}, t = \frac{U_0^2\bar{t}}{\nu}, Gr = \frac{\nu g\beta(T_w - T_\infty)}{U_0^3},$$

$$Gm = \frac{\nu g\bar{\beta}(C_w - C_\infty)}{U_0^3}, Pm = \frac{\nu}{\eta}, \theta = \frac{T - T_\infty}{T_w - T_\infty}, \phi = \frac{C - C_\infty}{C_w - C_\infty}, Pr = \frac{\mu C_p}{\kappa}, M = \frac{\sigma B_0^2 \nu}{\rho U_0^2}, Sc = \frac{\nu}{D_M}$$

$$K = \frac{\bar{K}\nu}{U_0^2}, B_x = \frac{B_x'}{H_0}, \Pi = \frac{H_0}{B_0}, \Lambda = 1 + \frac{4}{3N}, Q = \frac{\alpha\nu^2}{U_0^2\kappa}$$

The non-dimensional non-dimensional governing equations are

$$Pm \frac{\partial B_x}{\partial t} = \frac{\partial^2 B_x}{\partial y^2} \quad (2.22)$$

$$Pr \frac{\partial \theta}{\partial t} = \Lambda \frac{\partial^2 \theta}{\partial y^2} - Q\theta \quad (2.23)$$

$$Sc \frac{\partial \phi}{\partial t} = \frac{\partial^2 \phi}{\partial y^2} + SrSc \frac{\partial^2 \theta}{\partial y^2} - ScK\phi \quad (2.24)$$

$$Pm \frac{\partial u}{\partial t} = PmGr\theta + PmGm\phi + M\Pi \frac{\partial B_x}{\partial y} + Pm \frac{\partial^2 u}{\partial y^2} \quad (2.25)$$

The initial and boundary conditions becomes

$$\left. \begin{array}{l} \forall y \geq 0 : u = 0, \theta = 0, \phi = 0, B_x = 0; t \leq 0 \\ y = 0 : u = 1, \theta = 1, \phi = 1, B_x = 1; t > 0 \\ y \rightarrow \infty : u = 0, \theta = 0, \phi = 0, B_x = 0; t > 0 \end{array} \right\} \quad (2.26)$$

2.3 Method of Solution

Taking Laplace transform of the equations from (2.22) to (2.25) and applying the conditions (2.26), we get the following governing equations-

$$\frac{d^2 \bar{B}_x}{dy^2} - Pm.s \bar{B}_x = 0 \quad (2.27)$$

$$\Lambda \frac{d^2 \bar{\theta}}{dy^2} - (Pr.s + Q) \bar{\theta} = 0 \quad (2.28)$$

$$\frac{d^2\bar{\phi}}{dy^2} - Sc(K+s)\bar{\phi} = -SrSc\frac{d^2\bar{\theta}}{dy^2} \quad (2.29)$$

$$Pm\frac{d^2\bar{u}}{dy^2} + PmGr\bar{\theta} + PmGm\bar{\phi} + M\Pi\frac{d\bar{B}_x}{dy} = Pm.s\bar{u} \quad (2.30)$$

subject to the initial and boundary conditions

$$\left. \begin{aligned} y=0: \bar{u} &= \frac{1}{s}, \bar{\theta} = \frac{1}{s}, \bar{\phi} = \frac{1}{s}, \bar{B}_x = \frac{1}{s} \\ y \rightarrow \infty: \bar{u} &= 0, \bar{\theta} = 0, \bar{\phi} = 0, \bar{B}_x = 0 \end{aligned} \right\} \quad (2.31)$$

Solving the equations from (2.27) to (2.30) subject to the conditions (2.31) and taking inverse Laplace transform of the solutions, the expressions for the induced magnetic field B_x , temperature field θ , concentration field ϕ , and velocity field u are as follows-

$$B_x = \operatorname{erfc}\left(\frac{y\sqrt{Pm}}{2\sqrt{t}}\right) \quad (2.32)$$

$$\theta = \psi_1 \quad (2.33)$$

$$\phi = \psi_2 + \xi_1 - \xi_2 \quad (2.34)$$

$$u = \begin{cases} u_{1,1} + u_{1,2} + u_{1,3} + u_{1,4}; Pm \neq 1, Sc \neq 1, Pr \neq \Lambda \\ u_{2,1} + u_{2,2} + u_{2,3} + u_{2,4}; Pm = 1, Sc \neq 1, Pr \neq \Lambda \\ u_{3,1} + u_{3,2} + u_{3,3} + u_{3,4}; Pm \neq 1, Sc = 1, Pr \neq \Lambda \\ u_{4,1} + u_{4,2} + u_{4,3} + u_{4,4}; Pm \neq 1, Sc \neq 1, Pr = \Lambda \\ u_{5,1} + u_{5,2} + u_{5,3} + u_{5,4}; Pm = 1, Sc = 1, Pr \neq \Lambda \\ u_{6,1} + u_{6,2} + u_{6,3} + u_{6,4}; Pm = 1, Sc \neq 1, Pr = \Lambda \\ u_{7,1} + u_{7,2} + u_{7,3} + u_{7,4}; Pm \neq 1, Sc = 1, Pr = \Lambda \\ u_{8,1} + u_{8,2} + u_{8,3} + u_{8,4}; Pm = 1, Sc = 1, Pr = \Lambda \end{cases} \quad (2.35)$$

2.4 Nusselt Number

The heat flux q^* at the plate $\bar{y} = 0$ is obtained by Fourier's law of conduction is given by

$$q^* = -\kappa_0^* \left. \frac{\partial T}{\partial \bar{y}} \right]_{\bar{y}=0} \quad (2.36)$$

where $\kappa_0^* = \kappa + \frac{16\sigma^* T_\infty^3}{3\kappa^*}$ is the modified thermal conductivity.

Equation (2.36) yields

$$Nu = -\left. \frac{\partial \theta}{\partial y} \right]_{y=0} \quad (2.37)$$

where $Nu = \frac{q^* \nu}{\kappa_0^* U_0 (T_w - T_\infty)} = \frac{q^* \nu}{\kappa \Lambda (T_w - T_\infty) U_0}$ is called the Nusselt number which is concerned with the rate of heat transfer at the plate.

Equation (2.37) gives,

$$Nu = -\Omega_1 \quad (2.38)$$

2.5 Sherwood Number

The mass flux M_w at the plate $\bar{y} = 0$ is specified by Fick's law of diffusion is given by

$$M_w = -D_M \left. \frac{\partial C}{\partial \bar{y}} \right]_{\bar{y}=0} \quad (2.39)$$

Equation (2.39) gives

$$Sh = -\left. \frac{\partial \phi}{\partial y} \right]_{y=0} \quad (2.40)$$

In (2.40), $Sh = \frac{\nu M_w}{D_M (C_w - C_\infty)}$ is called the Sherwood number which is associated with the rate of mass transfer at the plate.

Equation (2.40) yields

$$Sh = -(\Omega_2 + \Lambda_1 - \Lambda_2) \quad (2.41)$$

2.6 Skin Friction

The viscous drag at the plate $\bar{y} = 0$ is determined by Newton's law of viscosity is given by

$$\bar{\tau} = -\mu \left. \frac{\partial u}{\partial y} \right]_{\bar{y}=0} \quad (2.42)$$

Equation (2.42) gives

$$\tau = -\left. \frac{\partial u}{\partial y} \right]_{y=0} \quad (2.43)$$

In (2.43), $\tau = \frac{\nu \bar{\tau}}{\mu U_0^2}$ is called the skin friction or coefficient of friction which is associated with the rate of momentum transfer at the plate.

Equation (2.43) yields,

$$\tau = - \begin{cases} \tau_{1,1} + \tau_{1,2} + \tau_{1,3} + \tau_{1,4}; Pm \neq 1, Sc \neq 1, Pr \neq \Lambda \\ \tau_{2,1} + \tau_{2,2} + \tau_{2,3} + \tau_{2,4}; Pm = 1, Sc = 1, Pr \neq \Lambda \\ \tau_{3,1} + \tau_{3,2} + \tau_{3,3} + \tau_{3,4}; Pm \neq 1, Sc = 1, Pr \neq \Lambda \\ \tau_{4,1} + \tau_{4,2} + \tau_{4,3} + \tau_{4,4}; Pm \neq 1, Sc \neq 1, Pr = \Lambda \\ \tau_{5,1} + \tau_{5,2} + \tau_{5,3} + \tau_{5,4}; Pm = 1, Sc = 1, Pr \neq \Lambda \\ \tau_{6,1} + \tau_{6,2} + \tau_{6,3} + \tau_{6,4}; Pm = 1, Sc \neq 1, Pr = \Lambda \\ \tau_{7,1} + \tau_{7,2} + \tau_{7,3} + \tau_{7,4}; Pm \neq 1, Sc = 1, Pr = \Lambda \\ \tau_{8,1} + \tau_{8,2} + \tau_{8,3} + \tau_{8,4}; Pm = 1, Sc = 1, Pr = \Lambda \end{cases} \quad (2.44)$$

2.7 Results and Discussion

In order to study the effects of the physical parameters involved in the problem on the flow and transport characteristics numerical calculations for induced magnetic field, temperature field, concentration field, velocity field, skin friction, Nusselt number, Sherwood number at the plate are carried out by assigning some specific values to the parameters and variables.

The numerically computed results are displayed graphically from Figures 2.2 to 2.19

Figure 2.2 and Figure 2.3 represent the variations of induced magnetic field versus normal co- ordinate y under magnetic Prandtl number Pm and time t . Figure 2.2 shows that there is a steady fall in induced magnetic field for increasing magnetic Prandtl number. This is due to the fact that increasing magnetic Prandtl number decreases magnetic diffusivity and consequently induced magnetic field loses its strength significantly. As time progresses,

induced magnetic field increases as it is reflected in Figure 2.3. Both figures uniquely establish the fact that the induced magnetic field falls asymptotically from its maximum value at $y = 0$ to its minimum value as $y \rightarrow \infty$.

Figures 2.4 to 2.6 represent the variations of temperature field versus normal coordinate y under Prandtl number Pr , time t , and heat absorption parameter Q . Figure 2.4 shows that there is a steady fall in temperature field for increasing Prandtl number. Increasing Prandtl number reduces thermal boundary layer and as a result heat diffuses quickly. Thus, temperature field reduces to a considerable extent. As time progresses, temperature field increases as it is reflected in Figure 2.5. It is informed from Figure 2.6 that the fluid temperature gets decreased significantly as the heat absorption parameter increases. When absorbed, heat weakens the inner- particle bond of the fluid and as a result temperature reduces as expected. From these figures, we can conclude that the temperature field falls asymptotically from its maximum value at $y = 0$ to its minimum value as $y \rightarrow \infty$.

Figures 2.7 to 2.10 represent the variations of concentration field versus normal coordinate y under Prandtl number Pr , time t , chemical reaction parameter K and Schmidt number Sc . Figure 2.7 shows that there is a steady rise in concentration field for increasing Prandtl number. It gives us an idea that higher thermal diffusivity lowers concentration field. Concentration field keeps increasing trend with time which is reflected in Figure 2.8. Figure 2.9 exhibits that there is a considerable decrement in temperature field for increasing chemical reaction parameter K . Higher chemical reaction parameter suggests that chemical substances of the fluid consumed rapidly and consequently concentration reduces. Figure 2.10 admits that concentration field gets lowered as the values of Schmidt number increases. It establishes the fact that increasing mass diffusivity results in a rise the concentration field. From these figures, we can conclude that the concentration field falls asymptotically from its maximum value at $y = 0$ to its minimum value as $y \rightarrow \infty$.

Figures 2.11 to 2.15 focus the variations of velocity field versus normal coordinate y under Soret number Sr , solutal Grashof number Gm , thermal Grashof number Gr , time t and heat absorption parameter Q . Figure 2.11 show that fluid velocity decreases with increasing values of Soret number. This gives us an idea that higher molar thermal diffusivity reduces the fluid velocity. Figure 2.12 admits that velocity hikes with increasing values of solutal Grashof number. Figure 2.13 shows that upsurge of thermal Grashof number increases the fluid velocity. Figure 2.12 and Figure 2.13 uniquely establish the fact that both solutal and

thermal buoyancy force hike fluid velocity. As time progresses, velocity hikes as it is reflected in Figure 2.14. Figure 2.15 indicates that increasing values of heat absorption parameter declines the fluid velocity. When heat is absorbed, inter particle bonds of the fluid weaken, and kinetic energy is lost. As a result motion of the fluid is retarded.

Figure 2.16 and Figure 2.17 represent the variations of Nusselt number versus time t under Prandtl number Pr and heat absorption parameter Q . Figure 2.16 shows that there is a steady rise in Nusselt number for increasing Prandtl number. This is because enhancement of molar thermal diffusivity lowers the rate of heat transfer from the plate to the fluid. Figure 2.17 depicts that Nusselt number keep on increasing for increasing values of heat absorption parameter. This is obvious that faster chemical consumption produces heat and it is transferred from plate to the fluid rapidly.

Figure 2.18 and Figure 2.19 represent the variations of Sherwood number versus time t under Prandtl number Pr and Soret number Sr . Figure 2.18 exhibit that there is a steady rise in Sherwood number for increasing Prandtl number. This gives us an idea that higher molar thermal diffusivity lowers the rate of mass transfer from the plate to the fluid. Figure 2.19 depicts that there is a comprehensive rise in Sherwood number for increasing values of Soret number. So, high temperature gradient compared to concentration gradient speed up rate of mass transfer.

Figure 2.20 and Figure 2.21 depict the variations of skin friction versus time t under thermal Grashof number Gr and Soret number Sr . Figure 2.20 shows that there is a comprehensive rise in Sherwood number for ascending Prandtl number. This is due to the fact that thermal buoyancy force has a tendency to increase rate of momentum transfer from the plate to the fluid. Figure 2.21 reveals that increasing Soret number hikes coefficient of friction. Thus, high temperature gradient rapidly hikes the rate of momentum transfer.

2.8 Comparison of Result

To check the accuracy of our result, we have compared one of our results with Ahmed and Sarmah (2009) who considered the thermal radiation effect on a transient MHD flow with mass transfer past an impulsively fixed infinite vertical plate. In absence of Soret effect and chemical reaction effect (i.e., $Sr=0$ and $K=0$), expression of concentration field of the present problem is

$$\phi = \operatorname{erfc}(\eta\sqrt{Sc})$$

where $\eta = \frac{y}{2\sqrt{t}}$

Figure 2.22 and Figure 2.23 display the concentration field versus η graphs for different Schmidt number obtained by Ahmed and Sarmah (2009) and present authors respectively. Both figures uniquely expresses the fact that concentration field declines for ascending values of Schmidt number. Hence, an excellent agreement of results between present authors and Ahmed and Sarmah (2009) is observed.

2.9 Conclusions

The key motive of the present investigation is to study exclusively the effects of radiation, heat absorption, chemical reaction, induced magnetic field and thermal diffusion effect of an unsteady MHD flow past a. Study of flow and transport properties under the action of different parameters was carried out with help of graphs. The major outcomes of the present work are as follows:

- i. Induced magnetic field falls for higher magnetic Prandtl number.
- ii. Increasing Prandtl number lowers temperature field.
- iii. Concentration field decreases as Schmidt number increases.
- iv. Higher solutal Grashof number hikes velocity field in a thin fluid layer adjacent to the plate and thereafter its behaviour takes a reverse turn.
- v. Nusselt number and Sherwood number decreases for small time and thereafter become stationary.
- vi. Increasing Soret number upsurges skin friction.

The solution of the present work also validates with the previous result obtained by Ahmed and Sarmah (2009) in particular case.

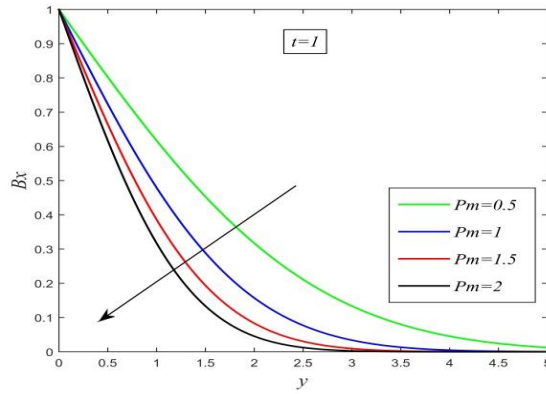


Figure 2.2: Induced magnetic field versus y for different Pm and $t=1$

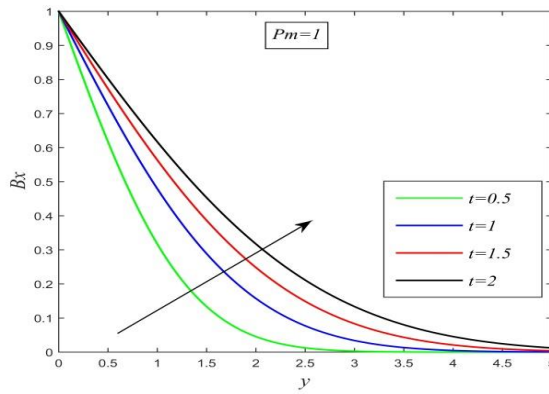


Figure 2.3: Induced magnetic field versus y for different t and $Pm=0.71$

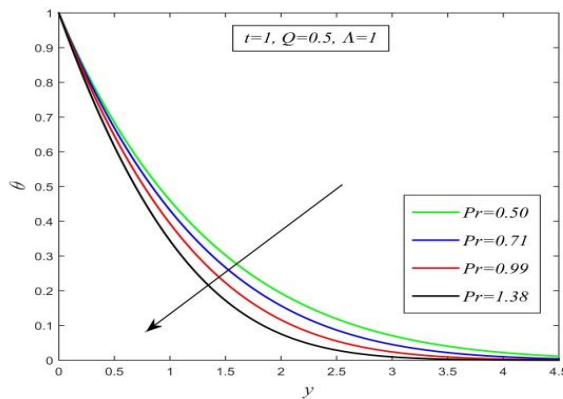


Figure 2.4: Temperature field versus y for different Pr and $t=1, Q=0.5, \Lambda=1$

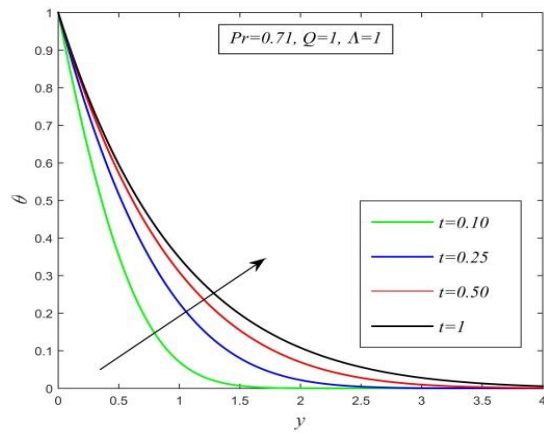


Figure 2.5: Temperature field versus y for different t and $Pr=0.71$, $Q=1$, $\Lambda=1$

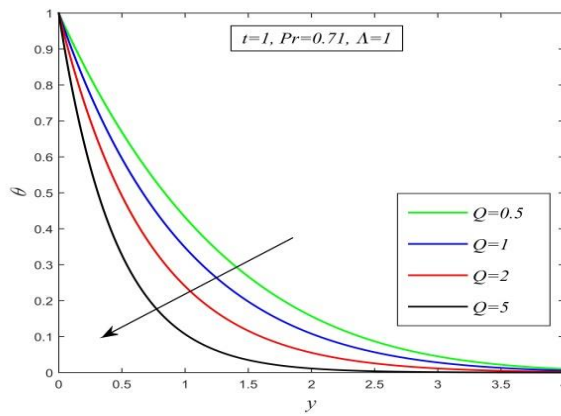


Figure 2.6: Temperature field versus y for different Q and $t=1$, $Pr=0.71$, $\Lambda=1$

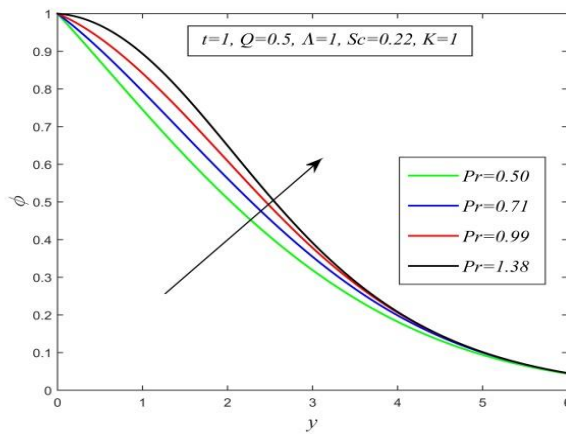


Figure 2.7: Concentration field versus y for different Pr and $t=1$, $Q=0.5$, $\Lambda=1$, $Sc=0.22$, $K=1$

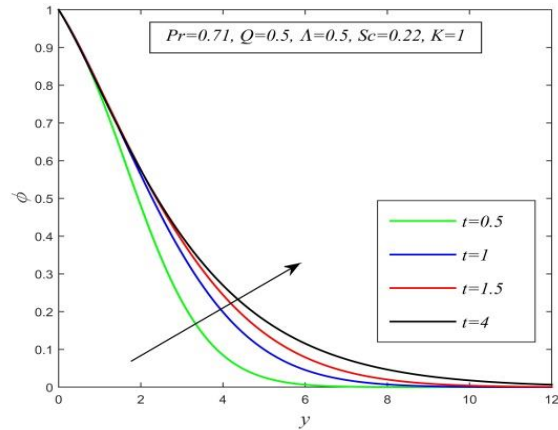


Figure 2.8: Concentration field versus y for different t and $Pr=0.71, Q=0.5, \Lambda=0.5, Sc=0.22, K=1$

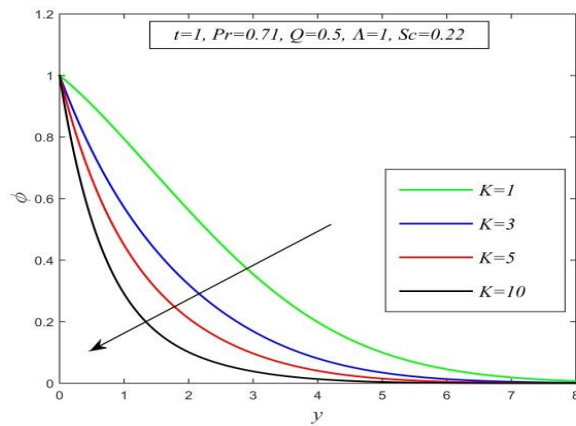


Figure 2.9: Concentration field versus y for different K and $t=1, Pr=0.71, Q=0.5, \Lambda=1, Sc=0.22$

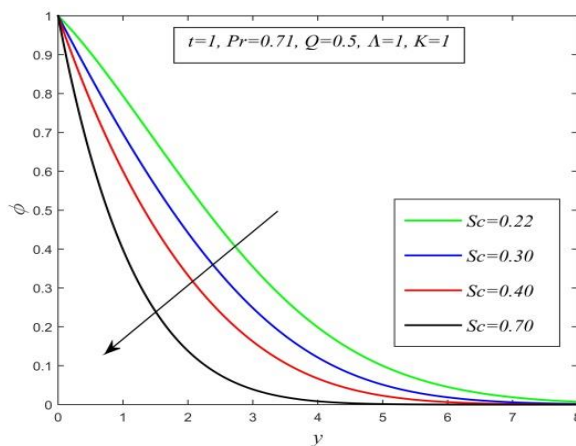


Figure 2.10: Concentration field versus y for different Sc and $t=1, Pr=0.71, Q=0.5, \Lambda=1, K=1$

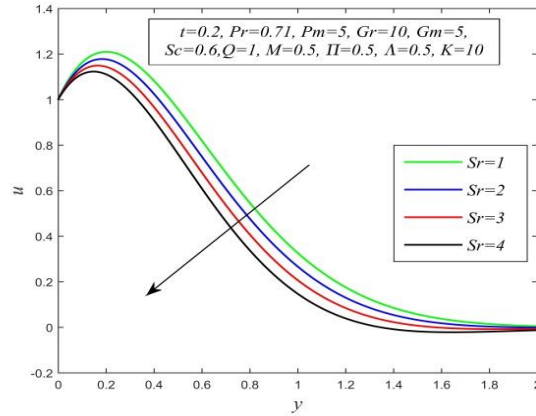


Figure 2.11: Velocity field versus y for different Sr and $t=0.2$, $Pr=0.71$, $Pm=5$, $Gr=10$, $Gm=5$, $Sc=0.6$, $Q=1$, $M=0.5$, $\Pi=0.5$, $\Lambda=0.5$, $K=10$

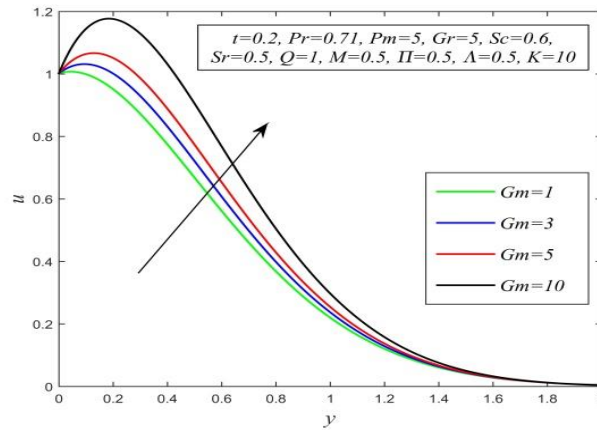


Figure 2.12: Velocity field versus y for different Gm and $t=0.2$, $Pr=0.71$, $Pm=5$, $Gr=5$, $Sc=0.6$, $Sr=0.5$, $Q=1$, $M=0.5$, $\Pi=0.5$, $\Lambda=0.5$, $K=10$

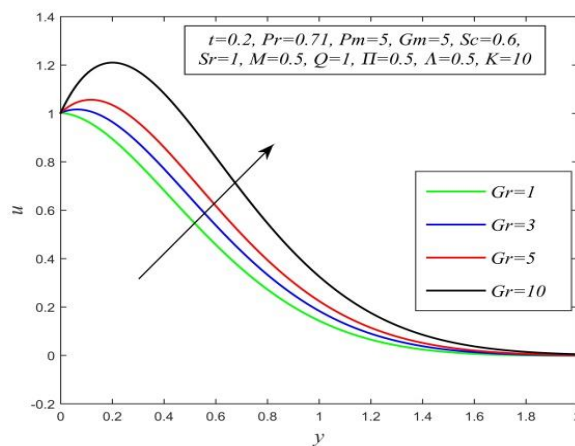


Figure 2.13: Velocity field versus y for different Gr and $t=0.2$, $Pr=0.71$, $Pm=5$, $Gm=5$, $Sc=0.6$, $Sr=1$, $Q=1$, $M=0.5$, $\Pi=0.5$, $\Lambda=0.5$, $K=10$

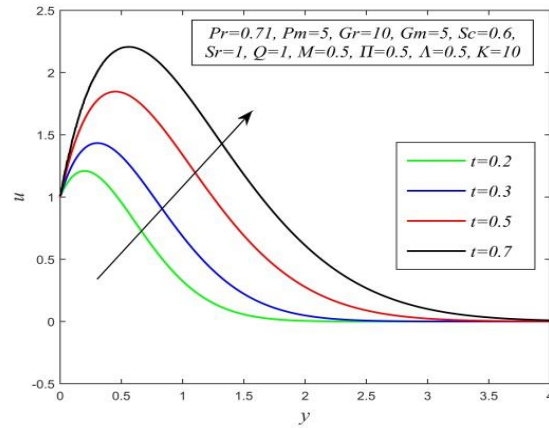


Figure 2.14: Velocity field versus y for different t and $Pr=0.71$, $Pm=5$, $Gr=10$, $Gm=5$, $Sc=0.6$, $Sr=1$, $Q=1$, $M=0.5$, $II=0.5$, $\Lambda=0.5$, $K=10$

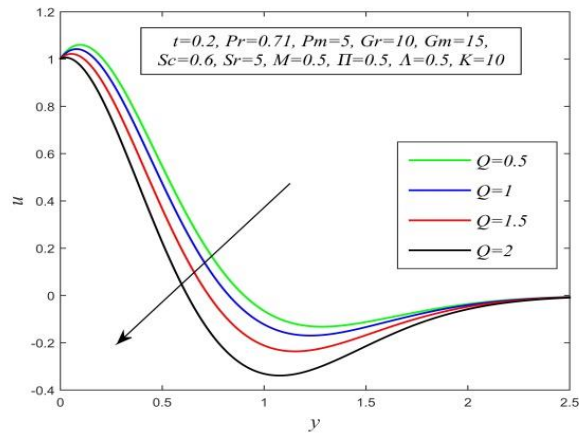


Figure 2.15: Velocity field versus y for different Q and $t=0.2$, $Pr=0.71$, $Pm=5$, $Gr=10$, $Gm=15$, $Sc=0.6$, $Sr=5$, $M=0.5$, $II=0.5$, $\Lambda=0.5$, $K=10$

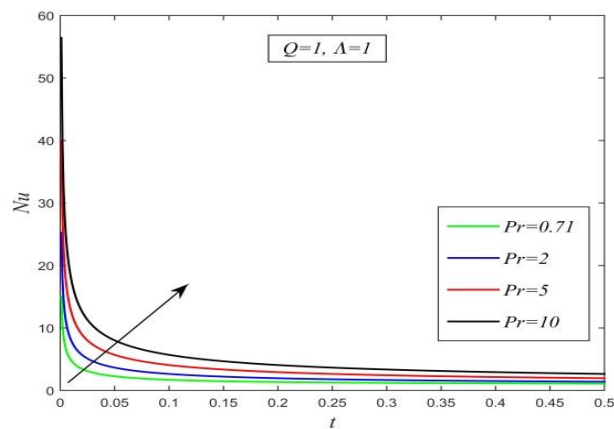


Figure 2.16: Nusselt number versus t for different Pr and $Q=1$, $\Lambda=1$

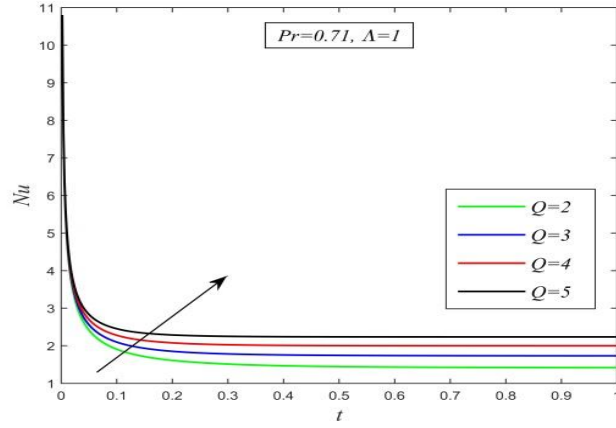


Figure 2.17: Nusselt number versus t for different Q and $Pr=0.71, \Lambda=1$

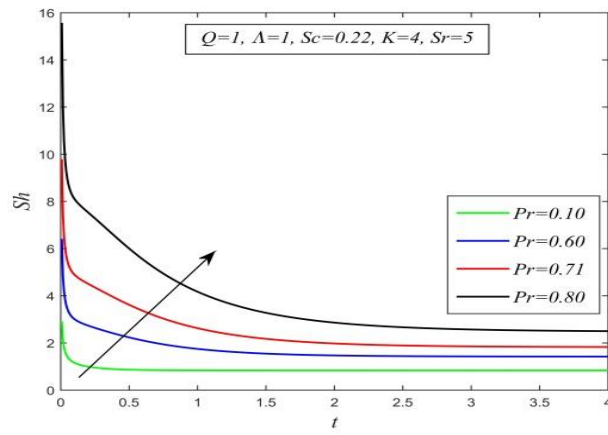


Figure 2.18: Sherwood number versus t for different Pr and $Q=1, \Lambda=1, Sc=0.22, K=4, Sr=5$

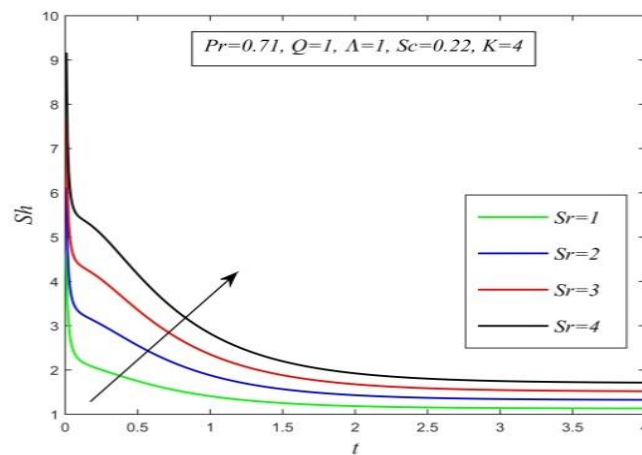


Figure 2.19: Sherwood number versus t for different Sr and $Pr=0.71, Q=1, \Lambda=1, Sc=0.22, K=4$

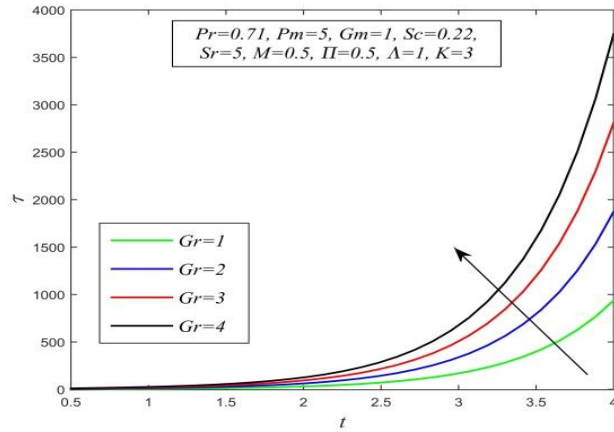


Figure 2.20: Skin friction versus t for different Gr and $Pr=0.71, Pm=5, Gm=1, Sr=5, M=0.5, II=0.5, A=1, Sc=0.22, K=3$

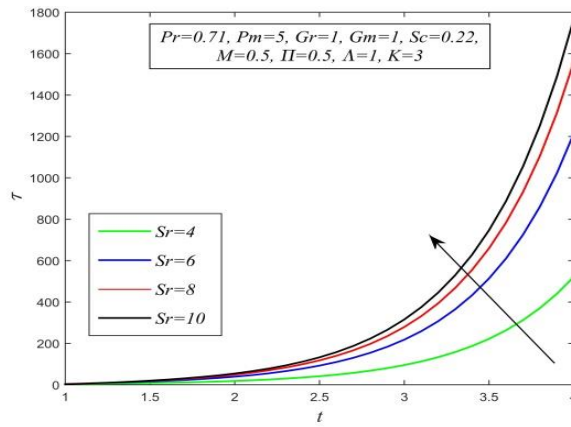


Figure 2.21: Skin friction versus t for different Sr and $Pr=0.71, Pm=5, Gr=1, Gm=1, M=0.5, II=0.5, A=1, Sc=0.22, K=3$

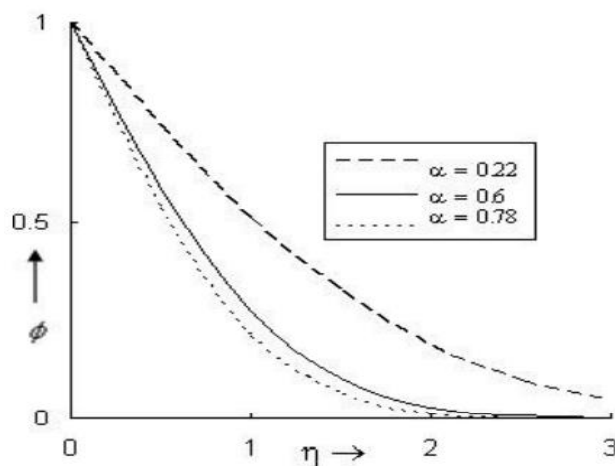


Figure 2.22: Scanned graph of concentration field versus η for different Schmidt number α drawn by Ahmed and Sarmah (2009)

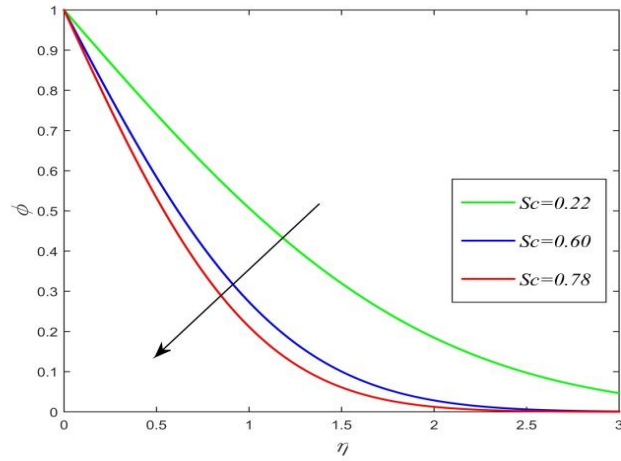


Figure 2.23: Concentration field versus η for different Schmidt number Sc drawn by present author

Nomenclature:

\vec{B} : Magnetic flux density

B_0 : Strength of the applied magnetic field

B_x' : Induced magnetic field

C : Molar species concentration

C_p : Specific heat at constant pressure

C_∞ : Concentration far away from the plate

C_w : Concentration at the plate

D_M : Mass diffusivity

D_T : Molar thermal diffusivity

\vec{g} : Gravitation acceleration vector

g : Gravitational acceleration

Gr : Thermal Grashof number

Gm : Solutal Grashof number

H_0 : Induced magnetic field

\vec{J} : Current density vector

κ^* : Mean absorption constant

\bar{K} : Chemical reaction rate

K : Chemical reaction parameter

M : Magnetic parameter

N : Radiation parameter

Q : Heat absorption parameter

p : pressure

Pm : Magnetic Prandtl number

Pr : Prandtl number

\vec{q} : Fluid velocity vector

\vec{q}_r : Radiation heat flux vector

q_r : Radiation heat flux

Sc : Schmidt number

\bar{t} : time

T : Fluid temperature

T_∞ : Undisturbed temperature

u' : X-component of fluid velocity

U_0 : Plate velocity

Greek Symbols:

η : Magnetic diffusivity

μ_e : Magnetic permeability

μ : Coefficient of viscosity

σ : Electrical conductivity

σ^* : Stefan-Boltzmann constant

ρ : Fluid density

ρ_∞ : Fluid density far away from the plate

κ : Thermal conductivity

α : Heat absorption rate

β : Volumetric coefficient of thermal expansion

$\bar{\beta}$: Volumetric coefficient of solutal expansion

ν : Kinematic viscosity

Subscripts:

w : Refers to physical quantity at the plate

∞ : Refers to physical quantity far away from the plate

Appendix

$$\begin{aligned}
\psi_1 &= \psi(a_1, a_3, y, t), \psi_2 = \psi(Sc, K, y, t), \xi_1 = a_5(A_1\psi_2 + A_2\psi_3), \psi_3 = \Psi(Sc, K, -a_4, y, t), \\
\xi_2 &= a_5(A_1\psi_1 + A_2\psi_4), \psi_4 = \Psi(a_1, a_3, -a_4, y, t), a_1 = \frac{Pr}{\Lambda}, a_2 = \frac{Q}{\Lambda}, a_3 = \frac{a_2}{a_1}, a_4 = \frac{a_3 a_1 - ScK}{a_1 - Sc}, \\
a_5 &= \frac{SrSca_1}{a_1 - Sc}, A_1 = \frac{a_3}{a_4}, A_2 = \frac{a_4 - a_3}{a_4}, u_{1,1} = u_{1,1,1} + u_{1,1,2} + u_{1,1,3} + u_{1,1,4}, u_{2,1} = u_{2,1,1} + u_{2,1,2} + u_{2,1,3}, \\
u_{3,1} &= u_{3,1,1} + u_{3,1,2} + u_{3,1,3} + u_{3,1,4}, u_{4,1} = u_{4,1,1} + u_{4,1,2} + u_{4,1,3} + u_{4,1,4}, u_{5,1} = u_{5,1,1} + u_{5,1,2} + u_{5,1,3}, \\
u_{6,1} &= u_{6,1,1} + u_{6,1,2} + u_{6,1,3}, u_{7,1} = u_{7,1,1} + u_{7,1,2} + u_{7,1,3} + u_{7,1,4}, u_{8,1} = u_{8,1,1} + u_{8,1,2} + u_{8,1,3}, a_6 = \frac{a_1 a_3}{a_1 - 1}, \\
a_7 &= \frac{KSc}{Sc - 1}, E_1 = \operatorname{erfc}\left(\frac{y}{2\sqrt{t}}\right), u_{1,1,1} = E_1, A_3 = \frac{a_3}{a_4 a_6}, A_4 = \frac{a_4 - a_3}{a_4(a_4 - a_6)}, A_5 = \frac{a_6 - a_3}{a_6(a_4 - a_6)}, \\
u_{1,1,2} &= M_{1,2} = \frac{1}{1 - a_1}(\xi_3 - \xi_4), \xi_3 = Gma_5(A_3E_1 + A_4\psi_5 + A_5\psi_6), \xi_4 = \frac{Gr}{a_5}(E_1 - \psi_6), \\
\psi_5 &= \Psi(1, 0, -a_4, y, t), \psi_6 = \Psi(1, 0, -a_6, y, t), u_{1,1,3} = M_{1,3} = \frac{Gm}{Sc - 1}(\xi_5 + \xi_6), \xi_5 = \frac{1}{a_7}(E_1 - \psi_7), \\
\psi_7 &= \Psi(1, 0, -a_7, y, t), \xi_6 = a_5(B_3E_1 + B_4\psi_5 + B_5\psi_7), B_3 = \frac{a_3}{a_4 a_7}, B_4 = \frac{a_4 - a_3}{a_4(a_4 - a_7)}, B_5 = \frac{a_7 - a_3}{a_7(a_4 - a_7)}, \\
u_{1,1,4} &= M_{1,4} = P(1, y, t) \frac{M\Pi}{(1 - Pm)\sqrt{Pm}}, u_{1,2} = M_2 = \frac{1}{a_1 - 1}(Gm\xi_7 - Gr\xi_8), \xi_7 = a_5(A_3\psi_1 + A_4\psi_4 + A_5\psi_8), \\
\psi_8 &= \Psi(a_1, a_3, -a_6, y, t), \xi_8 = \frac{1}{a_6}(\psi_1 - \psi_7), u_{1,3} = M_3 = -\frac{Gm}{Sc - 1}(\xi_9 + \xi_{10}), \xi_9 = \frac{1}{a_7}(\psi_2 - \psi_9), \\
\psi_9 &= \Psi(Sc, K, -a_7, y, t), \xi_{10} = a_5(B_3\psi_2 + B_4\psi_3 + B_5\psi_9), u_{1,4} = M_4 = \frac{M\Pi}{(1 - Pm)\sqrt{Pm}} K_1, K_1 = K(\sqrt{Pm}, y, t), \\
u_{2,1,1} &= E_1, u_{2,1,2} = u_{1,1,2}, u_{2,1,3} = u_{1,1,3}, u_{2,2} = u_{1,2}, u_{2,3} = u_{1,3}, u_{2,4} = -\frac{M\Pi y}{2} E_1, u_{3,1,1} = E_1, u_{3,1,2} = u_{1,1,2}, u_{3,1,3} = \xi_{11}, \\
\xi_{11} &= \frac{Gm}{K} [E_1(1 + a_5 G_1) + a_5 G_2 \psi_5], G_1 = \frac{a_3}{a_4}, G_2 = \frac{a_4 - a_3}{a_4}, u_{3,2} = u_{1,2}, u_{3,3} = \xi_{12}, \\
\xi_{12} &= -\frac{Gm}{K}(\psi_{10} + a_5 G_1 \psi_{10} + a_5 G_2 \psi_{11}), \psi_{10} = \psi(1, K, y, t) = \psi(Sc, K, y, t) = \psi_2, \\
\psi_{11} &= \Psi(1, K, -a_4, y, t) = \Psi(Sc, K, -a_4, y, t) = \psi_3, u_{4,1,1} = E_1, u_{4,1,2} = \xi_{13}, \\
\xi_{13} &= -\frac{1}{a_1 a_3} [(Gma_5 G_1 - Gr)E_1 + Gma_5 G_2 \psi_5], u_{4,1,3} = u_{1,1,3}, u_{4,1,4} = u_{1,1,4}, u_{4,2} = \frac{1}{a_1 a_3} (Gm\xi_{14} - Gr\psi_{13}), \\
\xi_{14} &= a_5(G_1\psi_{13} + G_2\psi_{14}), u_{4,3} = u_{1,3}, u_{4,4} = u_{1,4}, u_{5,1,1} = E_1, u_{5,1,2} = u_{1,1,2}, u_{5,1,3} = u_{3,1,3}, u_{5,2} = u_{1,2}, \\
u_{5,3} &= u_{3,3}, u_{5,4} = u_{2,4}, u_{6,1,1} = E_1, u_{6,1,2} = u_{4,1,2}, u_{6,1,3} = u_{1,1,3}, u_{6,2} = u_{4,2}, u_{6,3} = u_{1,3}, u_{6,4} = u_{2,4}, \\
u_{7,1,1} &= E_1, u_{7,1,2} = u_{4,1,2}, u_{7,1,3} = u_{3,1,3}, u_{7,1,4} = u_{1,1,4}, u_{7,2} = u_{4,2}, u_{7,3} = u_{3,3}, u_{7,4} = u_{1,4}, \\
u_{8,1,1} &= E_1, u_{8,1,2} = u_{4,1,2}, u_{8,1,3} = u_{3,1,3}, u_{8,2} = u_{4,2}, u_{8,3} = u_{3,3}, u_{8,4} = u_{2,4}
\end{aligned}$$

$$Nu = -\Omega_1, \Omega_2 = \Omega(Sc, K, t), \Lambda_1 = a_5(A_1\Omega_2 + A_2\Omega_3), \Omega_3 = Z(Sc, K, -a_4, t), \Lambda_2 = a_5(A_1\Omega_1 + A_2\Omega_4),$$

$$\begin{aligned}
\Omega_4 &= Z(a_1, a_3, -a_4, t), \tau_{1,1} = \tau_{1,1,1} + \tau_{1,1,2} + \tau_{1,1,3} + \tau_{1,1,4}, \tau_{1,1,1} = \alpha \left(\frac{1}{2\sqrt{t}} \right) = \alpha_1, \tau_{1,1,2} = \frac{1}{1-a_1} (\Lambda_3 - \Lambda_4), \\
\Lambda_3 &= Gma_5 (A_3\alpha_1 + A_4\Omega_5 + A_5\Omega_6), \Omega_5 = Z(1, 0, -a_4, t), \Omega_6 = Z(1, 0, -a_6, t), \Lambda_4 = \frac{Gr}{a_5} (\alpha_1 - \Omega_6), \\
\tau_{1,1,3} &= \frac{Gm}{Sc-1} (\Lambda_5 + \Lambda_6), \Lambda_5 = \frac{1}{a_7} (\alpha_1 - \Omega_7), \Omega_7 = Z(1, 0, -a_7, t), \Lambda_6 = a_5 (B_3\alpha_1 + B_4\Omega_5 + B_5\Omega_7), \\
\tau_{1,1,4} &= \frac{M\Pi}{(1-Pm)\sqrt{Pm}} P_y^0(1, y, t) = \Gamma I(y, t) = \Gamma I_1, \tau_{1,2} = \frac{1}{a_1-1} (Gm\Lambda_7 - Gr\Lambda_8), \\
\Lambda_7 &= a_5 (A_3\Omega_1 + A_4\Omega_4 + A_5\Omega_8), \Omega_8 = Z(a_1, a_3, -a_6, t), \Lambda_8 = \frac{1}{a_6} (-\Omega_1 - \Omega_8), \tau_{1,3} = -\frac{Gm}{Sc-1} (\Lambda_9 + \Lambda_{10}), \\
\Lambda_9 &= \frac{1}{a_7} (-\Omega_2 - \Omega_9), \Omega_9 = Z(Sc, K, -a_7, t), \Lambda_{10} = a_5 (B_3\Omega_2 + B_4\Omega_3 + B_5\Omega_7), \\
\tau_{1,4} &= -\Gamma K_y^0(\sqrt{Pm}, y, t) = -\Gamma\sqrt{Pm}, \tau_{2,1} = \tau_{2,1,1} + \tau_{2,1,2} + \tau_{2,1,3}, \tau_{2,1,1} = \alpha_1, \tau_{2,1,2} = \tau_{1,1,2}, \tau_{2,1,3} = \tau_{1,1,3}, \\
\tau_{2,2} &= \tau_{1,2}, \tau_{2,3} = \tau_{1,3}, \tau_{2,4} = -\frac{M\Pi E_1}{2}, \tau_{3,1} = \tau_{3,1,1} + \tau_{3,1,2} + \tau_{3,1,3}, \tau_{3,1,1} = \alpha_1, \tau_{3,1,2} = \tau_{1,1,2}, \tau_{3,1,3} = \Lambda_{11}, \\
\Lambda_{11} &= \frac{Gm}{K} [(1+a_5G_1)\alpha_1 + a_5G_2\Omega_5], \tau_{3,2} = \tau_{1,2}, \tau_{3,3} = \Lambda_{12}, \Lambda_{12} = -\frac{Gm}{K} (\Omega_2 + a_5G_1\Omega_2 + a_5G_2\Omega_3), \tau_{3,4} = \tau_{1,4}, \\
\tau_{4,1} &= \tau_{4,1,1} + \tau_{4,1,2} + \tau_{4,1,3} + \tau_{4,1,4}, \tau_{4,1,1} = \alpha_1, \tau_{4,1,2} = \Lambda_{13}, \Lambda_{13} = -\frac{1}{a_1a_3} [(Gma_5G_1 - Gr)\alpha_1 + Gma_5G_2\Omega_5], \\
\tau_{4,1,3} &= \tau_{1,1,3}, \tau_{4,1,4} = \tau_{1,1,4}, \tau_{4,2} = \frac{1}{a_1a_3} (Gm\Lambda_{14} - Gr\Omega_1), \Lambda_{14} = a_5 (G_1\Omega_1 + G_2\Omega_4), \tau_{4,3} = \tau_{1,3}, \tau_{4,4} = \tau_{1,4}, \\
\tau_{5,1} &= \tau_{5,1,1} + \tau_{5,1,2} + \tau_{5,1,3}, \tau_{5,1,1} = \alpha_1, \tau_{5,1,2} = \tau_{1,1,2}, \tau_{5,1,3} = \tau_{3,1,3}, \tau_{5,2} = \tau_{1,2}, \tau_{5,3} = \tau_{3,3}, \tau_{5,4} = \tau_{2,4}, \\
\tau_{6,1} &= \tau_{6,1,1} + \tau_{6,1,2} + \tau_{6,1,3}, \tau_{6,1,1} = \alpha_1, \tau_{6,1,2} = \tau_{4,1,2}, \tau_{6,1,3} = \tau_{1,1,3}, \tau_{6,2} = \tau_{4,2}, \tau_{6,3} = \tau_{1,3}, \tau_{6,4} = \tau_{2,4}, \\
\tau_{7,1} &= \tau_{7,1,1} + \tau_{7,1,2} + \tau_{7,1,3} + \tau_{7,1,4}, \tau_{7,1,1} = \alpha_1, \tau_{7,1,2} = \tau_{4,1,2}, \tau_{7,1,3} = \tau_{3,1,3}, \tau_{7,1,4} = \tau_{1,1,4}, \tau_{7,2} = \tau_{4,2}, \tau_{7,3} = \tau_{3,3}, \\
\tau_{7,4} &= \tau_{1,4}, \tau_{8,1} = \tau_{8,1,1} + \tau_{8,1,2} + \tau_{8,1,3}, \tau_{8,1,1} = \alpha_1, \tau_{8,1,2} = \tau_{4,1,2}, \tau_{8,1,3} = \tau_{3,1,3}, \tau_{8,2} = \tau_{4,2}, \tau_{8,3} = \tau_{3,3}, \tau_{8,4} = \tau_{2,4}
\end{aligned}$$

(The functions are defined in **Chapter I**)

CHAPTER III

Thermal Diffusion Effect on Unsteady MHD Free Convective Flow Past an Impulsively Started But Temporarily Accelerated Semi-Infinite Vertical Plate with Parabolic Ramped Conditions

Published in *Heat Transfer, Wiley (Scopus, ESCI)*, **50(4)**, 1-33, 2021.

3.1 Introduction

Magnetohydrodynamics (MHD) is the section of physics that deals with the dynamics of electrically conducting fluid under the influence of a magnetic field. Plasmas, liquid metals, electrolytes, ionized gases are some well-known examples of such fluids. MHD covers the connection between the magnetic field and the velocity of the conducting fluid. The field of MHD was initiated by Swiss physicist Hannes Alfvén (1942). There are several applications of MHD. Dynamo and motor work on principles of MHD. Engineers use MHD in metal dispersion, fusion reactors, metallurgy, etc. Besides these, MHD has vast applications in aeronautics, chemical and electrical engineering, medicine, and biological sciences. Pioneer authors due to whose contribution MHD is at present form are Cowling (1957), Ferraro and Plumpton (1966), Shercliff (1965), and Cramer and Pai (1973), etc.

Density variation in a fluid mixture occurs owing to the change in species concentration and fluid temperature. This variation generates buoyancy forces acting on the fluid. The flow arising due to this force is labeled as natural convection or free convection. Natural convection on MHD flow was studied exclusively by Raptis and Singh (1983), Hosain and Ahmed (1990), Takhar et al. (1996), Helmy (1998), etc. Nandi and Kumbhakar (2020) studied free convective MHD flow past a permeable vertical plate with periodic movement in presence of hall current and rotation.

The process of heat transfer through an electromagnetic wave is classified as radiation. Radiative convective flows can be found in numerous environmental and industrial processes. This type of flow takes a pivotal role in high-temperature processes and space technology. It is also used in the polymer processing industry. Influencing by the importance of applications, many authors have performed model research on free convection in many hydrodynamic and magnetohydrodynamics flow problems with thermal radiation effects under different physical and geometrical circumstances. Mbeledogu et al. (2007), Makinde (2005), Orhan and Ahmet (2008), Samad and Rahman (2006), Prasad et al. (2006), Seth et al. (2017), Balla and Naikoti (2015), Siviah et al. (2012), etc. are some authors in this field whose work are worth mentioning. Seth et al. (2016) discussed the effect of Hall current in a free convective, radiative, and heat-absorbing MHD flow past a moving vertical plate with ramped temperature. Ahmed and Dutta (2014) obtained the exact solution of a free convective transient MHD flow past an infinite vertical plate with radiation and ramped wall temperature.

When both thermal and solutal convection appears simultaneously on fluid motion, the relationship of driving potentials and fluxes are complex. Then mass flux is produced by both temperature gradient and concentration gradient. Effect of mass flux under temperature gradient is labeled as Soret effect or thermal diffusion effect. This effect appears when components of fluid are kept in different temperatures. This effect arises due to the flow of molecules from hotter regions to cooler regions. C. Ludwig first observed this effect in 1859. But the first experimental work on this effect was performed in the laboratory by noted Swiss chemist Charles Soret in 1879. This effect has numerous applications in many chemical and physical processes, isotope separation, etc. Consequences of the Soret effect in various mass transfer problems were studied by Kafoussias and Williams (1995), Eckert and Drake (1972), Postelnicu (2004), Ahmed (2010), and Ahmed and Sengupta (2011).

The present investigation aims to study and analyze the problem of a transient MHD flow past a suddenly accelerated semi-infinite vertical plate with parabolic ramped temperature along with concentration taking into account the thermal diffusion effect under the imposition of a uniform transverse magnetic field. Reviewing the literature, we found that no attempt has been made in this area. The governing equations of this problem are first transformed into a set of normalized equations and they are solved analytically with the help of the Laplace transformation technique. The flow phenomena are described using different parameters viz. magnetic parameter, Prandtl number, Ramped parameter, Schmidt number, thermal Grashof number, solutal Grashof number, etc. Effect of these parameters on the concentration field, temperature field, velocity field, Sherwood number, Nusselt number, and skin friction are analyzed and the results are discussed intensely with the assistance of graphs.

3.2 Mathematical Analysis

Equations that governs the convective flow of a viscous, radiating, electrically conducting, and incompressible fluid in presence of a magnetic field having constant mass diffusivity and thermal diffusivity considering thermo- diffusion effect are

Equation of continuity:

$$\vec{\nabla} \cdot \vec{q} = 0 \quad (3.1)$$

Equation of magnetic field continuity:

$$\vec{\nabla} \cdot \vec{B} = 0 \quad (3.2)$$

Ohm's Law:

$$\vec{J} = \sigma(\vec{E} + \vec{q} \times \vec{B}) \quad (3.3)$$

Equation of momentum:

$$\rho \left[\frac{\partial \vec{q}}{\partial t} + (\vec{q} \cdot \vec{\nabla}) \vec{q} \right] = -\vec{\nabla} p + \rho \vec{g} + \vec{J} \times \vec{B} + \mu \nabla^2 \vec{q} \quad (3.4)$$

Equation of energy:

$$\rho C_p \left[\frac{\partial T}{\partial t} + (\vec{q} \cdot \vec{\nabla}) T \right] = \kappa \nabla^2 T - \vec{\nabla} \cdot \vec{q}_r \quad (3.5)$$

Species continuity equation:

$$\frac{\partial C}{\partial t} + (\vec{q} \cdot \vec{\nabla}) C = D_M \nabla^2 C + D_T \nabla^2 T \quad (3.6)$$

Equation of state as per Boussinesq approximation:

$$\rho_\infty = \rho \left[1 + \beta(T - T_\infty) + \bar{\beta}(C - C_\infty) \right] \quad (3.7)$$

According to Rosseland approximation for optically thick and non-gray fluid, radiative heat flux is

$$\vec{q}_r = -\frac{4\sigma^*}{3\kappa^*} \vec{\nabla} T^4$$

Now,

$$T^4 = (T - T_\infty + T_\infty)^4 = 4TT_\infty^3 - 3T_\infty^4, \text{ as } |T - T_\infty| \ll 1$$

So,

$$\vec{\nabla} \cdot \vec{q}_r = -\frac{16\sigma^* T_\infty^3}{3\kappa^*} \nabla^2 T$$

Therefore, Energy equation (5) reduces to

$$\rho C_p \left[\frac{\partial T}{\partial \bar{t}} + (\vec{q} \cdot \vec{\nabla}) T \right] = \kappa \nabla^2 T + \frac{16\sigma^* T_\infty^3}{3\kappa^*} \nabla^2 T \quad (3.8)$$

Now we consider a transient MHD free convective flow of an incompressible, electrically conducting, and viscous fluid past a semi-infinite moving vertical plate. Suppose, a uniform magnetic field is applied normally to the plate, directed into the fluid region. Originally, the plate and neighboring fluid were static with uniform temperature T_∞ along with concentration C_∞ . The plate is allowed to move suddenly at $\bar{t} = 0^+$, with acceleration $\frac{U_0}{t_0}$ for $0 < \bar{t} \leq t_0$. For $\bar{t} > t_0$, the plate moves with a uniform speed U_0 . The plate concentration and temperature are instantaneously raised to $C_\infty + \frac{C_w - C_\infty}{t_0^2} \bar{t}^2$ and $T_\infty + \frac{T_w - T_\infty}{t_0^2} \bar{t}^2$ respectively, for $0 < \bar{t} \leq t_0$, where $T_w > T_\infty$, and $C_w > C_\infty$. Thereafter, the plate attains constant temperature T_w and constant concentration C_w for $\bar{t} > t_0$.

To idealize the mathematical model, the following constraints are imposed-

- I. Except for the density variation and buoyancy force, all other fluid characteristics are assumed to be constant.
- II. Dissipation of energy due to friction and Joule heating is negligible.
- III. Flow is parallel to the plate and one- dimensional.
- IV. Polarization voltage is negligible.
- V. The plate is insulating.

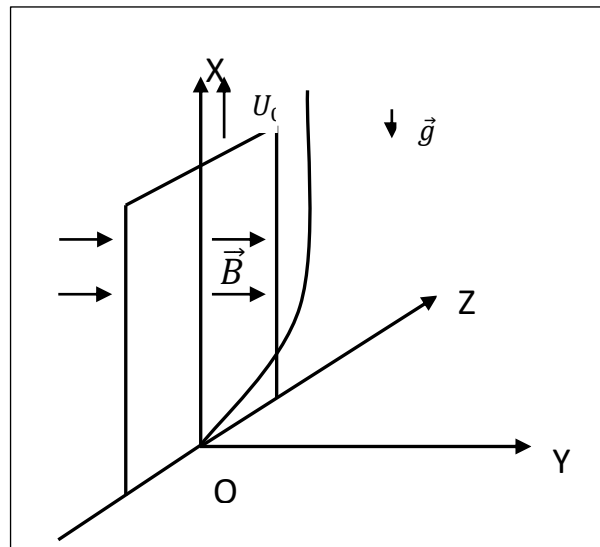


Figure 3.1: Flow Configuration

We now consider a tri- rectangular Cartesian coordinate $(\bar{x}, \bar{y}, \bar{z}, \bar{t})$ with X -axis is taken vertically upwards along the plate, Y -axis is taken normal to the plate directed into the fluid region and Z -axis is taken along the width of the plate. Let the fluid velocity be $\vec{q} = (u', 0, 0)$ and $\vec{B} = (0, B_0, 0)$ be the magnetic induction vector.

Equation (3.1) yields,

$$\begin{aligned} \frac{\partial u'}{\partial \bar{x}} &= 0 \\ \text{i.e., } u' &= u'(\bar{y}, \bar{t}) \end{aligned} \quad (3.9)$$

Equation (3.2) is satisfied trivially

Equation (3.4) reduces to

$$\rho \left[\frac{\partial u'}{\partial \bar{t}} \hat{i} + 0 \right] = -\hat{i} \frac{\partial p}{\partial \bar{x}} - \hat{j} \frac{\partial p}{\partial \bar{y}} - \rho g \hat{i} - \sigma B_0^2 u' \hat{i} + \mu \frac{\partial^2 u'}{\partial \bar{y}^2} \hat{i} \quad (3.10)$$

Equation (3.10) gives

$$\rho \frac{\partial u'}{\partial \bar{t}} = -\frac{\partial p}{\partial \bar{x}} - \rho g - \sigma B_0^2 u' + \mu \frac{\partial^2 u'}{\partial \bar{y}^2} \quad (3.11)$$

and

$$0 = -\frac{\partial p}{\partial \bar{y}} \quad (3.12)$$

Equation (3.12) shows that pressure near the plate and pressure far off the plate is the same along the normal to the plate.

For fluid far off the plate, equation (3.11) becomes

$$0 = -\frac{\partial p}{\partial \bar{x}} - \rho_\infty g \quad (3.13)$$

Eliminating $\frac{\partial p}{\partial \bar{x}}$ from (3.11) and (3.13), we get

$$\rho \frac{\partial u'}{\partial \bar{t}} = (\rho_\infty - \rho)g - \sigma B_0^2 u' + \mu \frac{\partial^2 u'}{\partial \bar{y}^2} \quad (3.14)$$

Now, (3.7) gives,

$$\rho_\infty - \rho = \rho [\beta(T - T_\infty) + \bar{\beta}(C - C_\infty)] \quad (3.15)$$

Putting value of (3.15) in (3.14),

$$\begin{aligned} \rho \frac{\partial u'}{\partial \bar{t}} &= \rho [\beta(T - T_\infty) + \bar{\beta}(C - C_\infty)]g - \sigma B_0^2 u' + \mu \frac{\partial^2 u'}{\partial \bar{y}^2} \\ \text{i.e., } \frac{\partial u'}{\partial \bar{t}} &= g\beta(T - T_\infty) + g\bar{\beta}(C - C_\infty) - \frac{\sigma B_0^2 u'}{\rho} + \nu \frac{\partial^2 u'}{\partial \bar{y}^2} \end{aligned} \quad (3.16)$$

Equation (3.8) yields,

$$\rho C_p \frac{\partial T}{\partial \bar{t}} = \kappa \frac{\partial^2 T}{\partial \bar{y}^2} + \frac{16\sigma^* T_\infty^3}{3\kappa^*} \frac{\partial^2 T}{\partial \bar{y}^2} \quad (3.17)$$

Equation (3.6) becomes,

$$\frac{\partial C}{\partial \bar{t}} = D_M \frac{\partial^2 C}{\partial \bar{y}^2} + D_T \frac{\partial^2 T}{\partial \bar{y}^2} \quad (3.18)$$

The relevant initial and boundary conditions are:

$$\left. \begin{aligned} \forall \bar{y} \geq 0: u' = 0, T = T_\infty, C = C_\infty; \bar{t} \leq 0 \\ \bar{y} = 0: u' = \frac{U_0 \bar{t}}{t_0}, T = T_\infty + \frac{T_w - T_\infty}{t_0^2} \bar{t}^2, C = C_\infty + \frac{C_w - C_\infty}{t_0^2} \bar{t}^2; 0 < \bar{t} \leq t_0 \\ \bar{y} = 0: u' = U_0, T = T_w, C = C_w; \bar{t} > t_0 \\ \bar{y} \rightarrow \infty: u' \rightarrow 0, T \rightarrow T_\infty, C \rightarrow C_\infty; \forall \bar{t} > 0 \end{aligned} \right\} \quad (3.19)$$

The mathematical model is normalized with the help of the following non-dimensional parameters and variables-

$$Sr = \frac{D_T(T_w - T_\infty)}{\nu(C_w - C_\infty)}, N = \frac{\kappa \kappa^*}{4\sigma^* T_\infty^3}, u = \frac{u'}{U_0}, y = \frac{\bar{y}}{U_0 t_0}, t = \frac{\bar{t}}{t_0}, Gr = \frac{\nu g \beta (T_w - T_\infty)}{U_0^3}, Ra = \frac{U_0^2 t_0}{\nu}$$

$$Gm = \frac{\nu g \bar{\beta} (C_w - C_\infty)}{U_0^3}, \theta = \frac{T - T_\infty}{T_w - T_\infty}, \phi = \frac{C - C_\infty}{C_w - C_\infty}, Pr = \frac{\mu C_p}{\kappa}, M = \frac{\sigma B_0^2 \nu}{\rho U_0^2}, Sc = \frac{\nu}{D_M}, \Lambda = 1 + \frac{4}{3N}$$

The non- dimensional governing equations are

$$\frac{\partial u}{\partial t} = \frac{1}{Ra} \frac{\partial^2 u}{\partial y^2} + RaGr\theta + RaGm\phi - uMRa \quad (3.20)$$

$$\frac{\partial \theta}{\partial t} = \frac{\Lambda}{RaPr} \frac{\partial^2 \theta}{\partial y^2} \quad (3.21)$$

$$\frac{\partial \phi}{\partial t} = \frac{1}{ScRa} \frac{\partial^2 \phi}{\partial y^2} + \frac{Sr}{Ra} \frac{\partial^2 \theta}{\partial y^2} \quad (3.22)$$

The relevant initial and boundary conditions are:

$$\left. \begin{aligned} \forall y \geq 0: u = 0, \theta = 0, \phi = 0; t \leq 0 \\ y = 0: u = t, \theta = t^2, \phi = t^2; 0 < t \leq 1 \\ y = 0: u = 1, \theta = 1, \phi = 1; t > 1 \\ y \rightarrow \infty: u \rightarrow 0, \theta \rightarrow 0, \phi \rightarrow 0; \forall t > 0 \end{aligned} \right\} \quad (3.23)$$

3.3 Method of Solution

On taking the Laplace transform of the equations (3.21), (3.22), and (3.20) respectively, we get:

$$s\bar{\theta} = \frac{\Lambda}{PrRa} \frac{d^2 \bar{\theta}}{dy^2} \quad (3.24)$$

$$s\bar{\phi} = \frac{1}{ScRa} \frac{d^2 \bar{\phi}}{dy^2} + \frac{Sr}{Ra} \frac{d^2 \bar{\theta}}{dy^2} \quad (3.25)$$

$$s\bar{u} = \frac{1}{Ra} \frac{d^2 \bar{u}}{dy^2} + RaGr\bar{\theta} + RaGm\bar{\phi} - MRa\bar{u} \quad (3.26)$$

Relevant initial and boundary conditions are:

$$\left. \begin{aligned} y = 0: \bar{\theta} = \frac{2}{s^3} (1 - e^{-s}) - \frac{2}{s^2} e^{-s}, \bar{\phi} = \frac{2}{s^3} (1 - e^{-s}) - \frac{2}{s^2} e^{-s}, \bar{u} = \frac{1}{s^2} (1 - e^{-s}) \\ y \rightarrow \infty: \bar{\theta} \rightarrow 0, \bar{\phi} \rightarrow 0, \bar{u} \rightarrow 0 \end{aligned} \right\} \quad (3.27)$$

Solving equations from (3.24) to (3.26) subject to the conditions (3.27) and obtaining inverse Laplace transform of the results, the expressions of temperature field θ , concentration field ϕ , and velocity field u are :

$$\theta = \theta_{1,1} - \theta_{1,2} \quad (3.28)$$

$$\phi = (1 + \eta)\phi_{1,1} - \eta\phi_{1,2} \quad (3.29)$$

$$u = \begin{cases} u_{1,1} + u_{1,2} + u_{1,3} + u_{1,4} : Sc \neq 1, Pr \neq \Lambda \\ u_{2,1} + u_{2,2} + u_{2,3} + u_{2,4} : Sc = 1, Pr \neq \Lambda \\ u_{3,1} + u_{3,2} + u_{3,3} + u_{3,4} : Sc \neq 1, Pr = \Lambda \\ u_{4,1} + u_{4,2} + u_{4,3} + u_{4,4} : Sc = 1, Pr = \Lambda \end{cases} \quad (3.30)$$

3.4 Nusselt Number

According to Fourier's law of conduction, heat flux q^* at the plate $\bar{y} = 0$ is

$$q^* = -\kappa_0^* \left. \frac{\partial T}{\partial \bar{y}} \right]_{\bar{y}=0} \quad (3.31)$$

Here, $\kappa_0^* = \kappa + \frac{16\sigma^* T_\infty^3}{3\kappa^*}$ is the modified thermal conductivity.

Equation (3.31) yields

$$Nu = - \left. \frac{\partial \theta}{\partial y} \right]_{y=0} \quad (3.32)$$

$Nu = \frac{q^* U_0 t_0}{\kappa_0^* (T_w - T_\infty)}$ is called the Nusselt number which is concerned with heat transfer rate at the plate.

Equation (3.32) gives,

$$Nu = -2(\Delta\zeta_1 - \bar{v}_1) \quad (3.33)$$

3.5 Sherwood Number

According to Fick's law of diffusion, mass flux M_w at the plate $\bar{y} = 0$ is

$$M_w = -D_M \left. \frac{\partial C}{\partial \bar{y}} \right]_{\bar{y}=0} \quad (3.34)$$

Equation (3.34) gives

$$Sh = - \left. \frac{\partial \phi}{\partial y} \right]_{y=0} \quad (3.35)$$

In (3.35), $Sh = \frac{M_w U_0 t_0}{D_M (C_w - C_\infty)}$ is called the Sherwood number which is associated with mass transfer rate at the plate.

Equation (3.35) yields

$$Sh = -2 \left[(1 + \eta) (\Delta \zeta_2 - \bar{v}_2) + \eta (\Delta \zeta_1 - \bar{v}_1) \right] \quad (3.36)$$

3.6 Skin Friction

According to Newton's law of viscosity, viscous drag $\bar{\tau}$ at the plate $\bar{y} = 0$ is

$$\bar{\tau} = -\mu \left. \frac{\partial u}{\partial \bar{y}} \right]_{\bar{y}=0} \quad (3.37)$$

Equation (3.37) gives

$$\tau = - \left. \frac{\partial u}{\partial y} \right]_{y=0} \quad (3.38)$$

In (3.38), $\tau = \frac{\bar{\tau} t_0}{\mu}$ is called the skin friction or coefficient of friction which is associated with the rate of momentum transfer at the plate.

Equation (3.38) yields,

$$\tau = - \begin{cases} \tau_{1,1} + \tau_{1,2} + \tau_{1,3} + \tau_{1,4} : Sc \neq 1, Pr \neq \Lambda \\ \tau_{2,1} + \tau_{2,2} + \tau_{2,3} + \tau_{2,4} : Sc = 1, Pr \neq \Lambda \\ \tau_{3,1} + \tau_{3,2} + \tau_{3,3} + \tau_{3,4} : Sc \neq 1, Pr = \Lambda \\ \tau_{4,1} + \tau_{4,2} + \tau_{4,3} + \tau_{4,4} : Sc = 1, Pr = \Lambda \end{cases} \quad (3.39)$$

3.7 Results and Discussion

We study how the flow parameters involved affect the flow and transport properties. The numerically computed results are displayed from Figures 3.2 to 3.33.

Figures 3.2 to 3.5 show the variation in temperature field versus normal co-ordinate y under time t , Prandtl number Pr , radiation parameter N , and Ramped parameter Ra . Figure 3.2 indicates that the temperature field hikes as time progresses. Figure 3.3 reveals that the temperature field gets lowered as the Prandtl number increases. In other words, higher thermal diffusivity upsurges the temperature field. Figure 3.4 displays that the temperature field decreases as the radiation parameter increases. In real life system, it is observed that radiation tends to decrease temperature. This physical observation is reflected here. Figure 3.5 admits that there is a comprehensive fall in the temperature field as Ramped parameter increases. An increase in Ra means a fall ν . Thus, the temperature rises as the friction of fluid increases. This observation is in excellent agreement with the fact that the fluid temperature increases for fluid having large friction. From these figures, we can conclude that the temperature field asymptotically declines from its highest value at $y = 0$ to lowest value as $y \rightarrow \infty$.

Figures 3.6 to 3.10 represent the variation in concentration field versus normal co-ordinate y under Prandtl number Pr , radiation parameter N and Ramped parameter Ra , Schmidt number Sc , and Soret number Sr . Figure 3.6 reveals that the concentration field decreases as the Prandtl number increases. This gives us an idea that higher thermal diffusivity upsurges the concentration field. Figure 3.7 indicates that the concentration field gets lowered with increment in radiation parameter. From a general idea in physics, it follows that fluid gets thinner as radiation from fluid to atmosphere increases. This phenomenon is reflected here. Figure 3.8 reveals that the concentration field decreases for increasing Ramped parameter. From the definition, it is noticed that Ramped parameter is inversely proportional to kinematic viscosity. Hence, fluid gets thicker for higher friction. Figure 3.9 suggests that a higher Schmidt number lowers the concentration field. This informs us that increment in

mass diffusivity upsurges concentration field. Figure 3.10 confesses us that a higher Soret number hikes the concentration field. The Soret effect is concerned with mass flux under temperature gradient. An increment in Soret number indicates a comprehensive rise in temperature gradient over the concentration gradient. Hence, an increment in temperature gradient results in a rise in the concentration level of the fluid.

Figures 3.11 to 3.18 explain the variation in velocity field versus normal co-ordinate y under time t , Prandtl number Pr , Ramped parameter Ra , Schmidt number Sc , thermal Grashof number Gr , solutal Grashof number Gm , magnetic parameter M and Soret number Sr . Velocity field hikes with time as shown in Figure 3.11. Figure 3.12 suggests that the velocity field decreases with increasing Prandtl number. Thus, higher thermal diffusivity upsurges the velocity field. Figure 3.13 gives us an idea that velocity increases with increasing Ramped parameter near the plate and its nature changes afterward. As the Ramped parameter is inversely proportional to kinematic viscosity, so, fluid velocity decreases in a thin layer adjacent to the plate but increases outside the layer as friction at the plate hikes. Velocity field hikes with increasing Schmidt number as shown in Figure 3.14. Hence, higher mass diffusivity declines fluid velocity. There is a comprehensive rise in velocity field with increasing thermal Grashof number as noticed in Figure 3.15. Higher solutal Grashof number upsurges velocity field as displayed in Figure 3.16. Thermal Grashof number refers to buoyancy force under temperature gradient whereas solutal Grashof number refers to buoyancy force under a concentration gradient. Thus both Figure 3.15 and Figure 3.16 assert that buoyancy force increases fluid velocity. Figure 3.17 indicates that the velocity field decline with increasing magnetic parameter. Since the electromagnetic field is applied in the transverse direction, so increase in electromagnetic force declines fluid velocity. Velocity field rises substantially for increasing Soret number as observed in Figure 3.18. So, if the temperature gradient is higher than the concentration gradient, then fluid velocity increases.

Figures 3.19 to 3.21 show the variation in Nusselt number versus time t under Prandtl number Pr , radiation parameter N , and Ramped parameter Ra . Figure 3.19 suggests that increment in the Prandtl number upsurges the Nusselt number. This indicates that higher thermal diffusivity lowers the Nusselt number. Figure 3.20 admits that the Nusselt number keep the increasing trend with higher radiation parameter. Thus, radiation accelerates the rate of heat transfer from the plate to the fluid. Nusselt number rises with increasing Ramped

parameter as shown in Figure 3.21. In other words, increasing viscosity decelerates the heat transfer process.

Figures 3.22 to 3.26 represent the variation in Sherwood number versus time t under Prandtl number Pr , radiation parameter N , Ramped parameter Ra , Soret number Sr , and Schmidt number Sc . Figure 3.22 reveals that the Sherwood number declines with increasing Prandtl number. Thus, higher thermal diffusivity increases the Sherwood number. Figure 3.23 admits that the Sherwood number gets lowered as the radiation parameter hikes. Thus radiation tends to slow down the mass transfer process from the plate to the fluid. Sherwood number upsurges with increment in Ramped parameter as shown in Figure 3.24. The friction declines the process of mass transfer to a good extent. Figure 3.25 gives us an idea that the higher Soret number declines Sherwood number. This establishes the fact that a lower concentration gradient compared to a high-temperature gradient decelerates the mass transfer process. Figure 3.26 suggests that there is an upsurge in Sherwood number as Schmidt number hikes. Alternatively, we can say that increasing mass diffusivity decreases the Sherwood number.

Figures 3.27 to 3.33 explain the variation in skin friction versus time t under Prandtl number Pr , Ramped parameter Ra , Schmidt number Sc , Soret number Sr , thermal Grashof number Gr , solutal Grashof number Gm , and magnetic parameter M . Skin friction falls comprehensively with an upsurge in Prandtl number as shown in Figure 3.27. In other words, we can say that higher thermal diffusivity raises skin friction. Figure 3.28 admits that skin friction declines as Ramped parameter hikes. So, increasing kinematic viscosity hikes frictional resistivity at the plate. Figure 3.29 reveals that skin friction gets decreased as Schmidt number increases. This admits that higher mass diffusivity enhances skin friction. Skin friction lowers with increasing Soret number as displayed in Figure 3.30. Hence, the concentration gradient offers more frictional resistance at the plate compared to the temperature gradient. Figure 3.31 suggests that skin friction gets lowered as the thermal Grashoff number increases. Skin friction falls significantly with increasing solutal Grashoff number as shown in Figure 3.32. Both Figures 3.31 and 3.32 express the fact that buoyancy force tends to lower frictional resistance at the plate. Figure 3.33 admits that skin friction hikes as magnetic parameter upsurges. In other words, the electromagnetic force increases frictional resistivity at the plate.

3.8 Conclusions

The significant findings of our investigation are as follows:

- i. The temperature field falls for a higher Ramped parameter.
- ii. Ascending values of the Prandtl number lowers the concentration field.
- iii. Velocity field accelerates for higher Soret number.
- iv. Nusselt number upsurges for increasing Ramped parameter.
- v. Higher Schmidt increases the Sherwood number.
- vi. Increasing Soret number declines skin friction.

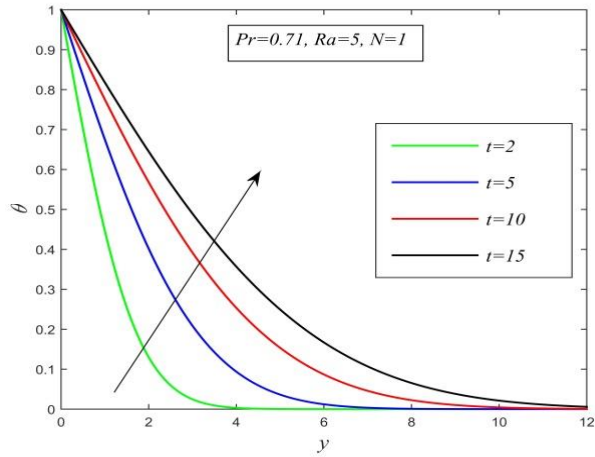


Figure 3.2: Temperature field versus y for different t and $Pr=0.71$, $Ra=5$, $N=1$

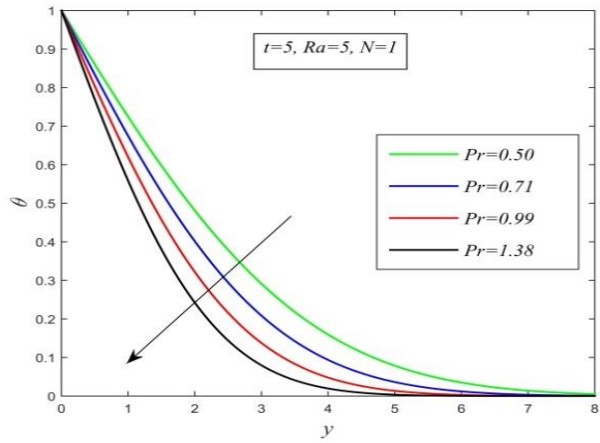


Figure 3.3: Temperature field versus y for different Pr and $t=5$, $Ra=5$, $N=1$

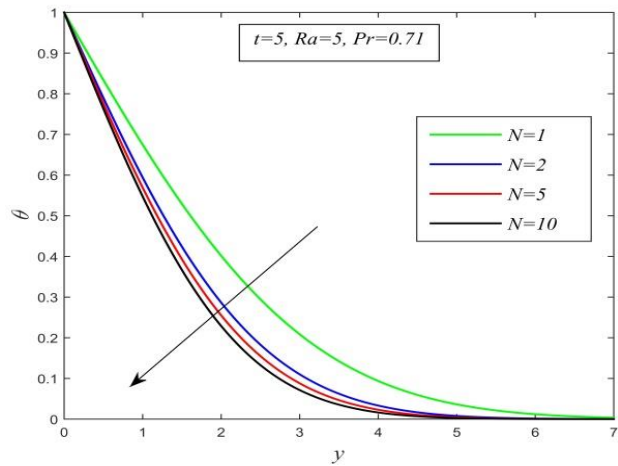


Figure 3.4: Temperature field versus y for different N and $t=5$, $Ra=5$, $Pr=0.71$

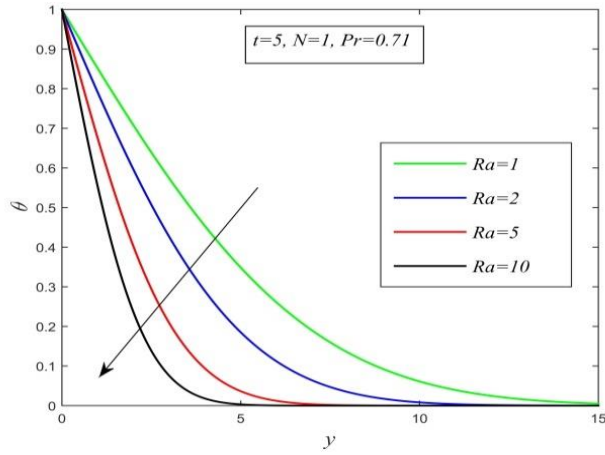


Figure 3.5: Temperature field versus y for different Ra and $t=5$, $N=1$, $Pr=0.71$

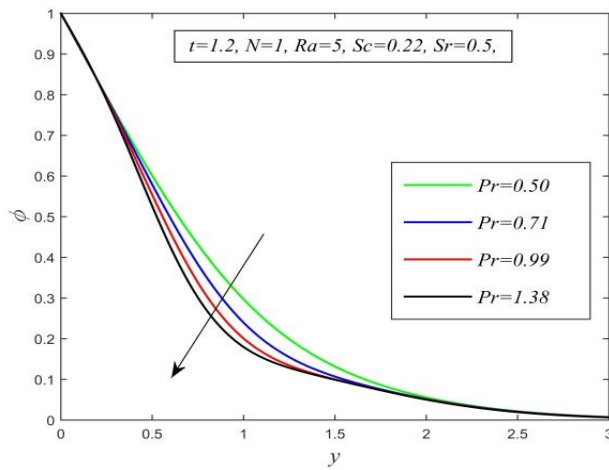


Figure 3.6: Concentration field versus y for different Pr and $t=1.2$, $N=1$, $Ra=5$, $Sc=0.22$, $Sr=0.5$

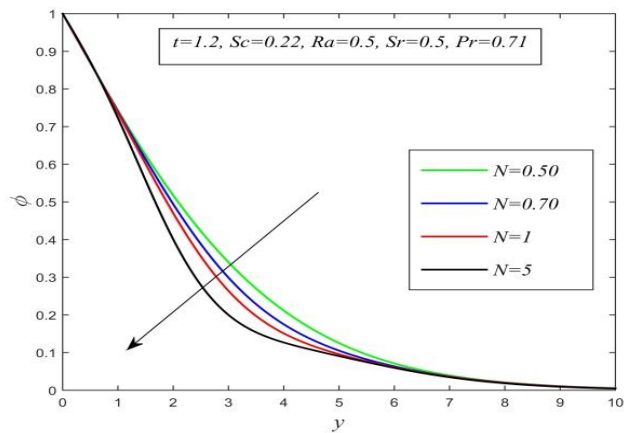


Figure 3.7: Concentration field versus y for different N and $t=1.2$, $Ra=5$, $Sc=0.22$, $Sr=0.5$, $Pr=0.71$

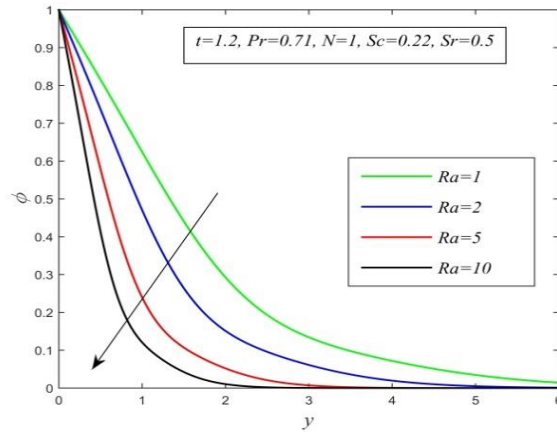


Figure 3.8: Concentration field versus y for different Ra and $t=1.2, N=1, Sc=0.22, Sr=0.5, Pr=0.71$

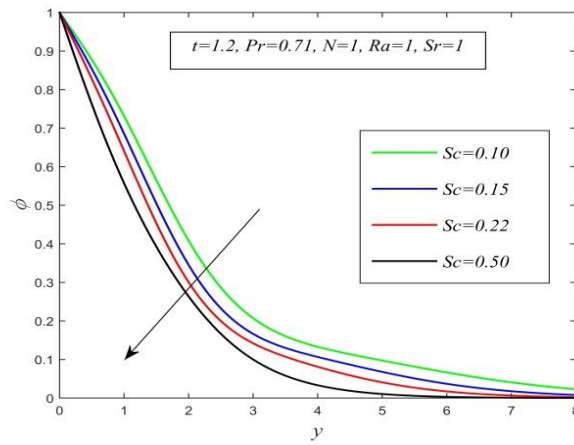


Figure 3.9: Concentration field versus y for different Sc and $t=1.2, Ra=1, Sr=1, Pr=0.71, N=1$

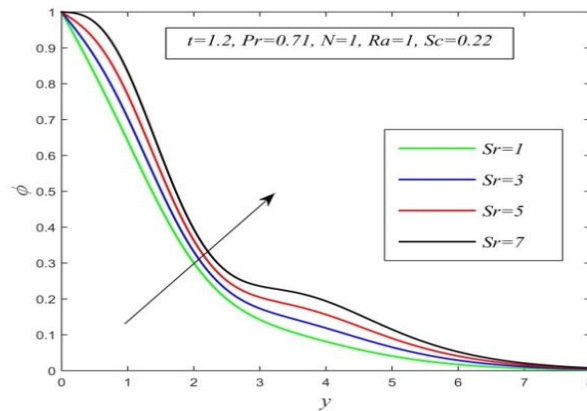


Figure 3.10: Concentration field versus y for different Sr and $t=1.2, Ra=1, Pr=0.71, N=1, Sc=0.22$

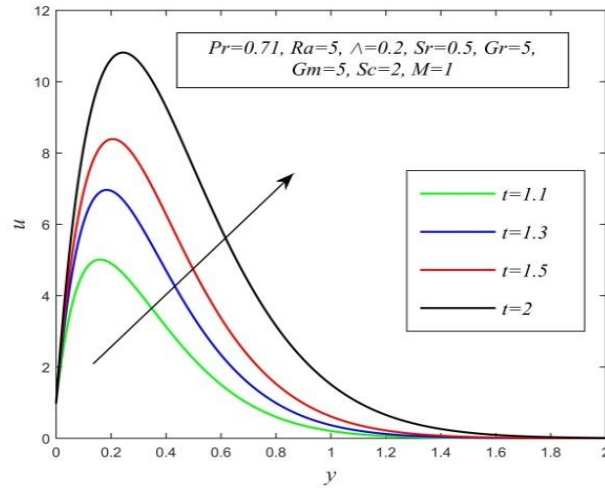


Figure 3.11: Velocity field versus y for different t and $Pr=0.71, Ra=5, \Lambda=0.2, Sr=0.5, Gr=5, Gm=5, Sc=2, M=1$

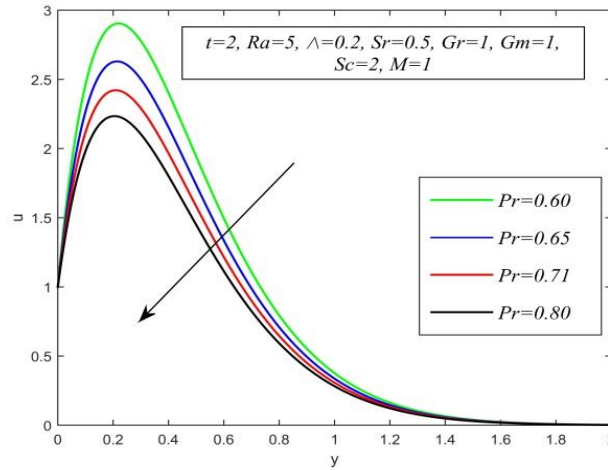


Figure 3.12: Velocity field versus y for different Pr and $t=2, Ra=5, \Lambda=0.2, Sr=0.5, Gr=1, Gm=1, Sc=2, M=1$

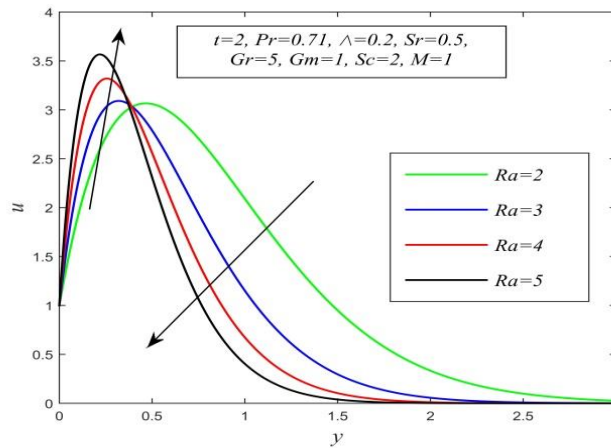


Figure 3.13: Velocity field versus y for different Ra and $t=2, Pr=0.71, \Lambda=0.2, Sr=0.5, Gr=5, Gm=1, Sc=2, M=1$

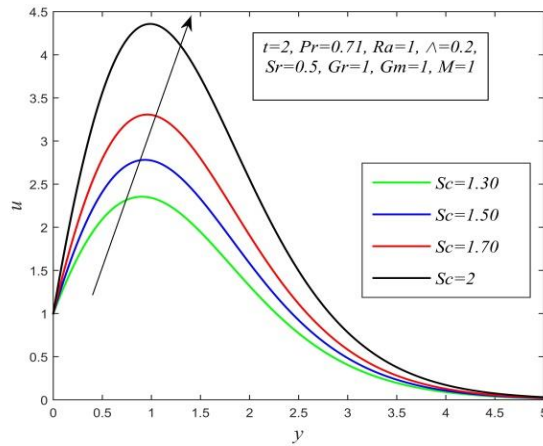


Figure 3.14: Velocity field versus y for different Sc and $t=2, Pr=0.71, Ra=1, \Lambda=0.2, Sr=0.5, Gr=1, Gm=1, M=1$

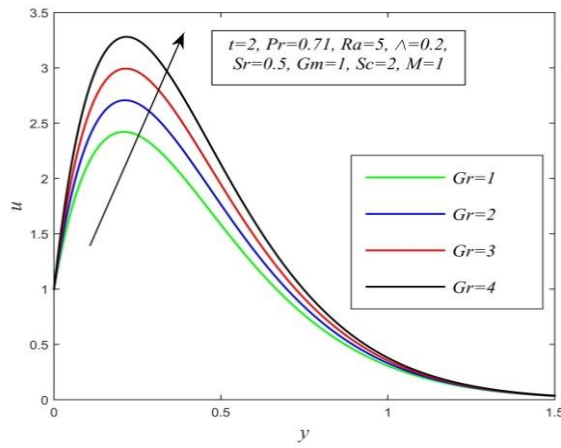


Figure 3.15: Velocity field versus y for different Gr and $t=2, Pr=0.71, Ra=5, \Lambda=0.2, Sr=0.5, Gm=1, Sc=2, M=1$

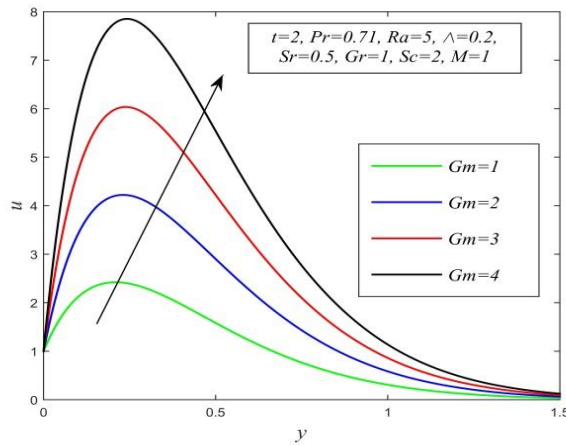


Figure 3.16: Velocity field versus y for different Gm and $t=2, Pr=0.71, Ra=5, \Lambda=0.2, Sr=0.5, Gr=1, Sc=2, M=1$

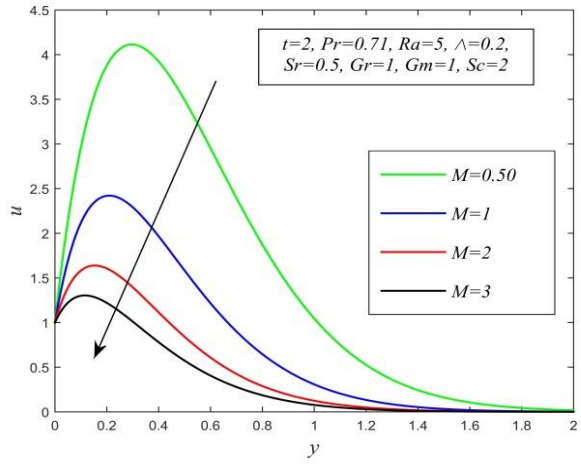


Figure 3.17: Velocity field versus y for different M and $t=2, Pr=0.71, Ra=5, \Lambda=0.2, Sr=0.5, Gr=1, Gm=1, Sc=2$

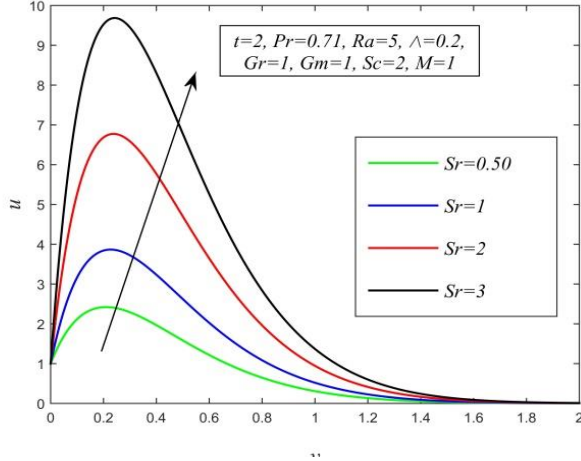


Figure 3.18: Velocity field versus y for different Sr and $t=2, Pr=0.71, Ra=5, \Lambda=0.2, Sr=0.5, Gr=1, Gm=1, Sc=2$

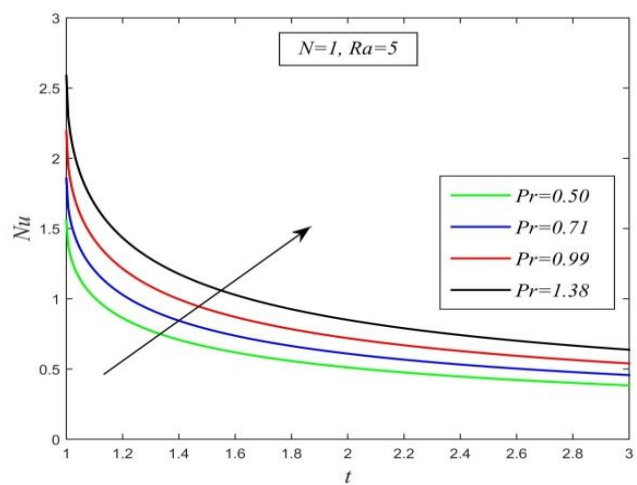


Figure 3.19: Nusselt number versus t for different Pr and $N=1, Ra=5$

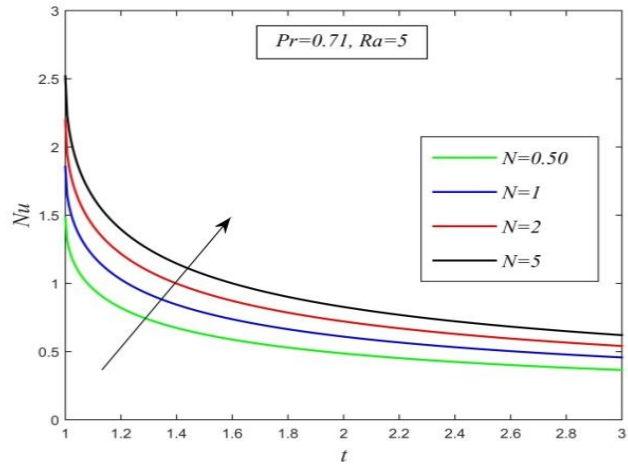


Figure 3.20: Nusselt number versus t for different N and $Pr=0.71, Ra=5$

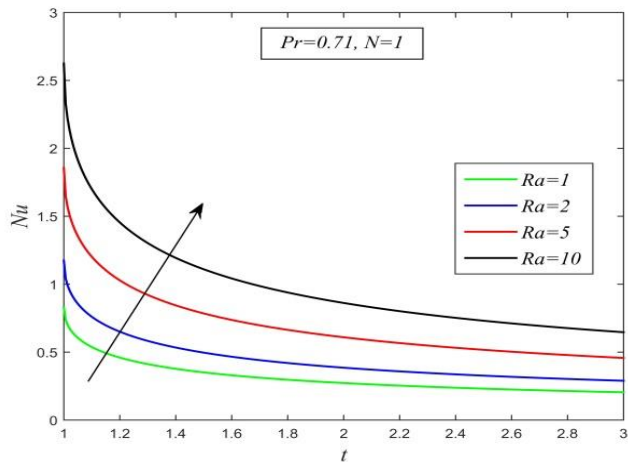


Figure 3.21: Nusselt number versus t for different Ra and $Pr=0.71, N=1$

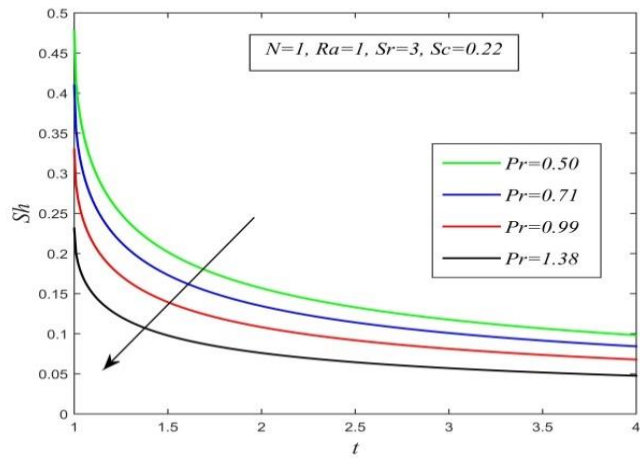


Figure 3.22: Sherwood number versus t for different Pr and $N=1, Ra=1, Sr=3, Sc=0.22$

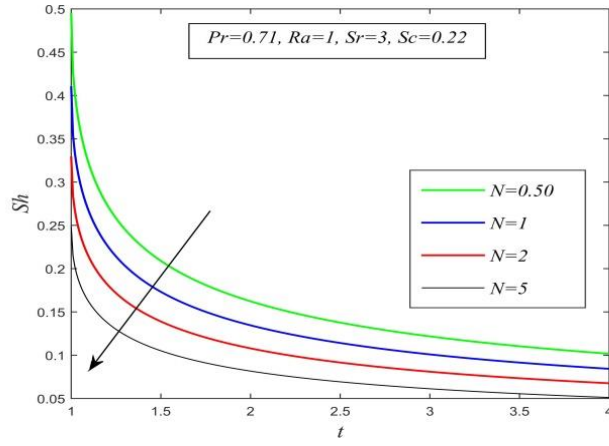


Figure 3.23: Sherwood number versus t for different N and $Pr=0.71, Ra=1, Sr=3, Sc=0.22$

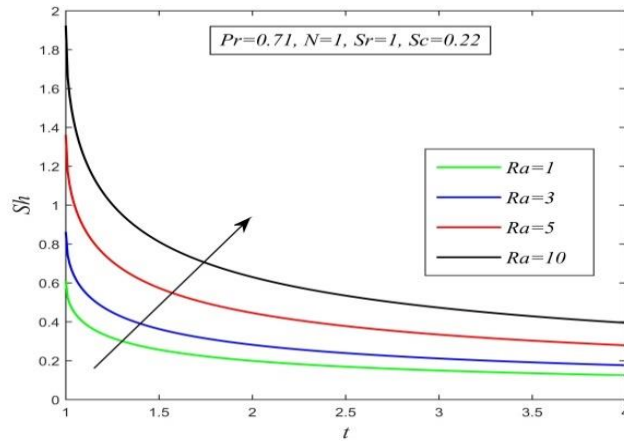


Figure 3.24: Sherwood number versus t for different Ra and $Pr=0.71, N=1, Sr=3, Sc=0.22$

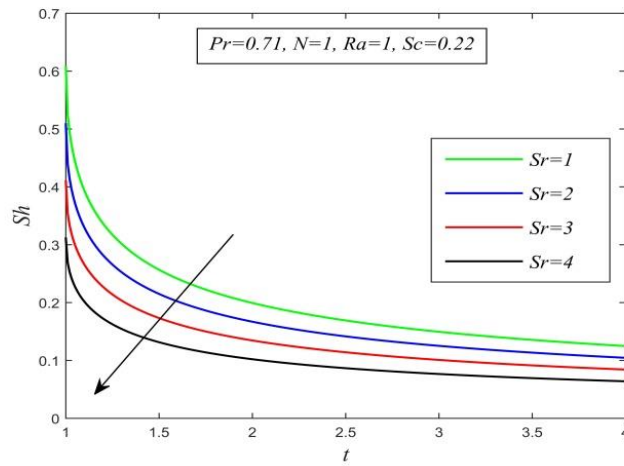


Figure 3.25: Sherwood number versus t for different Sr and $Pr=0.71, N=1, Ra=1, Sc=0.22$

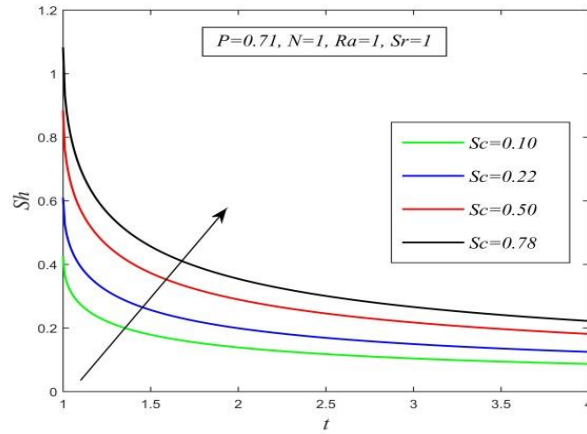


Figure 3.26: Sherwood number versus t for different Sc and $Pr=0.71, N=1, Ra=1, Sr=1$

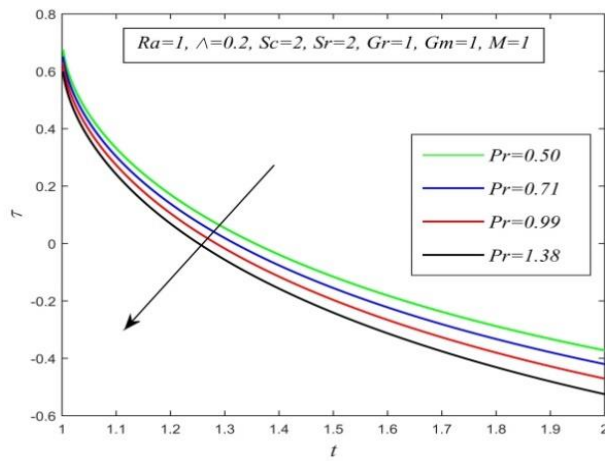


Figure 3.27: Skin friction versus t for different Pr and $Ra=1, \Lambda=0.2, Sc=2, Sr=2, Gr=1, Gm=1, M=1$

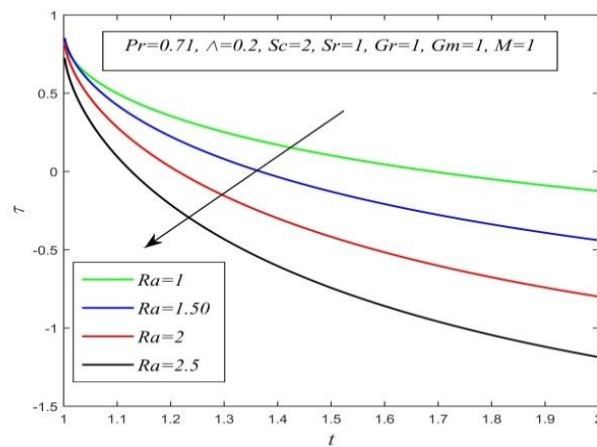


Figure 3.28: Skin friction versus t for different Ra and $Pr=0.71, \Lambda=0.2, Sc=2, Sr=2, Gr=1, Gm=1, M=1$

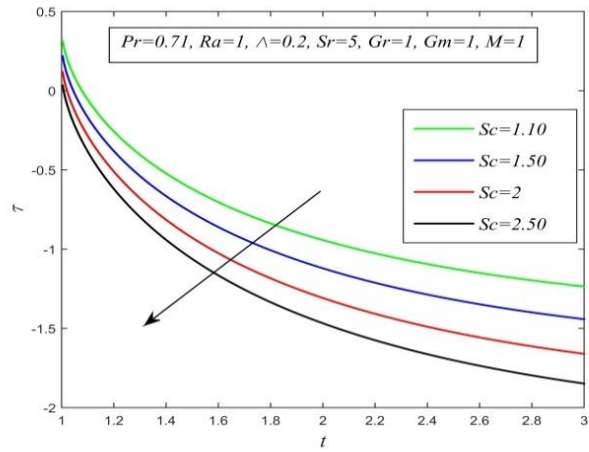


Figure 3.29: Skin friction versus t for different Sc and $Pr=0.71, Ra=1, \Lambda=0.2, Sr=5, Gr=1, Gm=1, M=1$

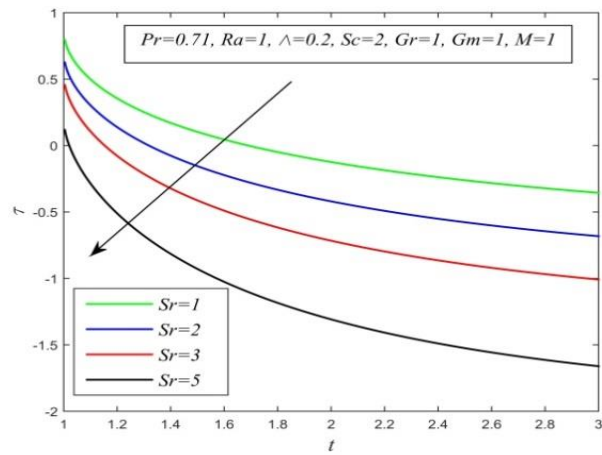


Figure 3.30: Skin friction versus t for different Sr and $Pr=0.71, Ra=1, \Lambda=0.2, Sc=2, Gr=1, Gm=1, M=1$

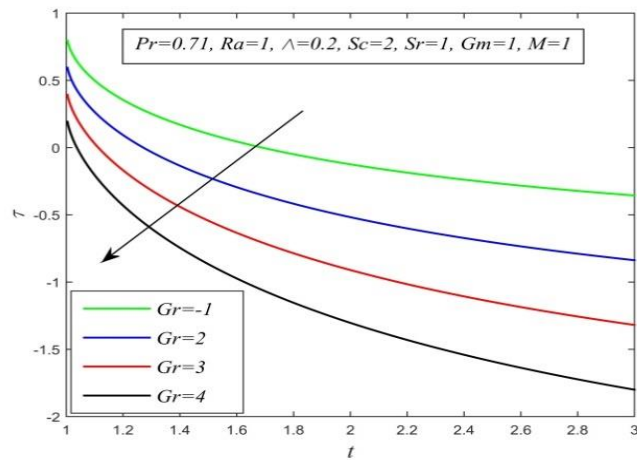


Figure 3.31: Skin friction versus t for different Gr and $Pr=0.71, Ra=1, \Lambda=0.2, Sc=2, Sr=1, Gm=1, M=1$

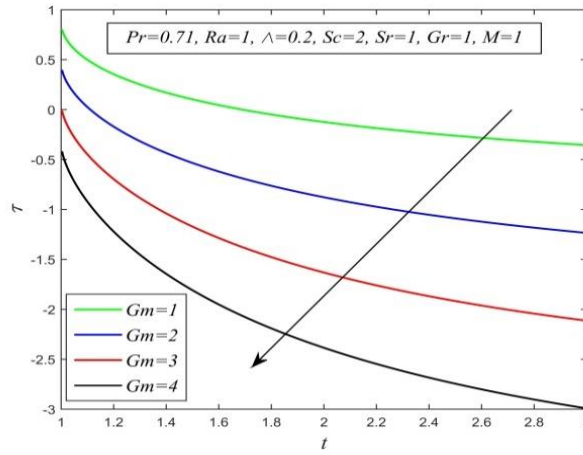


Figure 3.32: Skin friction versus t for different Gm and $Pr=0.71, Ra=1, \Lambda=0.2, Sc=2, Sr=1, Gr=1, M=1$

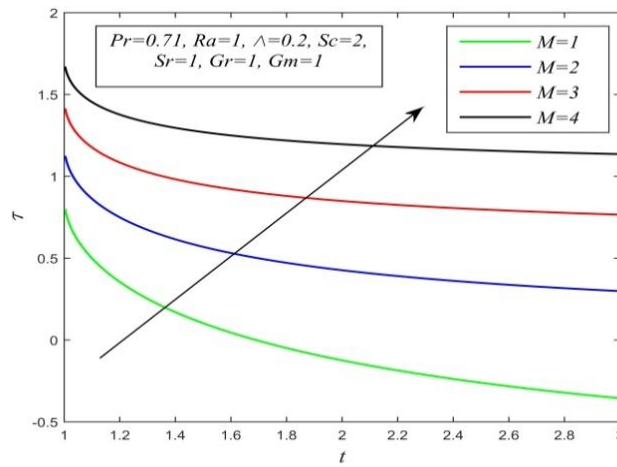


Figure 3.33: Skin friction versus t for different M and $Pr=0.71, Ra=1, \Lambda=0.2, Sc=2, Sr=1, Gr=1, Gm=1$

Nomenclature:

\vec{B} : Magnetic flux density

B_0 : Applied magnetic field strength $\left(\frac{\text{Weber}}{\text{m}^2}\right)$

C_∞ : Concentration far off the plate $\left(\frac{\text{mol}}{\text{m}^3}\right)$

C_w : Iso-solutal plate concentration $\left(\frac{\text{mol}}{\text{m}^3}\right)$

Ra : Ramped parameter

C : Molar species concentration $\left(\frac{\text{mol}}{\text{m}^3}\right)$

D_M : Mass diffusivity $\left(\frac{\text{m}^2}{\text{s}}\right)$

C_p : Specific heat at constant pressure $\left(\frac{\text{J}}{\text{Kg.K}}\right)$

D_T : Molar thermal diffusivity $\left(\frac{\text{J}}{\text{K.mol}}\right)$

\vec{g} : Gravitation acceleration vector

Gr : Thermal Grashof number

g : Gravitational acceleration $\left(\frac{\text{m}}{\text{s}^2}\right)$

Gm : Solutal Grashof number

\vec{J} : Current density vector $\left(\frac{\text{A}}{\text{m}^2}\right)$

N : Radiation parameter

p : Pressure $\left(\frac{\text{N}}{\text{m}^2}\right)$

Pr : Prandtl number

M : Magnetic parameter

\vec{q} : Fluid velocity vector

\vec{q}_r : Radiation heat flux vector

q_r : Radiation heat flux $\left(\frac{W}{m^2}\right)$

Sc : Schmidt number

U_0 : Plate velocity $\left(\frac{m}{s}\right)$

Sr : Soret number

\bar{t} : Time (s)

T : Fluid temperature (K)

T_∞ : Undisturbed temperature (K)

u' : X-component of fluid velocity $\left(\frac{m}{s}\right)$

Greek Symbols:

μ : Coefficient of viscosity $\left(\frac{Kg}{m.s}\right)$

σ : Electrical conductivity $\left(\frac{S}{m}\right)$

ρ : Fluid density $\left(\frac{Kg}{m^3}\right)$

σ^* : Stefan-Boltzmann constant $\left(\frac{W}{m^2.K^4}\right)$

ρ_∞ : Fluid density far off the plate $\left(\frac{Kg}{m^3}\right)$

β : Volumetric coefficient of thermal expansion $\left(\frac{1}{K}\right)$

κ : Thermal conductivity $\left(\frac{W}{m.K}\right)$

$\bar{\beta}$: Volumetric coefficient of solutal expansion $\left(\frac{1}{K.mol}\right)$

κ^* : Mean absorption constant $\left(\frac{1}{m}\right)$

ν : Kinematic viscosity $\left(\frac{m^2}{s}\right)$

Subscript:

w : Physical quantity at the plate

∞ : Physical quantity far off the plate

Appendix

$$\begin{aligned}
\xi &= \frac{\text{Pr} Ra}{\Lambda}, G_1 = G(y\sqrt{\xi}, t), \theta_{1,1} = 2\Delta G_1, \lambda_1 = \lambda(\xi, y, t), \theta_{1,2} = 2\bar{\lambda}_1, \eta = \frac{ScSr\xi}{\xi - ScRa}, \phi_{1,1} = \phi_{1,1,1} - \phi_{1,1,2} \\
\phi_{1,1,1} &= 2\Delta G_2, G_2 = G(y\sqrt{ScRa}, t), \phi_{1,1,2} = 2\bar{\lambda}_2, \lambda_2 = \lambda(ScRa, y, t), \phi_{1,2} = \theta, a_1 = M.Ra, a_2 = \frac{Ra.a_1}{\xi - Ra} \\
N_1 &= \frac{-Ra^2Gr}{\xi - Ra}, u_{1,1} = u_{1,1,1} - u_{1,1,2} + u_{1,1,3} + u_{1,1,4}, u_{1,1,1} = \Delta f_1, f_1 = f(Ra, a_1, y, t), u_{1,1,2} = u_{1,1,2,1} - u_{1,1,2,2} \\
u_{1,1,2,1} &= 2N_1\Delta(A_1\psi_2 + A_2\psi_1 + A_3f_1 + A_4\omega_1), \psi_1 = \psi(Ra, a_1, y, t), \psi_2 = \Psi(Ra, a_1, a_2, y, t) \\
\omega_1 &= \omega(Ra, a_1, y, t), A_1 = \frac{1}{a_2^3}, A_2 = -\frac{1}{a_2^3}, A_3 = -\frac{1}{a_2^2}, A_4 = -\frac{1}{a_2}, u_{1,1,2,2} = 2N_1(A_5\bar{\psi}_2 + A_3\bar{\psi}_1 + A_4\bar{f}_1) \\
A_5 &= \frac{1}{a_2^2}, u_{1,1,3} = u_{1,1,3,1} - u_{1,1,3,2}, u_{1,1,3,1} = 2N_2\Delta(A_6\psi_3 + A_7\psi_1 + A_8f_1 + A_9\omega_1), N_2 = \frac{RaGm(1+\eta)}{Sc-1} \\
a_3 &= \frac{a_1}{Sc-1}, A_6 = \frac{1}{a_3^3}, A_7 = -\frac{1}{a_3^3}, A_8 = -\frac{1}{a_3^2}, A_9 = -\frac{1}{a_3}, \psi_3 = \Psi(Ra, a_1, a_3, y, t) \\
u_{1,1,3,2} &= 2N_2(A_{10}\bar{\psi}_3 + A_8\bar{\psi}_1 + A_9\bar{f}_1), A_{10} = \frac{1}{a_3^2}, u_{1,1,4} = u_{1,1,4,1} - u_{1,1,4,2}, u_{1,1,4,1} = 2N_3\Delta(A_{11}\psi_4 + A_{12}\psi_1 + A_{13}f_1 + A_{14}\omega_1) \\
a_4 &= \frac{Ra.a_1}{Ra-\xi}, N_3 = \frac{Ra^2Gm\eta}{Ra-\xi}, A_{11} = -\frac{1}{a_4^3}, A_{12} = \frac{1}{a_4^3}, A_{13} = -\frac{1}{a_4^2}, A_{14} = \frac{1}{a_4}, \psi_4 = \Psi(Ra, a_1, -a_4, y, t) \\
u_{1,1,4,2} &= 2N_3(A_{15}\bar{\psi}_4 + A_{13}\bar{\psi}_1 + A_{14}\bar{f}_1), A_{15} = \frac{1}{a_4^2}, u_{1,2} = u_{1,2,1} - u_{1,2,2}, u_{1,2,1} = 2N_1\Delta(A_1\psi_5 + A_2E_1 + A_3\lambda_1 + A_4G_1), \\
\psi_5 &= \Psi(\xi, 0, a_2, y, t), E_1 = \text{erfc}\left(\frac{y\sqrt{\xi}}{2\sqrt{t}}\right), u_{1,2,2} = 2N_1(A_5\bar{\psi}_5 + A_3\bar{E}_1 + A_4\bar{\lambda}_1), u_{1,3} = -u_{1,3,1} + u_{1,3,2}, \\
u_{1,3,1} &= 2N_2\Delta(A_6\psi_6 + A_7E_2 + A_8\lambda_2 + A_9G_2), \psi_6 = \Psi(ScRa, 0, a_3, y, t), E_2 = \text{erfc}\left(\frac{y\sqrt{ScRa}}{2\sqrt{t}}\right), \\
u_{1,3,2} &= 2N_2(A_{10}\bar{\psi}_6 + A_8\bar{E}_2 + A_9\bar{\lambda}_2), u_{1,4} = -u_{1,4,1} + u_{1,4,2}, u_{1,4,1} = 2N_3\Delta(A_{11}\psi_7 + A_{12}E_1 + A_{13}\lambda_1 + A_{14}G_1), \\
\psi_7 &= \Psi(\xi, 0, -a_4, y, t), u_{1,4,2} = 2N_3(A_{15}\bar{\psi}_7 + A_{13}\bar{E}_1 + A_{14}\bar{\lambda}_1), u_{2,1} = u_{2,1,1} - u_{2,1,2} + u_{2,1,3} + u_{2,1,4}, \\
u_{2,1,1} &= u_{1,1,1}, u_{2,1,2} = u_{1,1,2}, u_{2,1,3} = u_{2,1,3,1} - u_{2,1,3,2}, u_{2,1,3,1} = 2N_4\Delta\omega_1, N_4 = -\frac{RaGm(1+\eta)}{a_1}, u_{2,1,3,2} = 2N_4\bar{f}_1, \\
u_{2,1,4} &= u_{1,1,4}, u_{2,2} = u_{1,2}, u_{2,3} = u_{2,3,1} - u_{2,3,2}, u_{2,3,1} = 2N_4\Delta G_2, u_{2,3,2} = 2N_4\bar{\lambda}_2, u_{2,4} = u_{1,4}, \\
u_{3,1} &= u_{3,1,1} - u_{3,1,2} + u_{3,1,3} + u_{3,1,4}, u_{3,1,1} = u_{1,1,1}, u_{3,1,2} = u_{3,1,2,1} - u_{3,1,2,2}, u_{3,1,2,1} = 2N_5\Delta\omega_1, N_5 = \frac{RaGr}{a_1}, \\
u_{3,1,2,2} &= 2N_5\bar{f}_1, u_{3,1,3} = u_{1,1,3}, u_{3,1,4} = u_{3,1,4,1} - u_{3,1,4,2}, u_{3,1,4,1} = 2N_6\Delta\omega_1, N_6 = \frac{RaGm\eta}{a_1}, u_{3,1,4,2} = 2N_6\bar{f}_1, \\
u_{3,2} &= u_{3,2,1} - u_{3,2,2}, u_{3,2,1} = 2N_5\Delta G_1, u_{3,2,2} = 2N_5\bar{\lambda}_1, u_{3,3} = u_{1,3}, u_{3,4} = u_{3,4,1} - u_{3,4,2}, u_{3,4,1} = 2N_6\Delta G_1, \\
u_{3,4,2} &= 2N_6\bar{\lambda}_1, u_{4,1} = u_{4,1,1} - u_{4,1,2} + u_{4,1,3} + u_{4,1,4}, u_{4,1,1} = u_{1,1,1}, u_{4,1,2} = u_{3,1,2}, u_{4,1,3} = u_{2,1,3}, u_{4,1,4} = u_{3,1,4}, \\
u_{4,2} &= u_{3,2}, u_{4,3} = u_{2,3}, u_{4,4} = u_{3,4}
\end{aligned}$$

$$\begin{aligned}
\zeta_1 &= \zeta\left(\sqrt{\xi}, t\right), v_1 = v(\xi, t), \zeta_2 = \zeta\left(\sqrt{ScRa}, t\right), v_2 = v(ScRa, t), \\
\tau_{1,1} &= \tau_{1,1,1} - \tau_{1,1,2} + \tau_{1,1,3} + \tau_{1,1,4}, \tau_{1,1,1} = \Delta\Phi_1, \Phi_1 = \Phi(Ra, a_1, t), \tau_{1,1,2} = \tau_{1,1,2,1} - \tau_{1,1,2,2} \\
\tau_{1,1,2,1} &= 2N_1\Delta(A_1Z_1 + A_2\Omega_1 + A_3\Phi_1 + A_4\Theta_1), Z_1 = Z(Ra, a_1, a_2, t), \Omega_1 = \Omega(Ra, a_1, t), \Theta_1 = \Theta(Ra, a_1, t) \\
\tau_{1,1,2,2} &= 2N_1\left(A_5\bar{Z}_1 + A_3\bar{\Omega}_1 + A_4\bar{\Phi}_1\right), \tau_{1,1,3} = \tau_{1,1,3,1} - \tau_{1,1,3,2}, \tau_{1,1,3,1} = 2N_2\Delta(A_6Z_2 + A_7\Omega_1 + A_8\Phi_1 + A_9\Theta_1) \\
Z_2 &= Z(Ra, a_1, a_3, t), \tau_{1,1,3,2} = 2N_2\left(A_{10}\bar{Z}_2 + A_8\bar{\Omega}_1 + A_9\bar{\Phi}_1\right), \tau_{1,1,4} = \tau_{1,1,4,1} - \tau_{1,1,4,2} \\
\tau_{1,1,4,1} &= 2N_3\Delta(A_{11}Z_3 + A_{12}\Omega_1 + A_{13}\Phi_1 + A_{14}\Theta_1), Z_3 = Z(Ra, a_1, -a_4, t), \tau_{1,1,4,2} = 2N_3\left(A_{15}\bar{Z}_3 + A_{13}\bar{\Omega}_1 + A_{14}\bar{\Phi}_1\right) \\
\tau_{1,2} &= \tau_{1,2,1} - \tau_{1,2,2}, \tau_{1,2,1} = 2N_1\Delta(A_1Z_4 + A_2\alpha_1 + A_3v_1 + A_4\zeta_1), Z_4 = Z(\xi, 0, a_2, t), \alpha_1 = \alpha\left(\frac{\sqrt{\xi}}{2\sqrt{t}}\right), \\
\tau_{1,2,2} &= 2N_1\left(A_5\bar{Z}_4 + A_3\bar{\alpha}_1 + A_4\bar{v}_1\right), \tau_{1,3} = -\tau_{1,3,1} + \tau_{1,3,2}, \tau_{1,3,1} = 2N_2\Delta(A_6Z_5 + A_7\alpha_2 + A_8v_2 + A_9\zeta_2), \\
Z_5 &= Z(ScRa, 0, a_3, t), \alpha_2 = \alpha\left(\frac{\sqrt{ScRa}}{2\sqrt{t}}\right), \tau_{1,3,2} = 2N_2\left(A_{10}\bar{Z}_5 + A_8\bar{\alpha}_2 + A_9\bar{v}_2\right), \tau_{1,4} = -\tau_{1,4,1} + \tau_{1,4,2}, \\
\tau_{1,4,1} &= 2N_3\Delta(A_{11}Z_6 + A_{12}\alpha_1 + A_{13}v_1 + A_{14}\zeta_1), Z_6 = Z(\xi, 0, -a_4, t), \tau_{1,4,2} = 2N_3\left(A_{15}\bar{Z}_6 + A_{13}\bar{\alpha}_1 + A_{14}\bar{v}_1\right) \\
\tau_{2,1} &= \tau_{2,1,1} - \tau_{2,1,2} + \tau_{2,1,3} + \tau_{2,1,4}, \tau_{2,1,1} = \tau_{1,1,1}, \tau_{2,1,2} = \tau_{1,1,2}, \tau_{2,1,3} = \tau_{2,1,3,1} - \tau_{2,1,3,2}, \tau_{2,1,3,1} = 2N_4\Delta\Theta_1, \\
\tau_{2,1,3,2} &= 2N_4\bar{\Phi}_1, \tau_{2,1,4} = \tau_{1,1,4}, \tau_{2,2} = \tau_{1,2}, \tau_{2,3} = \tau_{2,3,1} - \tau_{2,3,2}, \tau_{2,3,1} = 2N_4\Delta\zeta_2, \tau_{2,3,2} = 2N_4\bar{v}_2, \tau_{2,4} = \tau_{1,4}, \\
\tau_{3,1} &= \tau_{3,1,1} - \tau_{3,1,2} + \tau_{3,1,3} + \tau_{3,1,4}, \tau_{3,1,1} = \tau_{1,1,1}, \tau_{3,1,2} = \tau_{3,1,2,1} - \tau_{3,1,2,2}, \tau_{3,1,2,1} = 2N_5\Delta\Theta_1, \tau_{3,1,2,2} = 2N_5\bar{\Phi}_1, \\
\tau_{3,1,3} &= \tau_{1,1,3}, \tau_{3,1,4} = \tau_{3,1,4,1} - \tau_{3,1,4,2}, \tau_{3,1,4,1} = 2N_6\Delta\Theta_1, \tau_{3,1,4,2} = 2N_6\bar{\Phi}_1, \tau_{3,2} = \tau_{3,2,1} - \tau_{3,2,2}, \tau_{3,2,1} = 2N_5\Delta\zeta_1, \\
\tau_{3,2,2} &= 2N_5\bar{v}_1, \tau_{3,3} = \tau_{1,3}, \tau_{3,4} = \tau_{3,4,1} - \tau_{3,4,2}, \tau_{3,4,1} = 2N_6\Delta\zeta_1, \tau_{3,4,2} = 2N_6\bar{v}_1, \tau_{4,1} = \tau_{4,1,1} - \tau_{4,1,2} + \tau_{4,1,3} + \tau_{4,1,4}, \\
\tau_{4,1,1} &= \tau_{1,1,1}, \tau_{4,1,2} = \tau_{3,1,2}, \tau_{4,1,3} = \tau_{2,1,3}, \tau_{4,1,4} = \tau_{3,1,4}, \tau_{4,2} = \tau_{3,2}, \tau_{4,3} = \tau_{2,3}, \tau_{4,4} = \tau_{3,4}
\end{aligned}$$

(The functions are defined in **Chapter I**)

CHAPTER IV

Diffusion Thermo Effect on Free Convective Flow Past an Impulsively Started Semi- Infinite Moving Vertical Plate with Uniform Heat and Mass Flux

Published in *JP Journal of Heat and Mass Transfer (Scopus)*, **24(1)**, 37-62,
2021.

4.1 Introduction

Buoyancy force occurs due to density variation in fluid mixture. The flow generated by buoyancy force is termed as natural convection or free convection. Tornado, ocean currents, sea breeze, land breeze are some well-known environmental examples of natural convection. Mbledogu et al. (2007) considered the free convective compressible Boussinesq flow under the action of transverse magnetic field. Prasad et al. (2007) and Chandrakala (2010) studied the consequences of free convective flow past an impulsively started infinite vertical plate with uniform heat and mass flux in presence of thermal radiation. Ahmed et al. (2010), Makinde (2005), Samad and Rahman (2006) investigated the effect of natural convection through a porous vertical plate immersed in porous medium while Das and Jana (2010), Hazarika and Ahmed (2021) studied using non-porous vertical plate submerged in porous medium. Vedhanayagam et al. (1980), Martyneko et al. (1984), Kolar and Sastri (1988), Ramanaiah and Malarvizhi (1992), Carmago et al. (1996) studied intensively the behavior of free convective flow near vertical plate or surface under different conditions.

When two non-reacting and chemically different fluids are allowed to diffuse into each other at same temperature, the system generates a heat flux. It is the reverse phenomena of Soret effect. Effect of energy flux due to composition gradient in a chemical system is labeled as diffusion thermo effect or Dufour effect. This effect was discovered by noted Swiss scientist L Dufour in 1873. Eckert and Drake (1972) nicely illustrated this effect in their book. Kafoussias and Williams (1995) studied both Dufour and Soret effects in a mixed free- forced convective heat and mass transfer boundary layer flow problem. Jha and Ajibade (2011) investigated the influence of Dufour effect in a free convective heat and mass transfer flow in a vertical channel. Postelnicu (2004) examined consequences of both Soret and Dufour effects on a vertical surface embedded in porous medium. Ahmed et al. (2013) studied Dufour effect on a transient MHD flow past a uniformly moving porous plate with heat sink. Srinivasacharya et al. (2015) investigated roles of Soret and Dufour effects in a mixed convective heat and mass transfer problem along a wavy surface in porous medium. Ullah et al. (2017) studied unsteady mixed convective flow of Casson fluid over a non-linearly stretching sheet.

The purpose of the present investigation is to study the role of Dufour effect in a free convective flow past an impulsively started vertical moving plate with uniform heat and mass flux. Reviewing the existing literature, we found that no attempt has been made to study this

kind of problem. The governing equations are first normalized and they are solved by applying closed form of Laplace transform technique. Effect of different flow parameters, viz., Prandtl number, Schmidt number, Dufour number, thermal Grashoff number and solutal Grahof number on concentration field, temperature field, velocity field, plate concentration, plate temperature and skin friction are discussed exclusively with the help of graphs.

4.2 Mathematical Analysis

The governing equations of the convective flow of an electrically conducting, incompressible, viscous fluid having constant mass diffusivity and thermal diffusivity considering diffusion- thermo effect are

Continuity equation:

$$\vec{\nabla} \cdot \vec{q} = 0 \quad (4.1)$$

Momentum equation:

$$\rho \left[\frac{\partial \vec{q}}{\partial t'} + (\vec{q} \cdot \vec{\nabla}) \vec{q} \right] = -\vec{\nabla} p + \rho \vec{g} + \mu \nabla^2 \vec{q} \quad (4.2)$$

Energy equation:

$$\rho C_p \left[\frac{\partial T}{\partial t'} + (\vec{q} \cdot \vec{\nabla}) T \right] = \kappa \nabla^2 T + \frac{\rho D_M K_T}{C_s} \nabla^2 C \quad (4.3)$$

Species continuity equation:

$$\frac{\partial C}{\partial t'} + (\vec{q} \cdot \vec{\nabla}) C = D_M \nabla^2 C \quad (4.4)$$

Equation of state as per Boussinesq approximation:

$$\rho_\infty = \rho \left[1 + \beta (T - T_\infty) + \bar{\beta} (C - C_\infty) \right] \quad (4.5)$$

We consider natural convective heat and mass transfer flow of an electrically conducting, incompressible and viscous fluid past a semi- infinite vertical plate with uniform heat and mass flux. Let us introduce a rectangular co- ordinate system (x', y', z', t') with X axis vertically upwards, Y axis normal to the plate directed towards fluid region and Z axis

along the width of the plate. Let $q = (u', 0, 0)$ be the fluid velocity at the point (x', y', z', t') in the fluid.

Initially, the plate and the neighbouring fluid were at rest with uniform temperature T_∞ and concentration C_∞ at all points in the fluid. At time $\bar{t} = 0^+$, the plate suddenly starts to move in its own plane with speed U_0 along X axis. Instantaneously, the temperature and concentration of the plate are raised to $-\frac{q}{\kappa}$ and $-\frac{j''}{D}$ respectively, which are thereafter regarded as constant.

The foremost assumptions to idealize the mathematical model are-

- I. Except the variation in density in the buoyancy force term, all the fluid properties are constant.
- II. Dissipation of energy due to friction and Joule heating are negligible.
- III. Flow is one- dimensional which is parallel to the plate.
- IV. Plate is electrically non- conducting.
- V. No external electric field is applied for which the polarization voltage is negligible.

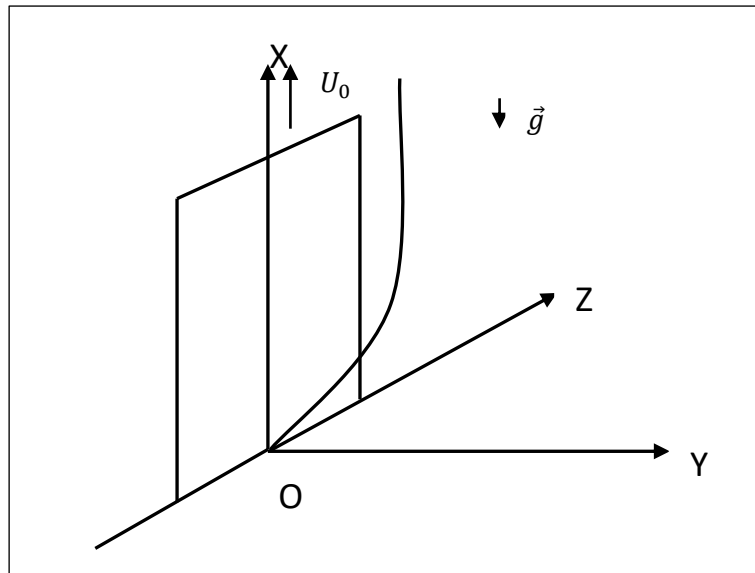


Figure 4.1: Flow Configuration

Equation (4.1) yields,

$$\frac{\partial u'}{\partial x'} = 0$$

$$i.e., u' = u'(y', t')$$
(4.6)

Equation (4.2) reduces to

$$\rho \left[\frac{\partial u'}{\partial t'} \hat{i} + 0 \right] = -\hat{i} \frac{\partial p}{\partial x'} - \hat{j} \frac{\partial p}{\partial y'} - \rho g \hat{i} + \mu \frac{\partial^2 u'}{\partial y'^2} \hat{i}$$
(4.7)

Equation (4.7) gives

$$\rho \frac{\partial u'}{\partial t'} = -\frac{\partial p}{\partial x'} - \rho g + \mu \frac{\partial^2 u'}{\partial y'^2}$$
(4.8)

and

$$0 = -\frac{\partial p}{\partial y'}$$
(4.9)

Equation (4.9) shows that pressure near the plate and pressure far away from the plate is same along the normal to the plate.

For fluid region far away from the plate, equation (4.8) takes the form

$$0 = -\frac{\partial p}{\partial x'} - \rho_\infty g$$
(4.10)

Eliminating $\frac{\partial p}{\partial x'}$ from (4.8) and (4.10), we get

$$\rho \frac{\partial u'}{\partial t'} = (\rho_\infty - \rho) g + \mu \frac{\partial^2 u'}{\partial y'^2}$$
(4.11)

Now, (4.5) gives,

$$\rho_\infty - \rho = \rho \left[\beta(T - T_\infty) + \bar{\beta}(C - C_\infty) \right]$$
(4.12)

Putting value of (4.12) in (4.11),

$$\rho \frac{\partial u'}{\partial t'} = \rho [\beta(T - T_\infty) + \bar{\beta}(C - C_\infty)]g + \mu \frac{\partial^2 u'}{\partial y'^2}$$

$$\text{i.e., } \frac{\partial u'}{\partial t'} = g\beta(T - T_\infty) + g\bar{\beta}(C - C_\infty) + \nu \frac{\partial^2 u'}{\partial y'^2} \quad (4.13)$$

Equation (4.3) yields,

$$\rho C_p \frac{\partial T}{\partial t'} = \kappa \frac{\partial^2 T}{\partial y'^2} + \frac{\rho D_M K_T}{C_s} \frac{\partial^2 C}{\partial y'^2} \quad (4.14)$$

Equation (4.4) yields,

$$\frac{\partial C}{\partial t'} = D_M \frac{\partial^2 C}{\partial y'^2} \quad (4.15)$$

The relevant initial and boundary conditions are:

$$\left. \begin{array}{l} \forall y' \geq 0 : u' = 0, T = T_\infty, C = C_\infty; t' \leq 0 \\ y' = 0 : u' = U_0, \frac{\partial T}{\partial y'} = -\frac{q}{\kappa}, \frac{\partial C}{\partial y'} = -\frac{j''}{D_M}; t' > 0 \\ y' \rightarrow \infty : u' \rightarrow 0, T \rightarrow T_\infty, C \rightarrow C_\infty; t' > 0 \end{array} \right\} \quad (4.16)$$

To normalize the mathematical model of the problem, we introduce the following non- dimensional quantities-

$$Du = \frac{D_M K_T (C_w - C_\infty)}{C_s C_p \nu (T_w - T_\infty)}, u = \frac{u'}{U_0}, y = \frac{y' U_0}{\nu}, t = \frac{t' U_0^2}{\nu}, Gr = \frac{\nu g \beta (T_w - T_\infty)}{U_0^3},$$

$$Gm = \frac{\nu g \bar{\beta} (C_w - C_\infty)}{U_0^3}, \theta = \frac{T - T_\infty}{T_w - T_\infty}, \phi = \frac{C - C_\infty}{C_w - C_\infty}, Pr = \frac{\mu C_p}{\kappa}, Sc = \frac{\nu}{D_M}$$

The non- dimensional governing equations are

$$\frac{\partial u}{\partial t} = \frac{\partial^2 u}{\partial y^2} + Gr\theta + Gm\phi \quad (4.17)$$

$$\frac{\partial \theta}{\partial t} = \frac{1}{Pr} \frac{\partial^2 \theta}{\partial y^2} + Du \frac{\partial^2 \phi}{\partial y^2} \quad (4.18)$$

$$\frac{\partial \phi}{\partial t} = \frac{1}{Sc} \frac{\partial^2 \phi}{\partial y^2} \quad (4.19)$$

Subject to the initial and boundary conditions:

$$\left. \begin{aligned} \forall y \geq 0 : u = 0, \theta = 0, \phi = 0; t \leq 0 \\ y = 0 : u = 1, \frac{\partial \theta}{\partial y} = -1, \frac{\partial \phi}{\partial y} = -1; t > 0 \\ y \rightarrow \infty : u \rightarrow 0, \theta \rightarrow 0, \phi \rightarrow 0; t > 0 \end{aligned} \right\} \quad (4.20)$$

4.3 Method of Solution

Taking Laplace transform of the equations (4.19), (4.18) and (4.17) respectively, we get the following ordinary differential equations:

$$s\bar{\phi} = \frac{1}{Sc} \frac{d^2 \bar{\phi}}{dy^2} \quad (4.21)$$

$$s\bar{\theta} = \frac{1}{Pr} \frac{d^2 \bar{\theta}}{dy^2} + Du \frac{d^2 \bar{\phi}}{dy^2} \quad (4.22)$$

$$s\bar{u} = \frac{d^2 \bar{u}}{dy^2} + Gr\bar{\theta} + Gm\bar{\phi} \quad (4.23)$$

Subject to the initial and boundary conditions:

$$\left. \begin{aligned} y = 0 : \bar{u} = \frac{1}{s}, \frac{d\bar{\theta}}{dy} = -\frac{1}{s}, \frac{d\bar{\phi}}{dy} = -\frac{1}{s} \\ y \rightarrow \infty : \bar{u} \rightarrow 0, \bar{\theta} \rightarrow 0, \bar{\phi} \rightarrow 0 \end{aligned} \right\} \quad (4.24)$$

Solving equations from (4.21) to (4.23) subject to the conditions (4.24) and taking inverse Laplace transform of the solutions, the expression for concentration field ϕ , temperature field θ , and velocity field u are as follows:

$$\phi = \frac{1}{\sqrt{Sc}} m_1 \quad (4.25)$$

$$\theta = \begin{cases} \theta_{1,1} + \theta_{1,2} : Pr \neq Sc \\ \theta_{2,1} + \theta_{2,2} : Pr = Sc \end{cases} \quad (4.26)$$

$$u = \begin{cases} u_{1,1} + u_{1,2} + u_{1,3} + u_{1,4} : \text{Pr} \neq \text{Sc}, \text{Pr} \neq 1, \text{Sc} \neq 1 \\ u_{2,1} + u_{2,2} + u_{2,3} + u_{2,4} : \text{Pr} = \text{Sc} \neq 1 \\ u_{3,1} + u_{3,2} + u_{3,3} + u_{3,4} : \text{Sc} \neq \text{Pr} = 1 \\ u_{4,1} + u_{4,2} + u_{4,3} + u_{4,4} : \text{Pr} \neq \text{Sc} = 1 \\ u_{5,1} + u_{5,2} + u_{5,3} + u_{5,4} : \text{Pr} = \text{Sc} = 1 \end{cases} \quad (4.27)$$

4.4 Plate Concentration

Plate concentration is determined as

$$\phi(0) = \frac{2\sqrt{t}}{\sqrt{\pi \text{Sc}}} \quad (4.28)$$

4.5 Plate Temperature

Plate temperature is found as

$$\theta(0) = \begin{cases} \theta(0)_{1,1} + \theta(0)_{1,2} : \text{Pr} \neq \text{Sc} \\ \theta(0)_{2,1} + \theta(0)_{2,2} : \text{Pr} = \text{Sc} \end{cases} \quad (4.29)$$

4.6 Sherwood Number

The mass flux M_w at the plate $y' = 0$ is characterized by Fick's law of diffusion is given by

$$M_w = -D_M \left. \frac{\partial C}{\partial y'} \right]_{y'=0} \quad (4.30)$$

Equation (4.30) gives

$$Sh = - \left. \frac{\partial \phi}{\partial y} \right]_{y=0} \quad (4.31)$$

In (4.31), $Sh = \frac{M_w \nu}{D_M (C_w - C_\infty) U_0}$ is known as the Sherwood number which is related to the rate of mass transfer at the plate.

Equation (4.31) yields

$$Sh = 1 \quad (4.32)$$

4.7 Nusselt Number

The heat flux q^* at the plate $\bar{y} = 0$ is determined by Fourier's law of conduction is given by

$$q^* = -\kappa_0^* \left. \frac{\partial T}{\partial y'} \right]_{y'=0} \quad (4.33)$$

where $\kappa_0^* = \kappa + \frac{16\sigma^* T_\infty^3}{3\kappa^*}$ is the modified thermal conductivity.

Equation (4.33) yields

$$Nu = - \left. \frac{\partial \theta}{\partial y} \right]_{y=0} \quad (4.34)$$

Where $Nu = \frac{q^* \nu}{\kappa_0^* (T_w - T_\infty) U_0}$ is called the Nusselt number which is correlated to the rate of heat transfer at the plate.

Equation (4.34) gives,

$$Nu = 1 \quad (4.35)$$

4.8 Skin Friction

The viscous drag at the plate $y' = 0$ is specified by Newton's law of viscosity is given by

$$\bar{\tau} = -\mu \left. \frac{\partial u}{\partial y'} \right]_{y'=0} \quad (4.36)$$

Equation (4.36) gives

$$\tau = - \left. \frac{\partial u}{\partial y} \right]_{y=0} \quad (4.37)$$

In (4.37), $\tau = \frac{\bar{\tau} \nu}{\mu U_0^2}$ is denoted as the skin friction or coefficient of friction which is

associated with the rate of momentum transfer at the plate.

Equation (4.38) yields,

$$\tau = - \begin{cases} \tau_{1,1} + \tau_{1,2} + \tau_{1,3} + \tau_{1,4} : \text{Pr} \neq \text{Sc}, \text{Pr} \neq 1, \text{Sc} \neq 1 \\ \tau_{2,1} + \tau_{2,2} + \tau_{2,3} + \tau_{2,4} : \text{Pr} = \text{Sc} \neq 1 \\ \tau_{3,1} + \tau_{3,2} + \tau_{3,3} + \tau_{3,4} : \text{Sc} \neq \text{Pr} = 1 \\ \tau_{4,1} + \tau_{4,2} + \tau_{4,3} + \tau_{4,4} : \text{Pr} \neq \text{Sc} = 1 \\ \tau_{5,1} + \tau_{5,2} + \tau_{5,3} + \tau_{5,4} : \text{Pr} = \text{Sc} = 1 \end{cases} \quad (4.38)$$

4.9 Results and Discussion

The effects of various flow parameters associated with the flow and transport properties are examined by assigning some specific values to variables and parameters. The results are demonstrated from Figures 4.2 to 4.22.

Figure 4.2 and Figure 4.3 display the variation of concentration field versus normal co- ordinate y . Figure 4.2 admits that concentration field keeps on increasing with time. Figure 4.3 reveals that there is a comprehensive fall in concentration field for increasing Schmidt number. Thus, higher mass diffusivity raises concentration field.

Figures 4.4 to 4.7 illustrate the variation of temperature field versus normal co- ordinate y . Figure 4.4 suggests that temperature field escalates with time. Figure 4.5 shows that temperature field upsurges in a thin layer adjacent to the plate and after that its behaviour changes as Schmidt number increases. In other words higher mass diffusivity first decreases temperature field in a thin layer adjacent to the plate and after that its behaviour reverses. Temperature field decelerates with increasing Prandtl number as shown in Figure 4.6. Accordingly, temperature field accelerates with higher thermal diffusivity. Figure 4.7 gives us an idea that temperature field rises with upsurge in Dufour number.

Figures 4.8 to 4.13 depict the variation of velocity field versus normal co- ordinate y . Figure 4.8 reveals that as time progresses, velocity field increases in a small layer adjoining the plate but decreases afterwards. Velocity field declines in a thin layer adjacent to the plate and its behaviour reverses as Schmidt number rises as shown in Figure 4.9. Velocity field falls in a slim layer neighbouring the plate and its nature takes reverse turn outside the layer as Prandtl number upsurges as demonstrated in Figure 4.10. Figure 4.11 exhibits that with increasing Dufour number, velocity field hikes near the plate, but after a critical point its nature reverses. Velocity rises with increment in both thermal Grashof number and solutal Grashof number but after a critical point its behaviour changes as noticed in Figure 4.12 and Figure 4.13 respectively.

Figure 4.14 displays the variation of plate concentration versus time t . It confirms that plate concentration decreases as Schmidt number increases. Thus, higher mass diffusivity raises plate concentration.

Figures 4.15 to 4.17 exhibit the variation of plate temperature versus time t . Figure 4.15 shows that plate temperature raises with increment in Schmidt number. In other words, we can say that higher mass diffusivity lowers temperature field. Enhancement in Prandtl number declines plate temperature as observed in Figure 4.16. Consequently, higher thermal diffusivity hikes plate temperature. Figure 4.17 admits that plate temperature rises considerably as Dufour number upsurges.

Variations of skin friction versus time t are demonstrated from Figures 4.18 to 4.22. Figure 4.18 admits that skin friction lowers as Schmidt number hikes. Thus, skin friction hikes as mass diffusivity increases. Skin friction falls substantially with increasing Prandtl number as observed in Figure 4.19. In other words, we can say that, enhancement in thermal diffusivity leads to rise in skin friction. Skin friction lifts with increment in Dufour number as noticed in Figure 4.20. There is a comprehensive rise in skin friction for increasing thermal Grashof number and solutal Grashof number as observed in Figure 4.21 and Figure 4.22 respectively.

4.10 Conclusions

The prominent outcomes of the present work are as follows:

- i. Both concentration field and temperature field accelerates with time.
- ii. Velocity field upsurges in a thin layer adjacent to the plate with increment in Dufour number, thermal Grashof number and solutal Grashof number and thereafter its behavior reverses.
- iii. Higher mass diffusivity increases plate concentration but decreases plate temperature.
- iv. There is a considerable fall in skin friction for higher Schmidt number and Prandtl number.

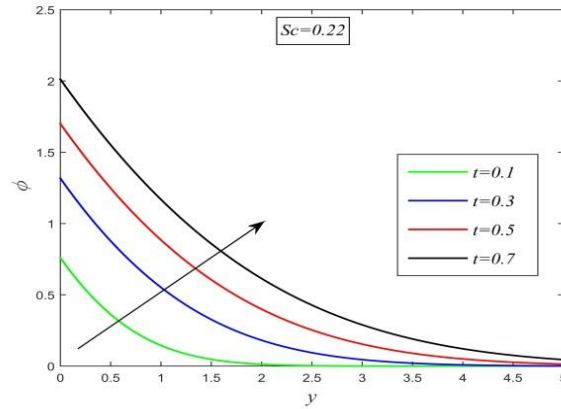


Figure 4.2: Concentration field versus y for different t and $Sc=0.22$

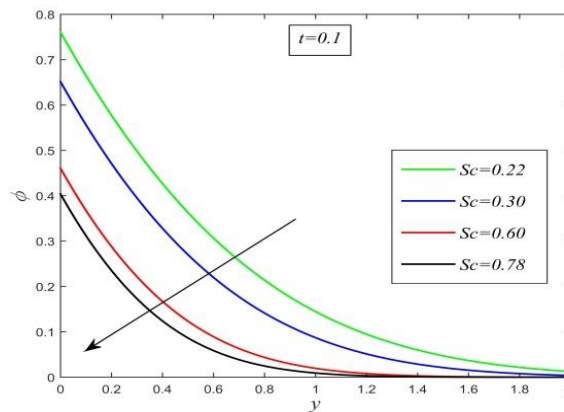


Figure 4.3: Concentration field versus y for different Sc and $t = 0.1$

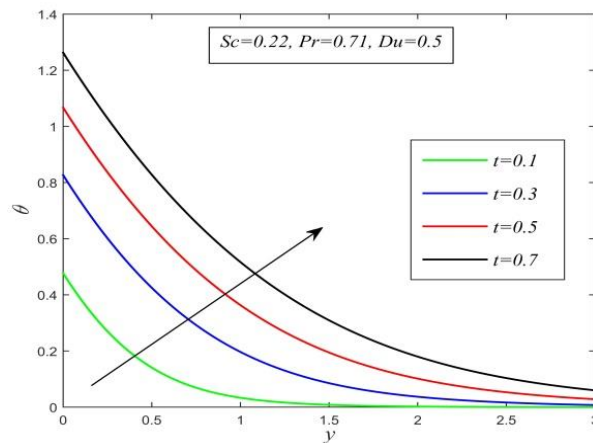


Figure 4.4: Temperature field versus y for different t and $Sc=0.22, Pr=0.71, Du=0.5$

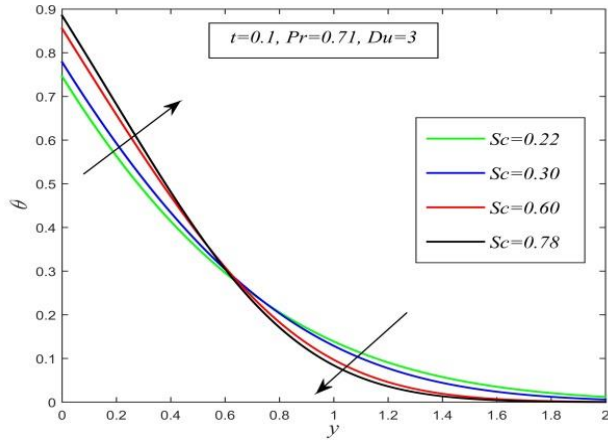


Figure 4.5: Temperature field versus y for different Sc and $t=0.1$, $Pr=0.71$, $Du=3$

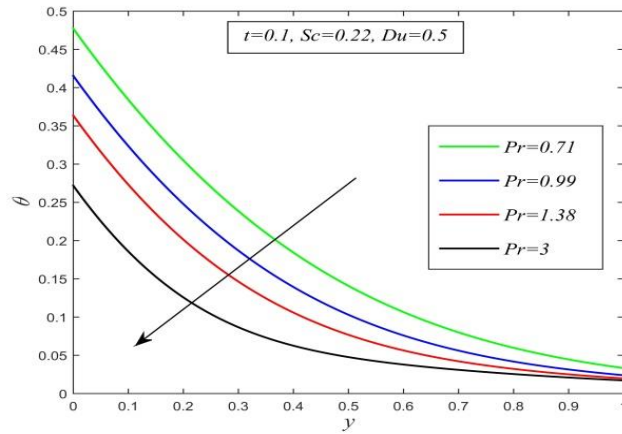


Figure 4.6: Temperature field versus y for different Pr and $t=0.1$, $Sc=0.22$, $Du=0.5$

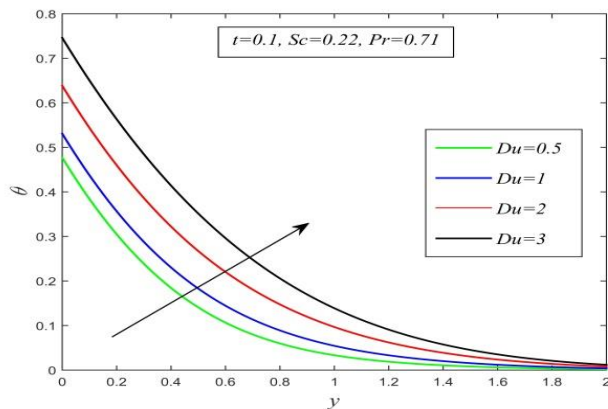


Figure 4.7: Temperature field versus y for different Du and $t=0.1$, $Sc=0.22$, $Pr=0.71$

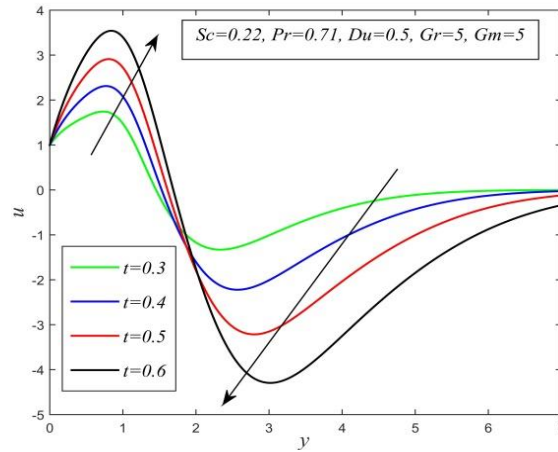


Figure 4.8: Velocity field versus y for different t and $Sc=0.22, Pr=0.71, Du=0.5, Gr=5, Gm=5$

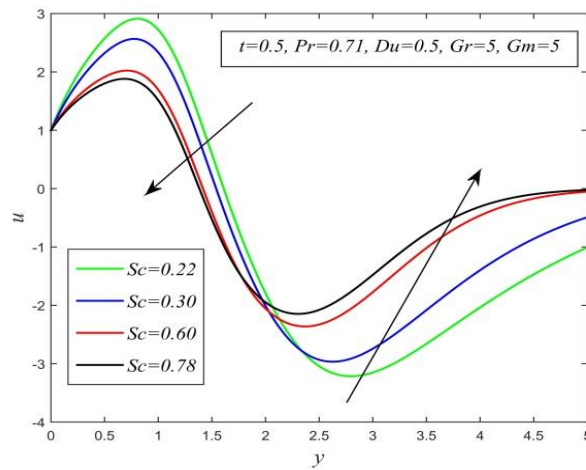


Figure 4.9: Velocity field versus y for different Sc and $t=0.5, Pr=0.71, Du=0.5, Gr=5, Gm=5$

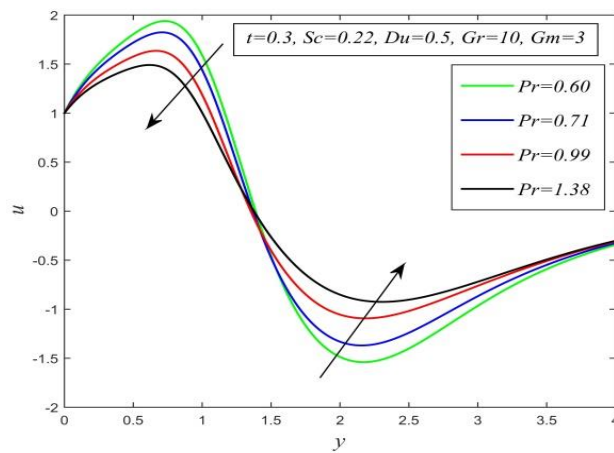


Figure 4.10: Velocity field versus y for different Pr and $t=0.3, Sc=0.22, Du=0.5, Gr=10, Gm=3$

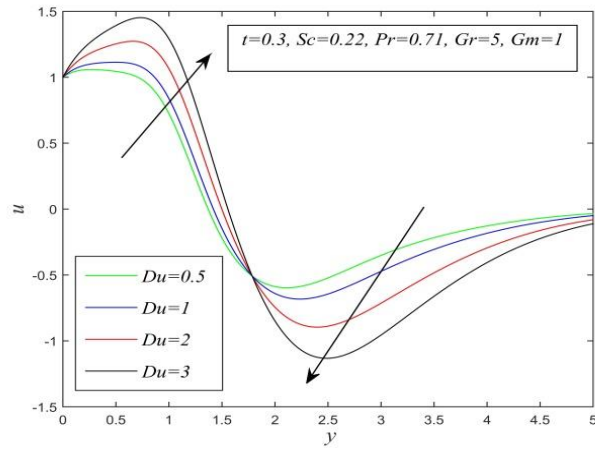


Figure 4.11: Velocity field versus y for different Du and $t=0.3, Sc=0.22, Pr=0.71, Gr=5, Gm=1$

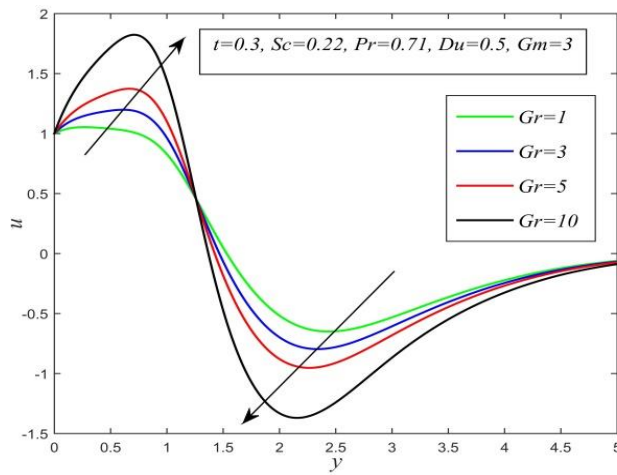


Figure 4.12: Velocity field versus y for different Gr and $t=0.3, Sc=0.22, Pr=0.71, Du=0.5, Gm=3$

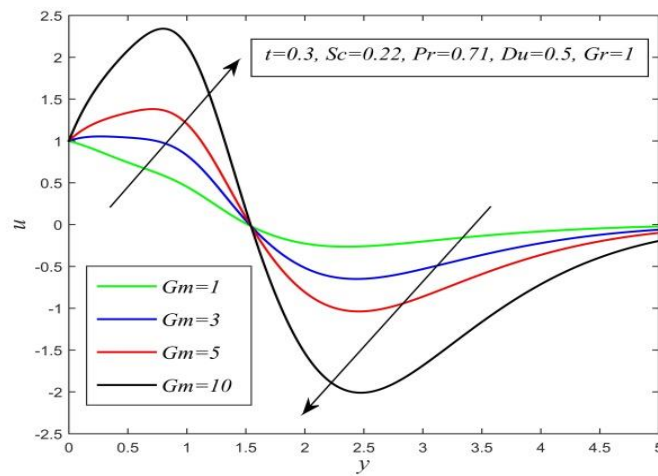


Figure 4.13: Velocity field versus y for different Gm and $t=0.3, Sc=0.22, Pr=0.71, Du=0.5, Gr=1$

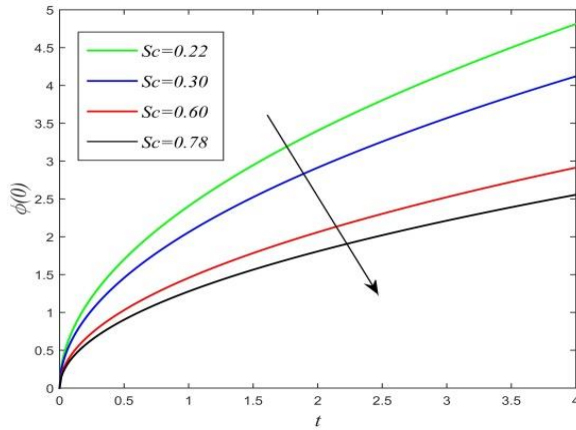


Figure 4.14: Plate concentration versus t for different Sc

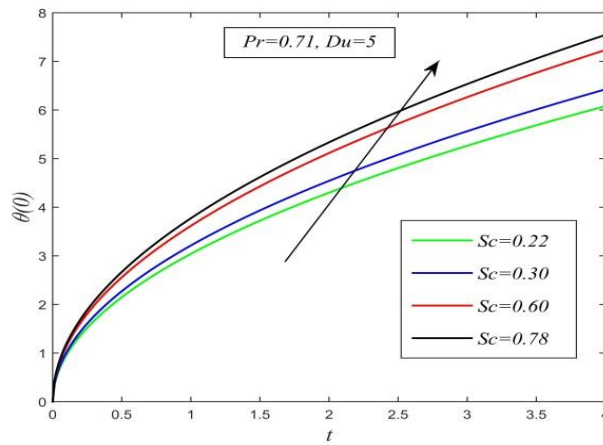


Figure 4.15: Plate temperature versus t for different Sc and $Pr=0.71, Du=5$

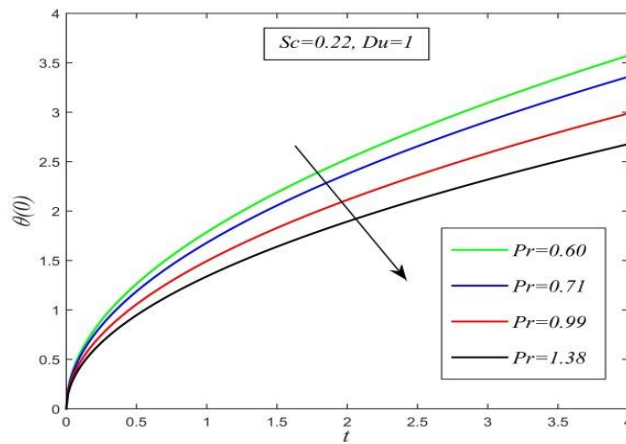


Figure 4.16: Plate temperature versus t for different Pr and $Sc=0.22, Du=1$

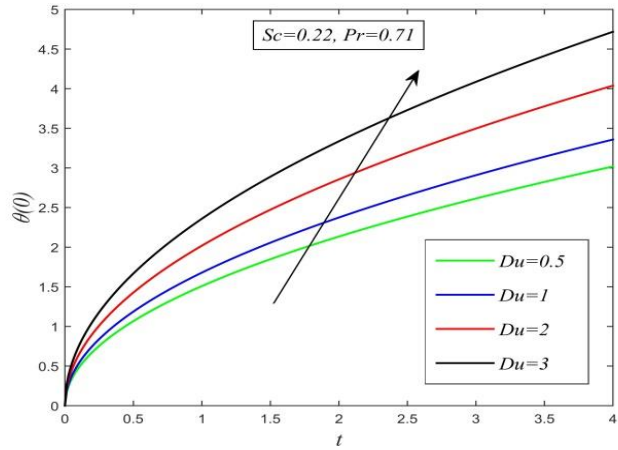


Figure 4.17: Plate temperature versus t for different Du and $Sc=0.22, Pr=0.71$

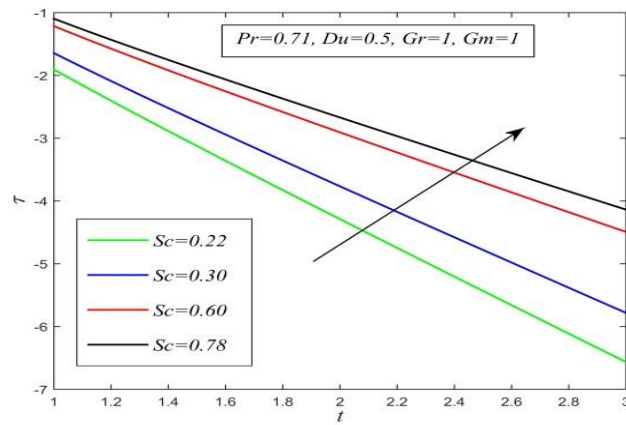


Figure 4.18: Skin friction versus t for different Sc and $Pr=0.71, Du=0.5, Gr=1, Gm=1$

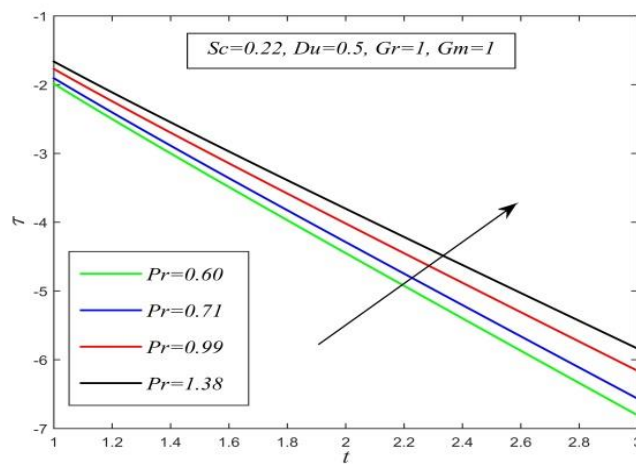


Figure 4.19: Skin friction versus t for different Pr and $Sc=0.22, Du=0.5, Gr=1, Gm=1$

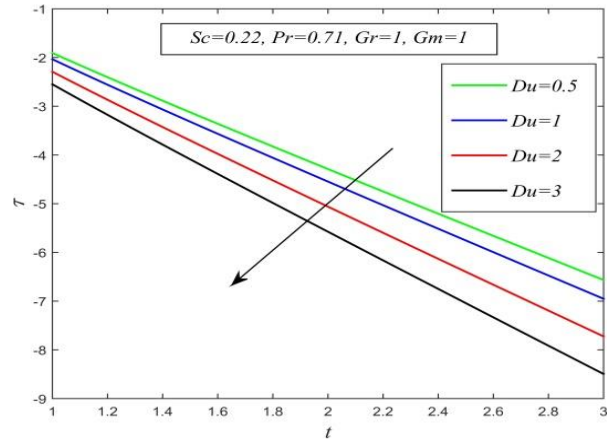


Figure 4.20: Skin friction versus t for different Du and $Sc=0.22, Pr=0.71, Gr=1, Gm=1$

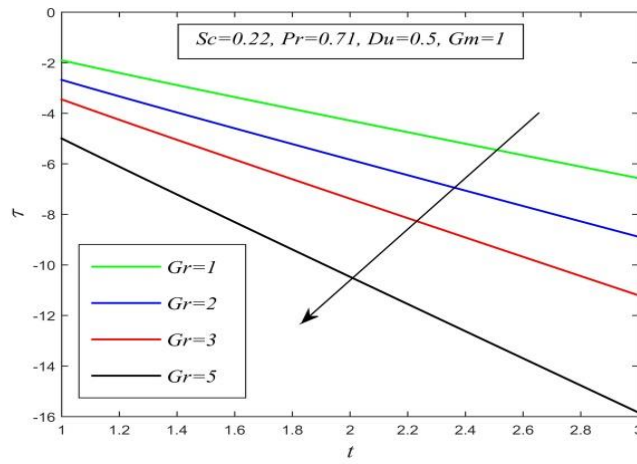


Figure 4.21: Skin friction versus t for different Gr and $Sc=0.22, Pr=0.71, Du=0.5, Gm=1$

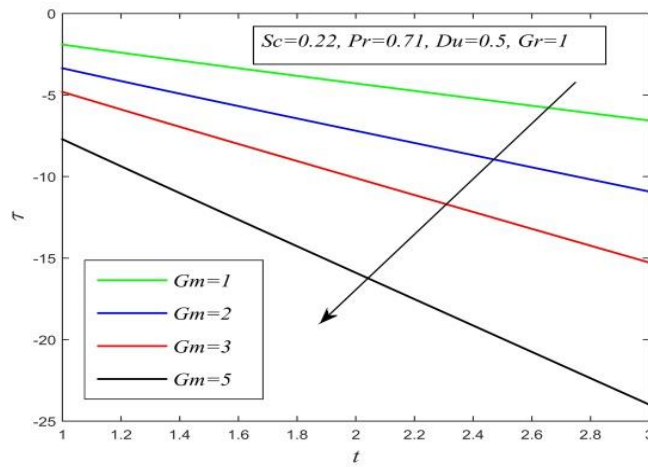


Figure 4.22: Skin friction versus t for different Gm and $Sc=0.22, Pr=0.71, Du=0.5, Gr=1$

Nomenclature:

C : Molar species concentration

C_p : Specific heat at constant pressure

C_s : Concentration susceptibility

C_∞ : Concentration far away from the plate

C_w : Iso-solutal plate concentration

D_M : Mass diffusivity

Du : Dufour number

\vec{g} : Gravitation acceleration vector

g : Gravitational acceleration

Gr : Thermal Grashof number

Gm : Solutal Grashof number

K_T : Thermal diffusion ratio

p : Pressure

Pr : Prandtl number

\vec{q} : Fluid velocity vector

Sc : Schmidt number

Sr : Soret number

t' : Time

T : Fluid temperature

T_∞ : Undisturbed temperature

T_w : Wall temperature

u' : X-component of fluid velocity

U_0 : Plate velocity

Greek Symbols:

μ : Coefficient of viscosity

ρ : Fluid density

ρ_∞ : Fluid density far away from the plate

κ : Thermal conductivity

κ^* : Mean absorption constant

κ : Thermal conductivity

β : Volumetric coefficient of thermal expansion

$\bar{\beta}$: Volumetric coefficient of solutal expansion

ν : Kinematic viscosity

Subscripts:

w : Refers to physical quantity at the plate

∞ : Refers to physical quantity far away from the plate

Appendix

$$\begin{aligned}
m_1 &= m(y\sqrt{Sc}, t), \xi = \frac{Du \Pr \sqrt{Sc}}{\Pr - Sc}, \theta_{1,1} = \frac{1 - \xi \sqrt{Sc}}{\sqrt{\Pr}} m_2, m_2 = m(y\sqrt{\Pr}, t), \theta_{1,2} = \xi m_1, \theta_{2,1} = Du \sqrt{\Pr} m_2, \\
\theta_{2,2} &= Du \sqrt{Sc} m_1, u_{1,1} = u_{1,1,1} - u_{1,1,2} - u_{1,1,3} - u_{1,1,4}, u_{1,1,1} = E_1, E_1 = \operatorname{erfc}(\eta), \eta = \frac{y}{2\sqrt{t}}, u_{1,1,2} = A_1 n_1, \\
A_1 &= -\frac{Gr(1 - \xi \sqrt{Sc})}{(\Pr - 1)\sqrt{\Pr}}, n_1 = n(y, t), u_{1,1,3} = A_2 n_1, A_2 = -\frac{Gr\xi}{Sc - 1}, u_{1,1,4} = A_3 n_1, A_3 = -\frac{Gm}{(Sc - 1)\sqrt{Sc}}, \\
u_{1,2} &= A_1 n_2, n_2 = n(y\sqrt{\Pr}, t), u_{1,3} = A_2 n_3, n_3 = n(y\sqrt{Sc}, t), u_{1,4} = A_3 n_3, u_{2,1} = u_{2,1,1} - u_{2,1,2} - u_{2,1,3} - u_{2,1,4}, \\
u_{2,1,1} &= u_{1,1,1}, u_{2,1,2} = A_4 n_1, A_4 = -\frac{Gr(1 + Du \Pr)}{(\Pr - 1)\sqrt{\Pr}}, u_{2,1,3} = A_5 n_1, A_5 = -\frac{Du Gr \sqrt{Sc}}{Sc - 1}, u_{2,1,4} = u_{1,1,4}, u_{2,2} = A_4 n_2, \\
u_{2,3} &= A_5 n_3, u_{2,4} = u_{1,4}, u_{3,1} = u_{3,1,1} - u_{3,1,2} - u_{3,1,3} - u_{3,1,4}, u_{3,1,1} = u_{1,1,1}, u_{3,1,2} = A_6 n_1, A_6 = \frac{Gr(Sc(Du + 1) - 1)}{1 - Sc}, \\
u_{3,1,3} &= A_7 n_1, A_7 = \frac{Gr Du \sqrt{Sc}}{(Sc - 1)^2}, u_{3,1,4} = u_{1,1,4}, u_{3,2} = A_6 n_1, u_{3,3} = A_7 n_3, u_{3,4} = u_{1,4}, u_{4,1} = u_{4,1,1} - u_{4,1,2} - u_{4,1,3} - u_{4,1,4}, \\
u_{4,1,1} &= u_{1,1,1}, u_{4,1,2} = A_8 n_1, A_8 = \frac{Gr(\Pr(Du - 1) + 1)}{(\Pr - 1)^2 \sqrt{\Pr}}, u_{4,1,3} = A_9 n_1, A_9 = \frac{Gr Du \Pr}{2(1 - \Pr)\sqrt{Sc}}, u_{4,1,4} = A_{10} n_1, \\
A_{10} &= -Gm, u_{4,2} = A_8 n_2, u_{4,3} = A_9 n_1, u_{4,4} = A_3 n_1, u_{5,1} = u_{5,1,1} - u_{5,1,2} - u_{5,1,3} - u_{5,1,4}, u_{5,1,1} = u_{1,1,1}, u_{5,1,2} = A_{11} n_1, \\
A_{11} &= -Gr(1 + Du), u_{5,1,3} = A_{12} n_1, A_{12} = -\frac{Du Gr}{2}, u_{5,1,4} = u_{4,1,4}, u_{5,2} = u_{5,1,2}, u_{5,3} = u_{5,1,3}, u_{5,4} = u_{4,4} \\
\theta(0)_{1,1} &= \frac{2\sqrt{t}(1 - \xi \sqrt{Sc})}{\sqrt{\pi \Pr}}, \theta(0)_{1,2} = 2\xi \sqrt{\frac{t}{\pi}}, \theta(0)_{2,1} = 2Du \sqrt{\frac{t \Pr}{\pi}}, \theta(0)_{2,2} = 2Du \sqrt{\frac{t Sc}{\pi}} \\
\tau_{1,1} &= \tau_{1,1,1} - \tau_{1,1,2} - \tau_{1,1,3} - \tau_{1,1,4}, \tau_{1,1,1} = \alpha_1, \alpha_1 = \alpha \left(\frac{1}{2\sqrt{t}} \right), \tau_{1,1,2} = -A_1 t, \tau_{1,1,3} = -A_2 t, \tau_{1,1,4} = -A_3 t, \\
\tau_{1,2} &= -A_1 t \sqrt{\Pr}, \tau_{1,3} = -A_2 t \sqrt{Sc}, \tau_{1,4} = -A_3 t \sqrt{Sc}, \tau_{2,1} = \tau_{2,1,1} - \tau_{2,1,2} - \tau_{2,1,3} - \tau_{2,1,4}, \tau_{2,1,1} = \alpha_1, \tau_{2,1,2} = -A_4 t, \\
\tau_{2,1,3} &= -A_5 t, \tau_{2,1,4} = \tau_{1,1,4}, \tau_{2,2} = -A_4 t \sqrt{\Pr}, \tau_{2,3} = -A_5 t \sqrt{Sc}, \tau_{2,4} = \tau_{1,4}, \tau_{3,1} = \tau_{3,1,1} - \tau_{3,1,2} - \tau_{3,1,3} - \tau_{3,1,4}, \\
\tau_{3,1,1} &= \tau_{1,1,1}, \tau_{3,1,2} = -A_6 t, \tau_{3,1,3} = -A_7 t, \tau_{3,1,4} = \tau_{1,1,4}, \tau_{3,2} = \tau_{3,1,2}, \tau_{3,3} = -A_7 t \sqrt{Sc}, \tau_{3,4} = \tau_{1,4}, \\
\tau_{4,1} &= \tau_{4,1,1} - \tau_{4,1,2} - \tau_{4,1,3} - \tau_{4,1,4}, \tau_{4,1,1} = \tau_{1,1,1}, \tau_{4,1,2} = -A_8 t, \tau_{4,1,3} = -A_9 t, \tau_{4,1,4} = -A_{10} t, \tau_{4,2} = -A_8 t \sqrt{\Pr}, \\
\tau_{4,3} &= \tau_{4,1,3}, \tau_{4,4} = -A_3 t, \tau_{5,1} = \tau_{5,1,1} - \tau_{5,1,2} - \tau_{5,1,3} - \tau_{5,1,4}, \tau_{5,1,1} = \tau_{1,1,1}, \tau_{5,1,2} = -A_{11} t, \tau_{5,1,3} = -A_{12} t, \\
\tau_{5,1,4} &= \tau_{4,1,4}, \tau_{5,2} = \tau_{5,1,2}, \tau_{5,3} = \tau_{5,1,3}, \tau_{5,4} = \tau_{4,4}
\end{aligned}$$

(The functions are defined in **Chapter I**)

CHAPTER V

Dufour Effect on Unsteady MHD Flow Past a Vertical Plate Embedded in Porous Medium with Ramped Temperature

Published in *Scientific Reports, Nature* (Scopus, SCIE), **12**(1), 2022.

5.1 Introduction

The branch of physics that deals with the interaction of the magnetic field with electrically conducting fluid are termed as Magnetohydrodynamics (MHD). Saltwater, liquid metals, plasmas, electrolytes are some common examples of such fluids. Noted Swiss scientist Hannes Alfvén (1942) initiated the field of MHD for which he received the Nobel prize in physics in the year 1970. But, due to substantial contributions from other authors like Cowling (1957), Shercliff (1965), Ferraro and Plumpton (1966), Roberts (1967), Cramer and Pai (1973), etc., MHD is at present form. There are several applications of MHD in modern technologies. Geophysical and astrophysical applications of MHD are nicely elaborated by Dormy and Nunez (2007). Dynamo, motor, fusion reactors, dispersion of metals, metallurgy, etc. are some engineering applications of MHD. Aeronautical applications of MHD were studied exclusively by Li et al. (2017). Farrokhi et al. (2019) studied biomedical applications of MHD.

Change in fluid temperature and species concentration generates density variation in the fluid mixture. This variation develops buoyancy forces that act on the fluid. The flow produced due to the buoyancy force is termed free convection or natural convection. Manh et al. (2020), Das and Ahmed (1992), Kafoussias (1992), Kumar and Singh (2013), etc. studied the effect of free convection on various MHD problems.

The porous medium contains holes or voids that are filled with solid particles which let the fluid pass through it. The mechanism of porous flow finds its applications in inkjet printing, nuclear waste disposal, electro-chemistry, combustion technology, etc. Dwivedi et al. (2018) studied MHD flow through the vertical channel in a porous medium while Raju et al. (2014) observed the MHD flow through horizontal channel taking viscous dissipation and Joule heating into account. Free convection in the porous media was investigated by Helmy (1998), Raju and Varma (2011), Pattnaik and Biswal (2015), Sinha et al. (2017), Basha and Nagarathna (2019).

Radiation is a form of heat transfer by electromagnetic waves. Many environmental and industrial procedures encounters with radiative convective flows. Flows of this kind take crucial role in space technology and high temperature activities. This influence many authors to perform model research on free convection with thermal radiation in several hydrodynamic and magnetohydrodynamic problems under various physical and geometrical conditions.

Mbeldogu et al. (2007), Makinde (2005), Samad and Rahman (2006), Orhan and Ahmet (2008), Prasad et al. (2006), Ahmed and Dutta (2014), Takhar et al. (1996), Seth et al. (2016), Balla and Naikoti (2015), Siviah et al. (2012) are some worth mentioning researchers in this area.

The effect of chemical reaction carries a great practical significance in heat and mass transfer problems. So, many researchers studied applications of chemical reaction in different MHD flow problems. Apelblat (1982) investigated chemical reaction effect in a mass transfer problem with axial diffusion. Mahapatra et al. (2010) examined the effects of chemical reaction in a free convective flow in a porous media surrounded by a vertical surface. Andersson et al. (1994) and Takhar et al. (2000) considered the diffusion of a chemically reactive species from a stretching sheet while Ganesan and Rani (2000) studied the diffusion of chemically reactive species through a vertical cylinder. Muthucumaraswamy and Ganesan (2001), Kandasamy et al. (2005), Raptis and Perdikis (2006), etc. investigated the effects of chemical reaction in various MHD problems. Arifuzzaman et al. (2018) studied chemically reactive and naturally convective high speed MHD flow through an oscillating vertical porous plate.

If two non-reacting and chemically different fluids are allowed to diffuse into each other at the same temperature, the system produces a heat flux. Effect of flux due to composition gradient is defined as Dufour effect or diffusion thermo effect. Renowned Swiss scientist L. Dufour discovered this effect in 1873. This effect is nicely elaborated by Eckert and Drake (1972). Swetha et al. (2015) analyzed Dufour and radiation effects on a free convective flow in a porous medium. Reddy et al. (2016) studied both Soret and Dufour effects of an MHD flow past a moving vertical plate immersed in a porous medium taking Hall current and rotating system into account. Oyekunle and Agunbiade (2020) explored the consequences of the Dufour and Soret effect of MHD flow on an inclined magnetic field. Kumaresan et al. (2018) analytically investigated the Dufour effect on unsteady free convective flow past an accelerated vertical plate. Vijaya Kumar et al. (2013) studied Dufour and radiation effects on a free convective MHD flow past an infinite vertical plate in presence of chemical reaction. Shateyi et al. (2010) studied the effects of Soret, Dufour, Hall current and radiation of a mixed convective flow in a porous medium. Postelnicu (2004) examined the consequences of both Soret and Dufour effects on a vertical surface embedded in a porous medium.

The present investigation aims to analyse the role of the diffusion thermo effect in a free convective, radiative, and chemically reacting fluid in a porous medium with arbitrary ramped temperature. Reviewing the existing literature, we found that no work has been done taking Dufour effect and ramped temperature with arbitrary characteristic time simultaneously in a flow past an exponentially started vertical plate. The governing equations are first converted to non-dimensional partial differential equations using some dimensionless quantities. A closed-form of the Laplace transform technique is adopted to solve the equations. Effects of different flow parameters like Prandtl number, Schmidt number, magnetic parameter, thermal Grashof number, solutal Grashof number, Dufour number, chemical reaction parameter, radiation parameter, porosity parameter, etc. on temperature field, concentration field, velocity field, Nusselt number, Sherwood number, and skin friction are discussed graphically. The obtained results are also verified with previously published work.

5.2 Mathematical Analysis

Equations that govern the convective flow of an electrically conducting, incompressible, viscous, chemically reactive, and radiating fluid in a porous medium in presence of a magnetic field having constant mass diffusivity and thermal diffusivity taking the diffusion- thermo effect into account are

Continuity equation:

$$\vec{\nabla} \cdot \vec{q} = 0 \quad (5.1)$$

Magnetic field continuity equation:

$$\vec{\nabla} \cdot \vec{B} = 0 \quad (5.2)$$

Ohm's Law:

$$\vec{J} = \sigma (\vec{E} + \vec{q} \times \vec{B}) \quad (5.3)$$

Momentum equation:

$$\rho \left[\frac{\partial \vec{q}}{\partial t'} + (\vec{q} \cdot \vec{\nabla}) \vec{q} \right] = -\vec{\nabla} p + \vec{J} \times \vec{B} + \rho \vec{g} + \mu \nabla^2 \vec{q} - \frac{\mu \vec{q}}{K^*} \quad (5.4)$$

Energy equation:

$$\rho C_p \left[\frac{\partial T}{\partial t'} + (\vec{q} \cdot \vec{\nabla}) T \right] = \kappa \nabla^2 T - \vec{\nabla} \cdot \vec{q}_r + \frac{\rho D_M K_T}{C_s} \nabla^2 C \quad (5.5)$$

Species continuity equation:

$$\frac{\partial C}{\partial t'} + (\vec{q} \cdot \vec{\nabla}) C = D_M \nabla^2 C + \bar{K} (C_\infty - C) \quad (5.6)$$

Equation of state as per Boussinesq approximation:

$$\rho_\infty = \rho \left[1 + \beta (T - T_\infty) + \bar{\beta} (C - C_\infty) \right] \quad (5.7)$$

The radiation heat flux as per Rosseland approximation is given by

$$\vec{q}_r = -\frac{4\sigma^*}{3\kappa^*} \vec{\nabla} T^4$$

Now,

$$T^4 = (T - T_\infty + T_\infty)^4 = 4TT_\infty^3 - 3T_\infty^4, \text{ as } |T - T_\infty| \ll 1$$

So,

$$\vec{\nabla} \cdot \vec{q}_r = -\frac{16\sigma^* T_\infty^3}{3\kappa^*} \nabla^2 T$$

Therefore, Energy equation (5.5) reduces to

$$\rho C_p \left[\frac{\partial T}{\partial t'} + (\vec{q} \cdot \vec{\nabla}) T \right] = \kappa \nabla^2 T + \frac{16\sigma^* T_\infty^3}{3\kappa^*} \nabla^2 T + \frac{\rho D_M K_T}{C_s} \nabla^2 C \quad (5.8)$$

We now consider a transient MHD free convection flow of a viscous incompressible electrically conducting fluid through a porous medium past a semi-infinite vertical plate in presence of a uniform magnetic field applied normal to the plate, directed into the fluid region. Initially, the plate and the surrounding fluid were at rest with uniform temperature T_∞ and concentration C_∞ at all points in the fluid. At time $t' > 0$, the plate is exponentially accelerated with velocity $U_0 e^{at'}$. The plate temperature is instantaneously elevated to

$T_\infty + (T_w - T_\infty) \frac{t'}{t_0}$, for $0 < t' \leq t_0$, and thereafter T_w when $t' > t_0$. The concentration is raised to C_w and maintained thereafter.

To idealize the mathematical model, we enforce the following constraints-

- I. Except the variation in density in the buoyancy force term, all the fluid properties are constant.
- II. Energy dissipation occurring from friction and Joule heating is negligible.
- III. Compared to applied magnetic field, induced magnetic field is negligible.
- IV. Flow is one- dimensional which is parallel to the plate.
- V. The plate is electrically insulating.
- VI. Polarization voltage is negligible because no external electric field is applied.

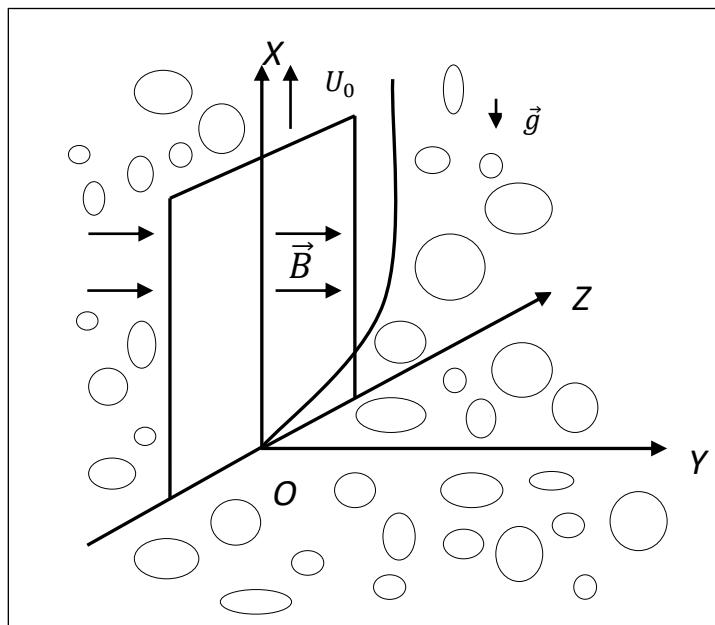


Figure 5.1: Flow configuration

We now consider a tri- rectangular Cartesian co-ordinate system (x', y', z', t') with X axis vertically upwards along the plate, Y axis normal to the plate directed into the fluid region, and Z axis along the width of the plate as displayed in Fig1. Let $\vec{q} = (u', 0, 0)$ be the fluid velocity and $\vec{B} = (0, B_0, 0)$ be the magnetic induction vector at the point (x', y', z', t') in the fluid.

Equation (5.1) yields,

$$\frac{\partial u'}{\partial x'} = 0 \quad (5.9)$$

i.e., u' = u'(y', t')

Equation (5.2) is trivially satisfied by $\vec{B} = (0, B_0, 0)$

Equation (5.4) reduces to

$$\rho \left[\frac{\partial u'}{\partial t'} \hat{i} + 0 \right] = -\hat{i} \frac{\partial p}{\partial x'} - \hat{j} \frac{\partial p}{\partial y'} - \rho g \hat{i} - \sigma B_0^2 u' \hat{i} + \mu \frac{\partial^2 u'}{\partial y'^2} \hat{i} - \frac{\mu u'}{K^*} \hat{i} \quad (5.10)$$

Equation (5.10) gives

$$\rho \frac{\partial u'}{\partial t'} = -\frac{\partial p}{\partial x'} - \rho g - \sigma B_0^2 u' + \mu \frac{\partial^2 u'}{\partial y'^2} - \frac{\mu u'}{K^*} \quad (5.11)$$

And

$$0 = -\frac{\partial p}{\partial y'} \quad (5.12)$$

Equation (5.12) shows that pressure near the plate and pressure far away from the plate are the same along the normal to the plate.

For fluid region far away from the plate, equation (5.11) takes the form

$$0 = -\frac{\partial p}{\partial x'} - \rho_\infty g \quad (5.13)$$

Eliminating $\frac{\partial p}{\partial x'}$ from (5.11) and (5.13), we get,

$$\rho \frac{\partial u'}{\partial t'} = (\rho_\infty - \rho) g - \sigma B_0^2 u' + \mu \frac{\partial^2 u'}{\partial y'^2} - \frac{\mu u'}{K^*} \quad (5.14)$$

Now, (5.7) gives,

$$\rho_\infty - \rho = \rho \left[\beta (T - T_\infty) + \bar{\beta} (C - C_\infty) \right] \quad (5.15)$$

Putting value of (5.15) in (5.14),

$$\rho \frac{\partial u'}{\partial t'} = \rho [\beta(T - T_\infty) + \bar{\beta}(C - C_\infty)]g - \sigma B_0^2 u' + \mu \frac{\partial^2 u'}{\partial y'^2} - \frac{\mu u'}{K^*}$$

$$i.e., \frac{\partial u'}{\partial t'} = g\beta(T - T_\infty) + g\bar{\beta}(C - C_\infty) - \frac{\sigma B_0^2 u'}{\rho} + \nu \frac{\partial^2 u'}{\partial y'^2} - \nu \frac{u'}{K^*} \quad (5.16)$$

Equation (5.8) yields,

$$\rho C_p \frac{\partial T}{\partial t'} = \kappa \frac{\partial^2 T}{\partial y'^2} + \frac{16\sigma^* T_\infty^3}{3\kappa^*} \frac{\partial^2 T}{\partial y'^2} + \frac{\rho D_M K_T}{C_S} \frac{\partial^2 C}{\partial y'^2} \quad (5.17)$$

Equation (5.6) becomes,

$$\frac{\partial C}{\partial t'} = D_M \frac{\partial^2 C}{\partial y'^2} + \bar{K}(C_\infty - C) \quad (5.18)$$

The relevant initial and boundary conditions are:

$$\left. \begin{aligned} u' = 0, T = T_\infty, C = C_\infty : \forall y' \geq 0; t' \leq 0 \\ u' = U_0 e^{at'}, C = C_w : y' = 0, t' > 0 \\ T = T_\infty + (T_w - T_\infty) \frac{t'}{t_0} : \bar{y} = 0; 0 < t' \leq t_0 \\ T = T_w : y' = 0; t' > t_0 \\ u' \rightarrow 0, T \rightarrow T_\infty, C \rightarrow C_\infty : y' \rightarrow \infty; t' > 0 \end{aligned} \right\} \quad (5.19)$$

For the sake of normalization of the mathematical model of the problem, we introduce the following non-dimensional quantities-

$$Du = \frac{D_M K_T (C_w - C_\infty)}{C_S C_P (T_w - T_\infty) \nu}, N = \frac{\kappa \kappa^*}{4\sigma^* T_\infty^3}, u = \frac{u'}{U_0}, y = \frac{U_0}{\nu} y', t = \frac{U_0^2}{\nu} t', Gr = \frac{\nu g \beta (T_w - T_\infty)}{U_0^3}, a = a' \frac{\nu}{U_0^2},$$

$$Gm = \frac{\nu g \bar{\beta} (C_w - C_\infty)}{U_0^3}, \theta = \frac{T - T_\infty}{T_w - T_\infty}, \phi = \frac{C - C_\infty}{C_w - C_\infty}, Pr = \frac{\mu C_p}{\kappa}, M = \frac{\sigma B_0^2 \nu}{\rho U_0^2}, Sc = \frac{\nu}{D_M}, \Lambda = 1 + \frac{4}{3N},$$

$$K = \frac{\nu \bar{K}}{U_0^2}, t_1 = \frac{U_0^2}{\nu} t_0, M_1 = M + \frac{1}{K^*}$$

The non-dimensional governing equations are

$$\frac{\partial u}{\partial t} = \frac{\partial^2 u}{\partial y^2} + Gr\theta + Gm\phi - M_1 u \quad (5.20)$$

$$\frac{\partial \theta}{\partial t} = \frac{\Lambda}{Pr} \frac{\partial^2 \theta}{\partial y^2} + Du \frac{\partial^2 \phi}{\partial y^2} \quad (5.21)$$

$$\frac{\partial \phi}{\partial t} = \frac{1}{Sc} \frac{\partial^2 \phi}{\partial y^2} - K\phi \quad (5.22)$$

Subject to the initial and boundary conditions

$$\left. \begin{aligned} u = 0, \theta = 0, \phi = 0 : \forall y \geq 0; t \leq 0 \\ u = e^{at}, \phi = 1 : y = 0, t > 0 \\ \theta = \frac{t}{t_1} : y = 0; 0 < t \leq t_1 \\ \theta = 1 : y = 0; t > t_1 \\ u \rightarrow 0, \theta \rightarrow 0, \phi \rightarrow 0 : y \rightarrow \infty; t > 0 \end{aligned} \right\} \quad (5.23)$$

5.3 Method of Solution

On taking Laplace transform of the equations (5.22), (5.21), and (5.20) respectively, we get the following equations:

$$s\bar{\phi} = \frac{1}{Sc} \frac{d^2 \bar{\phi}}{dy^2} - K\bar{\phi} \quad (5.24)$$

$$s\bar{\theta} = \frac{\Lambda}{Pr} \frac{d^2 \bar{\theta}}{dy^2} + Du \frac{d^2 \bar{\phi}}{dy^2} \quad (5.25)$$

$$s\bar{u} = \frac{d^2 \bar{u}}{dy^2} + Gr\bar{\theta} + Gm\bar{\phi} - M_1 \bar{u} \quad (5.26)$$

Subject to the initial and boundary conditions:

$$\left. \begin{aligned} y = 0 : \bar{\theta} = \frac{2}{s^2 t_1} (1 - e^{-st_1}), \bar{\phi} = \frac{1}{s}, \bar{u} = \frac{1}{s-a} \\ y \rightarrow \infty : \bar{\theta} \rightarrow 0, \bar{\phi} \rightarrow 0, \bar{u} \rightarrow 0 \end{aligned} \right\} \quad (5.27)$$

Solving equations from (5.24) to (5.26) subject to the conditions (5.27) and taking inverse Laplace transform of the solutions, the expression for temperature field θ , concentration field ϕ , and velocity field u are as follows:

$$\phi = \psi_1 \quad (5.28)$$

$$\theta = \begin{cases} \theta_{1,1} + \theta_{1,2} - \theta_{1,3} : \Lambda Sc \neq Pr \\ \theta_{2,1} + \theta_{2,2} - \theta_{2,3} : \Lambda Sc = Pr \end{cases} \quad (5.29)$$

$$u = \begin{cases} u_{1,1} + u_{1,2} + u_{1,3} + u_{1,4} + u_{1,5} : Pr \neq \Lambda, Sc \neq 1, Pr \neq \Lambda Sc \\ u_{2,1} + u_{2,2} + u_{2,3} + u_{2,4} + u_{2,5} : Pr = \Lambda, Sc \neq 1 \\ u_{3,1} + u_{3,2} + u_{3,3} + u_{3,4} + u_{3,5} : Pr \neq \Lambda, Sc = 1 \\ u_{4,1} + u_{4,2} + u_{4,3} + u_{4,4} + u_{4,5} : Pr = \Lambda, Sc = 1 \\ u_{5,1} + u_{5,2} + u_{5,3} + u_{5,4} + u_{5,5} : Pr \neq \Lambda, Sc \neq 1, Pr = \Lambda Sc \end{cases} \quad (5.30)$$

5.4 Nusselt Number

The heat flux q^* at the plate $y' = 0$ is obtained by Fourier's law of conduction is given by

$$q^* = -\kappa_0^* \left. \frac{\partial T}{\partial y'} \right]_{y'=0} \quad (5.31)$$

where $\kappa_0^* = \kappa + \frac{16\sigma^* T_\infty^3}{3\kappa^*}$ is the modified thermal conductivity.

Equation (5.31) yields

$$Nu = - \left. \frac{\partial \theta}{\partial y} \right]_{y=0} \quad (5.32)$$

where $Nu = \frac{q^* \nu}{\kappa_0^* U_0 (T_w - T_\infty)} = \frac{3Nq^* \nu}{\kappa(4+3N)(T_w - T_\infty)U_0}$ is called the Nusselt number which is

concerned with the rate of heat transfer at the plate.

Equation (5.32) gives,

$$Nu = - \begin{cases} Nu_{1,1} + Nu_{1,2} - Nu_{1,3} : \Lambda Sc \neq Pr \\ Nu_{2,1} + Nu_{2,2} - Nu_{2,3} : \Lambda Sc = Pr \end{cases} \quad (5.33)$$

5.5 Sherwood Number

The mass flux M_w at the plate $y' = 0$ is specified by Fick's law of diffusion is given by

$$M_w = -D_M \left. \frac{\partial C}{\partial y'} \right]_{y'=0} \quad (5.34)$$

Equation (5.34) gives

$$Sh = - \left. \frac{\partial \phi}{\partial y} \right]_{y=0} \quad (5.35)$$

In (5.35), $Sh = \frac{M_w \nu}{D_M U_0 (C_w - C_\infty)}$ is called the Sherwood number which is associated with the rate of mass transfer at the plate.

Equation (5.35) yields

$$Sh = -\Omega_1 \quad (5.36)$$

5.6 Skin Friction

The viscous drag at the plate $y' = 0$ is determined by Newton's law of viscosity is given by

$$\bar{\tau} = -\mu \left. \frac{\partial u}{\partial y'} \right]_{y'=0} \quad (5.37)$$

Equation (5.37) gives

$$\tau = - \left. \frac{\partial u}{\partial y} \right]_{y=0} \quad (5.38)$$

In (5.38), $\tau = \frac{\bar{\tau} \nu}{\mu U_0^2}$ is called the skin friction or coefficient of friction which is associated with the rate of momentum transfer at the plate.

Equation (5.38) yields,

$$\tau = - \begin{cases} \tau_{1,1} + \tau_{1,2} + \tau_{1,3} + \tau_{1,4} + \tau_{1,5} : \text{Pr} \neq \Lambda, \text{Sc} \neq 1, \text{Pr} \neq \Lambda \text{Sc} \\ \tau_{2,1} + \tau_{2,2} + \tau_{2,3} + \tau_{2,4} + \tau_{2,5} : \text{Pr} = \Lambda, \text{Sc} \neq 1 \\ \tau_{3,1} + \tau_{3,2} + \tau_{3,3} + \tau_{3,4} + \tau_{3,5} : \text{Pr} \neq \Lambda, \text{Sc} = 1 \\ \tau_{4,1} + \tau_{4,2} + \tau_{4,3} + \tau_{4,4} + \tau_{4,5} : \text{Pr} = \Lambda, \text{Sc} = 1 \\ \tau_{5,1} + \tau_{5,2} + \tau_{5,3} + \tau_{5,4} + \tau_{5,5} : \text{Pr} \neq \Lambda, \text{Sc} \neq 1, \text{Pr} = \Lambda \text{Sc} \end{cases} \quad (5.39)$$

5.7 Results and Discussion

The effects of various flow parameters associated with the flow and transport properties are examined by assigning some specific values. The results are demonstrated from Figures 5.2 to 5.35.

Figures 5.2 to 5.4 display the variation of concentration field versus normal coordinate y . Figure 5.2 admits that the concentration field keeps on increasing with time. Figure 5.3 reveals that there is a comprehensive fall in the concentration field for increasing chemical reaction parameter. A faster chemical reaction consumes chemical substances present in the fluid rapidly and as a result concentration of the fluid declines. The behaviour of concentration profiles for various fluids such as hydrogen ($Sc=0.22$), helium ($Sc=0.30$), water vapour ($Sc=0.60$) and ammonia ($Sc=0.78$) are demonstrated in Figure 5.4. It suggests that a higher Schmidt number lowers the concentration field. Thus higher mass diffusivity hikes the concentration field.

Figures 5.5 to 5.10 illustrate the variation of temperature field versus normal coordinate y . Figure 5.5 suggests that the temperature field escalates with time. Figure 5.6 shows that the temperature field upsurges with increment in chemical reaction parameter. Increasing chemical reaction parameter upsurges collision between fluid molecules and as a result temperature of fluid hikes. Figure 5.7 displays that increasing the Dufour number hikes temperature field. An increment in the Dufour number indicates a comprehensive rise in concentration gradient over temperature gradient. Hence, increasing concentration gradient upsurges the temperature field. Figure 5.8 suggests that the temperature field elevates with uplift in Schmidt number. Thus, the temperature field decreases with increasing mass diffusivity. The temperature field decelerates with increasing radiation parameter as noticed in Figure 5.9. It is in agreement with the fact that radiation tends to decline temperature. The nature of temperature profiles for various fluids such as oxygen ($Pr=0.60$), air ($Pr=0.71$), ammonia ($Pr=1.38$) etc. are demonstrated in Figure 5.10. It shows that the temperature field

falls with ascending values of the Prandtl number. This informs that the temperature field accelerates with higher thermal diffusivity.

Figures 5.11 to 5.20 depict the variation of velocity field versus normal co-ordinate y . Figure 5.11 reveals that as time progresses, the velocity field increases. Figure 5.12 admits that the velocity field declines considerably as the Dufour number rises. Consequently, a large concentration gradient relative to the temperature gradient results in a dip in the velocity field. Figure 5.13 shows that velocity reduces with increasing chemical reaction parameter. This is because increasing chemical reaction parameter accelerates the process of collision between fluid molecules and as a result, kinetic energy is lost. Velocity falls with increasing magnetic parameter as noticed in Figure 5.14. Application of transverse magnetic field produces a resistive force known as Lorentz force, which slows down fluid velocity. Figure 5.15 exhibits that increasing Schmidt number decrease velocity field. Thus, high mass diffusivity escalates fluid velocity. Velocity field upsurges in a thin layer adjacent to the plate and its nature take reverse turn outside the layer as thermal Grashof number upsurges as demonstrated in Figure 5.16. So, thermal buoyancy force hikes velocity in a small layer surrounding the plate but lowers velocity outside the layer. Velocity rises with increment in solutal Grashof number as noticed in Figure 5.17. Thus, solutal buoyancy force upsurges velocity. Hence higher mass diffusivity raises velocity field but increasing thermal diffusivity reduces velocity. Increasing porosity parameter means the fluid gets more free space to flow. As a result fluid velocity hikes. This phenomenon is reflected in Figure 5.18. Increasing radiation parameter accelerates fluid velocity as observed in Figure 5.19. The reason behind it is that when the radiation increases, chemical bonding between the fluid molecules becomes weak so that velocity hikes. Figure 5.20 shows that ascending values of Prandtl number uplift velocity. Thus, higher thermal diffusivity diminishes velocity.

Figures 5.21 and 5.22 demonstrate the variation of Sherwood number versus time t . Sherwood number increases with increment in chemical reaction parameter as noticed in Figure 5.11. From Figure 5.22, it is observed that increasing Schmidt number upsurges Sherwood number. This result establishes the fact that higher mass diffusivity accelerates the process of mass transfer from the plate to the fluid.

Figures 5.23 to 5.27 exhibit the variation of Nusselt number versus time t . Nusselt number increases for a small time but decreases thereafter for increasing radiation parameter as noticed in Figure 5.23. Thus, radiation increases the rate of heat transfer from the plate to

the fluid for a small time and decreases afterward. Figure 5.24 shows that the Nusselt number hikes for a small time but declines thereafter with ascending values of the Prandtl number. So, higher thermal diffusivity lessens the rate of heat transfer for a small time but increases as time progresses. From Figure 5.25 and Figure 5.27, it is observed that the Nusselt number declines for a small time but upsurges thereafter with increment in Dufour number and Schmidt number respectively. Figure 5.26 show that higher chemical reaction parameter hikes Nusselt number. Increasing chemical reaction parameter suggests a hike in heat generation. So, the process of heat transfer is accelerated.

Variations of skin friction versus time t are demonstrated from Figures 5.28 to 5.35. Figure 5.28 admits that there is a comprehensive rise in skin friction as Dufour number hikes. Thus, the concentration gradient generates more frictional resistance compared to the temperature gradient. Skin friction uplifts with increment in thermal Grashof number as noticed in Figure 5.29. Thus, thermal buoyancy force hikes frictional resistivity at the plate. Skin friction hikes with an upsurge in both chemical reaction parameter and porosity parameter as shown in Figure 5.30 and Figure 5.31 respectively. Figure 5.32 reveals that increasing magnetic parameter raises skin friction. Hence Lorentz force accelerates frictional resistivity of the plate. Higher Schmidt number hikes skin friction as displayed in Figure 5.33. Therefore, increasing mass diffusivity lowers the frictional resistance of the plate. Figure 5.34 and Figure 5.35 give us an idea that enhancement in radiation parameter and Prandtl number lowers skin friction.

Numerical values of Nusselt number Nu against different time t , Dufour number Du and radiation parameter are analyzed in Table 5.1. It is observed that for a small time, the Nusselt number decreases with increment in Dufour number but its behaviour reverses as time progresses. An opposite behaviour is noticed for increasing radiation parameter. This asserts that a high concentration gradient decelerates but radiation accelerates the process of heat transfer from the plate to the fluid. This is in complete agreement with our results from Figure 5.23 and Figure 5.25. Numerical values of skin friction τ against different time t , chemical reaction parameter K , radiation parameter N , Dufour number Du , thermal Grashof number Gr and solutal Grashof number Gm are demonstrated in Table 5.2. It is noticed that ascending values of time, chemical reaction parameter, Dufour number and thermal Grashof number hike skin friction whereas ascending values of radiation parameter and solutal Grashof number declines the value of skin friction. This is in accordance with our result from Figure 5.30, Figure 5.28, Figure 5.29 and Figure 5.34 respectively.

5.8 Comparison of Results

To check the validity of our result, we have compared one of our results with Seth et al. (2016b) who considered the unsteady free convective MHD flow of a chemically reactive, radiative flow past a moving vertical plate immersed in a porous medium. In absence of Dufour and chemical reaction effects and for vanishing Schmidt number (i.e., $Du=0$, $K=0$ and $Sc=0$), expression of temperature field of the present problem is

$$\theta = \theta_{1,1}$$

Figure 5.36 and Figure 5.37 display the temperature field versus normal co- ordinate y for different t_1 obtained by Seth et al. (2016b) and present author respectively. Both figures uniquely expresses the fact that temperature field declines for ascending values of critical time of rampedness. Hence, an excellent agreement of results between present author and Seth et al. (2016b) is observed.

Table 5.3 display the variation of Sherwood number for different K , Sc and t obtained by Asogwa et al. (2021), Seth et al. (2014), Kataria and Patel (2019) and present author respectively. This table indicates that current study is in line with the results obtained by these authors.

5.9 Conclusions

The prime purpose of the present work was to study exclusively the effects of radiation, chemical reaction and Diffusion thermo effect of an unsteady MHD flow past a moving vertical plate embedded in a porous medium with ramped temperature. The behavioural study of flow and transport characteristics under the action of different parameters was carried out with aid of graphs. The prominent outcomes of the present work are as follows:

- i. Velocity field, concentration field, and temperature field accelerate with time.
- ii. Fluid gets thinner rapidly as chemical reaction parameter and Schmidt number hikes.
- iii. Radiation and Lorentz force resists fluid velocity.
- iv. Higher mass diffusivity results in a fall in Nusselt Number, Sherwood number, and skin friction.
- v. Radiation slows down rate of momentum transfer.

The solution of the present work also validates with the previous result obtained by Seth et al. (2016b), Asogwa et al. (2021), Seth et al. (2014) and Kataria and Patel (2019) in particular case.

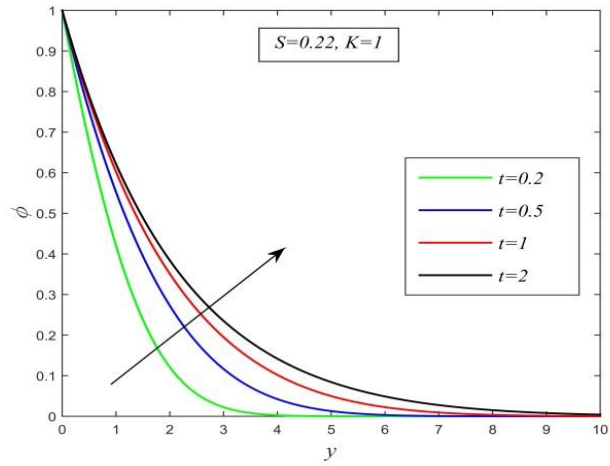


Figure 5.2: Concentration field versus y for different t and $Sc=0.22, K=1$

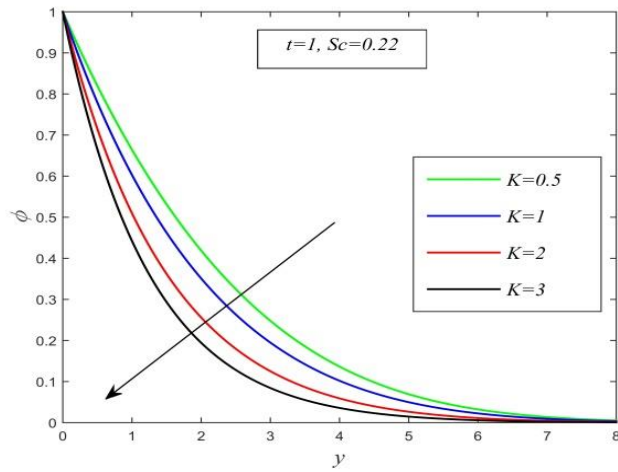


Figure 5.3: Concentration field versus y for different K and $t=1, Sc=0.22$

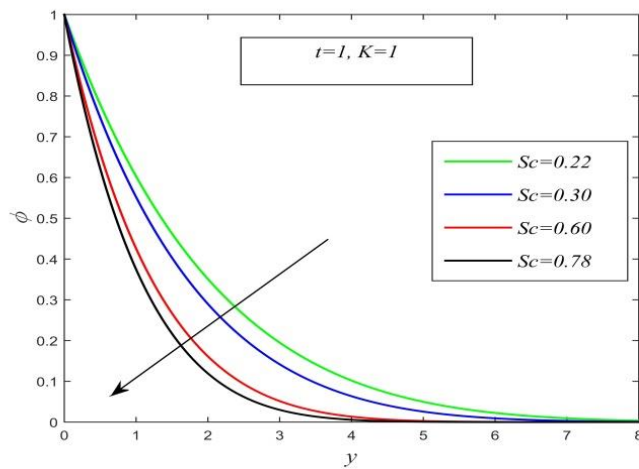


Figure 5.4: Concentration field versus y for different Sc and $t=1, K=0.22$

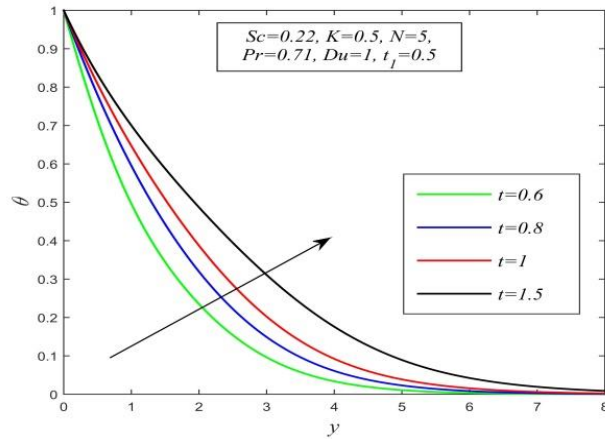


Figure 5.5: Temperature field versus y for different t and $Sc=0.22$, $K=0.5$, $N=5$, $Pr=0.71$, $Du=1$, $t_1=0.5$

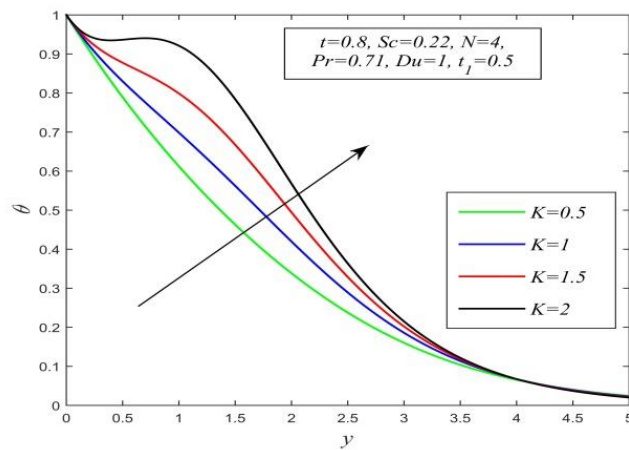


Figure 5.6: Temperature field versus y for different K and $t=0.8$, $Sc=0.22$, $N=4$, $Pr=0.71$, $Du=1$, $t_1=0.5$

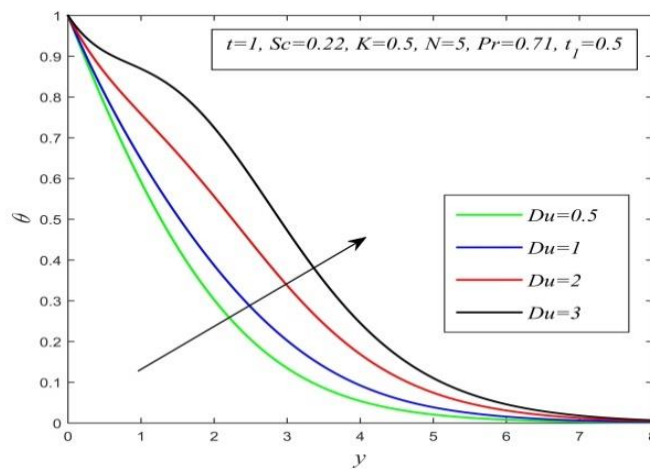


Figure 5.7: Temperature field versus y for different Du and $t=1$, $Sc=0.22$, $K=0.5$, $N=5$, $Pr=0.71$, $t_1=0.5$

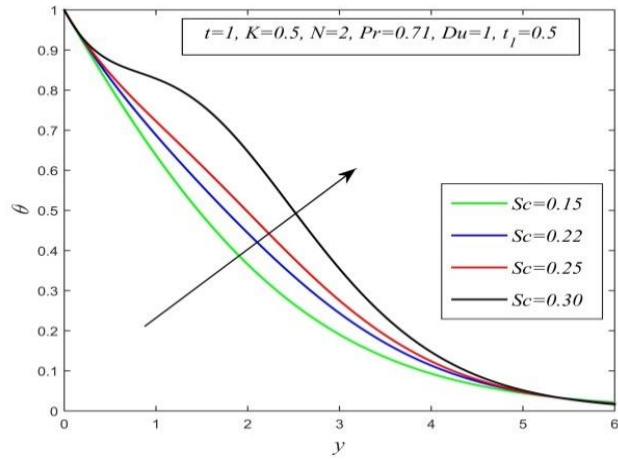


Figure 5.8: Temperature field versus y for different Sc and $t=1, K=0.5, N=2, Pr=0.71, Du=1, t_1=0.5$

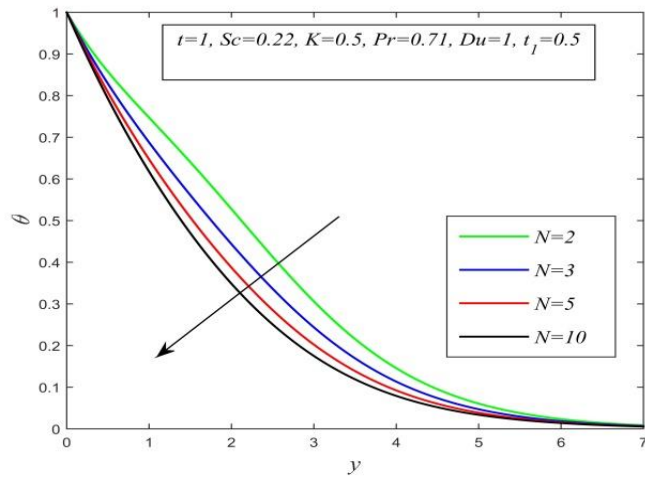


Figure 5.9: Temperature field versus y for different N and $t=1, Sc=0.22, K=0.5, Pr=0.71, Du=1, t_1=0.5$

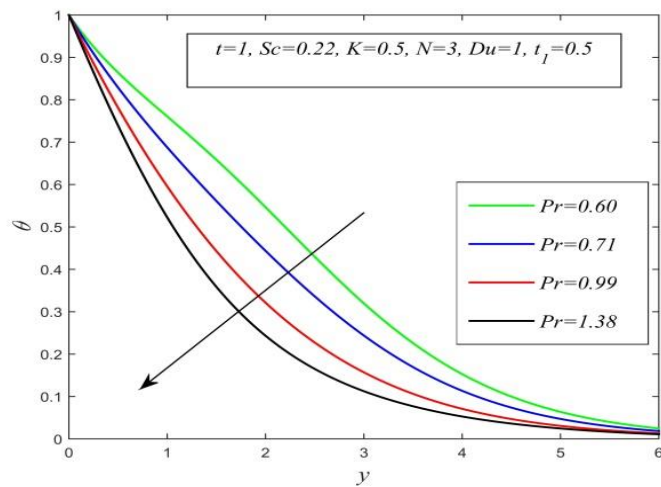


Figure 5.10: Temperature field versus y for different Pr and $t=1, Sc=0.22, K=0.5, N=3, Du=1, t_1=0.5$

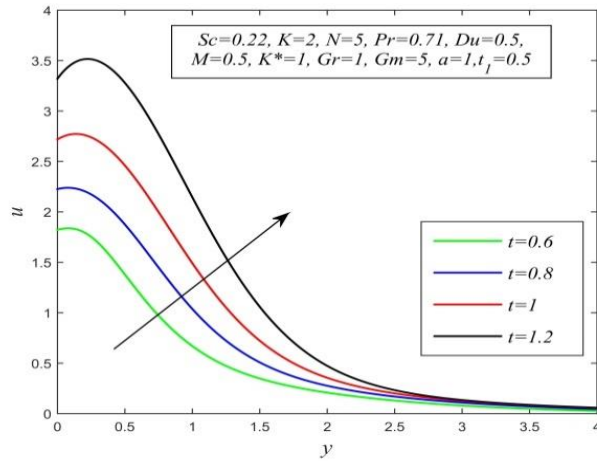


Figure 5.11: Velocity field versus y for different t and $Sc=0.22$, $K=2$, $N=5$, $Pr=0.71$, $Du=0.5$, $M=0.5$, $K^*=1$, $Gr=1$, $Gm=10$, $a=1$, $t_1=0.5$

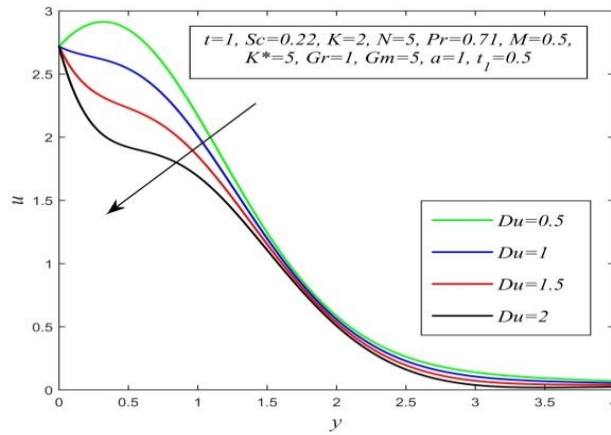


Figure 5.12: Velocity field versus y for different Du and $t=1$, $Sc=0.22$, $K=2$, $N=5$, $Pr=0.71$, $M=0.5$, $K^*=1$, $Gr=1$, $Gm=5$, $a=1$, $t_1=0.5$

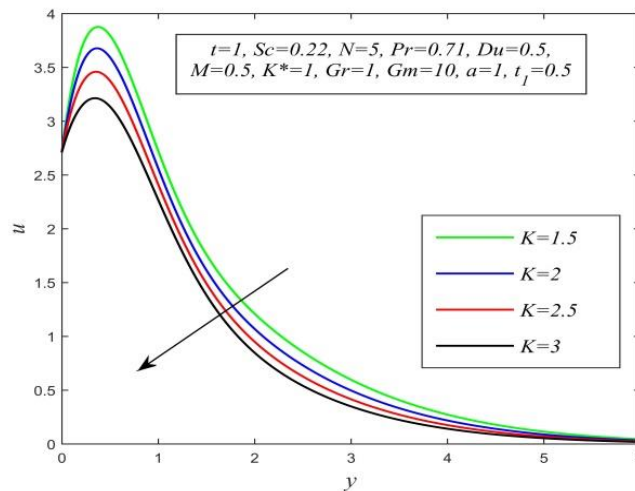


Figure 5.13: Velocity field versus y for different K and $t=1$, $Sc=0.22$, $N=5$, $Pr=0.71$, $Du=0.5$, $M=0.5$, $K^*=1$, $Gr=1$, $Gm=10$, $a=1$, $t_1=0.5$

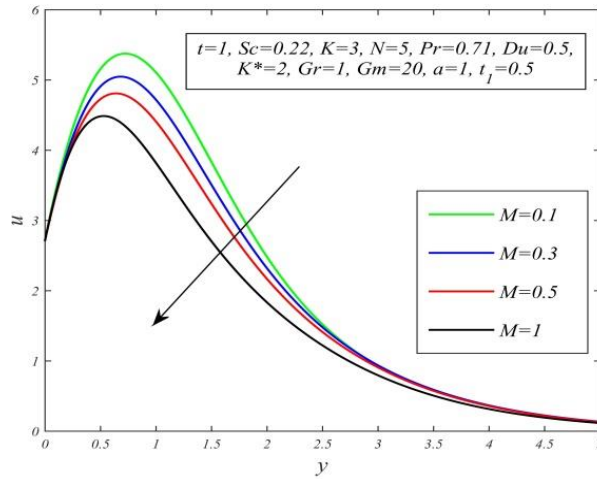


Figure 5.14: Velocity field versus y for different M and $t=1, Sc=0.22, K=3, N=5, Pr=0.71, Du=0.5, K^*=2, Gr=1, Gm=20, a=1, t_1=0.5$

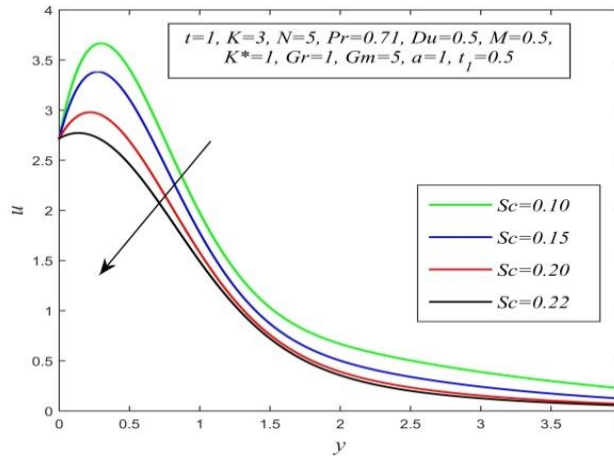


Figure 5.15: Velocity field versus y for different Sc and $t=1, K=3, N=5, Pr=0.71, Du=0.5, M=0.5, K^*=1, Gr=1, Gm=10, a=1, t_1=0.5$

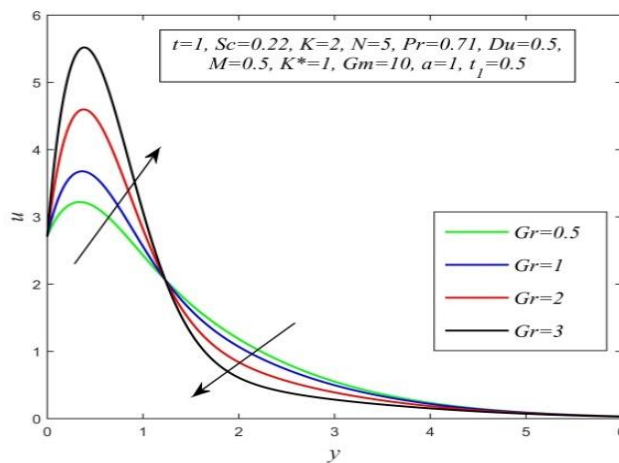


Figure 5.16: Velocity field versus y for different Gr and $t=1, Sc=0.22, K=2, N=5, Pr=0.71, Du=0.5, M=0.5, K^*=1, Gm=10, a=1, t_1=0.5$

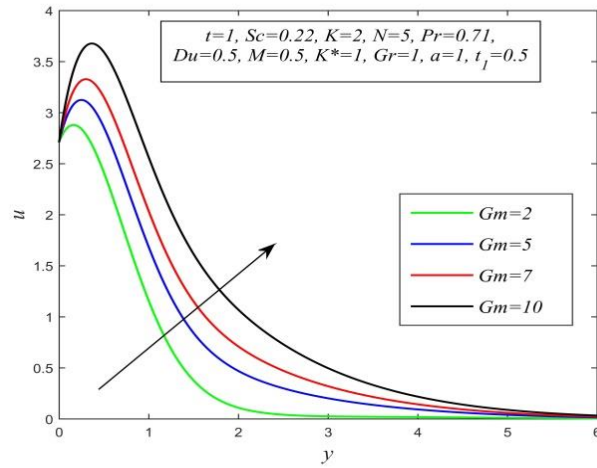


Figure 5.17: Velocity field versus y for different Gm and $t=1, Sc=0.22, K=2, N=5, Pr=0.71, Du=0.5, M=0.5, K^*=1, Gr=1, a=1, t_1=0.5$

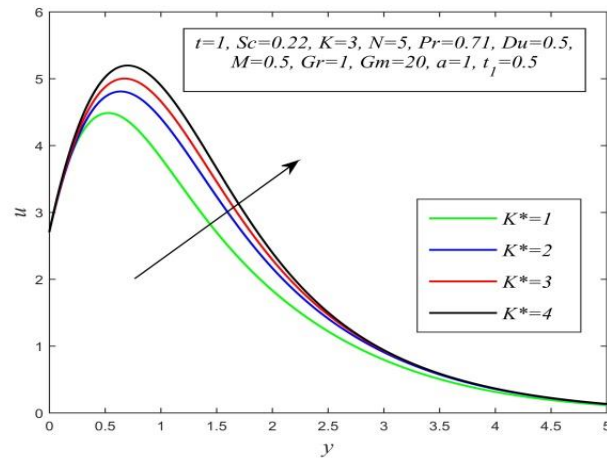


Figure 5.18: Velocity field versus y for different K^* and $t=1, Sc=0.22, K=3, N=5, Pr=0.71, Du=0.5, M=0.5, Gr=1, Gm=20, a=1, t_1=0.5$

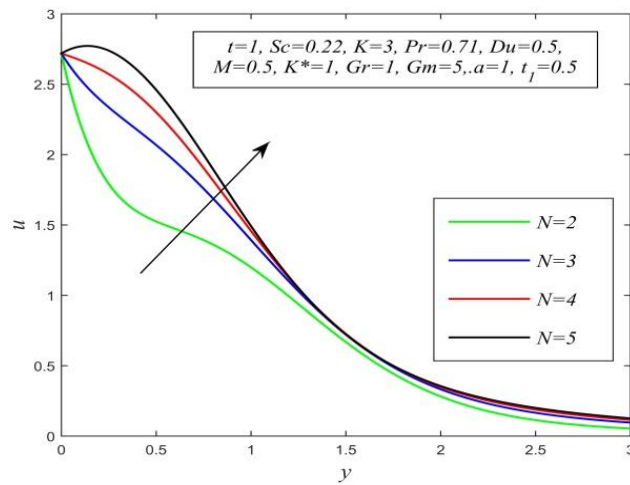


Figure 5.19: Velocity field versus y for different N and $t=1, Sc=0.22, K=3, Pr=0.71, Du=0.5, M=0.5, K^*=1, Gr=1, Gm=5, a=1, t_1=0.5$

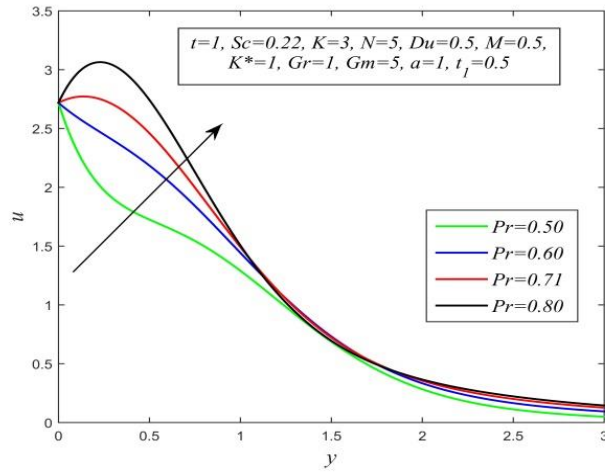


Figure 5.20: Velocity field versus y for different Pr and $t=1$, $Sc=0.22$, $K=3$, $N=5$, $Du=0.5$, $M=0.5$, $K^*=1$, $Gr=1$, $Gm=5$, $a=1$, $t_1=0.5$

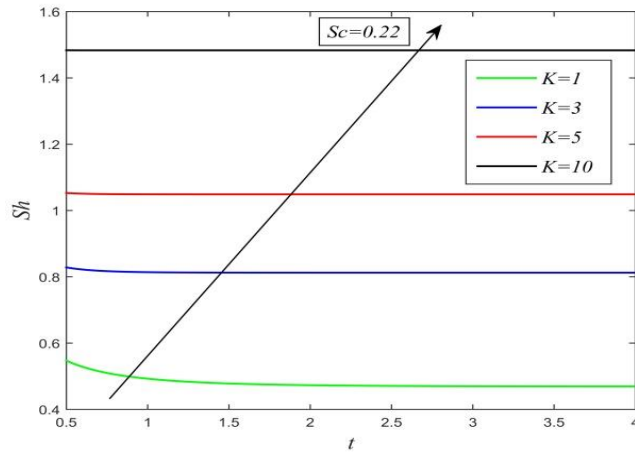


Figure 5.21: Sherwood number versus t for different K and $Sc=0.22$

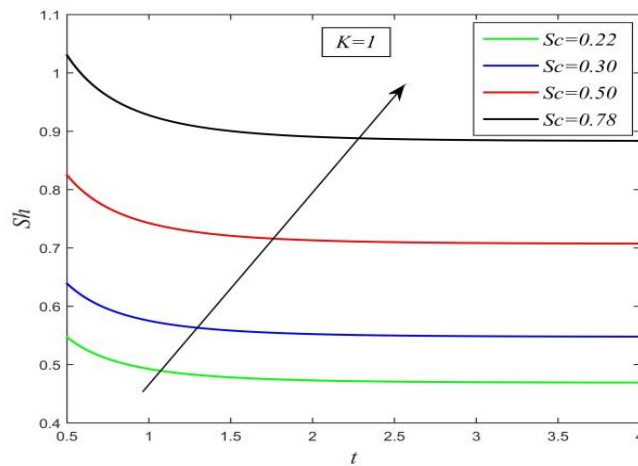


Figure 5.22: Sherwood number versus t for different Sc and $K=1$

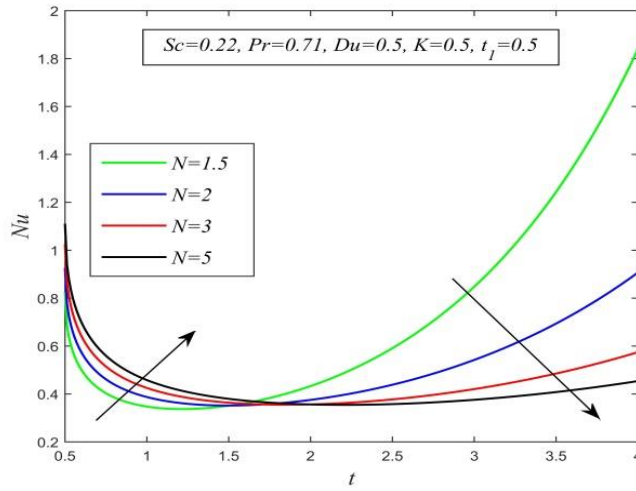


Figure 5.23: Nusselt number versus t for different N and $Sc=0.22, Pr=0.71, Du=0.5, K=0.5, t_1=0.5$

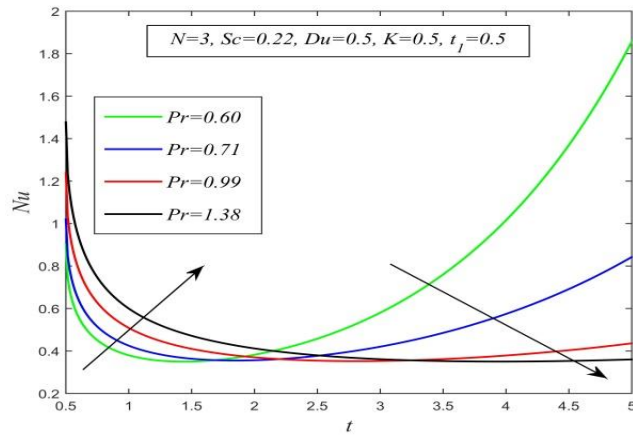


Figure 5.24: Nusselt number versus t for different Pr and $Sc=0.22, N=3, Du=0.5, K=0.5, t_1=0.5$

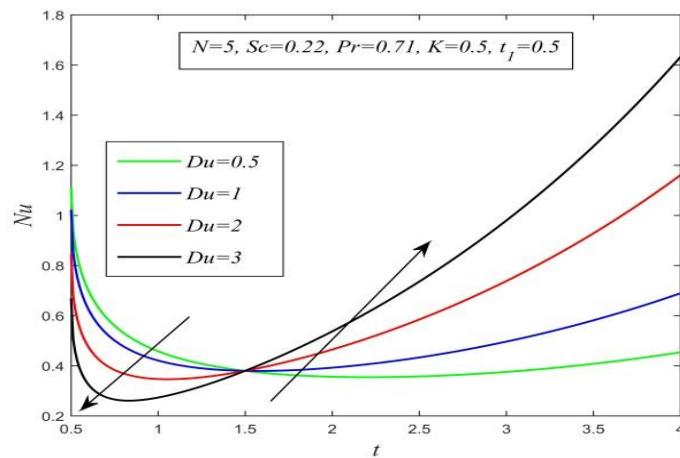


Figure 5.25: Nusselt number versus t for different Du and $Sc=0.22, N=5, Pr=0.71, K=0.5, t_1=0.5$

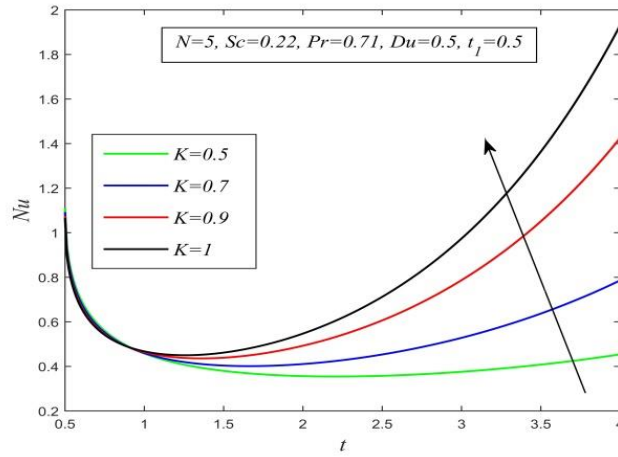


Figure 5.26: Nusselt number versus t for different K and $Sc=0.22$, $N=5$, $Pr=0.71$, $Du=0.5$, $t_1=0.5$

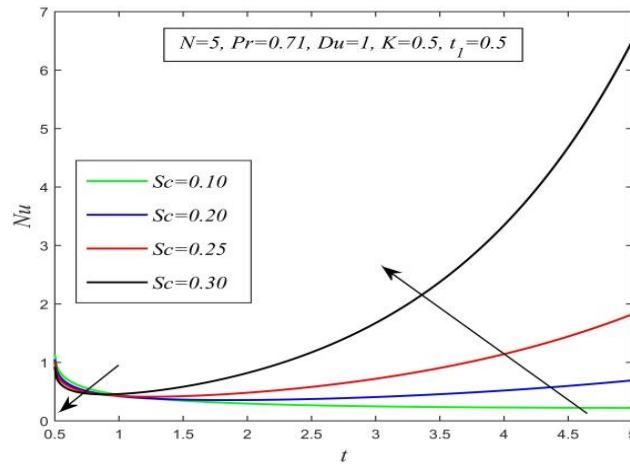


Figure 5.27: Nusselt number versus t for different Sc and $N=5$, $Pr=0.71$, $Du=0.5$, $K=0.5$, $t_1=0.5$

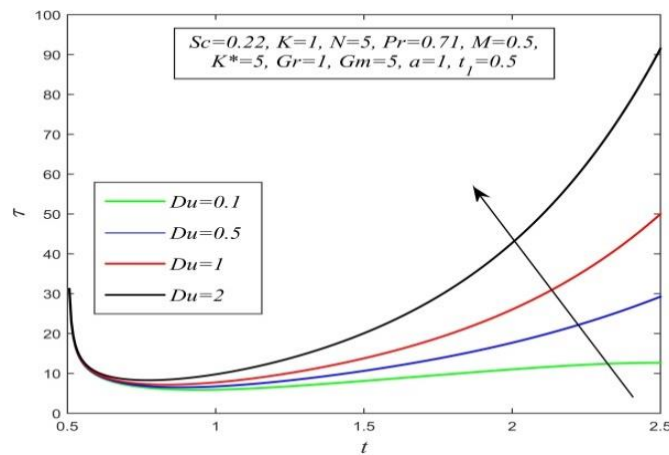


Figure 5.28: Skin friction versus t for different Du and $Sc=0.22$, $K=1$, $N=5$, $Pr=0.71$, $M=0.5$, $K^*=5$, $Gr=1$, $Gm=5$, $a=1$, $t_1=0.5$

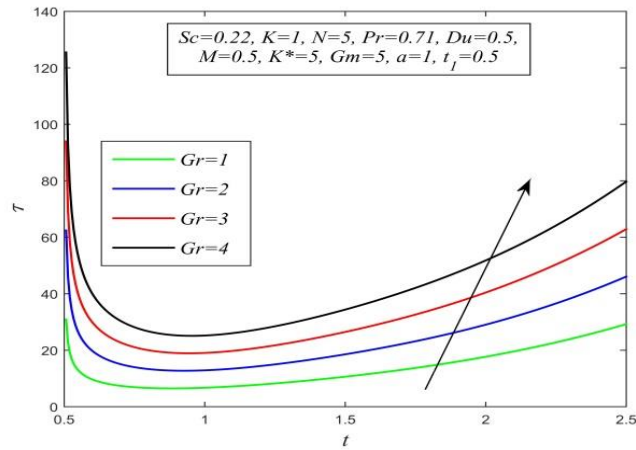


Figure 5.29: Skin friction versus t for different Gr and $Sc=0.22$, $K=1$, $N=5$, $Pr=0.71$, $Du=0.5$, $M=0.5$, $K^*=5$, $Gm=5$, $a=1$, $t_1=0.5$

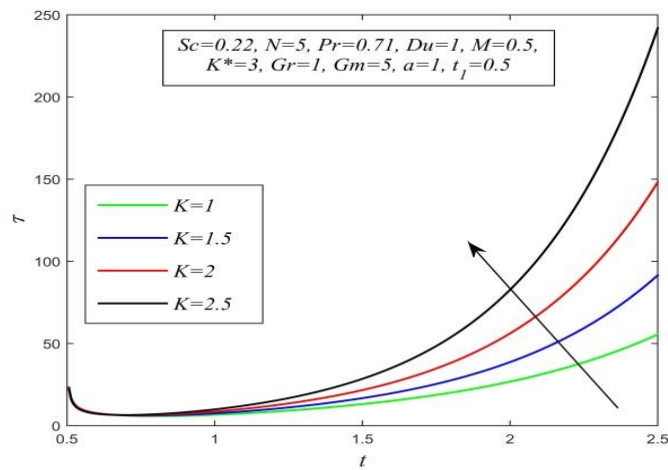


Figure 5.30: Skin friction versus t for different K and $Sc=0.22$, $N=5$, $Pr=0.71$, $Du=1$, $M=0.5$, $K^*=3$, $Gr=1$, $Gm=5$, $a=1$, $t_1=0.5$

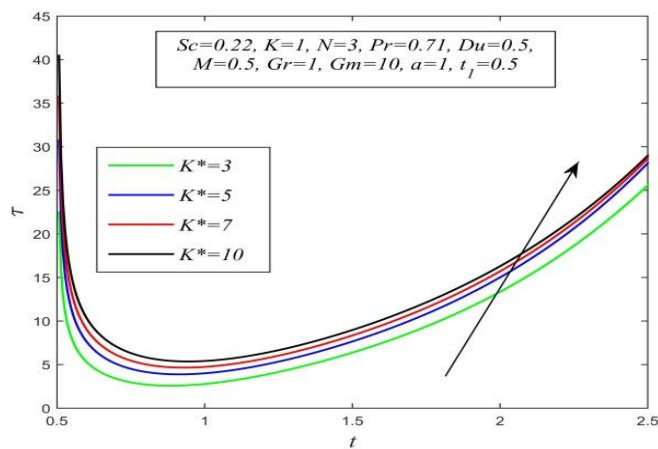


Figure 5.31: Skin friction versus t for different K^* and $Sc=0.22$, $K=1$, $N=3$, $Pr=0.71$, $Du=0.5$, $M=0.5$, $Gr=1$, $Gm=10$, $a=1$, $t_1=0.5$

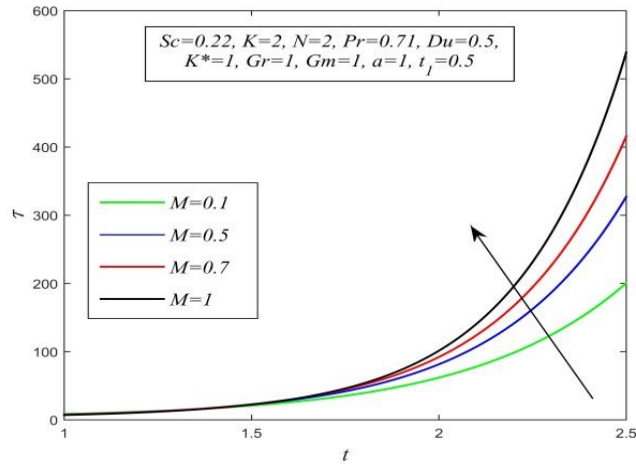


Figure 5.32: Skin friction versus t for different M and $Sc=0.22$, $K=2$, $N=2$, $Pr=0.71$, $Du=0.5$, $K^*=1$, $Gr=1$, $Gm=1$, $a=1$, $t_1=0.5$

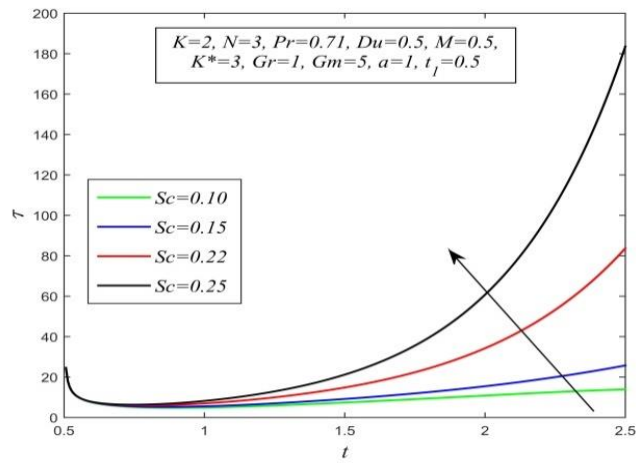


Figure 5.33: Skin friction versus t for different Sc and $K=2$, $N=3$, $Pr=0.71$, $M=0.5$, $Du=0.5$, $K^*=3$, $Gr=1$, $Gm=5$, $a=1$, $t_1=0.5$

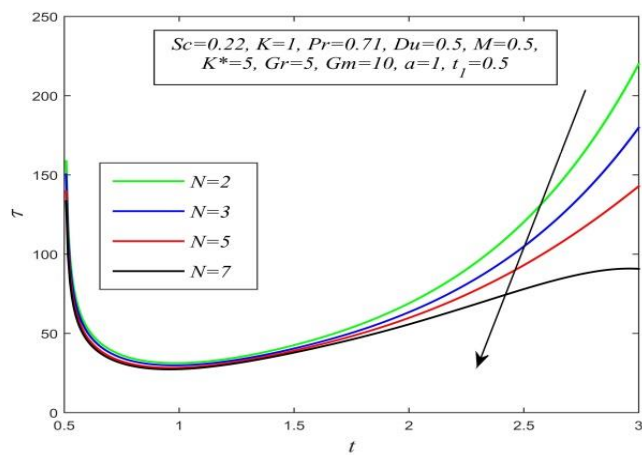


Figure 5.34: Skin friction versus t for different N and $Sc=0.22$, $K=1$, $Pr=0.71$, $M=0.5$, $Du=0.5$, $K^*=5$, $Gr=5$, $Gm=10$, $a=1$, $t_1=0.5$

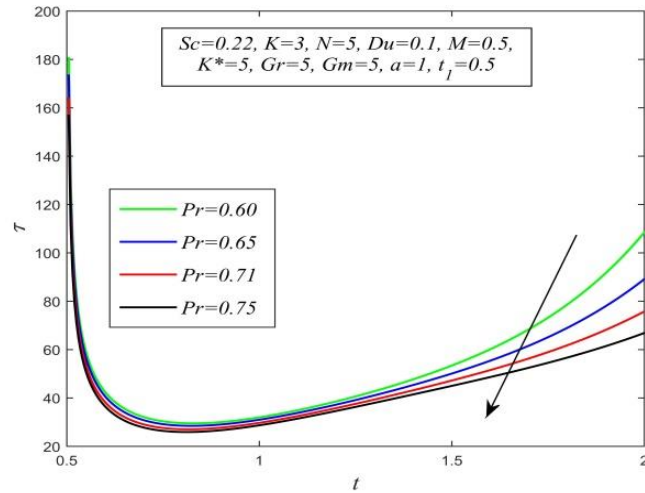


Figure 5.35: Skin friction versus t for different Pr and $Sc=0.22$, $K=3$, $N=5$, $M=0.5$, $Du=0.1$, $K^*=5$, $Gr=5$, $Gm=5$, $a=1$, $t_1=0.5$

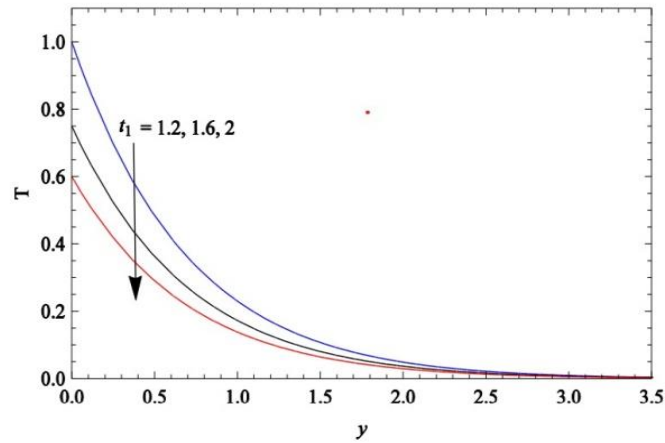


Figure 5.36: Scanned graph of temperature field versus y for different t_1 when $t=1.2$, $N=2$, $Pr=0.71$ drawn by Seth et al. (2016b)

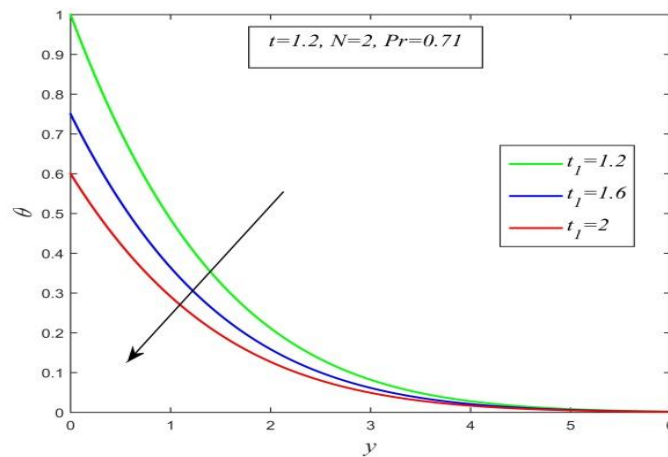


Figure 5.37: Temperature field versus y for different t_1 when $t=1.2$, $N=2$, $Pr=0.71$, $Sc=0$, $Du=0$, $K=0$ drawn by present author

t	Du	N	Nu
0.5	0.5	5	1.1016
0.5	1	5	1.0184
0.5	1.5	5	0.9302
2	0.5	5	0.3564
2	1	5	0.3926
2	1.5	5	0.4288
0.5	0.5	2	0.9218
0.5	0.5	3	1.0204
0.5	0.5	4	1.0730
2	0.5	2	0.3753
2	0.5	3	0.3565
2	0.5	4	0.3552

Table 5.1: Computational values of Nusselt number for various t , Du and N when $Pr=0.71$, $Sc=0.22$, $K=0.5$, $t_1=0.5$

t	K	N	Du	Gr	Gm	τ
1	1	5	0.5	1	1	9.1499
1.5						13.2425
2						20.4193
1	2	5	0.5	1	1	9.9629
	3					11.2420
	5					16.8475
1	1	2	0.5	1	1	9.7355
		5				9.1499
		7				8.9585
1	1	5	1	1	1	10.1642
			2			14.2214
			3			18.2786
1	1	5	0.5	1	1	9.1499
				3		21.4736
				5		33.7974
1	1	5	0.5	1	1	9.1499
					3	7.9392
					5	6.7286

Table 5.2: Computational values of skin friction for various t , K , N , Du , Gr and Gm when $Pr=0.71$, $Sc=0.22$, $a=1$, $M=0.5$, $K^*=0.5$, $t_1=0.5$

K	Sc	t	Asogwa et. al (2021) (isothermal condition)	Seth et. al (2014) (isothermal condition)	Kataria and Patel (2019) (isothermal condition)	Present study (isothermal condition)
5	0.66	0.4	1.8320	1.8320	1.8320	1.8320
5.1	0.66	0.4	1.8493	1.8493	1.8493	1.8493
5.2	0.66	0.4	1.8664	1.8664	1.8664	1.8664
5	0.7	0.4	1.8867	1.8867	1.8867	1.8867
5	0.8	0.4	2.0170	2.0170	2.0170	2.0170
5	0.66	0.5	1.8238	1.8238	1.8238	1.8238
5	0.66	0.6	1.8201	1.8201	1.8201	1.8201
5	1.24	0.4	2.5111	-	-	2.5117
5	2.01	0.4	3.1971	-	-	3.1971

Table 5.3: Comparison of computational values of Sherwood number for various K , Sc and t obtained by Asogwa et.al (2021), Seth et. Al (2014), Kataria and Patel (2019) and present author

Nomenclature:

a : Surface acceleration parameter

\vec{B} : Magnetic flux density

B_0 : Strength of the applied magnetic field $\left(\frac{\text{Weber}}{\text{m}^2}\right)$

C : Molar species concentration $\left(\frac{\text{mol}}{\text{m}^3}\right)$

C_p : Specific heat at constant pressure $\left(\frac{\text{J}}{\text{Kg.K}}\right)$

C_s : Concentration susceptibility

C_∞ : Concentration far away from the plate $\left(\frac{\text{mol}}{\text{m}^3}\right)$

C_w : Concentration at the plate $\left(\frac{\text{mol}}{\text{m}^3}\right)$

D_M : Mass diffusivity $\left(\frac{\text{m}^2}{\text{s}}\right)$

Du : Dufour number

\vec{g} : Gravitation acceleration vector

g : Gravitational acceleration $\left(\frac{\text{m}}{\text{s}^2}\right)$

Gr : Thermal Grashof number

Gm : Solutal Grashof number

K_T : Thermal diffusion ratio

K^* : Porosity parameter

\vec{J} : Current density vector $\left(\frac{\text{A}}{\text{m}^2}\right)$

\bar{K} : Chemical reaction rate $\left(\frac{\text{mol}}{\text{m}^2\text{s}}\right)$

K : Chemical reaction parameter

M : Magnetic parameter

N : Radiation parameter

p : Pressure $\left(\frac{N}{m^2}\right)$

Pr : Prandtl number

\vec{q} : Fluid velocity vector

\vec{q}_r : Radiation heat flux vector

q_r : Radiation heat flux $\left(\frac{W}{m^2}\right)$

Sc : Schmidt number

t' : Time (s)

t_0 : Critical time for rampedness (s)

t_1 : Non- dimensional critical time for rampedness

T : Fluid temperature (K)

T_w : Temperature at the plate (K)

T_∞ : Undisturbed temperature (K)

u' : X-component of fluid velocity $\left(\frac{m}{s}\right)$

U_0 : Plate velocity $\left(\frac{m}{s}\right)$

Greek Symbols:

μ : Coefficient of viscosity $\left(\frac{Kg}{m.s}\right)$

σ : Electrical conductivity $\left(\frac{S}{m}\right)$

σ^* : Stefan-Boltzmann constant $\left(\frac{W}{m^2.K^4}\right)$

ρ : Fluid density $\left(\frac{Kg}{m^3}\right)$

ρ_∞ : Fluid density far away from the plate $\left(\frac{Kg}{m^3}\right)$

κ : Thermal conductivity $\left(\frac{W}{m.K}\right)$

κ^* : Mean absorption constant $\left(\frac{1}{m}\right)$

β : Volumetric coefficient of thermal expansion $\left(\frac{1}{K}\right)$

$\bar{\beta}$: Volumetric coefficient of solutal expansion $\left(\frac{1}{K.mol}\right)$

ν : Kinematic viscosity $\left(\frac{m^2}{s}\right)$

Subscripts:

w : Refers to physical quantity at the plate

∞ : Refers to physical quantity far away from the plate

Appendix

$$\begin{aligned}
\psi_1 &= \psi(Sc, K, y, t), a_1 = \frac{Pr}{\Lambda}, a_2 = \frac{\Lambda Sc K}{\Lambda Sc - Pr}, a_3 = \frac{Du Pr Sc}{\Lambda Sc - Pr}, \theta_{1,1} = \frac{1}{t_1} \Delta \lambda_1, \lambda_1 = \lambda(a_1, y, t), \\
\theta_{1,2} &= a_3 (A_1 E_1 + A_2 E_3), E_1 = \operatorname{erfc} \left(\frac{y \sqrt{a_1}}{2\sqrt{t}} \right), E_2 = \operatorname{erfc} \left(\frac{y \sqrt{a_1 - a_2}}{2\sqrt{t}} \right), E_3 = e^{-a_2 t} E_2, A_1 = \frac{K}{a_2}, \\
A_2 &= \frac{a_2 - K}{a_2}, \theta_{1,3} = a_3 (A_1 \psi_1 + A_2 \psi_2), \psi_2 = \Psi(Sc, K, -a_2, y, t), \theta_{2,1} = \theta_{1,1}, a_4 = \frac{Du Pr}{\Lambda K}, \\
\theta_{2,2} &= a_4 (K \lambda_1 + P_1), P_1 = P(a_1, y, t), \theta_{2,3} = a_4 (K \psi_1 + l_1), l_1 = l(Sc, K, y, t), \\
u_{1,1} &= u_{1,1,1} + u_{1,1,2} + u_{1,1,3} + u_{1,1,4} + u_{1,1,5}, u_{1,1,1} = h_2, h_2 = e^{at} h_1, h_1 = h(M_1 + a, y, t), a_5 = \frac{M_1}{a_1 - 1}, \\
a_6 &= \frac{K Sc - M_1}{Sc - 1}, a_7 = \frac{Gr}{t_1 (a_1 - 1)}, u_{1,1,2} = a_7 (A_3 \Delta h_5 + A_4 \Delta h_3 + A_5 \Delta r_1), A_3 = \frac{1}{a_5^2}, A_4 = -A_3, A_5 = \frac{1}{a_5}, \\
h_3 &= h(M_1, y, t), h_5 = e^{-a_5 t} h_4, h_4 = h(M_1 - a_5, y, t), r_1 = r(M_1, y, t), a_8 = \frac{Gra_3}{a_1 - 1}, \\
u_{1,1,3} &= a_8 (A_6 h_7 + A_7 h_5 + A_8 h_3), A_6 = \frac{a_2 - K}{a_2 (a_5 - a_2)}, A_7 = \frac{a_5 - K}{a_5 (a_2 - a_5)}, A_8 = \frac{K}{a_2 a_5}, h_7 = e^{-a_2 t} h_6, \\
h_6 &= h(M_1 - a_2, y, t), a_9 = \frac{Gra_3}{Sc - 1}, u_{1,1,4} = a_9 (A_9 h_7 + A_{10} h_9 + A_{11} h_3), h_9 = e^{-a_6 t} h_8, h_8 = h(M_1 - a_6, y, t), \\
A_9 &= \frac{a_2 - K}{a_2 (a_6 - a_2)}, A_{10} = \frac{a_6 - K}{a_6 (a_2 - a_6)}, A_{11} = \frac{K}{a_2 a_6}, a_{10} = \frac{Gm}{Sc - 1}, u_{1,1,5} = a_{10} (A_{12} h_9 + A_{13} h_3), A_{12} = -\frac{1}{a_6}, \\
A_{13} &= -A_{12}, u_{1,2} = -a_7 (A_3 \Delta E_5 + A_4 \Delta E_1 + A_5 \Delta \lambda_1), E_5 = e^{-a_5 t} E_4, E_4 = \operatorname{erfc} \left(\frac{y \sqrt{a_1 - a_5}}{2\sqrt{t}} \right), \\
u_{1,3} &= -a_8 (A_6 E_3 + A_7 E_5 + A_8 E_1), u_{1,4} = -a_9 (A_9 \psi_2 + A_{10} \psi_3 + A_{11} \psi_1), \psi_3 = \Psi(Sc, K, -a_6, y, t), \\
u_{1,5} &= -a_{10} (A_{12} \psi_3 + A_{13} \psi_1), u_{2,1} = u_{2,1,1} + u_{2,1,2} + u_{2,1,3} + u_{2,1,4} + u_{2,1,5}, u_{2,1,1} = u_{1,1,1}, a_{11} = \frac{Gr}{M_1 t_1}, \\
u_{2,1,2} &= a_{11} \Delta r_1, a_{12} = \frac{Gra_3}{M_1}, u_{2,1,3} = a_{12} (A_{14} h_7 + A_{15} h_3), A_{14} = -\frac{K}{a_2}, A_{15} = -A_{14}, u_{2,1,4} = u_{1,1,4}, u_{2,1,5} = u_{1,1,5}, \\
u_{2,2} &= -a_{11} \Delta \lambda_2, \lambda_2 = \lambda(1, y, t), u_{2,3} = -a_{12} (A_{14} E_8 + A_{15} E_6), E_6 = \operatorname{erfc} \left(\frac{y}{2\sqrt{t}} \right), E_8 = e^{-a_2 t} E_7, \\
E_7 &= \operatorname{erfc} \left(\frac{y \sqrt{1 - a_2}}{2\sqrt{t}} \right), u_{2,4} = u_{1,4}, u_{2,5} = u_{1,5}, u_{3,1} = u_{3,1,1} + u_{3,1,2} + u_{3,1,3} + u_{3,1,4} + u_{3,1,5}, u_{3,1,1} = u_{1,1,1}, \\
u_{3,1,2} &= u_{1,1,2}, u_{3,1,3} = u_{1,1,3}, u_{3,1,4} = a_{13} (A_{14} h_7 + A_{15} h_3), a_{13} = \frac{Gra_3}{K - M_1}, u_{3,1,5} = a_{14} h_3, a_{14} = \frac{Gm}{K - M_1}, \\
u_{3,2} &= u_{1,2}, u_{3,3} = u_{1,3}, u_{3,4} = -a_{13} (A_{14} h_{11} + A_{15} h_{12}), h_{10} = h(K - a_2, y, t), h_{11} = e^{-a_2 t} h_{10}, h_{12} = h(K, y, t), \\
u_{3,5} &= -a_{13} \psi_1, u_{4,1} = u_{4,1,1} + u_{4,1,2} + u_{4,1,3} + u_{4,1,4} + u_{4,1,5}, u_{4,1,1} = u_{1,1,1}, u_{4,1,2} = u_{2,1,2}, a_{15} = \frac{Gr Du}{KM_1},
\end{aligned}$$

$$\begin{aligned}
u_{4,1,3} &= a_{15}(Kh_3 + q_1), q_1 = q(M_1, y, t), u_{4,1,4} = a_{16}(Kh_3 + q_1), u_{4,1,5} = a_{17}h_3, a_{17} = \frac{Gm}{K - M_1}, u_{4,2} = u_{2,2}, \\
u_{4,3} &= -a_{15}E_6, E_6 = \operatorname{erfc}\left(\frac{y}{2\sqrt{t}}\right), u_{4,4} = -a_{16}(Kh_{12} + q_2), h_{12} = h(K, y, t), q_2 = q(K, y, t), \\
u_{4,5} &= -a_{17}h_{10}, u_{5,1} = u_{5,1,1} + u_{5,1,2} + u_{5,1,3} + u_{5,1,4} + u_{5,1,5}, u_{5,1,1} = u_{1,1,1}, u_{5,1,2} = u_{1,1,2}, \\
u_{5,1,3} &= a_{18}(A_{16}h_5 + A_{17}h_3), a_{18} = \frac{GrDuSc}{(a_1 - 1)K}, A_{16} = \frac{a_5 - K}{a_5}, A_{17} = \frac{K}{a_5}, u_{5,1,4} = a_{18}(A_{18}h_3 + A_{19}h_9), \\
A_{18} &= \frac{K}{a_6}, A_{19} = \frac{a_6 - K}{a_6}, u_{5,1,5} = u_{1,1,5}, u_{5,2} = u_{1,2}, u_{5,3} = -a_{18}(A_{16}\psi_4 + A_{17}\psi_1), \psi_4 = \Psi(Sc, K, -a_5, y, t), \\
u_{5,4} &= -a_{18}(A_{18}\psi_1 + A_{19}\psi_3), u_{5,5} = u_{1,5} \\
Nu_{1,1} &= \frac{1}{t_1}\Delta v_1, v_1 = v(a_1, t), Nu_{1,2} = a_3(A_1\alpha_1 + A_2\alpha_3), \alpha_1 = \alpha\left(\frac{\sqrt{a_1}}{2\sqrt{t}}\right), \alpha_2 = \alpha\left(\frac{\sqrt{a_1 - a_2}}{2\sqrt{t}}\right), \\
\alpha_3 &= e^{-a_2 t}\alpha_2, Nu_{1,3} = a_3(A_1\Omega_1 + A_2Z_1), \Omega_1 = \Omega(Sc, K, t), Z_1 = Z(Sc, K, -a_2, t), Nu_{2,1} = Nu_{1,1}, \\
Nu_{2,2} &= a_4(Kv_1 + I_1), I_1 = I(a_1, t), Nu_{2,3} = a_4(K\Omega_1 + T_1), T_1 = T(Sc, K, t) \\
\tau_{1,1} &= \tau_{1,1,1} + \tau_{1,1,2} + \tau_{1,1,3} + \tau_{1,1,4}, \tau_{1,1,1} = N_2, N_2 = e^{at}N_1, N_1 = N(M_1 + a, t), \\
\tau_{1,1,2} &= a_7(A_3\Delta N_5 + A_4\Delta N_3 + A_5\Delta O_1), N_3 = N(M_1, t), N_4 = N(M_1 - a_5, t), N_5 = e^{-a_5 t}N_4, \\
O_1 &= O(M_1, t), \tau_{1,1,3} = a_8(A_6N_7 + A_7N_5 + A_8N_3), N_7 = e^{-a_2 t}N_6, N_6 = N(M_1 - a_2, t), \\
\tau_{1,1,4} &= a_9(A_9N_7 + A_{10}N_9 + A_{11}N_3), N_9 = e^{-a_6 t}N_8, N_8 = N(M_1 - a_6, t), \tau_{1,1,5} = a_{10}(A_{12}N_9 + A_{13}N_3), \\
\tau_{1,2} &= -a_7(A_3\Delta\alpha_5 + A_4\Delta\alpha_1 + A_5\Delta v_1), \alpha_5 = e^{-a_5 t}\alpha_4, \alpha_4 = \alpha\left(\frac{\sqrt{a_1 - a_5}}{2\sqrt{t}}\right), \\
\tau_{1,3} &= -a_8(A_6\alpha_3 + A_7\alpha_5 + A_8\alpha_1), \tau_{1,4} = -a_9(A_9Z_1 + A_{10}Z_2 + A_{11}\Omega_1), Z_2 = Z(Sc, K, -a_6, t), \\
\tau_{1,5} &= -a_{10}(A_{12}Z_2 + A_{13}\Omega_1), \tau_{2,1} = \tau_{2,1,1} + \tau_{2,1,2} + \tau_{2,1,3} + \tau_{2,1,4} + \tau_{2,1,5}, \tau_{2,1,1} = \tau_{1,1,1}, \tau_{2,1,2} = a_{11}\Delta O_1, \\
\tau_{2,1,3} &= a_{12}(A_{14}N_7 + A_{15}N_3), \tau_{2,1,4} = \tau_{1,1,4}, \tau_{2,1,5} = \tau_{1,1,5}, \tau_{2,2} = -a_{11}\Delta v_2, v_2 = v(1, t), \\
\tau_{2,3} &= -a_{12}(A_{14}\alpha_8 + A_{15}\alpha_6), \alpha_6 = \alpha\left(\frac{1}{2\sqrt{t}}\right), \alpha_8 = e^{-a_2 t}\alpha_7, \alpha_7 = \alpha\left(\frac{\sqrt{1 - a_2}}{2\sqrt{t}}\right), \tau_{2,4} = \tau_{1,4}, \tau_{2,5} = \tau_{1,5}, \\
\tau_{3,1} &= \tau_{3,1,1} + \tau_{3,1,2} + \tau_{3,1,3} + \tau_{3,1,4} + \tau_{3,1,5}, \tau_{3,1,1} = \tau_{1,1,1}, \tau_{3,1,2} = \tau_{1,1,2}, \tau_{3,1,3} = \tau_{1,1,3}, \\
\tau_{3,1,4} &= a_{13}(A_{14}N_7 + A_{15}N_3), \tau_{3,1,5} = a_{14}N_3, \tau_{3,2} = \tau_{1,2}, \tau_{3,3} = \tau_{1,3}, \tau_{3,4} = -a_{13}(A_{14}N_{11} + A_{15}N_{12}), \\
\tau_{3,5} &= -a_{13}\Omega_1, N_{10} = N(K - a_2, t), N_{11} = e^{-a_2 t}N_{10}, N_{12} = N(K, t), \\
\tau_{4,1} &= \tau_{4,1,1} + \tau_{4,1,2} + \tau_{4,1,3} + \tau_{4,1,4} + \tau_{4,1,5}, \tau_{4,1,1} = \tau_{1,1,1}, \tau_{4,1,2} = \tau_{2,1,2}, \tau_{4,1,3} = a_{15}(KN_3 + Y_1), Y_1 = Y(M_1, t), \\
\tau_{4,1,4} &= a_{16}(KN_3 + Y_1), \tau_{4,1,5} = a_{17}N_3, \tau_{4,2} = \tau_{2,2}, \tau_{4,3} = -a_{15}\alpha_6, \alpha_6 = \alpha\left(\frac{1}{2\sqrt{t}}\right), \tau_{4,4} = -a_{16}(KN_{12} + Y_2), \\
Y_2 &= Y(K, t), \tau_{4,5} = -a_{17}N_{12}, \tau_{5,1} = \tau_{5,1,1} + \tau_{5,1,2} + \tau_{5,1,3} + \tau_{5,1,4} + \tau_{5,1,5}, \tau_{5,1,1} = \tau_{1,1,1}, \tau_{5,1,2} = \tau_{1,1,2}, \\
\tau_{5,1,3} &= a_{18}(A_{16}N_5 + A_{17}N_3), \tau_{5,1,4} = a_{18}(A_{18}N_3 + A_{19}N_9), \tau_{5,1,5} = \tau_{1,1,5}, \tau_{5,2} = \tau_{1,2}, \\
\tau_{5,3} &= -a_{18}(A_{16}Z_3 + A_{17}\Omega_1), Z_3 = Z(Sc, K, -a_5, t), \tau_{5,4} = -a_{18}(A_{18}\Omega_1 + A_{19}Z_2), \tau_{5,5} = \tau_{1,5}
\end{aligned}$$

(The functions are defined in **Chapter I**)

CHAPTER VI

Thermal Diffusion Effect on Unsteady MHD Free Convective Flow Past a Semi- Infinite Exponentially Accelerated Vertical Plate in a Porous Medium

Published in *Canadian Journal of Physics* (Scopus, SCI), **100**, 437-451, 2022.

6.1 Introduction

Magnetohydrodynamics (MHD) is the branch of physics associated with the interaction of electrically conducting fluids with a magnetic field. Plasmas, electrolytes, liquid metals, saltwater are some common examples of such fluids. Renowned Swiss scientist Hannes Alfvén (1942) introduced the concept of MHD for which he received the Nobel Prize in 1970. But, MHD is at present form due to significant contributions from other authors like Cowling (1957), Shercliff (1965), Ferraro and Plumpton (1966), Roberts (1967), Cramer and Pai (1973), Davidson (2001) etc. Engineering applications of MHD include motor, dynamo, MHD generator, plasma confinement, cooling of liquid metals, nuclear reactors, etc. applications of MHD in biological systems were studied by Rashidi et al. (2017). Farrokhi et al. (2019) investigated biomedical applications of MHD. Besides these, MHD has vast applications in astrophysics, geophysics, chemical sciences, nanotechnology, etc.

In a fluid mixture, density variation takes place due to changes in both species concentration and fluid temperature. This variation develops buoyancy force which acts on the fluid. The flow produced by this force is termed natural convection or free convection. Asimoni et al. (2017) studied free convective viscous MHD flow past a vertical plate. Bulinda et al. (2020) investigated the effect of MHD free convection over a vibrating bottom surface with Hall current. Sravan Kumar et al. (2020) examined the behavior of Lorentz force and viscous dissipation on unsteady nanofluid convection flow over an exponentially moving vertical plate. Anwar et al. (2020) investigated combined effects of ramped wall temperature and ramped wall velocity in a convective Maxwell fluid flow.

The method of heat transfer through electromagnetic waves is termed radiation. Applications of radiative-convective heat transfer can be found in space technology, industrial and environmental processes, climate engineering, the human body, etc. Orhan and Ahmet (2008) studied the effect of radiation in MHD mixed convection flow about a permeable vertical plate. Pattnaik et al. (2017) analyzed the effect of radiation in an MHD flow in a porous medium past an exponentially accelerated inclined plate with variable temperature. Ahmed and Dutta (2014) obtained an analytical solution of an MHD transient flow problem past an infinite vertical plate with radiation and ramped wall temperature. Seth et al. (2017) considered MHD double-diffusive natural convective flow over an exponentially accelerated inclined plate. Seth and Sarkar (2015) investigated the impact of radiation, chemical reaction, and Hall current in a free convective MHD flow past a moving vertical

plate. Das et al. (2020) considered the combined effects of radiation and chemical reaction of Casson fluid over a stretching sheet in a porous medium. Das et al. (2019) studied the influence of rotational buoyancy force on a radiative convective MHD flow near a rotating plate.

Medium containing pores or voids through which fluid passes through is called porous medium. Wood, Rubber, Sponge are some common examples of a porous medium. Fluid flow through a porous medium has significant application in combustion technology, nuclear waste disposal, drying of biological materials, etc. Megahed (1984) obtained exact solution of unsteady MHD flow through porous medium while Raghunath et al. (2020) discussed unsteady MHD flow through a porous medium bounded by two vertical porous plates. Acharya et al. (2014) studied unsteady convective MHD flow in porous medium past a vertical porous plate with heat source and variable temperature. Sinha et al. (2017) considered MHD free convective flow through a porous medium past a vertical plate with ramped wall temperature. Venkateswarlu and Makinde (2018) studied MHD slip flow with radiative heat and mass transfer over an inclined plate immersed in a porous medium.

The chemical reaction effect draws the attention of many researchers due to its great practical significance in many technological, industrial and natural processes. Jonnadula et al. (2015) observed the outcome of radiation and chemical reaction in an MHD flow over a stretching surface. The chemical reaction effect in an MHD flow due to rotating disk in the porous medium was studied by Hayat et al. (2017). Zigta (2019) observed the effects of radiation, chemical reaction, and viscous dissipation in an unsteady MHD flow in a porous medium. Seth and Sarkar (2015) investigated the impact of Hall current, chemical reaction, and radiation in MHD free convective flow past a moving vertical plate. Eid and Makinde (2018) studied the effect of solar radiation on a nanofluid flow in a porous medium with chemically reactive species. Rajesh and Chamkha (2014) investigated the effects of radiation, chemical reaction and ramped wall temperature in an unsteady two dimensional flow.

Heat absorption/ generation carry great importance in different free convective MHD problems. Srinivasa and Eswara (2016) discussed the consequences of heat generation on an MHD free convection flow from an isothermal cone. Rajput and Kumar (2017) studied the heat absorption effect on an MHD flow over a plate with variable wall temperature. Nandkeolyar and Das (2014) considered MHD free convection flow of heat-absorbing dusty fluid past a flat plate with ramped wall temperature. Consequences of Hall current and heat

absorption in an MHD flow past an oscillating vertical plate in a porous medium were studied by Rajput and Kanaujia (2019). Nandkeolyar et al. (2013) obtained the exact solution of an unsteady MHD free convection flow past a flat plate considering the heat absorption effect.

When both solutal and thermal convection simultaneously takes place in a fluid mixture, then mass flux is produced by temperature gradient and concentration gradient. Effect of mass flux under temperature gradient is termed as thermal diffusion effect or Soret effect or Ludwig- Soret effect. Carl Ludwig observed and reported about this effect in 1856. Later, Charles Soret analyzed the effect in 1879. Ahmed (2012) discussed the combined effects of Soret and radiation in a free convective MHD flow past an infinite vertical plate. Oyekunle and Agunbiade (2020) studied MHD slip flow over permeable vertical plate taking both Soret and Dufour effects into account. Sivaiah et al. (2012) considered thermal diffusion and radiation effects on an MHD free convective flow past an infinitely heated vertical plate in a porous medium. Effects of thermal diffusion and radiation in a chemically reactive MHD flow past a vertical plate were discussed by Raju et al. (2019). Mohanty et al. (2014) considered thermal diffusion, radiation, chemical reaction, and periodic permeability in a three-dimensional MHD flow in a porous medium. Anil Kumar et al. (2021) discussed how Soret, Dufour, Hall current, rotation, and radiation influence MHD free convective flow past an accelerated vertical plate. Influences of radiation, thermal diffusion, chemical reaction, and heat generation in an MHD flow over a vertical surface in a porous medium were investigated by Lavanya and Kesavaiah (2014). Pal and Mondal (2012) discussed Soret, Dufour, chemical reaction, and radiation effects in a mixed convection flow. Raju et al. (2017) investigated thermal diffusion, radiation, heat absorption, and chemical reaction effects in a mixed convective MHD flow.

The objective of the present investigation is to study and analyse the thermal diffusion effect in a radiative, free convective, chemically reacting unsteady MHD flow past a semi-infinite vertical plate embedded in a porous medium with heat absorption and arbitrary ramped temperature. Equations governing the flow are converted to a set of non-dimensional partial differential equations with the help of some dimensionless variables and parameters. Solutions of these equations are obtained adopting a closed-form of Laplace transformation technique. Effects of various flow parameters such as Prandtl number, Schmidt number, heat absorption parameter, chemical reaction parameter, magnetic parameter, radiation parameter, porosity parameter, Soret number, thermal Grashof number, and solutal Grashof number on flow and transport characteristics are discussed graphically. Some results are compared with

previously published work. The present paper will be useful in designing cooling systems, flow meters, continuous casting of metals, MHD generators, etc. This paper will also help scientists and researchers in the field of heat and mass transfer.

6.2 Mathematical Analysis

Governing equations of the convective flow of an incompressible, electrically conducting, viscous, chemically reacting, heat-absorbing, and radiating fluid in a porous medium in presence of a magnetic field having constant mass diffusivity and thermal diffusivity considering thermal diffusion effect are

Continuity equation:

$$\vec{\nabla} \cdot \vec{q} = 0 \quad (6.1)$$

Magnetic field continuity equation:

$$\vec{\nabla} \cdot \vec{B} = 0 \quad (6.2)$$

Ohm's Law:

$$\vec{J} = \sigma (\vec{E} + \vec{q} \times \vec{B}) \quad (6.3)$$

Momentum equation:

$$\rho \left[\frac{\partial \vec{q}}{\partial t} + (\vec{q} \cdot \vec{\nabla}) \vec{q} \right] = -\vec{\nabla} p + \vec{J} \times \vec{B} + \rho \vec{g} + \mu \nabla^2 \vec{q} - \frac{\mu \vec{q}}{K^*} \quad (6.4)$$

Energy equation:

$$\rho C_p \left[\frac{\partial T}{\partial t} + (\vec{q} \cdot \vec{\nabla}) T \right] = \kappa \nabla^2 T - \vec{\nabla} \cdot \vec{q}_r + \alpha (T_\infty - T) \quad (6.5)$$

Species continuity equation:

$$\frac{\partial C}{\partial t} + (\vec{q} \cdot \vec{\nabla}) C = D_M \nabla^2 C + D_T \nabla^2 T + \bar{K} (C_\infty - C) \quad (6.6)$$

Equation of state as per Boussinesq approximation:

$$\rho_\infty = \rho \left[1 + \beta(T - T_\infty) + \bar{\beta}(C - C_\infty) \right] \quad (6.7)$$

For optically thick and non-gray fluid, the radiation heat flux as per Rosseland approximation is given by

$$\vec{q}_r = -\frac{4\sigma^*}{3\kappa^*} \vec{\nabla} T^4$$

Now,

$$T^4 = (T - T_\infty + T_\infty)^4 = 4TT_\infty^3 - 3T_\infty^4, \text{ as } |T - T_\infty| \ll 1$$

So,

$$\vec{\nabla} \cdot \vec{q}_r = -\frac{16\sigma^* T_\infty^3}{3\kappa^*} \nabla^2 T$$

Therefore, Energy equation (5) reduces to

$$\rho C_p \left[\frac{\partial T}{\partial \bar{t}} + (\vec{q} \cdot \vec{\nabla}) T \right] = \kappa \nabla^2 T + \frac{16\sigma^* T_\infty^3}{3\kappa^*} \nabla^2 T + \alpha (T_\infty - T) \quad (6.8)$$

We, now consider a transient MHD free convective flow of a viscous incompressible electrically conducting fluid through a porous medium past a semi-infinite vertical plate in presence of a uniform magnetic field applied normal to the plate, directed into the fluid region. Initially, the plate and the surrounding fluid were at rest with uniform temperature T_∞ and concentration C_∞ at all points in the fluid. At time $\bar{t} > 0$, the plate is exponentially accelerated with velocity $U_o e^{a\bar{t}}$. The plate temperature is instantly raised to $T_\infty + (T_w - T_\infty) \frac{\bar{t}}{t_0}$, for $0 < \bar{t} \leq t_0$, and thereafter T_w when $\bar{t} > t_0$. The concentration is raised to C_w and maintained thereafter.

To idealize the mathematical model of the problem, we impose the following constraints-

- I. All the fluid properties are constant except the variation in density in the buoyancy force term.

- II. Viscous dissipation, Joule heating and porous medium resistance are negligible as velocity and velocity gradient are small.
- III. The induced magnetic field in comparison to the applied magnetic field is negligible.
- IV. Flow is one- dimensional which is parallel to the plate.
- V. The plate is electrically non-conducting.
- VI. No external electric field is applied for which the polarization voltage is negligible.

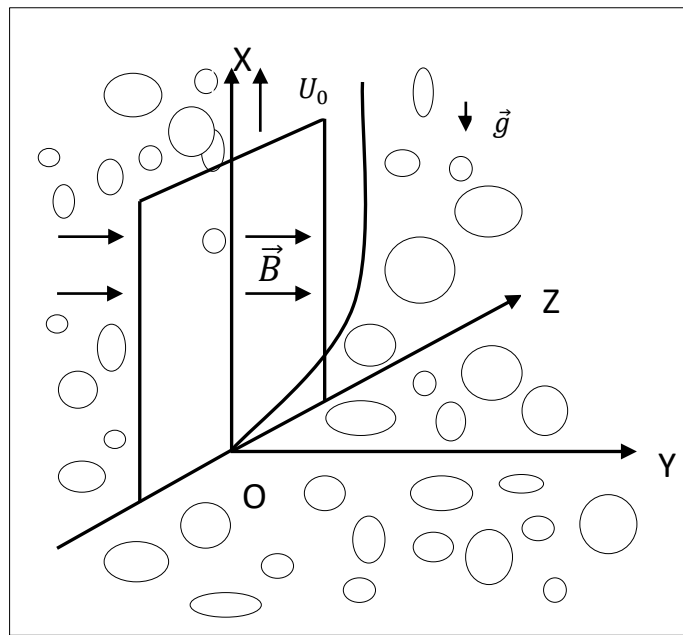


Figure 6.1: Flow configuration

We now consider a tri- rectangular Cartesian co-ordinate system $(\bar{x}, \bar{y}, \bar{z}, \bar{t})$ with X axis vertically upwards along with the plate, Y axis normal to the plate directed into the fluid region, and Z axis along the width of the plate as shown in Figure 6.1. Let $\vec{q} = (u', 0, 0)$ be the fluid velocity and $\vec{B} = (0, B_0, 0)$ be the magnetic induction vector at the point $(\bar{x}, \bar{y}, \bar{z}, \bar{t})$ in the fluid.

Equation (6.1) yields,

$$\frac{\partial u'}{\partial \bar{x}} = 0$$

$$i.e., u' = u'(\bar{y}, \bar{t}) \quad (6.9)$$

Equation (6.2) is trivially satisfied by $\vec{B} = (0, B_0, 0)$

Equation (6.4) reduces to

$$\rho \left[\frac{\partial u'}{\partial t} \hat{i} + 0 \right] = -\hat{i} \frac{\partial p}{\partial x} - \hat{j} \frac{\partial p}{\partial y} - \rho g \hat{i} - \sigma B_0^2 u' \hat{i} + \mu \frac{\partial^2 u'}{\partial y^2} \hat{i} - \frac{\mu u'}{K^*} \hat{i} \quad (6.10)$$

Equation (6.10) gives

$$\rho \frac{\partial u'}{\partial t} = -\frac{\partial p}{\partial x} - \rho g - \sigma B_0^2 u' + \mu \frac{\partial^2 u'}{\partial y^2} - \frac{\mu u'}{K^*} \quad (6.11)$$

And

$$0 = -\frac{\partial p}{\partial y} \quad (6.12)$$

Equation (6.12) shows that pressure near the plate and pressure far away from the plate are the same along the normal to the plate.

For fluid region far away from the plate, equation (6.11) takes the form

$$0 = -\frac{\partial p}{\partial x} - \rho_\infty g \quad (6.13)$$

Eliminating $\frac{\partial p}{\partial x}$ from (6.11) and (6.13), we get,

$$\rho \frac{\partial u'}{\partial t} = (\rho_\infty - \rho) g - \sigma B_0^2 u' + \mu \frac{\partial^2 u'}{\partial y^2} - \frac{\mu u'}{K^*} \quad (6.14)$$

Now, (6.7) gives,

$$\rho_\infty - \rho = \rho \left[\beta (T - T_\infty) + \bar{\beta} (C - C_\infty) \right] \quad (6.15)$$

Putting value of (6.15) in (6.14),

$$\rho \frac{\partial u'}{\partial t} = \rho \left[\beta (T - T_\infty) + \bar{\beta} (C - C_\infty) \right] g - \sigma B_0^2 u' + \mu \frac{\partial^2 u'}{\partial y^2} - \frac{\mu u'}{K^*}$$

$$i.e., \frac{\partial u'}{\partial \bar{t}} = g\beta(T - T_\infty) + g\bar{\beta}(C - C_\infty) - \frac{\sigma B_0^2 u'}{\rho} + \nu \frac{\partial^2 u'}{\partial \bar{y}^2} - \nu \frac{u'}{K^*} \quad (6.16)$$

Equation (6.8) yields,

$$\rho C_p \frac{\partial T}{\partial \bar{t}} = \kappa \frac{\partial^2 T}{\partial \bar{y}^2} + \frac{16\sigma^* T_\infty^3}{3\kappa^*} \frac{\partial^2 T}{\partial \bar{y}^2} + \alpha(T_\infty - T) \quad (6.17)$$

Equation (6.6) becomes,

$$\frac{\partial C}{\partial \bar{t}} = D_M \frac{\partial^2 C}{\partial \bar{y}^2} + D_T \frac{\partial^2 T}{\partial \bar{y}^2} + \bar{K}(C_\infty - C) \quad (6.18)$$

The relevant initial and boundary conditions are:

$$\left. \begin{aligned} u' = 0, T = T_\infty, C = C_\infty : \forall \bar{y} \geq 0; \bar{t} \leq 0 \\ u' = U_0 e^{a\bar{t}}, C = C_w : \bar{y} = 0, \bar{t} > 0 \\ T = T_\infty + (T_w - T_\infty) \frac{\bar{t}}{t_0} : \bar{y} = 0; 0 < \bar{t} \leq t_0 \\ T = T_w : \bar{y} = 0; \bar{t} > t_0 \\ u' \rightarrow 0, T \rightarrow T_\infty, C \rightarrow C_\infty : \bar{y} \rightarrow \infty; \bar{t} > 0 \end{aligned} \right\} \quad (6.19)$$

For the sake of normalization of the mathematical model of the problem, we introduce the following non-dimensional quantities-

$$Sr = \frac{D_T(T_w - T_\infty)}{(C_w - C_\infty)\nu}, N = \frac{\kappa\kappa^*}{4\sigma^* T_\infty^3}, u = \frac{u'}{U_0}, y = \frac{U_0}{\nu} \bar{y}, t = \frac{U_0^2}{\nu} \bar{t}, Gr = \frac{\nu g\beta(T_w - T_\infty)}{U_0^3}, a = a' \frac{\nu}{U_0^2},$$

$$Gm = \frac{\nu g\bar{\beta}(C_w - C_\infty)}{U_0^3}, \theta = \frac{T - T_\infty}{T_w - T_\infty}, \phi = \frac{C - C_\infty}{C_w - C_\infty}, Pr = \frac{\mu C_p}{\kappa}, M = \frac{\sigma B_0^2 \nu}{\rho U_0^2}, Sc = \frac{\nu}{D_M}, \Lambda = 1 + \frac{4}{3N},$$

$$Q = \frac{\alpha \nu^2}{U_0^2 \kappa}, K = \frac{\nu \bar{K}}{U_0^2}, t_1 = \frac{U_0^2}{\nu} t_0, M_1 = M + \frac{1}{K^*}$$

The non-dimensional governing equations are

$$\frac{\partial u}{\partial t} = \frac{\partial^2 u}{\partial y^2} + Gr\theta + Gm\phi - M_1 u \quad (6.20)$$

$$\frac{\partial \theta}{\partial t} = \frac{\Lambda}{Pr} \frac{\partial^2 \theta}{\partial y^2} - \frac{Q}{Pr} \theta \quad (6.21)$$

$$\frac{\partial \phi}{\partial t} = \frac{1}{Sc} \frac{\partial^2 \phi}{\partial y^2} + Sr \frac{\partial^2 \theta}{\partial y^2} - K\phi \quad (6.22)$$

Subject to the initial and boundary conditions

$$\left. \begin{aligned} u = 0, \theta = 0, \phi = 0 : \forall y \geq 0; t \leq 0 \\ u = e^{at}, \phi = 1 : y = 0, t > 0 \\ \theta = \frac{t}{t_1} : y = 0; 0 < t \leq t_1 \\ \theta = 1 : y = 0; t > t_1 \\ u \rightarrow 0, \theta \rightarrow 0, \phi \rightarrow 0 : y \rightarrow \infty; t > 0 \end{aligned} \right\} \quad (6.23)$$

6.3 Method of Solution

On taking Laplace transform of the equations (6.22), (6.21) and (6.20) respectively, we get the following equations:

$$s\bar{\phi} = \frac{1}{Sc} \frac{d^2 \bar{\phi}}{dy^2} + Sr \frac{d^2 \bar{\theta}}{dy^2} - K\bar{\phi} \quad (6.24)$$

$$s\bar{\theta} = \frac{\Lambda}{Pr} \frac{d^2 \bar{\theta}}{dy^2} - \frac{Q}{Pr} \bar{\theta} \quad (6.25)$$

$$s\bar{u} = \frac{d^2 \bar{u}}{dy^2} + Gr\bar{\theta} + Gm\bar{\phi} - M_1\bar{u} \quad (6.26)$$

Subject to the initial and boundary conditions:

$$\left. \begin{aligned} y = 0 : \bar{\theta} = \frac{2}{s^2 t_1} (1 - e^{-st_1}), \bar{\phi} = \frac{1}{s}, \bar{u} = \frac{1}{s-a} \\ y \rightarrow \infty : \bar{\theta} \rightarrow 0, \bar{\phi} \rightarrow 0, \bar{u} \rightarrow 0 \end{aligned} \right\} \quad (6.27)$$

Solving equations from (6.24) to (6.26) subject to the conditions (6.27) and taking inverse Laplace transform of the solutions, the expression for temperature field θ , concentration field ϕ , and velocity field u are as follows:

$$\theta = \frac{1}{t_1} \Delta f_1 \quad (6.28)$$

$$\phi = \begin{cases} \phi_{1,1} + \phi_{1,2} - \phi_{1,3} : \Lambda Sc \neq Pr \\ \phi_{2,1} + \phi_{2,2} - \phi_{2,3} : \Lambda Sc = Pr \end{cases} \quad (6.29)$$

$$u = \begin{cases} u_{1,1} - u_{1,2} - u_{1,3} - u_{1,4} + u_{1,5} : Pr \neq \Lambda, Sc \neq 1, Pr \neq \Lambda Sc \\ u_{2,1} - u_{2,2} - u_{2,3} - u_{2,4} + u_{2,5} : Pr = \Lambda, Sc \neq 1 \\ u_{3,1} - u_{3,2} - u_{3,3} - u_{3,4} + u_{3,5} : Pr \neq \Lambda, Sc = 1 \\ u_{4,1} - u_{4,2} - u_{4,3} - u_{4,4} + u_{4,5} : Pr = \Lambda, Sc = 1 \\ u_{5,1} - u_{5,2} - u_{5,3} - u_{5,4} + u_{5,5} : Pr \neq \Lambda, Sc \neq 1, Pr = \Lambda Sc \end{cases} \quad (6.30)$$

6.4 Nusselt Number

By Fourier's law of conduction, the heat flux q^* at the plate $\bar{y} = 0$ is given by

$$q^* = -\kappa_0^* \left. \frac{\partial T}{\partial \bar{y}} \right]_{\bar{y}=0} \quad (6.31)$$

Here, $\kappa_0^* = \kappa + \frac{16\sigma^* T_\infty^3}{3\kappa^*}$ is modified thermal conductivity.

Equation (6.31) yields

$$Nu = - \left. \frac{\partial \theta}{\partial y} \right]_{y=0} \quad (6.32)$$

Here, $Nu = \frac{q^* \nu}{\kappa_0^* U_0 (T_w - T_\infty)} = \frac{q^* \nu}{\kappa \Lambda (T_w - T_\infty) U_0} = \frac{3Nq^* \nu}{\kappa(4+3N)(T_w - T_\infty) U_0}$ is termed as Nusselt number which is associated with the rate of heat transfer at the plate.

Equation (6.32) gives,

$$Nu = - \frac{1}{t_1} \Delta \Phi_1 \quad (6.33)$$

6.5 Sherwood Number

By Fick's law of diffusion, the mass flux M_w at the plate $\bar{y} = 0$ is given by

$$M_w = -D_M \left. \frac{\partial C}{\partial \bar{y}} \right]_{\bar{y}=0} \quad (6.34)$$

Equation (6.34) gives

$$Sh = - \left. \frac{\partial \phi}{\partial y} \right]_{y=0} \quad (6.35)$$

In (6.35), $Sh = \frac{M_w \nu}{D_M U_0 (C_w - C_\infty)}$ is labeled as the Sherwood number which determines the rate of mass transfer at the plate.

Equation (6.35) yields

$$Sh = - \begin{cases} Sh_{1,1} + Sh_{1,2} - Sh_{1,3} : Pr \neq \Lambda Sc \\ Sh_{2,1} + Sh_{2,2} - Sh_{2,3} : Pr = \Lambda Sc \end{cases} \quad (6.36)$$

6.6 Skin Friction

By Newton's law of viscosity, the viscous drag at the plate $\bar{y} = 0$ is given by

$$\bar{\tau} = -\mu \left. \frac{\partial u'}{\partial \bar{y}} \right]_{\bar{y}=0} \quad (6.37)$$

Equation (6.37) gives

$$\tau = - \left. \frac{\partial u}{\partial y} \right]_{y=0} \quad (6.38)$$

In (6.38), $\tau = \frac{\bar{\tau} \nu}{\mu U_0^2}$ is entitled as the skin friction or coefficient of friction which gives the rate of momentum transfer at the plate.

Equation (6.38) yields,

$$\tau = - \begin{cases} \tau_{1,1} - \tau_{1,2} - \tau_{1,3} - \tau_{1,4} + \tau_{1,5} : \text{Pr} \neq \Lambda, \text{Sc} \neq 1, \text{Pr} \neq \Lambda \text{Sc} \\ \tau_{2,1} - \tau_{2,2} - \tau_{2,3} - \tau_{2,4} + \tau_{2,5} : \text{Pr} = \Lambda, \text{Sc} \neq 1 \\ \tau_{3,1} - \tau_{3,2} - \tau_{3,3} - \tau_{3,4} + \tau_{3,5} : \text{Pr} \neq \Lambda, \text{Sc} = 1 \\ \tau_{4,1} - \tau_{4,2} - \tau_{4,3} - \tau_{4,4} + \tau_{4,5} : \text{Pr} = \Lambda, \text{Sc} = 1 \\ \tau_{5,1} - \tau_{5,2} - \tau_{5,3} - \tau_{5,4} + \tau_{5,5} : \text{Pr} \neq \Lambda, \text{Sc} \neq 1, \text{Pr} = \Lambda \text{Sc} \end{cases} \quad (6.39)$$

6.7 Results and Discussion

To analyse the effects of the physical parameters involved in the flow and transport characteristics, numerical calculations for temperature field, concentration field, velocity field, skin friction, Nusselt number, Sherwood number at the plate are carried out by assigning some specific values to the parameters and variables.

The numerically computed results are displayed from Figure 6.2 to Figure 6.26.

Figures 6.2 to 6.4 display the variation of temperature field versus normal co-ordinate y . There is a comprehensive fall in the temperature field for increasing radiation parameter as displayed in Figure 6.2. Thus, radiation tends to reduce fluid temperature. This is in agreement with the result obtained by Nandkeolyar et al. (2013). Figure 6.3 depicts that ascending values of the heat absorption parameter lessens temperature. From Figure 6.4, it is observed that a higher Prandtl number declines fluid temperature. Thus, temperature hikes with increasing thermal diffusivity.

Figures 6.5 to 6.8 show the variation of concentration field versus normal co-ordinate y . The concentration field declines with enhancement in chemical reaction parameter as depicted in Figure 6.5. Increasing chemical reaction devours chemical substances present in the fluid rapidly and as a result fluid concentration gets reduced. Ascending values of Schmidt number diminishes concentration field as noticed in Figure 6.6. Consequently, higher mass diffusivity upsurges the concentration field. This is in line with the result obtained by Seth and Sarkar (2015). Figure 6.7 admits that concentration hikes with growing Soret number. Thus, the temperature gradient increases the concentration field more rapidly compared to the concentration gradient. The concentration field escalates in a thin layer adjacent to the plate but declines outside with increment in radiation parameter as noticed in Figure 6.8. Thus, radiation hikes concentration in a small layer adjoining the plate but its behaviour takes a reverse turn outside the layer.

Figures 6.9 to 6.16 exhibit the variation of velocity field versus normal co-ordinate y . Figure 6.9 reveals that velocity field declines for ascending values of radiation parameter. Increasing radiation parameter decreases the fluid temperature and as a result, the flow becomes slow. Higher magnetic parameter reduces fluid velocity as displayed in Figure 6.10. The magnetic field, which is applied in the transverse direction to the flow, generates a resistive force known as Lorentz force, which drops fluid velocity. This agrees the result obtained by Sinha et al. (2017). Figure 6.11 asserts that there is a comprehensive fall in velocity field as chemical reaction parameter hikes. Increasing chemical reaction parameter enhances the process of collision between fluid molecules and as a result, kinetic energy is lost. Subsequently, fluid velocity declines. Ascending values of Prandtl number diminishes the velocity field as shown in Figure 6.12. Thus, higher thermal diffusivity hikes the velocity field. Figure 6.13 admits that fluid velocity falls rapidly as Schmidt number hikes. Hence, increment in mass diffusivity hikes velocity field. Growing porosity parameter means there is more free space in the system for the fluid to flow. Accordingly, the velocity of the fluid upsurges. This phenomenon is reflected in Figure 6.14. Ascending Soret number accelerates fluid flow as noticed in Figure 6.15. An increment in Soret number suggests an extensive rise in temperature gradient over the concentration gradient. . This gives us an idea that if the temperature gradient is higher than the concentration gradient, then fluid motion is accelerated. Increasing thermal Grashof number lifts velocity field as noticed in Figure 6.16. Thus, thermal buoyancy force escalates fluid velocity.

Figures 6.17 and 6.18 depict the variation of Nusselt number versus time t . Nusselt number hikes for ascending values of radiation parameter as noticed in Figure 6.17. Hence, radiation amplifies the process of heat transfer from the plate to the fluid. Growing Prandtl number hikes Nusselt number as shown in Figure 6.18. Thus, higher thermal diffusivity declines the heat transfer process.

Figures 6.19 to 6.22 illustrate the variation of Sherwood number versus time t . There is a comprehensive rise in Sherwood number for ascending values of chemical reaction parameter as shown in Figure 6.19. From Figure 6.20, it is observed that the Sherwood number lowers with rising values of the radiation parameter. Thus, radiation weakens the rate of mass transfer from the plate to the fluid. Sherwood number declines substantially for increasing values of Prandtl number as displayed in Figure 6.21. Hence, growing thermal diffusivity accelerates the process of mass transfer. Increasing Soret number reduces

Sherwood number as shown in Figure 6.22. So, a high concentration gradient compared to a low-temperature gradient quickens the process of mass transfer.

Figures 6.23 to 6.26 illuminate the change in skin friction versus time t . Skin friction upsurges for a small time but reverses its behaviour afterward with increasing values of radiation parameters as observed in Figure 6.23. Increasing porosity parameter hikes skin friction for a small time but reduces thereafter as noticed in Figure 6.24. Figure 6.25 asserts that skin friction upsurges for a small time and reduces after that as Soret number hikes. Thus, growing temperature gradient hikes frictional resistivity for small-time but reduces afterward. Higher solutal Grashof number raises skin friction for small time but reverses its behavior as noticed in Figure 6.26. Thus, solutal buoyancy force first increase frictional resistivity for small time but decrease afterwards.

6.8 Comparison of Result

To check the accuracy of our result, we have compared one of our results with Seth et al. (2016b) who considered the unsteady free convective MHD flow of a chemically reactive, radiative flow past a moving vertical plate submerged in a porous medium. In absence of the Soret effect (i.e., $Sr=0$), expression of concentration field of the present problem is

$$\phi = \psi_1$$

Figure 6.27 and Figure 6.28 display the concentration field versus normal co-ordinate y for different chemical reaction parameter obtained by Seth et al. (2016b) and present authors respectively. Both figures uniquely express the fact that the concentration field declines for ascending values of chemical reaction parameter. Hence, an excellent agreement of results between the present authors and Seth et al. (2016b) is observed.

6.9 Conclusions

The purpose of the present work is to study exclusively the effects of radiation, chemical reaction and thermal diffusion effect of an unsteady MHD flow past a moving vertical plate immersed in a porous medium with ramped temperature. The study of flow and transport characteristics under the action of different parameters was carried out with the help of graphs. The leading outcomes of the present work are as follows:

- i. Radiation declines both temperature and velocity fields.
- ii. Increasing heat absorption process lowers the fluid temperature.

- iii. Higher chemical reaction reduces both concentration and velocity profiles.
- iv. Lorentz force decelerates fluid velocity but hikes skin friction.
- v. Ascending Prandtl number upsurges Nusselt number but diminish Sherwood number.

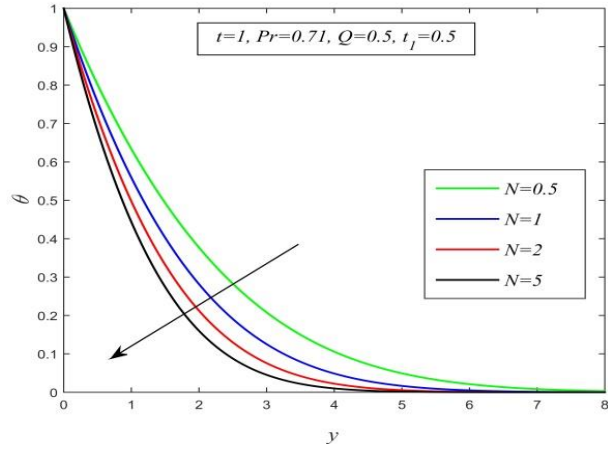


Figure 6.2: Temperature field versus y for different N and $t=1, Pr=0.71, Q=0.5, t_1=0.5$

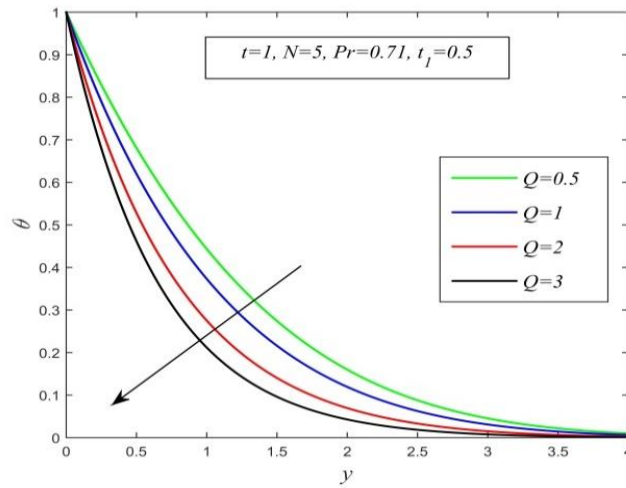


Figure 6.3: Temperature field versus y for different Q and $t=1, Pr=0.71, N=5, t_1=0.5$

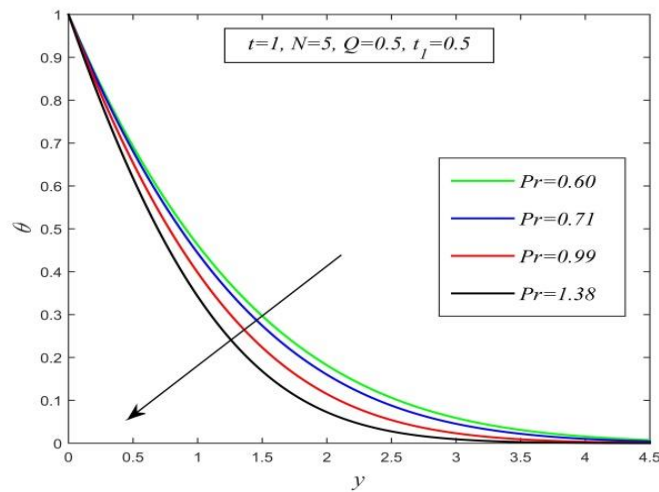


Figure 6.4: Temperature field versus y for different Pr and $t=1, N=5, Q=0.5, t_1=0.5$

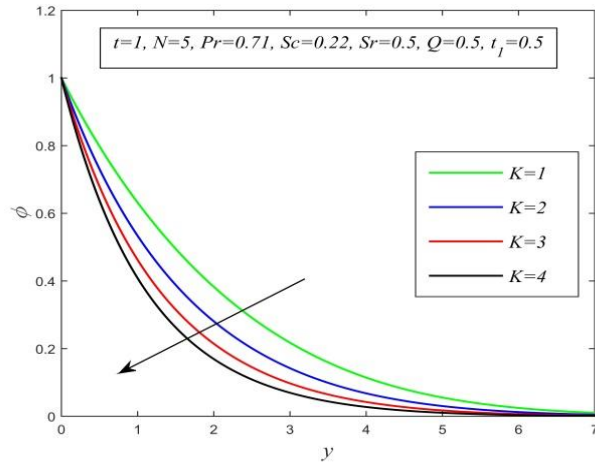


Figure 6.5: Concentration field versus y for different K and $t=1, N=5, Pr=0.71, Sc=0.22, Sr=0.5, Q=0.5, t_1=0.5$

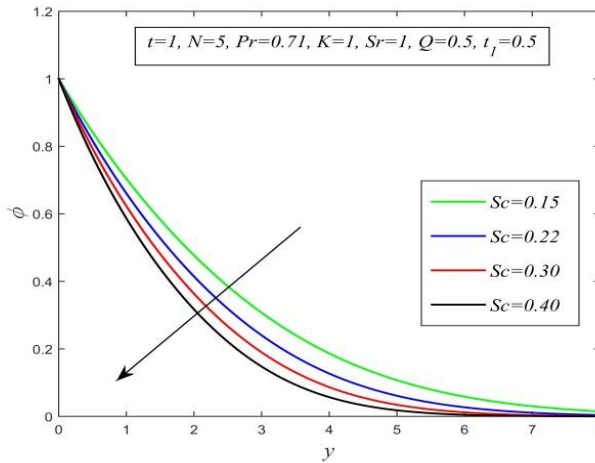


Figure 6.6: Concentration field versus y for different Sc and $t=1, N=5, Pr=0.71, K=1, Sr=1, Q=0.5, t_1=0.5$

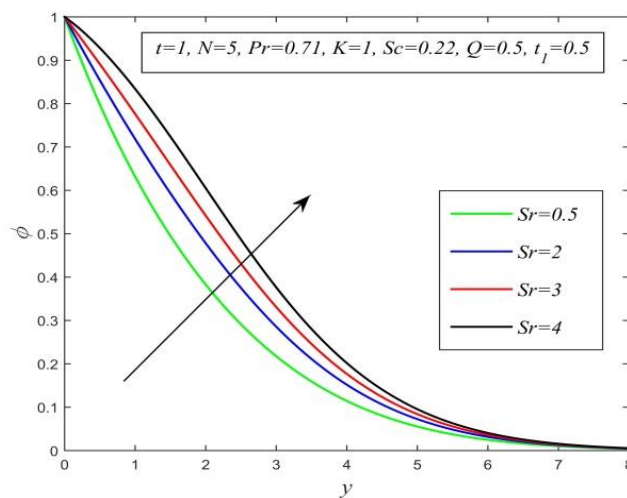


Figure 6.7: Concentration field versus y for different Sr and $t=1, N=5, Pr=0.71, K=1, Sc=0.22, Q=0.5, t_1=0.5$

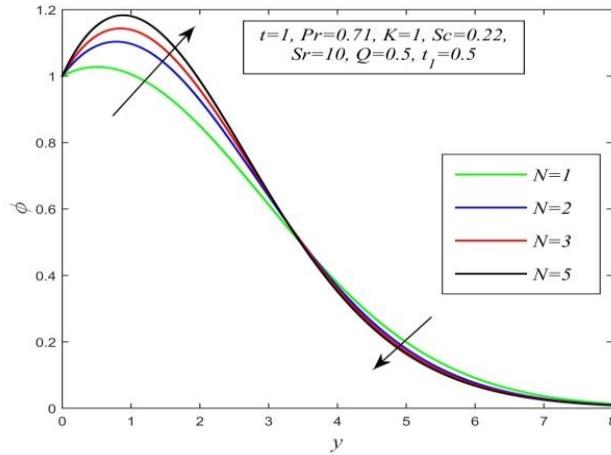


Figure 6.8: Concentration field versus y for different N and $t=1, Pr=0.71, K=1, Sc=0.22, Sr=10, Q=0.5, t_1=0.5$

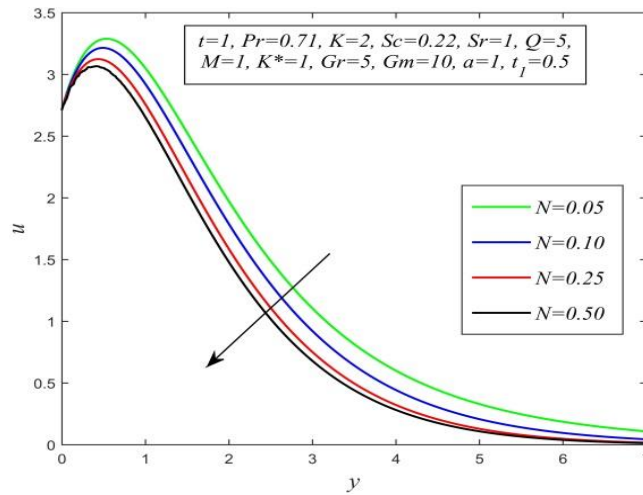


Figure 6.9: Velocity field versus y for different N and $t=1, Pr=0.71, K=2, Sc=0.22, Sr=1, Q=5, M=1, K^*=1, Gr=5, Gm=10, a=1, t_1=0.5$

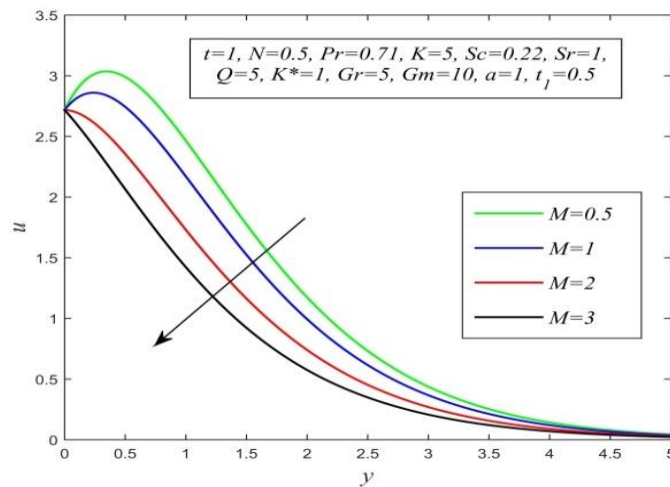


Figure 6.10: Velocity field versus y for different M and $t=1, N=0.5, Pr=0.71, K=5, Sc=0.22, Sr=1, Q=5, K^*=1, Gr=5, Gm=10, a=1, t_1=0.5$

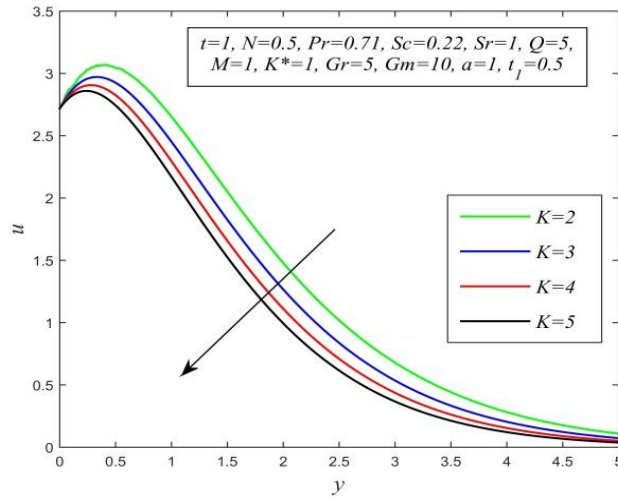


Figure 6.11: Velocity field versus y for different K and $t=1, N=0.5, Pr=0.71, Sc=0.22, Sr=1, Q=5, M=1, K^*=1, Gr=5, Gm=10, a=1, t_1=0.5$

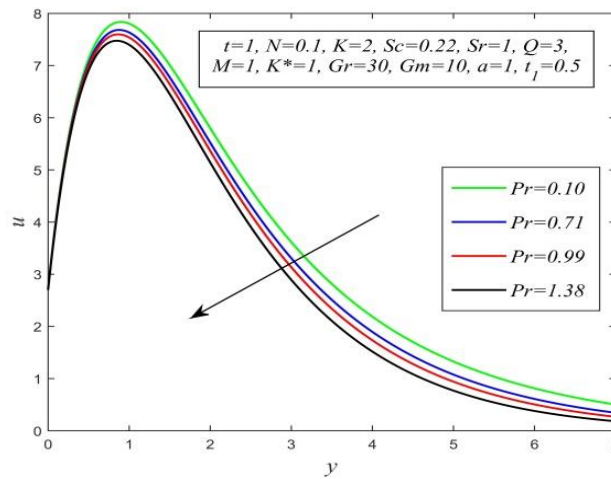


Figure 6.12: Velocity field versus y for different Pr and $t=1, N=0.1, K=2, Sc=0.22, Sr=1, Q=3, M=1, K^*=1, Gr=30, Gm=10, a=1, t_1=0.5$

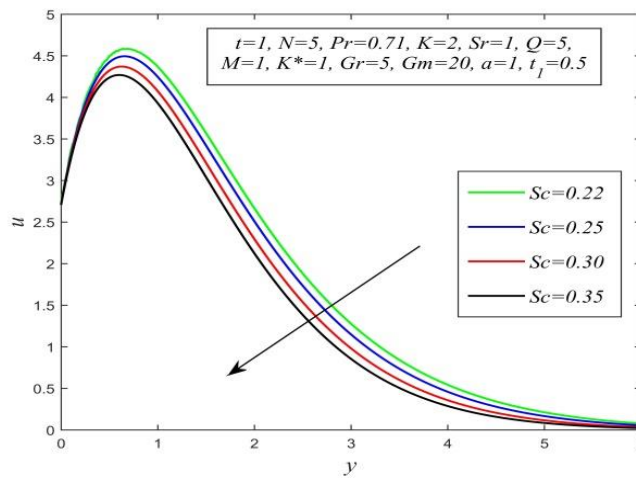


Figure 6.13: Velocity field versus y for different Sc and $t=1, N=5, K=2, Pr=0.71, Sr=1, Q=5, M=1, K^*=1, Gr=5, Gm=20, a=1, t_1=0.5$

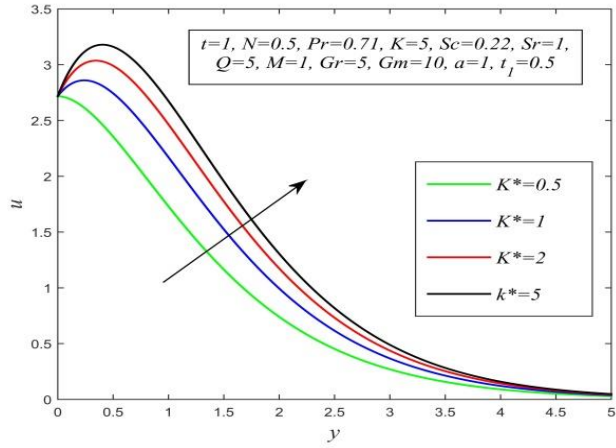


Figure 6.14: Velocity field versus y for different K^* and $t=1, N=0.5, K=5, Pr=0.71, Sc=0.22, Sr=1, Q=5, M=1, Gr=5, Gm=10, a=1, t_1=0.5$

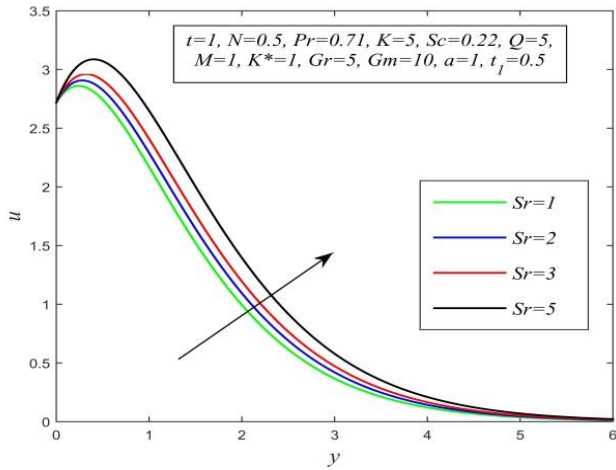


Figure 6.15: Velocity field versus y for different Sr and $t=1, N=0.5, K=5, Pr=0.71, Sc=0.22, Q=5, M=1, K^*=1, Gr=5, Gm=10, a=1, t_1=0.5$

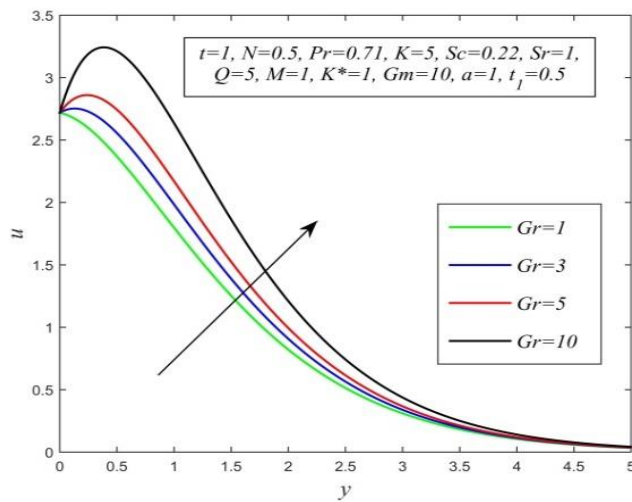


Figure 6.16: Velocity field versus y for different Sr and $t=1, N=0.5, K=5, Pr=0.71, Sc=0.22, Q=5, M=1, K^*=1, Gr=5, Gm=10, a=1, t_1=0.5$

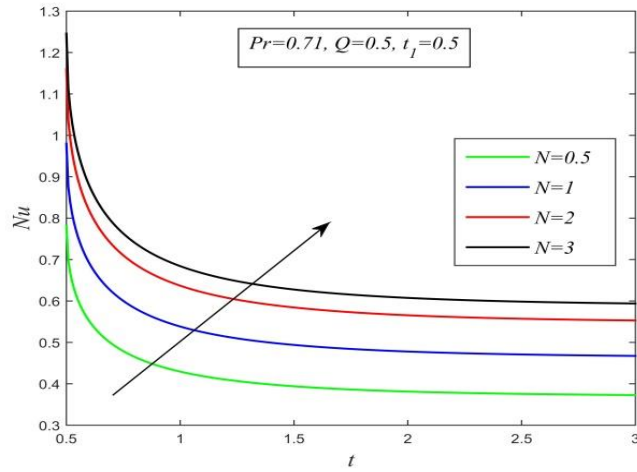


Figure 6.17: Nusselt number versus t for different N and $Pr=0.71, Q=0.5, t_1=0.5$

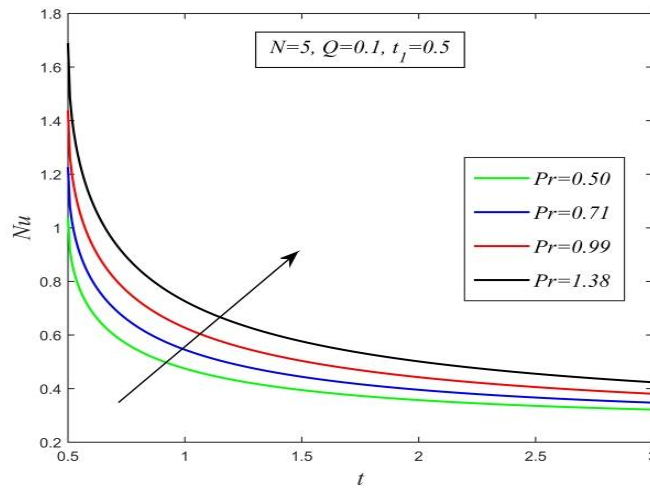


Figure 6.18: Nusselt Number versus t for different Pr and $N=5, Q=0.1, t_1=0.5$

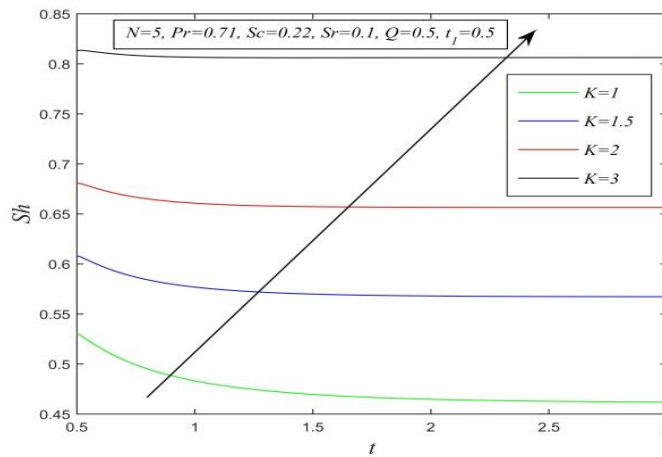


Figure 6.19: Sherwood Number versus t for different K and $N=5, Pr=0.71, Sc=0.22, Sr=0.1, Q=0.5, t_1=0.5$

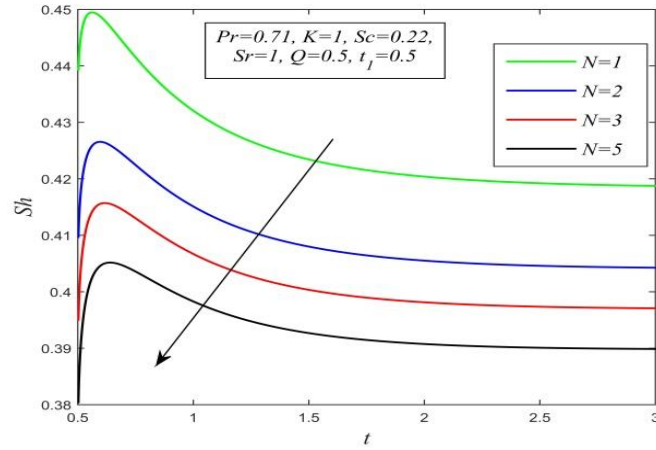


Figure 6.20: Sherwood Number versus t for different N and $Pr=0.71, K=1, Sc=0.22, Sr=1, Q=0.5, t_1=0.5$

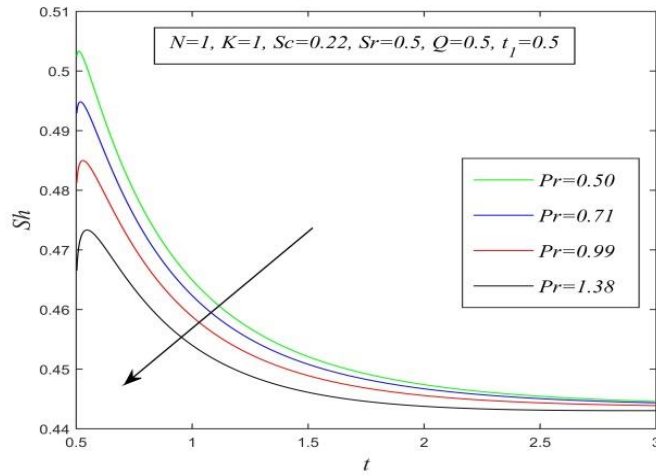


Figure 6.21: Sherwood Number versus t for different Pr and $N=1, K=1, Sc=0.22, Sr=0.5, Q=0.5, t_1=0.5$

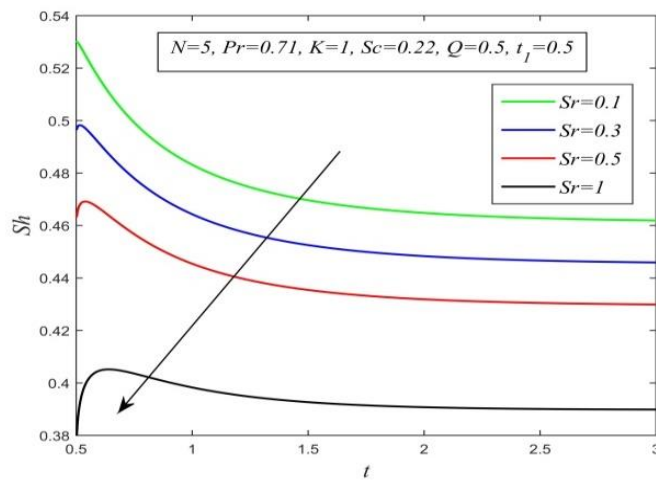


Figure 6.22: Sherwood Number versus t for different Sr and $N=5, Pr=0.71, K=1, Sc=0.22, Q=0.5, t_1=0.5$

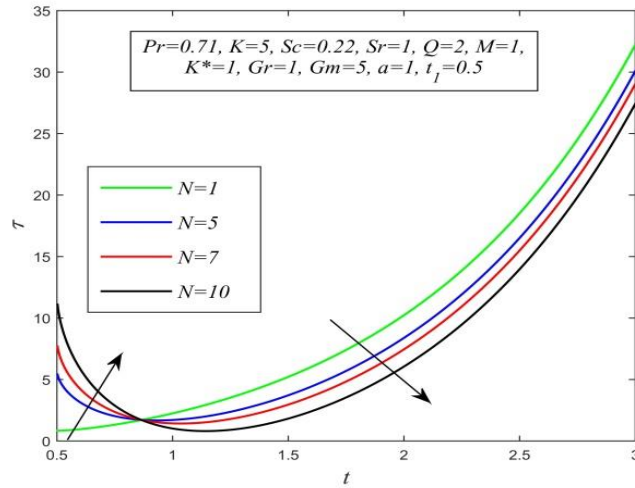


Figure 6.23: Skin friction versus t for different N and $Pr=0.71$, $K=5$, $Sc=0.22$, $Sr=1$, $Q=2$, $M=1$, $K^*=1$, $Gr=1$, $Gm=5$, $a=1$, $t_1=0.5$

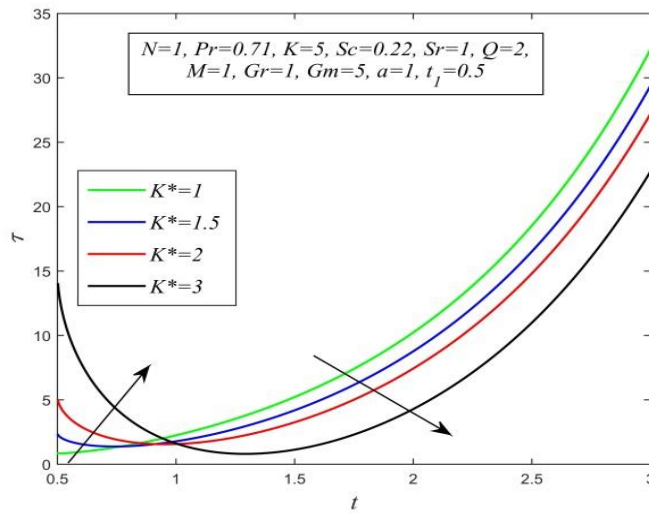


Figure 6.24: Skin friction versus t for different K^* and $N=1$, $Pr=0.71$, $K=5$, $Sc=0.22$, $Sr=1$, $Q=2$, $M=1$, $Gr=1$, $Gm=5$, $a=1$, $t_1=0.5$

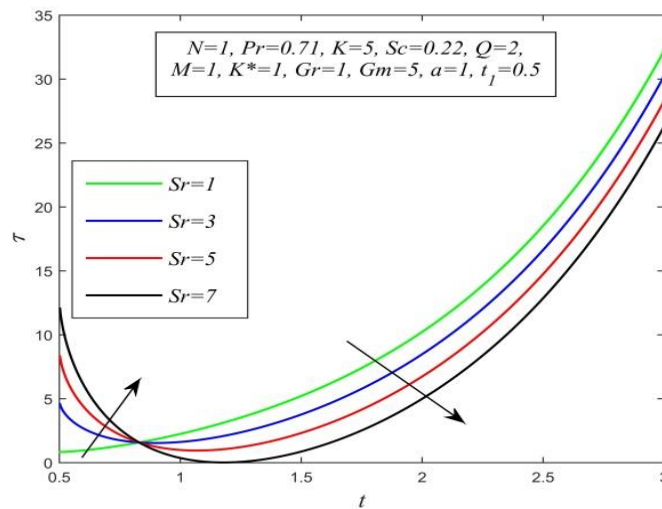


Figure 6.25: Skin friction versus t for different Sr and $N=1$, $Pr=0.71$, $K=5$, $Sc=0.22$, $Q=2$, $M=1$, $K^*=1$, $Gr=1$, $Gm=5$, $a=1$, $t_1=0.5$

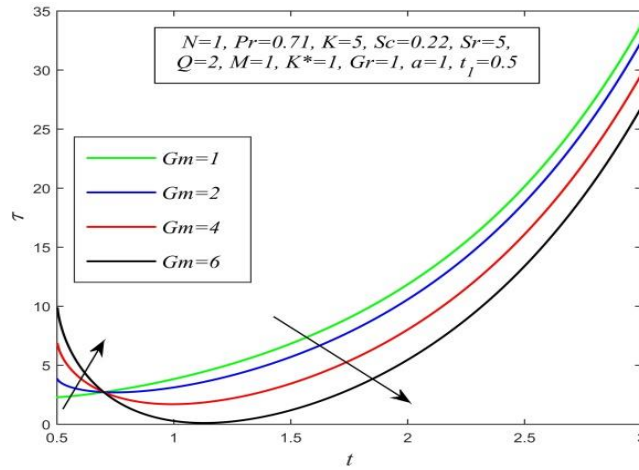


Figure 6.26: Skin friction versus t for different Gm and $N=1$, $Pr=0.71$, $K=5$, $Sc=0.22$, $Sr=5$, $Q=2$, $M=1$, $K^*=1$, $Gr=1$, $a=1$, $t_1=0.5$

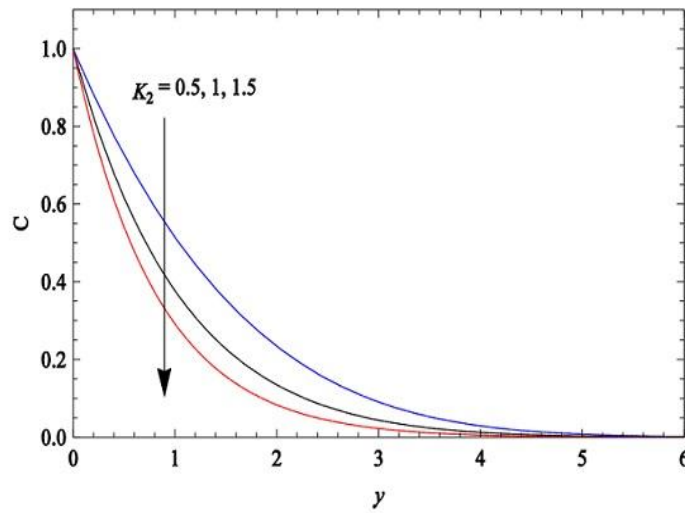


Figure 6.27: Scanned graph of concentration field versus y for different K when $t=1.2$, $Sc=0.6$ drawn by Seth et al. (2016b)

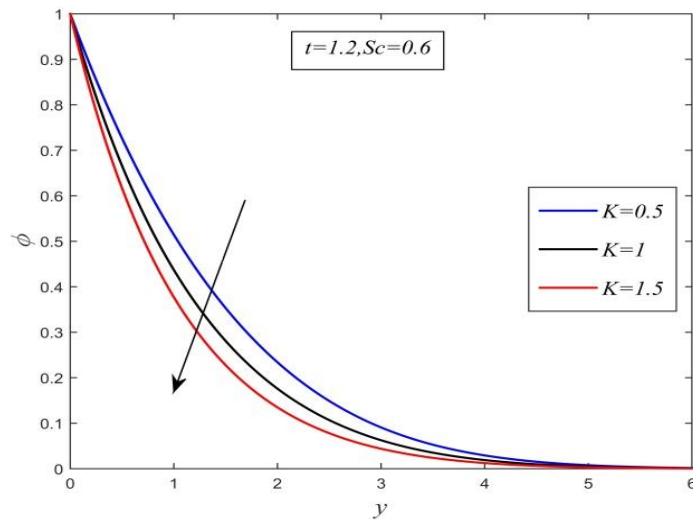


Figure 6.28: Concentration field versus y for different K when $t=1.2$, $Sc=0.6$, $Sr=0$ drawn by author

Nomenclature

a : Surface acceleration parameter

a^* : Absorption coefficient $\left(\frac{m^2}{mol}\right)$

\vec{B} : Magnetic flux density

B_0 : Strength of the applied magnetic field $\left(\frac{Weber}{m^2}\right)$

C : Molar species concentration $\left(\frac{mol}{m^3}\right)$

C_p : Specific heat at constant pressure $\left(\frac{J}{Kg.K}\right)$

C_∞ : Concentration far away from the plate $\left(\frac{mol}{m^3}\right)$

C_w : Concentration at the plate $\left(\frac{mol}{m^3}\right)$

D_M : Mass diffusivity $\left(\frac{m^2}{s}\right)$

D_T : Molar thermal diffusivity $\left(\frac{J}{K.mol}\right)$

\vec{g} : Gravitation acceleration vector

g : Gravitational acceleration $\left(\frac{m}{s^2}\right)$

Gr : Thermal Grashof number

Gm : Solutal Grashof number

K_T : Thermal diffusion ratio

K^* : Porosity parameter

\vec{J} : Current density vector $\left(\frac{A}{m^2}\right)$

\bar{K} : Chemical reaction rate $\left(\frac{mol}{m^2.s}\right)$

K : Chemical reaction parameter

M : Magnetic parameter

N : Radiation parameter

p : Pressure $\left(\frac{N}{m^2}\right)$

Pr : Prandtl number

Q : Heat absorption parameter

\vec{q} : Fluid velocity vector

\vec{q}_r : Radiation heat flux vector

q_r : Radiation heat flux $\left(\frac{W}{m^2}\right)$

Sc : Schmidt number

Sr : Soret number

\bar{t} : Time (s)

t_0 : Critical time for rampedness (s)

t_1 : Non- dimensional critical time for rampedness

T : Fluid temperature (K)

T_w : Temperature at the plate (K)

T_∞ : Undisturbed temperature (K)

u' : X-component of fluid velocity $\left(\frac{m}{s}\right)$

U_0 : Plate velocity $\left(\frac{m}{s}\right)$

Greek Symbols:

α : Heat absorption rate $\left(\frac{J}{s}\right)$

η : Magnetic diffusivity $\left(\frac{m^2}{s}\right)$

μ : Coefficient of viscosity $\left(\frac{Kg}{m.s}\right)$

σ : Electrical conductivity $\left(\frac{S}{m}\right)$

σ^* : Stefan-Boltzmann constant $\left(\frac{W}{m^2.K^4}\right)$

ρ : Fluid density $\left(\frac{Kg}{m^3}\right)$

ρ_∞ : Fluid density far away from the plate $\left(\frac{Kg}{m^3}\right)$

κ : Thermal conductivity $\left(\frac{W}{m.K}\right)$

κ^* : Mean absorption constant $\left(\frac{1}{m}\right)$

β : Volumetric coefficient of thermal expansion $\left(\frac{1}{K}\right)$

$\bar{\beta}$: Volumetric coefficient of solutal expansion $\left(\frac{1}{K.mol}\right)$

ν : Kinematic viscosity $\left(\frac{m^2}{s}\right)$

Subscripts:

w : Refers to physical quantity at the plate

∞ : Refers to physical quantity far away from the plate

Appendix

$$\begin{aligned}
a_1 &= \frac{\text{Pr}}{\Lambda}, a_2 = \frac{Q}{\lambda}, a_3 = \frac{a_2}{a_1}, f_1 = f(a_1, a_3, y, t), a_4 = \frac{a_2 - \text{Sc} \cdot K}{a_1 - \text{Sc}}, a_5 = \frac{\text{SrSc} a_1}{t_1 (a_1 - \text{Sc})}, \phi_{1,1} = \psi_1, \\
\psi_1 &= \psi(\text{Sc}, K, y, t), A_1 = \frac{a_3 - a_4}{a_4^2}, A_2 = -A_1, A_3 = \frac{a_3}{a_4}, \phi_{1,2} = a_5 (A_1 \Delta \psi_2 + A_2 \Delta \psi_1 + A_3 \Delta f_2), \\
\psi_2 &= \Psi(\text{Sc}, K, -a_4, y, t), f_2 = f(\text{Sc}, K, y, t), \phi_{1,3} = a_5 (A_1 \Delta \psi_4 + A_2 \Delta \psi_3 + A_3 \Delta f_1), \\
\psi_3 &= \psi(a_1, a_3, y, t), \psi_4 = \Psi(a_1, a_3, -a_4, y, t), \phi_{2,1} = \phi_{1,1}, \phi_{2,2} = a_6 (\Delta \psi_1 + a_3 \Delta f_2), a_6 = \frac{\text{SrSc} \cdot a_1}{t_1 (a_2 - \text{Sc} \cdot K)}, \\
\phi_{2,3} &= a_6 (\Delta \psi_3 + a_3 \Delta f_1), a_7 = \frac{a_2 - M_1}{a_1 - 1}, a_8 = \frac{\text{Gr}}{t_1 (a_1 - 1)}, a_9 = \frac{K \text{Sc} - M_1}{\text{Sc} - 1}, \\
u_{1,1} &= u_{1,1,1} + u_{1,1,2} + u_{1,1,3} + u_{1,1,4} - u_{1,1,5}, u_{1,1,1} = h_2, h_2 = e^{at} h_1, h_1 = h(M_1 + a, y, t), \\
u_{1,1,2} &= a_8 (A_4 \Delta h_5 + A_5 \Delta h_3 + A_6 \Delta r_1), A_4 = \frac{1}{a_7^2}, A_5 = -A_4, A_6 = \frac{1}{a_7}, h_3 = h(M_1, y, t), \\
h_4 &= h(M_1 - a_7, y, t), h_5 = e^{-a_7 t} h_4, r_1 = r(M_1, y, t), u_{1,1,3} = a_{10} (A_7 h_7 + A_8 h_3), a_{10} = \frac{\text{Gm}}{\text{Sc} - 1}, A_7 = -\frac{1}{a_9}, \\
A_8 &= -A_7, h_7 = e^{-a_9 t} h_6, h_6 = h(M_1 - a_9, y, t), u_{1,1,4} = a_{11} (A_9 \Delta h_9 + A_{10} \Delta h_7 + A_{11} \Delta h_3 + A_{12} \Delta r_1), \\
a_{11} &= \frac{\text{Gm} \cdot a_5}{\text{Sc} - 1}, A_9 = \frac{a_3 - a_4}{(a_9 - a_4) a_4^2}, A_{10} = \frac{a_3 - a_9}{(a_4 - a_9) a_9^2}, A_{11} = -(A_9 + A_{10}), A_{12} = \frac{a_3}{a_4 a_9}, h_9 = e^{-a_4 t} h_8, \\
h_8 &= h(M - a_4, y, t), u_{1,1,5} = a_{12} (A_{13} \Delta h_9 + A_{14} \Delta h_5 + A_{15} \Delta h_3 + A_{16} \Delta r_1), a_{12} = \frac{\text{Gm} \cdot a_5}{a_1 - 1}, A_{13} = \frac{a_3 - a_4}{(a_7 - a_4) a_4^2}, \\
A_{14} &= \frac{a_3 - a_7}{(a_4 - a_7) a_7^2}, A_{15} = -(A_{13} + A_{14}), A_{16} = \frac{a_3}{a_4 a_7}, u_{1,2} = a_8 (A_4 \Delta \psi_5 + A_5 \Delta \psi_3 + A_6 \Delta f_1), \\
\psi_5 &= \Psi(a_1, a_3, -a_7, y, t), u_{1,3} = a_{10} (A_7 \psi_6 + A_8 \psi_1), \psi_6 = \Psi(\text{Sc}, K, -a_9, y, t), \\
u_{1,4} &= a_{11} (A_9 \Delta \psi_2 + A_{10} \Delta \psi_6 + A_{11} \Delta \psi_1 + A_{12} \Delta f_2), u_{1,5} = a_{12} (A_{13} \Delta \psi_4 + A_{14} \Delta \psi_5 + A_{15} \Delta \psi_3 + A_{16} \Delta f_1), \\
u_{2,1} &= u_{2,1,1} + u_{2,1,2} + u_{2,1,3} + u_{2,1,4} - u_{2,1,5}, u_{2,1,1} = u_{1,1,1}, u_{2,1,2} = a_{13} \Delta r_1, a_{13} = \frac{\text{Gr}}{t_1 (a_2 - M_1)}, u_{2,1,3} = u_{1,1,3}, \\
u_{2,1,4} &= u_{1,1,4}, u_{2,1,5} = a_{14} (A_1 \Delta h_9 + A_2 \Delta h_3 + A_3 \Delta r_1), a_{14} = \text{Gm} \cdot a_5, u_{2,2} = a_{13} \Delta r_2, r_2 = r(a_2, y, t), u_{2,3} = u_{1,3}, \\
u_{2,4} &= u_{1,4}, u_{2,5} = a_{14} (A_1 \Delta h_{11} + A_2 \Delta h_{12} + A_3 \Delta r_2), h_{10} = h(a_2 - a_4, y, t), h_{11} = e^{-a_4 t} h_{10}, h_{12} = h(a_2, y, t), \\
u_{3,1} &= u_{3,1,1} + u_{3,1,2} + u_{3,1,3} + u_{3,1,4} - u_{3,1,5}, u_{3,1,1} = u_{1,1,1}, u_{3,1,2} = u_{1,1,2}, u_{3,1,3} = a_{15} h_3, a_{15} = \frac{\text{Gm}}{K - 1}, \\
u_{3,1,4} &= a_{16} (A_1 \Delta h_9 + A_2 \Delta h_3 + A_3 \Delta r_1), a_{16} = \frac{\text{Gm} \cdot a_5}{K - 1}, u_{3,1,5} = u_{1,1,5}, u_{3,2} = u_{1,2}, u_{3,3} = a_{15} h_{13}, h_{13} = h(K, y, t), \\
u_{3,4} &= a_{16} (A_1 \Delta h_5 + A_2 \Delta h_3 + A_3 \Delta r_3), h_{14} = h(K - a_4, y, t), h_{15} = e^{-a_4 t} h_{14}, r_3 = r(K, y, t), u_{3,5} = u_{1,5}, \\
u_{4,1} &= u_{4,1,1} + u_{4,1,2} + u_{4,1,3} + u_{4,1,4} - u_{4,1,5}, u_{4,1,1} = u_{1,1,1}, u_{4,1,2} = u_{2,1,2}, u_{4,1,3} = u_{3,1,3}, u_{4,1,4} = a_{17} (\Delta h_3 + a_3 \Delta r_1), \\
a_{17} &= \frac{\text{GmSr}}{t_1 (a_2 - K)(K - 1)}, u_{4,1,5} = u_{4,1,4}, u_{4,2} = u_{2,2}, u_{4,3} = u_{3,3}, u_{4,4} = a_{17} (\Delta h_{13} + a_3 \Delta r_3), \\
u_{4,5} &= a_{17} (\Delta h_{12} + a_3 \Delta r_2), u_{5,1} = u_{5,1,1} + u_{5,1,2} + u_{5,1,3} + u_{5,1,4} - u_{5,1,5}, u_{5,1,1} = u_{1,1,1}, u_{5,1,2} = u_{1,1,2}, u_{5,1,3} = u_{1,1,3},
\end{aligned}$$

$$u_{5,1,4} = a_{18} (A_{17}\Delta h_7 + A_{18}\Delta h_3 + A_{19}\Delta r_1), a_{18} = \frac{GmSrSc^2}{t_1(Sc-1)(a_2 - ScK)}, A_{17} = \frac{a_3 - a_9}{a_9^2}, A_{18} = -A_{17},$$

$$A_{19} = \frac{a_3}{a_9}, u_{5,1,5} = a_{18} (A_4\Delta h_5 + A_5\Delta h_3 + A_6\Delta r_1), u_{5,2} = u_{5,2}, u_{5,3} = u_{1,3},$$

$$u_{5,4} = a_{18} (A_{17}\Delta \psi_6 + A_{18}\Delta \psi_1 + A_{19}\Delta f_2), u_{5,5} = a_{18} (A_4\Delta \psi_5 + A_5\Delta \psi_3 + A_6\Delta f_1) \Phi_1 = \Phi(a_1, a_3, t)$$

$$Sh_{1,1} = \Omega_1, \Omega_1 = \Omega(Sc, K, t), Sh_{1,2} = a_5 (A_1\Delta Z_1 + A_2\Delta \Omega_1 + A_3\Delta \Phi_2), Z_1 = Z(Sc, K, -a_4, t),$$

$$\Phi_2 = \Phi(Sc, K, t), Sh_{1,3} = a_5 (A_1\Delta Z_2 + A_2\Delta \Omega_2 + A_3\Delta \Phi_1), Z_2 = Z(a_1, a_3, -a_4, t), \Omega_2 = \Omega(a_1, a_3, t),$$

$$Sh_{2,1} = Sh_{1,1}, Sh_{2,2} = a_6 (\Delta \Omega_1 + a_3\Delta \Phi_2), Sh_{2,3} = a_6 (\Delta \Omega_2 + a_3\Delta \Phi_1)$$

$$\tau_{1,1} = \tau_{1,1,1} + \tau_{1,1,2} + \tau_{1,1,3} + \tau_{1,1,4} - \tau_{1,1,5}, \tau_{1,1,1} = N_2, N_2 = e^{at} N_1, N_1 = N(M_1 + a, t),$$

$$\tau_{1,1,2} = a_8 (A_4\Delta N_5 + A_5\Delta N_3 + A_6\Delta O_1) N_3 = N(M_1, t), N_4 = N(M_1 - a_7, t), N_5 = e^{-at} N_4,$$

$$O_1 = O(M_1, t), \tau_{1,1,3} = a_{10} (A_7 N_7 + A_8 N_3), N_7 = e^{-a_9 t} N_6, N_6 = N(M_1 - a_9, t),$$

$$\tau_{1,1,4} = a_{11} (A_9\Delta N_9 + A_{10}\Delta N_7 + A_{11}\Delta N_3 + A_{12}\Delta O_1), N_8 = N(M_1 - a_4, t), N_9 = e^{-a_4 t} N_8,$$

$$\tau_{1,1,5} = a_{12} (A_{13}\Delta N_9 + A_{14}\Delta N_5 + A_{15}\Delta N_3 + A_{16}\Delta O_1), \tau_{1,2} = a_8 (A_4\Delta Z_3 + A_5\Delta \Omega_2 + A_6\Delta \Phi_1),$$

$$Z_3 = Z(a_1, a_3, -a_7, t), \tau_{1,3} = a_{10} (A_7 Z_4 + A_8 \Omega_1), Z_4 = Z(Sc, K, -a_9, t),$$

$$\tau_{1,4} = a_{11} (A_9\Delta Z_1 + A_{10}\Delta Z_4 + A_{11}\Omega_1 + A_{12}\Delta \Phi_2), \tau_{1,5} = a_{12} (A_{13}\Delta Z_2 + A_{14}\Delta Z_3 + A_{15}\Omega_2 + A_{16}\Delta \Phi_1),$$

$$\tau_{2,1} = \tau_{2,1,1} + \tau_{2,1,2} + \tau_{2,1,3} + \tau_{2,1,4} - \tau_{2,1,5}, \tau_{2,1,1} = \tau_{1,1,1}, \tau_{2,1,2} = a_{13}\Delta O_1, \tau_{2,1,3} = \tau_{1,1,3}, \tau_{2,1,4} = \tau_{1,1,4},$$

$$\tau_{2,1,5} = a_{14} (A_1\Delta N_9 + A_2\Delta N_3 + A_3\Delta O_1), \tau_{2,2} = a_{13}\Delta O_2, O_2 = O(a_2, t), \tau_{2,3} = \tau_{1,3}, \tau_{2,4} = \tau_{1,4},$$

$$\tau_{2,5} = a_{14} (A_1\Delta N_{11} + A_2\Delta N_{12} + A_3\Delta O_2), N_{10} = N(a_2 - a_4, t), N_{11} = e^{-a_4 t} N_{10}, N_{12} = N(a_2, t),$$

$$\tau_{3,1} = \tau_{3,1,1} + \tau_{3,1,2} + \tau_{3,1,3} + \tau_{3,1,4} - \tau_{3,1,5}, \tau_{3,1,1} = \tau_{1,1,1}, \tau_{3,1,2} = \tau_{1,1,2}, \tau_{3,1,3} = a_{15} N_3,$$

$$\tau_{3,1,4} = a_{16} (A_1\Delta N_9 + A_2\Delta N_3 + A_3\Delta O_1), \tau_{3,1,5} = \tau_{1,1,5}, \tau_{3,2} = \tau_{1,2}, \tau_{3,3} = a_{15} N_{13}, N_{13} = N(K, t),$$

$$\tau_{3,4} = a_{16} (A_1\Delta N_{15} + A_2\Delta N_{13} + A_3\Delta O_3), N_{14} = N(K - a_4, t), N_{15} = e^{-a_4 t} N_{14}, O_3 = O(K, t), \tau_{3,5} = \tau_{1,5},$$

$$\tau_{4,1} = \tau_{4,1,1} + \tau_{4,1,2} + \tau_{4,1,3} + \tau_{4,1,4} - \tau_{4,1,5}, \tau_{4,1,1} = \tau_{1,1,1}, \tau_{4,1,2} = \tau_{1,1,2}, \tau_{4,1,3} = \tau_{3,1,3}, \tau_{4,1,4} = a_{17} (\Delta N_3 + a_3\Delta O_1),$$

$$\tau_{4,1,5} = \tau_{4,1,4}, \tau_{4,2} = \tau_{2,2}, \tau_{4,3} = \tau_{3,3}, \tau_{4,4} = a_{17} (\Delta N_{13} + a_3\Delta O_3), \tau_{4,5} = a_{17} (\Delta N_{12} + a_3\Delta O_2),$$

$$\tau_{5,1} = \tau_{5,1,1} + \tau_{5,1,2} + \tau_{5,1,3} + \tau_{5,1,4} - \tau_{5,1,5}, \tau_{5,1,1} = \tau_{1,1,1}, \tau_{5,1,2} = \tau_{1,1,2}, \tau_{5,1,3} = \tau_{1,1,3},$$

$$\tau_{5,1,4} = a_{18} (A_{17}\Delta N_7 + A_{18}\Delta N_3 + A_{19}\Delta O_1), \tau_{5,1,5} = a_{18} (A_4\Delta N_5 + A_5\Delta N_3 + A_6\Delta O_1), \tau_{5,2} = \tau_{1,2}, \tau_{5,3} = \tau_{1,3},$$

$$\tau_{5,4} = a_{18} (A_{17}\Delta Z_4 + A_{18}\Delta \Omega_1 + A_{19}\Delta \Phi_2), \tau_{5,5} = a_{18} (A_4\Delta Z_3 + A_5\Delta \Omega_2 + A_6\Delta \Phi_1)$$

(The functions are defined in **Chapter I**)

CHAPTER VII

Influence of Thermal Diffusion on Unsteady MHD Free Convective, Chemically Reactive, and Radiating Flow Past a Semi-Infinite Inclined Moving Plate in a Porous Medium with Arbitrary Ramped Temperature

7.1 Introduction

Magnetohydrodynamics (MHD) is a branch of physics that is concerned with the interaction of the magnetic field with electrically conducting fluid. Some common examples of this kind of fluids are plasmas, liquid metals (e.g. mercury), electrolytes, etc. The basic principle behind MHD is that magnetic fields can induce a current in moving conducting fluids which in turn polarizes the fluid and as a result changes the magnetic field. Renowned Swiss scientist Hannes Alfvén (1942) initiated the concept of MHD for which he received the prestigious Nobel Prize in physics in 1970. But, MHD is at present form due to valuable contributions from researchers like Cowling (1957), Shercliff (1965), Ferraro and Plumpton (1966), Roberts (1967), Cramer and Pai (1973) etc. There are numerous applications of MHD in present-day technologies. Many geophysical and astrophysical phenomena can be elaborated by the MHD principle. Engineering applications of MHD include Dynamo, motor, fusion reactors, dispersion of metals, metallurgy, MHD pumps, etc. Farrokhi et al. (2019) studied biomedical applications of MHD.

Density variation in fluid mixture arises owing to changes in fluid temperature and species concentration. This variation generates buoyancy force which acts on the fluid. The flow produced by these forces is termed free convection or natural convection. Ullah et al. (2021) studied two-dimensional unsteady MHD free convection flow over a vertical plate. Abdullah (2018) considered free convection MHD flow past an accelerated vertical plate with periodic temperature. Kumar and Singh (2013) studied unsteady MHD free convective flow over an infinite vertical moving plate.

The process of heat transfer through electromagnetic waves is defined as radiation. Radiative convective flow occurs in many environmental and industrial processes. This is the reason behind many model researches by researchers on free convection with thermal radiation under various physical and geometrical circumstances. Mbeldogu (2007) explored unsteady free convection on a compressible fluid past a moving vertical plate with radiative heat transfer. Orhan and Ahmet (2008) considered the effect of radiation on MHD mixed convection flow about a permeable vertical plate. Prasad et al. (2006) studied transient radiative free convection flow past an impulsively started vertical plate. Takhar et al. (1996) explored radiation effects on MHD free convection flow of a radiating gas. Ghaly (2002) studied radiation effects in certain MHD convection flows. Sheikholeslami et al. (2016) explored free convection and thermal radiation effects on $Al_2O_3-H_2O$ nanofluid. Ali et al.

(2013) considered radiation effects on MHD free convection flow along the vertical flat plate with Joule heating and heat generation.

A medium containing holes or voids so that fluid can pass through it is termed a porous medium. Sponge, wood, cork, etc. are some well-known examples of porous materials. The concept of the porous medium is widely used in many disciplines of applied science and chemistry such as filtration, solid mechanics, geomechanics, soil mechanics, bio remediation, construction engineering, material science, fuel cells, etc. Sharma and Gupta (2018) studied the effect of radiation on MHD boundary layer flow along a stretching cylinder in a porous medium. Raju and Varma (2011) considered unsteady MHD Couette flow through a porous medium with periodic wall temperature. Pattnaik and Biswal (2015) obtained an analytical solution of an MHD free convection flow through a porous medium with time-dependent temperature and concentration. Sinha et al. (2017) explored MHD free convection flow through a porous medium past a vertical plate with ramped wall temperature. Basha and Nagarathna (2019) observed the process of heat and mass transfer on a free convective MHD flow through a porous medium past an infinite vertical plate.

The chemical reaction effect has great practical importance in many heat and mass transfer processes. Suresh et al (2019) studied the combined effects of chemical reaction and radiation on MHD flow along a moving vertical porous plate with heat source and suction. Rudraswamy and Gireesha (2014) explored the influences of both chemical reactions and thermal radiation in an MHD boundary layer flow. Mohamed and Abo- Daheb (2009) studied the effects of chemical reaction and heat generation in an MHD micropolar flow over a vertically moving porous plate in a porous medium while Babu et al. (2013) extended this work by considering viscous dissipation. Malathy et al (2017) considered both chemical reaction and radiation effects on an *Oldroyd-B* fluid in a porous medium. Lavanya (2020) examined the effects of chemical reaction, heat generation, and radiation on MHD convective flow over a porous plate through a porous medium. Sumathi et al. (2017) numerically investigated the effects of thermal radiation and chemical reaction on three-dimensional MHD flow in a porous medium.

When both thermal and solutal convection occurs simultaneously in a fluid mixture, then the relation between driving potential and flux becomes more complicated. The mass flux is generated by both temperature gradient and concentration gradient. The effect of mass flux under temperature gradient is termed the Soret effect or thermal diffusion effect. This

effect appears due to the flow of fluid molecules from the hotter region to the cooler region. This effect was first observed by Ludwig in 1859. But, the first experimental work was done by Swiss chemist Charles Soret in 1879. This effect has many applications in different chemical and physical processes, isotope separation, etc. Ahmed and Sarma (2021) studied the thermal diffusion effect in an MHD free convective flow past an impulsively started semi-infinite vertical plate considering parabolic ramped conditions. Ahmed (2012) considered the combined effects of Soret and radiation in a free convective transient MHD flow past an infinite vertical plate. Sivaiah et al. (2012) considered the combined effects of thermal diffusion and radiation on unsteady MHD free convective flow past an infinite heated vertical plate in a porous medium. Narahari et al (2021) explored the effects of Soret, heat generation, and radiation in a free convective MHD flow past an infinite plate with oscillating temperature in a porous medium.

The objective of the present investigation is to analyse the problem of a free convective MHD flow past an exponentially accelerated inclined plate. Thermal radiation, chemical reaction, ramped wall temperature and thermal diffusion effects are also considered. The flow medium is taken to be porous. Reviewing the existing literature, we have not found any work considering all these effects simultaneously. The equations governing the flow are first normalized into non – dimensional equations and they are solved analytically using a closed form of the Laplace transformation technique. The effects of different flow parameters on the velocity field, temperature field, concentration field, Nusselt number, Sherwood number, and skin friction are analysed and results are discussed with the assistance of graphs and tables.

7.2 Mathematical Analysis

Consider convective flow of an incompressible, electrically conducting, viscous, and radiating fluid in a porous medium in presence of a magnetic field having constant mass diffusivity and thermal diffusivity past an inclined plate considering the thermal diffusion effect with arbitrary ramped temperature past an infinite inclined plate. A uniform magnetic field applied normally to the plate, directed into the fluid region. Initially, the plate and the surrounding fluid were at rest with uniform temperature T_∞ and concentration C_∞ at all points in the fluid. At time $\bar{t} > 0$, the plate is exponentially accelerated with velocity $U_o e^{a't}$. The

plate temperature is instantly raised to $T_\infty + (T_w - T_\infty) \frac{\bar{t}}{t_0}$, for $0 < \bar{t} \leq t_0$, and thereafter T_w when $\bar{t} > t_0$. The concentration is raised to C_w and maintained thereafter.

To idealize the mathematical model of the problem, we impose the following constraints-

- I. All the fluid properties are constant except for the variation in density in the buoyancy force term.
- II. Dissipation of energy due to friction and Joule heating is negligible.
- III. The induced magnetic field in comparison to the applied magnetic field is negligible.
- IV. Flow is one- dimensional and is parallel to the plate.
- V. The plate is electrically non-conducting.
- VI. No external electric field is applied for which the polarization voltage is negligible.

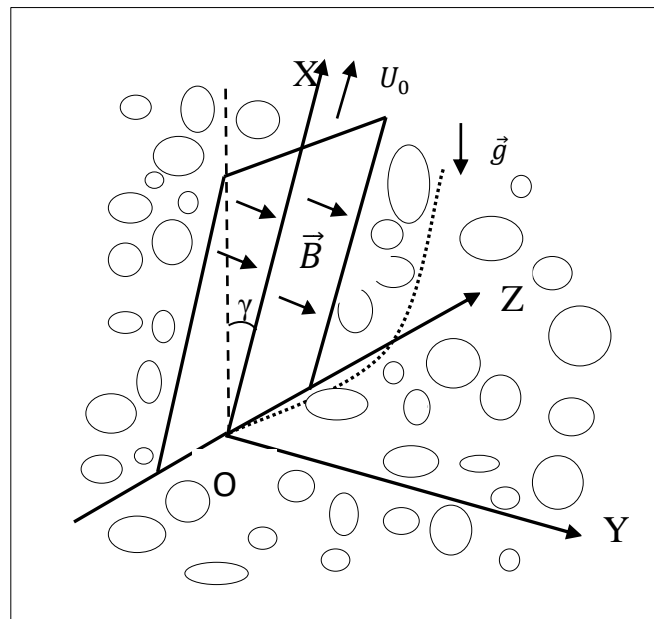


Figure 7.1: Flow Geometry

We now consider a tri- rectangular Cartesian co-ordinate system $(\bar{x}, \bar{y}, \bar{z}, \bar{t})$ with X axis vertically upwards along the plate, Y axis normal to the plate directed into the fluid region, and Z axis along the width of the plate. Let $\vec{q} = (u', 0, 0)$ be the fluid velocity and $\vec{B} = (0, B_0, 0)$ be the magnetic induction vector at the point $(\bar{x}, \bar{y}, \bar{z}, \bar{t})$ in the fluid. Let the

plate is inclined to vertical direction by an angle γ . With the above assumptions, the governing equations for unsteady magnetohydrodynamic free convective flow of an viscous, incompressible, electrically conducting, chemically reactive, radiative and optically thick fluid past an inclined plate through a porous medium are given by

$$\frac{\partial u'}{\partial \bar{t}} = g\beta(T - T_\infty)\cos\gamma + g\bar{\beta}(C - C_\infty)\cos\gamma - \frac{\sigma B_0^2 u'}{\rho} + \nu \frac{\partial^2 u'}{\partial \bar{y}^2} - \nu \frac{u'}{K^*} \quad (7.1)$$

$$\rho C_p \frac{\partial T}{\partial \bar{t}} = \kappa \frac{\partial^2 T}{\partial \bar{y}^2} + \frac{16\sigma^* T_\infty^3}{3\kappa^*} \frac{\partial^2 T}{\partial \bar{y}^2} \quad (7.2)$$

$$\frac{\partial C}{\partial \bar{t}} = D_M \frac{\partial^2 C}{\partial \bar{y}^2} + D_T \frac{\partial^2 T}{\partial \bar{y}^2} + \bar{K}(C_\infty - C) \quad (7.3)$$

Here, we have used Rosseland approximation method for the radiation heat flux term that appears in the energy equation.

$$\vec{q}_r = -\frac{4\sigma^*}{3\kappa^*} \vec{\nabla} T^4$$

The relevant initial and boundary conditions are:

$$\left. \begin{aligned} u' = 0, T = T_\infty, C = C_\infty : \forall \bar{y} \geq 0; \bar{t} \leq 0 \\ u' = U_0 e^{a\bar{t}}, C = C_w : \bar{y} = 0, \bar{t} > 0 \\ T = T_\infty + (T_w - T_\infty) \frac{\bar{t}}{t_0} : \bar{y} = 0; 0 < \bar{t} \leq t_0 \\ T = T_w : \bar{y} = 0; \bar{t} > t_0 \\ u' \rightarrow 0, T \rightarrow T_\infty, C \rightarrow C_\infty : \bar{y} \rightarrow \infty; \bar{t} > 0 \end{aligned} \right\} \quad (7.4)$$

For the sake of normalization of the mathematical model of the problem, we introduce the following non-dimensional quantities-

$$Sr = \frac{D_T(T_w - T_\infty)}{(C_w - C_\infty)\nu}, N = \frac{\kappa\kappa^*}{4\sigma^* T_\infty^3}, u = \frac{u'}{U_0}, y = \frac{U_0}{\nu} \bar{y}, t = \frac{U_0^2}{\nu} \bar{t}, Gr = \frac{\nu g\beta(T_w - T_\infty)}{U_0^3}, a = a' \frac{\nu}{U_0^2},$$

$$Gm = \frac{\nu g\bar{\beta}(C_w - C_\infty)}{U_0^3}, \theta = \frac{T - T_\infty}{T_w - T_\infty}, \phi = \frac{C - C_\infty}{C_w - C_\infty}, Pr = \frac{\mu C_p}{\kappa}, M = \frac{\sigma B_0^2 \nu}{\rho U_0^2}, Sc = \frac{\nu}{D_M}, \Lambda = 1 + \frac{4}{3N},$$

$$K = \frac{\nu \bar{K}}{U_0^2}, t_1 = \frac{U_0^2}{\nu} t_0, M_1 = M + \frac{1}{K^*}$$

The non- dimensional governing equations are

$$\frac{\partial u}{\partial t} = \frac{\partial^2 u}{\partial y^2} + Gr\theta \cos \gamma + Gm\phi \cos \gamma - M_1 u \quad (7.5)$$

$$\frac{\partial \theta}{\partial t} = \frac{\Lambda}{Pr} \frac{\partial^2 \theta}{\partial y^2} \quad (7.6)$$

$$\frac{\partial \phi}{\partial t} = \frac{1}{Sc} \frac{\partial^2 \phi}{\partial y^2} + Sr \frac{\partial^2 \theta}{\partial y^2} - K\phi \quad (7.7)$$

Subject to the initial and boundary conditions

$$\left. \begin{aligned} u = 0, \theta = 0, \phi = 0 : \forall y \geq 0; t \leq 0 \\ u = e^{at}, \phi = 1 : y = 0, t > 0 \\ \theta = \frac{t}{t_1} : y = 0; 0 < t \leq t_1 \\ \theta = 1 : y = 0; t > t_1 \\ u \rightarrow 0, \theta \rightarrow 0, \phi \rightarrow 0 : y \rightarrow \infty; t > 0 \end{aligned} \right\} \quad (7.8)$$

7.3 Method of Solution

On taking Laplace transform of the equations (7.7), (7.6) and (7.5) respectively, we get the following equations:

$$s\bar{\phi} = \frac{1}{Sc} \frac{d^2 \bar{\phi}}{dy^2} + Sr \frac{d^2 \bar{\theta}}{dy^2} - K\bar{\phi} \quad (7.9)$$

$$s\bar{\theta} = \frac{\Lambda}{Pr} \frac{d^2 \bar{\theta}}{dy^2} \quad (7.10)$$

$$s\bar{u} = \frac{d^2 \bar{u}}{dy^2} + Gr \cos \gamma \bar{\theta} + Gm \cos \gamma \bar{\phi} - M_1 \bar{u} \quad (7.11)$$

Subject to the initial and boundary conditions:

$$\left. \begin{aligned} y=0: \bar{\theta} &= \frac{2}{s^2 t_1} (1 - e^{-st_1}), \bar{\phi} = \frac{1}{s}, \bar{u} = \frac{1}{s-a} \\ y \rightarrow \infty: \bar{\theta} &\rightarrow 0, \bar{\phi} \rightarrow 0, \bar{u} \rightarrow 0 \end{aligned} \right\} \quad (7.12)$$

Solving equations from (7.9) to (7.11) subject to the conditions (7.12) and taking inverse Laplace transform of the solutions, the expression for temperature field θ , concentration field ϕ , and velocity field u are as follows:

$$\theta = \frac{1}{t_1} \Delta \lambda_1 \quad (7.13)$$

$$\phi = \begin{cases} \phi_{1,1} + \phi_{1,2} - \phi_{1,3} : \Lambda Sc \neq Pr \\ \phi_{2,1} + \phi_{2,2} - \phi_{2,3} : \Lambda Sc = Pr \end{cases} \quad (7.14)$$

$$u = \begin{cases} u_{1,1} - u_{1,2} - u_{1,3} - u_{1,4} + u_{1,5} : Pr \neq \Lambda, Sc \neq 1, Pr \neq \Lambda Sc \\ u_{2,1} - u_{2,2} - u_{2,3} - u_{2,4} + u_{2,5} : Pr = \Lambda, Sc \neq 1 \\ u_{3,1} - u_{3,2} - u_{3,3} - u_{3,4} + u_{3,5} : Pr \neq \Lambda, Sc = 1 \\ u_{4,1} - u_{4,2} - u_{4,3} - u_{4,4} + u_{4,5} : Pr = \Lambda, Sc = 1 \\ u_{5,1} - u_{5,2} - u_{5,3} - u_{5,4} + u_{5,5} : Pr \neq \Lambda, Sc \neq 1, Pr = \Lambda Sc \end{cases} \quad (7.15)$$

7.4 Nusselt Number

By Fourier's law of conduction, the heat flux q^* at the plate $\bar{y} = 0$ is given by

$$q^* = -\kappa_0^* \left. \frac{\partial T}{\partial \bar{y}} \right]_{\bar{y}=0} \quad (7.16)$$

Here, $\kappa_0^* = \kappa + \frac{16\sigma^* T_\infty^3}{3\kappa^*}$ is modified thermal conductivity.

Equation (7.16) yields

$$Nu = - \left. \frac{\partial \theta}{\partial y} \right]_{y=0} \quad (7.17)$$

Here, $Nu = \frac{q^* \nu}{\kappa_0^* U_0 (T_w - T_\infty)}$ is termed as Nusselt number which is associated with the rate of heat transfer at the plate.

Equation (7.17) gives,

$$Nu = -\frac{1}{t_1} \Delta v_1 \quad (7.18)$$

7.5 Sherwood Number

By Fick's law of diffusion, the mass flux M_w at the plate $\bar{y} = 0$ is given by

$$M_w = -D_M \left. \frac{\partial C}{\partial \bar{y}} \right]_{\bar{y}=0} \quad (7.19)$$

Equation (7.19) gives

$$Sh = -\left. \frac{\partial \phi}{\partial y} \right]_{y=0} \quad (7.20)$$

In (7.20), $Sh = \frac{M_w \nu}{D_M U_0 (C_w - C_\infty)}$ is labelled as the Sherwood number which determines the rate of mass transfer at the plate.

Equation (7.20) yields

$$Sh = -\begin{cases} Sh_{1,1} + Sh_{1,2} - Sh_{1,3} : Pr \neq \Lambda Sc \\ Sh_{2,1} + Sh_{2,2} - Sh_{2,3} : Pr = \Lambda Sc \end{cases} \quad (7.21)$$

7.6 Skin Friction

By Newton's law of viscosity, the viscous drag at the plate $\bar{y} = 0$ is given by

$$\bar{\tau} = -\mu \left. \frac{\partial u}{\partial \bar{y}} \right]_{\bar{y}=0} \quad (7.22)$$

Equation (7.22) gives

$$\tau = -\left. \frac{\partial u}{\partial y} \right]_{y=0} \quad (7.23)$$

In (7.23), $\tau = \frac{\bar{\tau} \nu}{\mu U_0^2}$ is entitled as the skin friction or coefficient of friction which gives the rate of momentum transfer at the plate.

Equation (7.23) yields,

$$\tau = - \begin{cases} \tau_{1,1} - \tau_{1,2} - \tau_{1,3} - \tau_{1,4} + \tau_{1,5} : \text{Pr} \neq \Lambda, Sc \neq 1, \text{Pr} \neq \Lambda Sc \\ \tau_{2,1} - \tau_{2,2} - \tau_{2,3} - \tau_{2,4} + \tau_{2,5} : \text{Pr} = \Lambda, Sc \neq 1 \\ \tau_{3,1} - \tau_{3,2} - \tau_{3,3} - \tau_{3,4} + \tau_{3,5} : \text{Pr} \neq \Lambda, Sc = 1 \\ \tau_{4,1} - \tau_{4,2} - \tau_{4,3} - \tau_{4,4} + \tau_{4,5} : \text{Pr} = \Lambda, Sc = 1 \\ \tau_{5,1} - \tau_{5,2} - \tau_{5,3} - \tau_{5,4} + \tau_{5,5} : \text{Pr} \neq \Lambda, Sc \neq 1, \text{Pr} = \Lambda Sc \end{cases} \quad (7.24)$$

7.7 Results and Discussion

The effects of various flow parameters on flow and transport characteristics are analyzed by assigning some specific values.

Figures 7.2 to 7.5 display the variation of concentration field versus normal coordinate y . Figure 7.2 reveals that the concentration field keeps on decreasing with an increment in the chemical reaction parameter. Increasing chemical reaction absorbs the chemical substances present in the fluid quickly and as a result fluid concentration reduces. Figure 7.3 admits that concentration hikes in a thin layer adjacent to the plate but its behavior reverses outside the layer with ascending values of Prandtl number. This implies that higher thermal diffusivity decreases the fluid concentration in a slim layer adjoining the plate but its nature takes a reverse turn outside the layer. There is a comprehensive fall in fluid concentration with increasing Schmidt number as displayed in Figure 7.4. Thus, greater mass diffusivity hikes fluid concentration. Figure 7.5 suggests that ascending Soret number raises the concentration field. As the Soret number is the ratio of temperature gradient to concentration gradient, so rapid change in temperature hikes the concentration field speedily.

Figures 7.6 and 7.7 depict the variation of temperature field versus normal coordinate y . Figure 7.6 suggests that the temperature field falls with increasing radiation parameter. It establishes the fact that radiation tends to decline fluid temperature. The temperature field declines with an uplift in the Prandtl number as displayed in Figure 7.7. Thus, higher thermal diffusivity hikes fluid temperature.

Figures 7.8 to 7.15 show the variation of velocity field versus normal co- ordinate y . Figure 7.8 displays that increasing chemical reaction parameter decline fluid velocity. The collision between fluid molecules increases as the chemical reaction parameter hikes. As a result, Kinetic energy is lost and velocity decelerates. There is a comprehensive rise in velocity field with increasing porosity parameter as shown in Figure 7.9. Ascending values of the porosity parameter indicate that there is more free space in the medium for the fluid to flow and accordingly, fluid velocity accelerates. Figure 7.10 admits that an increment in the Schmidt number diminishes fluid velocity. Consequently, higher mass diffusivity hikes fluid velocity. Growing Soret number escalates velocity field as noticed in Figure 7.11. This implies that a high-temperature gradient compared to concentration gradient results in a hike in the velocity field. Increasing thermal Grashof number lowers velocity as noticed in Figure 7.12. Thus high thermal diffusivity leads to a dip in the velocity field. Figure 7.13 displays that ascending values of solutal Grashof number upsurges velocity field. This asserts to us that rising solutal diffusivity upsurges fluid velocity. Figure 7.14 demonstrate that growing magnetic parameter slow down fluid velocity. This is because the application of a transverse magnetic field generates a resistive force known as Lorentz force, which declines fluid velocity. Figure 7.15 displays that an increment in the angle of inclination diminishes velocity at all points of the fluid.

Figures 7.16 and 7.17 demonstrate the variation of Nusselt number versus time t . Nusselt number hikes with increment in radiation parameter as noticed in Figure 7.16. Thus, radiation accelerates the process of heat transfer from the plate to the fluid. From Figure 7.17, it is observed that increasing the Prandtl number lifts the Nusselt number. This result establishes the fact that higher thermal diffusivity speed up the rate of heat transfer.

Figures 7.18 to 7.21 exhibit the variation of Sherwood number versus time t . Sherwood number decreases with ascending radiation parameter as noticed in Figure 7.18. This implies that radiation slows down the rate of mass transfer from the plate to the fluid. Figure 7.19 reveals that the Sherwood number declines with an increment in the Prandtl number. Thus, higher thermal diffusivity speeds up the rate of mass transfer time progresses. Increasing chemical reaction parameter lifts Sherwood number as displayed in Figure 7.20. It is noticed from Figure 7.21 that increasing Soret number declines the Sherwood number. This result agrees with the fact that a high concentration gradient compared to a temperature gradient accelerates the process of mass transfer from the plate to the fluid.

Numerical values of Skin friction τ against different time t , radiation parameter N , Soret number Sr and magnetic parameter M are demonstrated in Table 7.1. It is noticed that skin friction upsurges as time progresses. Skin friction hikes as radiation parameter increases. Thus, radiation accelerates the process of momentum transfer. Increasing Soret number hikes skin friction. This is because a high-temperature gradient exerts more drag force. An opposite behavior is noticed for increasing magnetic parameter. This asserts that Lorentz force arising from the application of transverse magnetic field reduces the frictional resistance of the plate.

Numerical values of skin friction τ against different thermal Grashof number Gr , solutal Grashof number Gm , porosity parameter K^* , and angle of inclination γ of the plate are analyzed in Table 7.2. It is observed that increasing thermal Grashof number hikes skin friction, but ascending solutal Grashof number lowers skin friction. Thus, thermal buoyancy force accelerates the process of momentum transfer, whereas, solutal buoyancy force shows its reverse character. Increasing porosity parameter hikes the viscous drag of the plate. The increasing angle of inclination of the plate hikes skin friction. The more the plate is inclined from the vertical, the more it experiences frictional resistance.

7.8 Conclusions

A study of unsteady free convective hydromagnetic flow with heat and mass transfer of a viscous, incompressible, chemically reactive, electrically conducting, radiative and optically thick fluid past an exponentially accelerated moving inclined plate with variable ramped temperature embedded in a porous medium is carried out. The prominent outcomes of our investigation are:

- i. The chemical reaction effect lowers the concentration field.
- ii. Soret effect upsurges both concentration and velocity fields.
- iii. Radiation tends to decline temperature field.
- iv. Both Lorentz force and increasing angle of inclination slow down fluid velocity.
- v. Ascending Prandtl number uplifts Nusselt number, but diminishes Sherwood number.
- vi. Skin friction gets enhanced with increment in Soret number, porosity parameter, and angle of inclination.

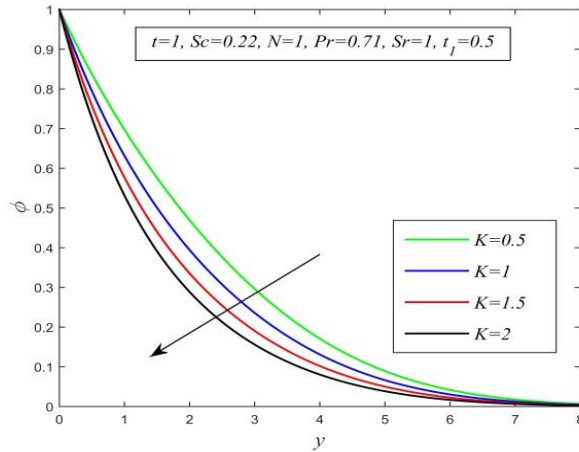


Figure 7.2: Concentration field versus y for different K and $t=1, Sc=0.22, N=1, Pr=0.71, Sr=1, t_I=0.5$

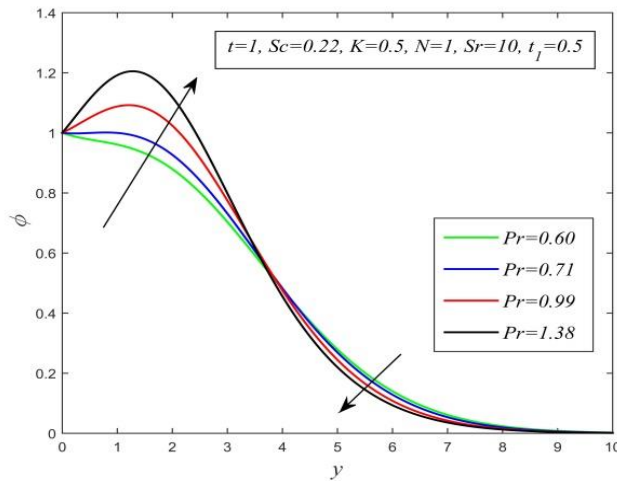


Figure 7.3: Concentration field versus y for different Pr and $t=1, Sc=0.22, K=0.5, N=1, Sr=10, t_I=0.5$

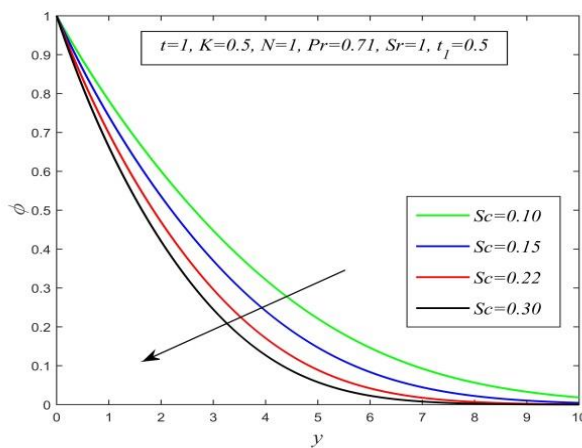


Figure 7.4: Concentration field versus y for different Sc and $t=1, K=0.5, N=1, Pr=0.71, Sr=1, t_I=0.5$

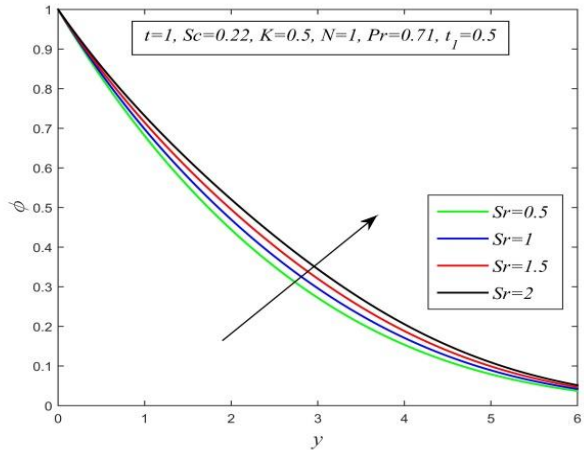


Figure 7.5: Concentration field versus y for different Sr and $t=1, Sc=0.22, K=0.5, N=1, Pr=0.71, t_1=0.5$

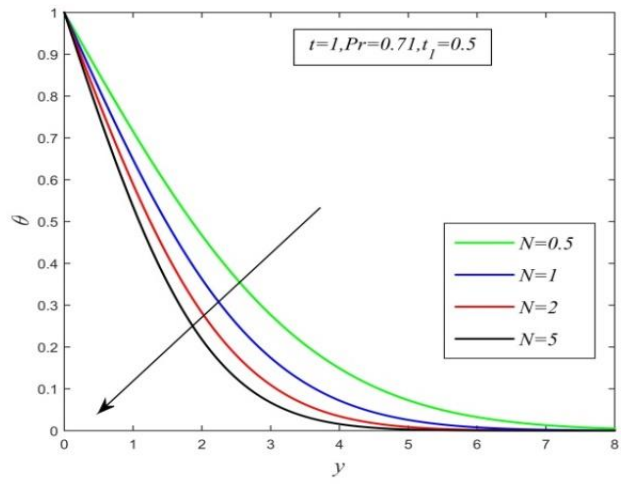


Figure 7.6: Temperature field versus y for different N and $t=1, Pr=0.71, t_1=0.5$

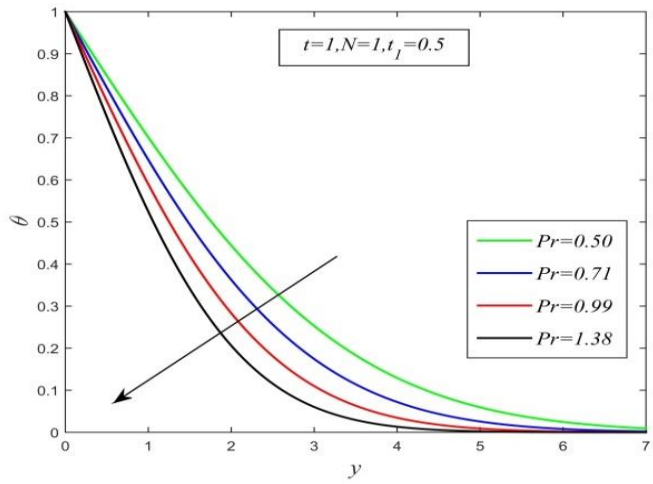


Figure 7.7: Temperature field versus y for different Pr and $t=1, N=1, t_1=0.5$

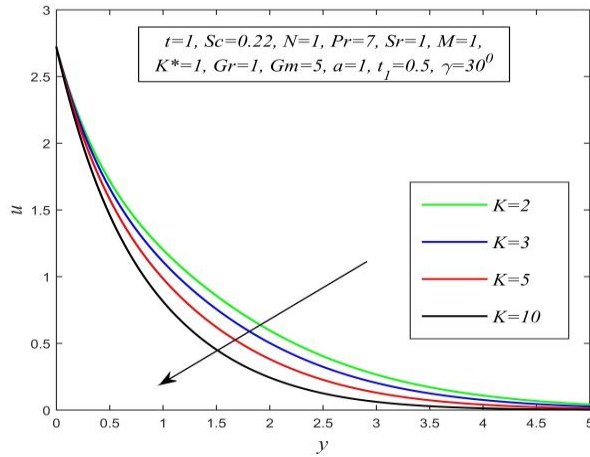


Figure 7.8: Velocity field versus y for different K and $t=1$, $Sc=0.22$, $N=1$, $Pr=7$, $Sr=1$, $M=1$, $K^*=1$, $Gr=1$, $Gm=5$, $a=1$, $t_1=0.5$, $\gamma=30^\circ$

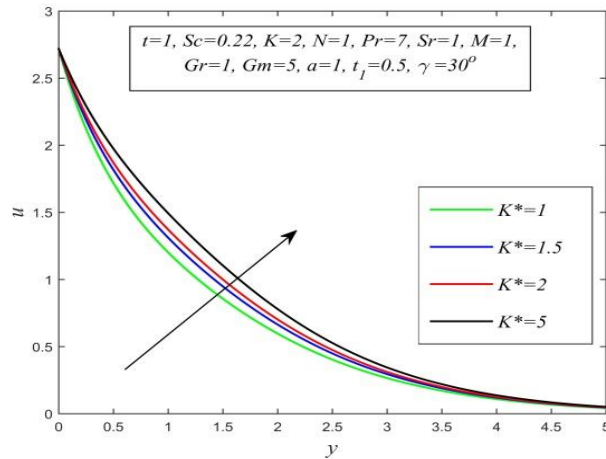


Figure 7.9: Velocity field versus y for different K^* and $t=1$, $Sc=0.22$, $K=2$, $N=1$, $Pr=7$, $Sr=1$, $M=1$, $Gr=1$, $Gm=5$, $a=1$, $t_1=0.5$, $\gamma=30^\circ$

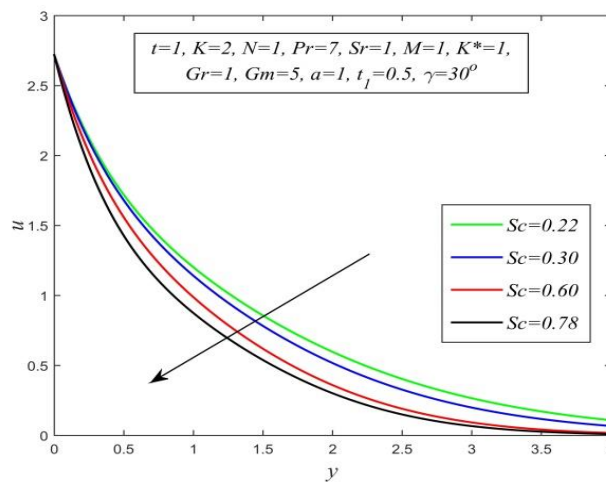


Figure 7.10: Velocity field versus y for different Sc and $t=1$, $K=2$, $N=1$, $Pr=7$, $Sr=1$, $M=1$, $K^*=1$, $Gr=1$, $Gm=5$, $a=1$, $t_1=0.5$, $\gamma=30^\circ$

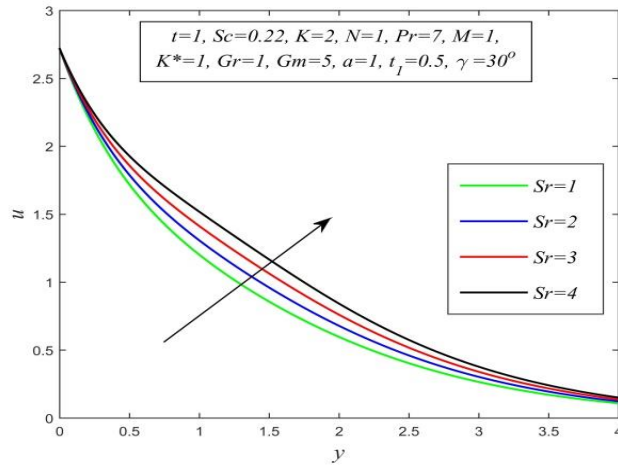


Figure 7.11: Velocity field versus y for different Sr and $t=1, Sc=0.22, K=2, N=1, Pr=7, M=1, K^*=1, Gr=1, Gm=5, a=1, t_1=0.5, \gamma=30^\circ$

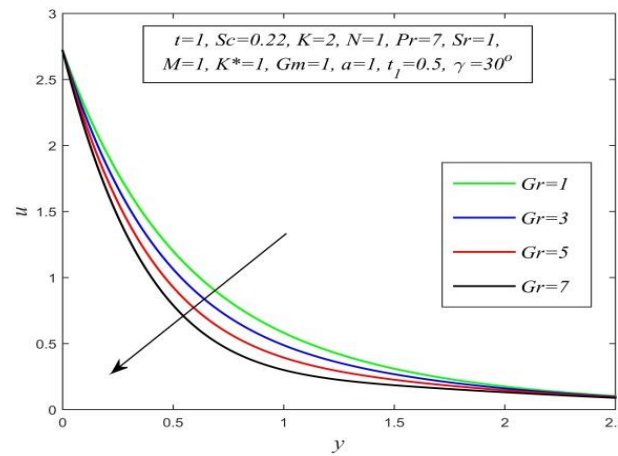


Figure 7.12: Velocity field versus y for different Gr and $t=1, Sc=0.22, K=2, N=1, Pr=7, Sr=1, M=1, K^*=1, Gm=1, a=1, t_1=0.5, \gamma=30^\circ$

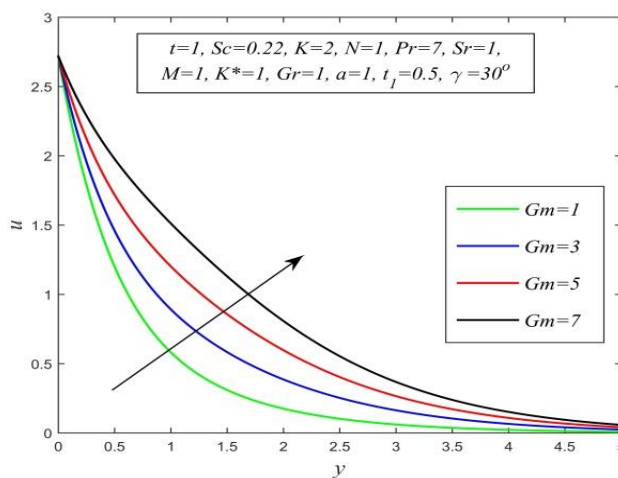


Figure 7.13: Velocity field versus y for different Gm and $t=1, Sc=0.22, K=2, N=1, Pr=7, Sr=1, M=1, K^*=1, Gr=1, a=1, t_1=0.5, \gamma=30^\circ$

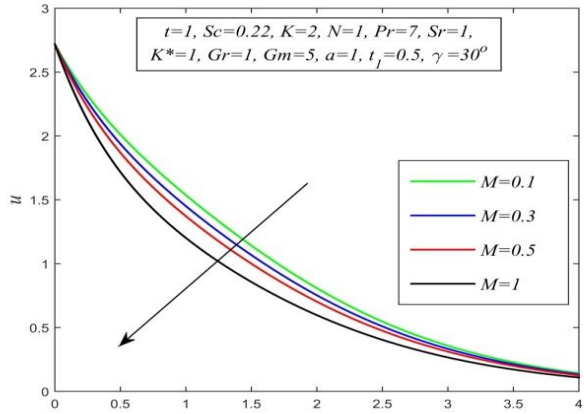


Figure 7.14: Velocity field versus y for different M and $t=1$, $Sc=0.22$, $K=2$, $N=1$, $Pr=7$, $Sr=1$, $K^*=1$, $Gr=1$, $Gm=5$, $a=1$, $t_1=0.5$, $\gamma=30^\circ$

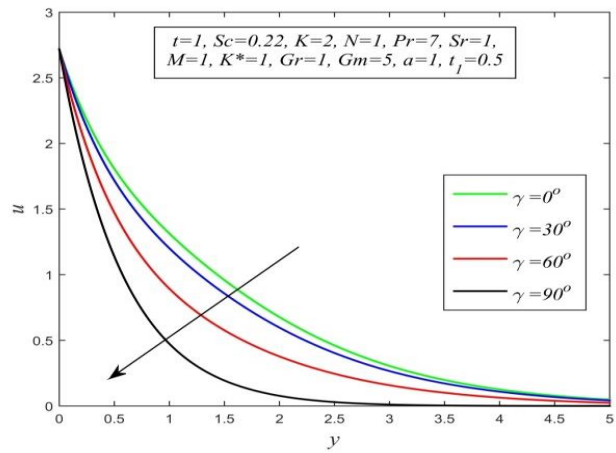


Figure 7.15: Velocity field versus y for different γ and $t=1$, $Sc=0.22$, $K=2$, $N=1$, $Pr=7$, $Sr=1$, $M=1$, $K^*=1$, $Gr=1$, $Gm=5$, $a=1$, $t_1=0.5$

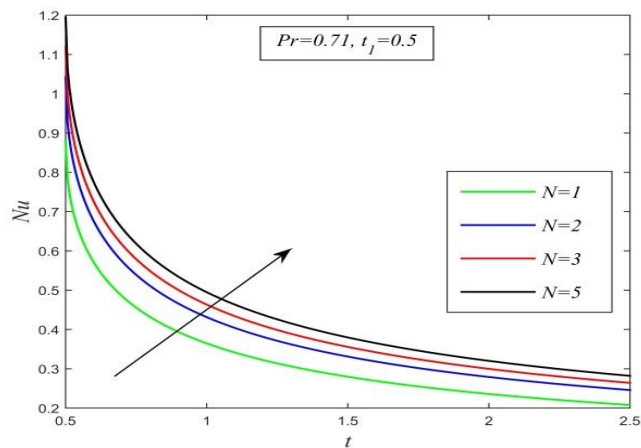


Figure 7.16: Nusselt number versus t for different N and $Pr=0.71$, $t_1=0.5$

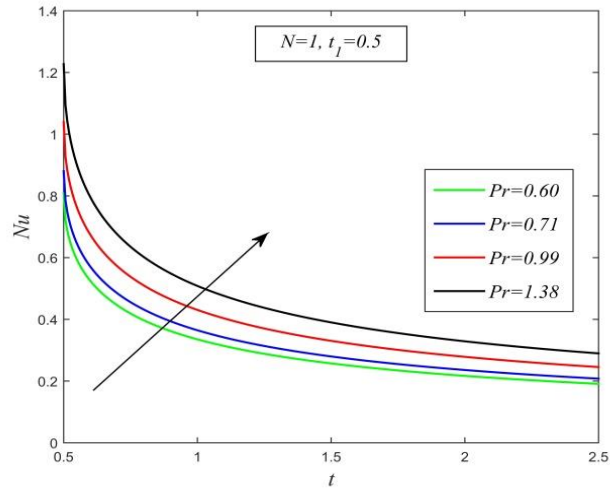


Figure 7.17: Nusselt number versus t for different Pr and $N=1, t_1=0.5$

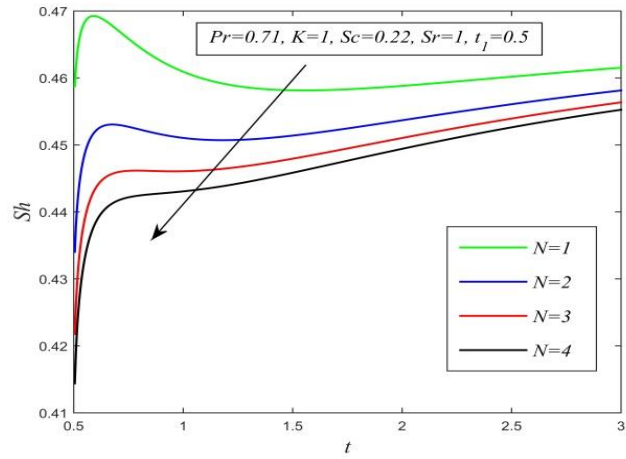


Figure 7.18: Sherwood number versus t for different N and $Pr=0.71, K=1, Sc=0.22, Sr=1, t_1=0.5$

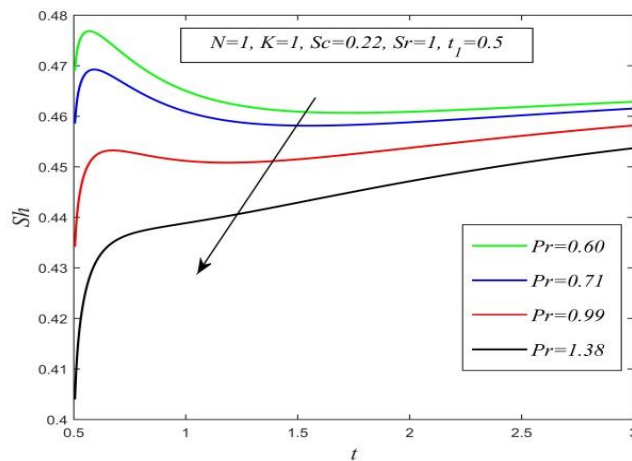


Figure 7.19: Sherwood number versus t for different Pr and $N=1, K=1, Sc=0.22, Sr=1, t_1=0.5$

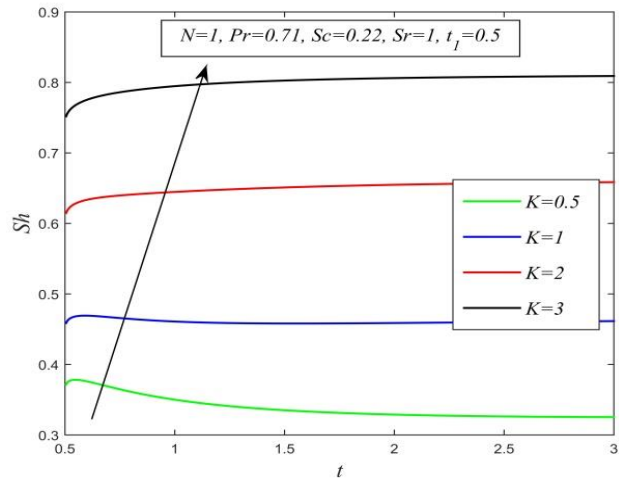


Figure 7.20: Sherwood number versus t for different K and $N=1, Pr=0.71, Sc=0.22, Sr=1, t_1=0.5$

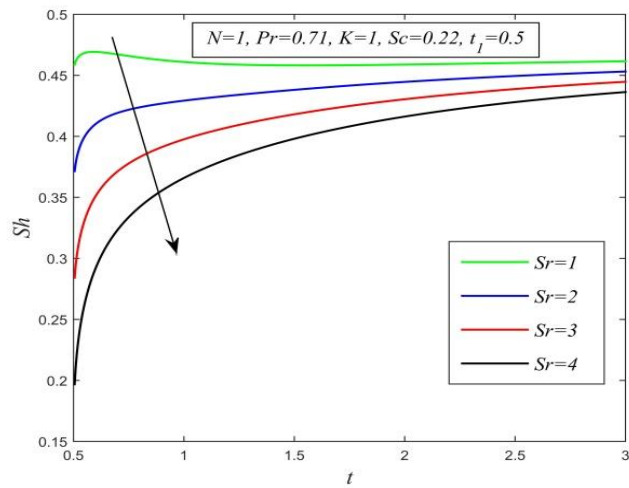


Figure 7.21: Sherwood number versus t for different Sr and $N=1, Pr=0.71, K=1, Sc=0.22, t_1=0.5$

t	N	Sr	M	τ
1	1	1	1	4.0964
1.5				4.5736
2				5.8117
1	1	1	1	4.0964
	1.5			4.8201
	2			5.4763
	3			6.5574
1	1	1	1	4.0964
		1.5		4.5147
		2		4.9385
		3		5.7806
1	5		0.1	6.3056
			0.5	4.6683
			1	4.0964

Table 7.1: Computational values of skin friction for various t , N , Sr , and M when $Pr=7$, $Sc=0.22$, $K=2$, $a=1$, $K^*=1$, $Gr=1$, $Gm=5$, $\gamma=30^\circ$, $t_1=0.5$

Gr	Gm	K^*	γ	τ
1	5	1	30°	4.0964
3				5.1495
5				6.2027
1	1	1	30°	5.0143
	3			4.5554
	5			4.0964
1	5	1	30°	4.0964
		2		4.6683
		5		5.6991
1	5	1	30°	4.0964
			45°	4.2103
			60°	4.3588
			90°	4.7172

Table 7.2: Computational values of skin friction for various Gr , Gm , K^* and γ when $t=1$, $Pr=7$, $Sc=0.22$, $K=2$, $N=1$, $Sr=1$, $M=1$, $a=1$, $t_1=0.5$

Nomenclature

a : Surface acceleration parameter

a^* : Absorption coefficient $\left(\frac{m^2}{mol}\right)$

\vec{B} : Magnetic flux density

B_0 : Strength of the applied magnetic field $\left(\frac{Weber}{m^2}\right)$

C : Molar species concentration $\left(\frac{mol}{m^3}\right)$

C_p : Specific heat at constant pressure $\left(\frac{J}{Kg.K}\right)$

C_∞ : Concentration far away from the plate $\left(\frac{mol}{m^3}\right)$

C_w : Concentration at the plate $\left(\frac{mol}{m^3}\right)$

D_M : Mass diffusivity $\left(\frac{m^2}{s}\right)$

D_T : Molar thermal diffusivity $\left(\frac{J}{K.mol}\right)$

\vec{g} : Gravitation acceleration vector

g : Gravitational acceleration $\left(\frac{m}{s^2}\right)$

Gr : Thermal Grashof number

Gm : Solutal Grashof number

K^* : Porosity parameter

\vec{J} : Current density vector $\left(\frac{A}{m^2}\right)$

\bar{K} : Chemical reaction rate $\left(\frac{mol}{m^2.s}\right)$

K : Chemical reaction parameter

M : Magnetic parameter

N : Radiation parameter

p : Pressure $\left(\frac{N}{m^2}\right)$

Pr : Prandtl number

\vec{q} : Fluid velocity vector

\vec{q}_r : Radiation heat flux vector

q_r : Radiation heat flux $\left(\frac{W}{m^2}\right)$

Sc : Schmidt number

Sr : Soret number

\bar{t} : Time (s)

t_0 : Critical time for rampedness (s)

t_1 : Non- dimensional critical time for rampedness

T_w : Temperature at the plate (K)

T_∞ : Undisturbed temperature (K)

u' : X-component of fluid velocity $\left(\frac{m}{s}\right)$

U_0 : Plate velocity $\left(\frac{m}{s}\right)$

Greek Symbols:

γ : Angle of inclination to the vertical

μ : Coefficient of viscosity $\left(\frac{Kg}{m.s}\right)$

σ : Electrical conductivity $\left(\frac{S}{m}\right)$

σ^* : Stefan-Boltzmann constant $\left(\frac{W}{m^2.K^4}\right)$

ρ : Fluid density $\left(\frac{Kg}{m^3}\right)$

ρ_∞ : Fluid density far away from the plate $\left(\frac{Kg}{m^3}\right)$

κ : Thermal conductivity $\left(\frac{W}{m.K}\right)$

κ^* : Mean absorption constant $\left(\frac{1}{m}\right)$

β : Volumetric coefficient of thermal expansion $\left(\frac{1}{K}\right)$

$\bar{\beta}$: Volumetric coefficient of solutal expansion $\left(\frac{1}{K.mol}\right)$

ν : Kinematic viscosity $\left(\frac{m^2}{s}\right)$

Subscripts:

w : Refers to physical quantity at the plate

∞ : Refers to physical quantity far away from the plate

Appendix

$$\begin{aligned}
a_1 &= \frac{\text{Pr}}{\Lambda}, \lambda_1 = \lambda(a_1, y, t) a_2 = \frac{\text{SrSca}_1}{t_1(a_1 - \text{Sc})}, a_3 = \frac{\text{Sc}K}{a_1 - \text{Sc}}, \phi_{1,1} = \psi_1, \psi_1 = \Psi(\text{Sc}, K, y, t), A_1 = \frac{1}{a_3}, \\
A_2 &= -A_1, \phi_{1,2} = a_2(A_1\Delta\psi_2 + A_2\Delta\psi_1), \psi_2 = \Psi(\text{Sc}, K, a_3, y, t), \phi_{1,3} = a_2(A_1\Delta\psi_3 + A_2\Delta E_1), \\
\psi_3 &= \Psi(a_1, 0, a_3, y, t), E_1 = \text{erfc}\left(\frac{y\sqrt{a_1}}{2\sqrt{t}}\right), \phi_{2,1} = \phi_{1,1}, a_4 = -\frac{\text{SrSc}}{K}, \phi_{2,2} = a_4\Delta\psi_1, \phi_{2,3} = a_4\Delta E_1, \\
a_5 &= \frac{M_1}{a_1 - 1}, a_6 = \frac{\text{Gr}\cos\gamma}{t_1(a_1 - 1)}, u_{1,1} = u_{1,1,1} + u_{1,1,2} + u_{1,1,3} + u_{1,1,4} - u_{1,1,5}, u_{1,1,1} = h_2, h_2 = e^{at}h_1, \\
h_1 &= h(M_1 + a, y, t), A_3 = \frac{1}{a_5^2}, A_4 = -A_3, A_5 = -\frac{1}{a_5}, u_{1,1,2} = a_6(A_3\Delta h_5 + A_4\Delta h_3 + A_5\Delta r_1), \\
h_3 &= h(M_1, y, t), h_4 = h(M_1 + a_5, y, t), h_5 = e^{ast}h_4, r_1 = r(M_1, y, t), a_7 = \frac{\text{Sc}K - M_1}{\text{Sc} - 1}, a_8 = \frac{\text{Gm}\cos\gamma}{\text{Sc} - 1}, \\
A_6 &= -\frac{1}{a_7}, A_7 = -A_6, u_{1,1,3} = a_8(A_6h_7 + A_7h_3), h_7 = e^{-at}h_6, h_6 = h(M_1 - a_7, y, t), a_9 = \frac{\text{Gm}\cos\gamma a_2}{\text{Sc} - 1}, \\
A_8 &= \frac{1}{(a_3 + a_7)a_7}, A_9 = \frac{1}{(a_3 + a_7)a_3}, A_{10} = -\frac{1}{a_3a_7}, u_{1,1,4} = a_{11}(A_9\Delta h_9 + A_{10}\Delta h_7 + A_{11}\Delta h_3 + A_{12}\Delta r_1), \\
h_9 &= e^{ast}h_8, h_8 = h(M + a_3, y, t), a_{10} = \frac{\text{Gm}\cos\gamma a_2}{a_1 - 1}, A_{11} = \frac{1}{(a_5 - a_3)a_5}, A_{12} = \frac{1}{(a_3 - a_5)a_3}, A_{13} = \frac{1}{a_3a_5}, \\
u_{1,1,5} &= a_{10}(A_{11}\Delta h_{11} + A_{12}\Delta h_9 + A_{13}\Delta h_3), h_{11} = e^{ast}h_{10}, h_{10} = h(M_1 + a_5, y, t), \\
u_{1,2} &= a_6(A_3\Delta\psi_4 + A_4\Delta E_1 + A_5\Delta\lambda_1), \psi_4 = \Psi(a_1, 0, a_5, y, t), u_{1,3} = a_8(A_6\psi_5 + A_7\psi_1), \\
\psi_5 &= \Psi(\text{Sc}, K, -a_7, y, t), u_{1,4} = a_9(A_8\Delta\psi_5 + A_9\Delta\psi_2 + A_{10}\Delta\psi_1), \\
u_{1,5} &= a_{10}(A_{11}\Delta\psi_6 + A_{12}\Delta\psi_3 + A_{13}\Delta E_1), \psi_6 = \Psi(a_1, 0, a_8, y, t), u_{2,1} = u_{2,1,1} + u_{2,1,2} + u_{2,1,3} + u_{2,1,4} - u_{2,1,5}, \\
u_{2,1,1} &= u_{1,1,1}, a_{11} = -\frac{\text{Gr}\cos\gamma}{M_1 t_1}, u_{2,1,2} = a_{11}\Delta r_1, u_{2,1,3} = u_{1,1,3}, u_{2,1,4} = u_{1,1,4}, u_{2,1,5} = a_{12}(A_1\Delta h_9 + A_2\Delta h_3), \\
a_{12} &= -\frac{\text{Gm}\cos\gamma a_2}{M_1}, u_{2,2} = a_{11}\Delta\lambda_1, u_{2,3} = u_{1,3}, u_{2,4} = u_{1,4}, u_{2,5} = a_{12}(A_1\Delta\psi_3 + A_2\Delta E_1), \\
u_{3,1} &= u_{3,1,1} + u_{3,1,2} + u_{3,1,3} + u_{3,1,4} - u_{3,1,5}, u_{3,1,1} = u_{1,1,1}, u_{3,1,2} = u_{1,1,2}, u_{3,1,3} = a_{12}h_3, a_{13} = \frac{\text{Gm}\cos\gamma}{K - 1}, \\
u_{3,1,4} &= a_{14}(A_1\Delta h_9 + A_2\Delta h_3), a_{14} = \frac{\text{Gm}\cos\gamma a_2}{K - 1}, u_{3,1,5} = u_{1,1,5}, u_{3,2} = u_{1,2}, u_{3,3} = a_{13}\psi_1, \\
u_{3,4} &= a_{14}(A_1\Delta\psi_2 + A_2\Delta\psi_1), u_{3,5} = u_{1,5}, u_{4,1} = u_{4,1,1} + u_{4,1,2} + u_{4,1,3} + u_{4,1,4} - u_{4,1,5}, u_{4,1,1} = u_{1,1,1}, \\
u_{4,1,2} &= u_{2,1,2}, u_{4,1,3} = u_{3,1,3}, u_{4,1,4} = a_{15}\Delta h_3, a_{15} = \frac{\text{Gm}\cos\gamma \text{Sr}}{t_1 K (K - 1)}, u_{4,1,5} = a_{16}\Delta h_3, a_{16} = \frac{\text{Gm}\cos\gamma \text{Sr}}{t_1 K M_1}, \\
u_{4,2} &= u_{2,2}, u_{4,3} = u_{3,3}, u_{4,4} = a_{15}\Delta\psi_1, u_{4,5} = a_{16}\Delta E_1, u_{5,1} = u_{5,1,1} + u_{5,1,2} + u_{5,1,3} + u_{5,1,4} - u_{5,1,5}, u_{5,1,1} = u_{1,1,1}, \\
u_{5,1,2} &= u_{1,1,2}, u_{5,1,3} = u_{1,1,3}, u_{5,1,4} = a_{17}(A_6\Delta h_7 + A_7\Delta h_3), a_{17} = -\frac{\text{Gm}\cos\gamma \text{Sra}_1}{t_1 K},
\end{aligned}$$

$$\begin{aligned}
u_{5,1,5} &= a_{17} (A_{14} \Delta h_{11} + A_{15} \Delta h_3), A_{14} = \frac{1}{a_8}, A_{15} = -A_{14}, u_{5,2} = u_{1,2}, u_{5,3} = u_{1,3}, \\
u_{5,4} &= a_{17} (A_6 \Delta \psi_5 + A_7 \Delta \psi_1), u_{5,5} = a_{17} (A_{14} \Delta \psi_6 + A_{15} \Delta E_1) \\
v_1 &= v(a_1, t), Sh_{1,1} = \Omega_1, \Omega_1 = \Omega(Sc, K, t), Sh_{1,2} = a_2 (A_1 \Delta Z_1 + A_2 \Delta \Omega_1), Z_1 = Z(Sc, K, a_3, t), \\
Sh_{1,3} &= a_2 (A_1 \Delta Z_2 + A_2 \Delta \alpha_1), Z_2 = Z(a_1, 0, a_3, t), \alpha_1 = \alpha \left(\frac{\sqrt{a_1}}{2\sqrt{t}} \right), Sh_{2,1} = Sh_{1,1}, Sh_{2,2} = a_4 \Delta \Omega_1, \\
Sh_{2,3} &= a_4 \Delta \alpha_1, Sh_{2,2} = a_4 \Delta \Omega_1, Sh_{2,3} = a_4 \Delta \alpha_1 \\
\tau_{1,1} &= \tau_{1,1,1} + \tau_{1,1,2} + \tau_{1,1,3} + \tau_{1,1,4} - \tau_{1,1,5}, \tau_{1,1,1} = N_2, N_2 = e^{at} N_1, N_1 = N(M_1 + a, t), \\
\tau_{1,1,2} &= a_6 (A_3 \Delta N_5 + A_4 \Delta N_3 + A_5 \Delta O_1) N_3 = N(M_1, t), N_4 = N(M_1 + a_5, t), N_5 = e^{a_5 t} N_4, \\
O_1 &= O(M_1, t), \tau_{1,1,3} = a_8 (A_6 N_7 + A_7 N_3), N_7 = e^{-a_6 t} N_6, N_6 = N(M_1 - a_7, t), \\
\tau_{1,1,4} &= a_9 (A_8 \Delta N_7 + A_9 \Delta N_9 + A_{10} \Delta N_3), N_8 = N(M_1 + a_3, t), N_9 = e^{a_3 t} N_8, \\
\tau_{1,1,5} &= a_{10} (A_{11} \Delta N_{11} + A_{12} \Delta N_9 + A_{13} \Delta N_3), N_{11} = e^{a_5 t} N_{10}, N_{10} = N(M_1 + a_5), \\
\tau_{1,2} &= a_6 (A_3 \Delta Z_3 + A_4 \Delta \alpha_1 + A_5 \Delta v_1), Z_3 = Z(a_1, 0, a_5, t), \tau_{1,3} = a_8 (A_6 Z_4 + A_7 \Omega_1), Z_4 = Z(Sc, K, -a_7, t), \\
\tau_{2,1} &= \tau_{2,1,1} + \tau_{2,1,2} + \tau_{2,1,3} + \tau_{2,1,4} - \tau_{2,1,5}, \tau_{2,1,1} = \tau_{1,1,1}, \tau_{2,1,2} = a_{11} \Delta O_1, \tau_{2,1,3} = \tau_{1,1,3}, \tau_{2,1,4} = \tau_{1,1,4}, \\
\tau_{1,4} &= a_9 (A_8 \Delta Z_4 + A_9 \Delta Z_1 + A_{10} \Omega_1), \tau_{1,5} = a_{10} (A_{11} \Delta Z_5 + A_9 \Delta Z_2 + A_3 \Delta \alpha_1), Z_5 = Z(a_1, 0, a_8, t), \\
\tau_{2,1,5} &= a_{12} (A_1 \Delta N_9 + A_2 \Delta N_3), \tau_{2,2} = a_{11} \Delta v_1, \tau_{2,3} = \tau_{1,3}, \tau_{2,4} = \tau_{1,4}, \tau_{2,5} = a_{12} (A_1 \Delta Z_2 + A_2 \Delta \alpha_1), \\
\tau_{3,1} &= \tau_{3,1,1} + \tau_{3,1,2} + \tau_{3,1,3} + \tau_{3,1,4} - \tau_{3,1,5}, \tau_{3,1,1} = \tau_{1,1,1}, \tau_{3,1,2} = \tau_{1,1,2}, \tau_{3,1,3} = a_{14} N_3, \\
\tau_{3,1,4} &= a_{14} (A_1 \Delta N_9 + A_2 \Delta N_3), \tau_{3,1,5} = \tau_{1,1,5}, \tau_{3,2} = \tau_{1,2}, \tau_{3,3} = a_{13} \Omega_1, \tau_{3,4} = a_{14} (A_1 \Delta Z_1 + A_2 \Delta \Omega_1), \\
\tau_{3,5} &= \tau_{1,5}, \tau_{4,1} = \tau_{4,1,1} + \tau_{4,1,2} + \tau_{4,1,3} + \tau_{4,1,4} - \tau_{4,1,5}, \tau_{4,1,1} = \tau_{1,1,1}, \tau_{4,1,2} = \tau_{1,1,2}, \tau_{4,1,3} = \tau_{3,1,3}, \tau_{4,1,4} = a_{15} \Delta N_3, \\
\tau_{4,1,5} &= a_{16} \Delta N_3, \tau_{4,2} = \tau_{2,2}, \tau_{4,3} = \tau_{3,3}, \tau_{4,4} = a_{15} \Delta \Omega_1, \tau_{4,5} = a_{16} \Delta \alpha_1, \\
\tau_{5,1} &= \tau_{5,1,1} + \tau_{5,1,2} + \tau_{5,1,3} + \tau_{5,1,4} - \tau_{5,1,5}, \tau_{5,1,1} = \tau_{1,1,1}, \tau_{5,1,2} = \tau_{1,1,2}, \tau_{5,1,3} = \tau_{1,1,3}, \\
\tau_{5,1,4} &= a_{17} (A_6 \Delta N_7 + A_7 \Delta N_3), \tau_{5,1,5} = a_{17} (A_{14} \Delta N_{11} + A_{15} \Delta N_3), \tau_{5,2} = \tau_{1,2}, \tau_{5,3} = \tau_{1,3}, \\
\tau_{5,4} &= a_{17} (A_6 \Delta Z_4 + A_7 \Delta \Omega_1), \tau_{5,5} = a_{17} (A_{14} \Delta Z_5 + A_{15} \Delta \alpha_1)
\end{aligned}$$

(The functions are defined in **Chapter I**)

CHAPTER VIII

Induced Magnetic Field and Thermal Diffusion Effects on Unsteady MHD Free Convective, Chemically Reactive and Radiating Flow Past a Semi-Infinite Moving Vertical Plate with Arbitrary Ramped Temperature

8.1 Introduction

The branch of physical science which is associated with the interaction of electrically conducting fluid with a magnetic field is called magnetohydrodynamics (MHD). Plasmas, electrolytes, liquid metals (for example, mercury) are some well-known conducting fluids. Interaction of a magnetic field with electrically conducting fluids generates current which polarizes the fluid and subsequently it perturbs the magnetic field. Fundamental concepts of MHD were given by Hannes Alfvén (1942) and for that, he received the Nobel Prize in physics in 1970. Cowling (1957), Roberts (1967), Shercliff (1965), Ferraro and Plumpton (1966), Cramer and Pai (1973) are some pioneer researchers in the field of MHD. Numerous modern-day technologies are based on the application of the MHD principle. Liquid metal cooling of nuclear reactors, continuous casting process of metals, magnetic behavior of plasmas in fusion reactors, principles of dynamo and motor etc. are some common applications of MHD in engineering. Astrophysical applications of MHD include solar wind, Sunspots, etc.

Difference in both fluid temperature and species concentration develops density variation in the fluid mixture. This difference produces buoyancy force which acts on the fluid. The flow generated by this force is called natural convection or free convection. Das et al. (2012) studied free convection in an MHD Couette flow in presence of heat generation. Agrawal et al. (1989) investigated the effects of free convection on an MHD flow past a vibrating infinite vertical cylinder. Afsana et al. (2021) explored MHD-free convection of power-law fluids.

Radiation is a powerful form of heat transfer as it does not necessarily need a material medium for heat transfer, unlike conduction and convection. Many industrial and environmental processes encounter convective flow with radiation. This persuades many researchers to carry on model research on radiative free convection flow under different physical and geometrical restrictions. Anwar et al. (2020) obtained exact solutions of unsteady MHD radiative free convective flow. Goud et al. (2020) observed the influence of MHD-free convection across a vertical surface in a porous medium with radiation. Ibrahim et al. (2013) considered the effects of radiation on MHD-free convection flow of a micropolar fluid.

Many heat and mass transfer processes encounter chemical reactions. So, this effect has great practical importance in many MHD flow investigations. Reddy et al. (2020) examined how chemical reaction affects radiative MHD flow near the stagnation point. Zhang et al. (2022) investigated the chemical reaction effect on Newtonian MHD flow on a vertical plate immersed in a porous medium. Joshna et al. (2022) obtained an analytical solution of chemically reactive MHD flow in a vertical surface filled with porous materials. Narayana et al. (2022) investigated chemical reaction on MHD couple-stress nanofluid flow. Patil et al. (2022) studied thermally and chemically reactive MHD Maxwell nanofluid flow past an inclined permeable stretching surface. Reddy et al. (2021) studied impact of chemical reaction on free convective MHD flow through a porous medium. Sarma and Ahmed (2022b) explored the combined effects of radiation, Dufour, and chemical reaction on a free convective MHD flow past a vertical plate in a porous medium.

When both thermal and solutal convection occurs at the same time, then mass flux is produced by both temperature gradient and concentration gradient. The effect of mass flux occurring from temperature gradient is called the thermal diffusion effect or Soret effect. This effect takes place due to the movement of fluid molecules from a hotter region to a cooler region. Though this effect was first observed by Ludwig in 1859, but first experimental research was carried out by Charles Soret in 1879. Many chemical and physical processes, isotope separation processes, etc. are based on this effect. Sarma and Ahmed (2022a) studied the thermal diffusion effect on unsteady MHD free convective flow past a semi-infinite exponentially accelerated vertical plate submerged in a porous medium. Gulle and Kodi (2022) explored the Soret effect on MHD Jeffery fluid past an inclined vertical plate in a porous medium taking radiation and chemical reaction into account. Niranjana et al. (2017) investigated the combined effects of radiation, chemical reaction, Soret, and Dufour on an MHD mixed convection stagnation point flow. Jayakar et al. (2018) studied thermal diffusion effect on chemically reacting MHD flow past an inclined plate in a slip flow regime. Oyekunle and Agunbiade (2020) explored both Soret and Dufour effects with an inclined magnetic field on unsteady MHD flow. Ahmed and Sarma (2021) studied thermal diffusion effect on unsteady MHD free convective flow past a semi-infinite vertical plate with parabolic ramped temperature.

In most works of MHD, the effect of the induced magnetic field is neglected on the assumption that for many natural gases, electrical conductivity is very low and as a result, the magnetic Reynolds number is very small. But, when a missile travels through the earth's

atmosphere, a huge amount of heat is generated due to friction and it sometimes ionizes the gas in the surrounding air near the stagnation point. This ionized gas in the stagnation region is electrically conducting. When a magnetic field is applied in this region, an electromagnetic force is induced in the air and consequently, it affects the motion. Acknowledging the importance of induced hydromagnetic effects on flows of electrically conducting fluid, some researchers carried out model research on the consequences of the induced magnetic field. Goud et al. (2021) considered the induced magnetic field effect on MHD free convective flow in conducting and non-conducting vertical microchannel walls. Jha and Aina (2016) explored the role of an induced magnetic field on free convective MHD flow in a vertical microchannel. Poddar et al. (2021) analysed the effect of magnetic field induction in a radiating MHD flow. Sarveshanand and Singh (2015) examined the effects of the induced magnetic field in a free convective MHD flow between two parallel plates.

The purpose of our current study is to analyse the combined impacts of induced magnetic field and thermal diffusion on a free convective and chemically reactive MHD flow past an exponentially accelerated flat vertical plate. The wall temperature is taken to be ramped. Studying the available literature, we have not found any work considering the above effects together. The governing equations are converted to non-dimensional equations with the help of some non-dimensional variables and parameters. Then they are solved using a closed form of the Laplace transform technique. Effects of various flow parameters on velocity, temperature, concentration, Nusselt number, and Sherwood number are discussed with the help of graphs. Variation of skin friction is demonstrated with the assistance of tables.

8.2 Mathematical Analysis

The equations that govern the motion of an electrically conducting, radiative, and chemically reacting fluid in the existence of a magnetic field with constant mass diffusivity and constant thermal diffusivity taking Soret effect into account are

Equation of continuity (based on the law of conservation of mass and Newton's 2nd law of motion)

$$\vec{\nabla} \cdot \vec{q} = 0 \quad (8.1)$$

Magnetic field continuity equation

$$\vec{\nabla} \cdot \vec{B} = 0 \quad (8.2)$$

Ampere's law

$$\vec{\nabla} \times \vec{B} = \mu_e \vec{J} \quad (8.3)$$

Momentum equation (based on the law of conservation of linear momentum)

$$\rho \left[\frac{\partial \vec{q}}{\partial t} + (\vec{q} \cdot \vec{\nabla}) \vec{q} \right] = -\vec{\nabla} p + \rho \vec{g} + \vec{J} \times \vec{B} + \mu \nabla^2 \vec{q} \quad (8.4)$$

Energy equation (based on the law of conservation of energy)

$$\rho C_p \left[\frac{\partial T}{\partial t} + (\vec{q} \cdot \vec{\nabla}) T \right] = \kappa \nabla^2 T - \vec{\nabla} \cdot \vec{q}_r \quad (8.5)$$

Species continuity equation (based on the law of conservation of species)

$$\frac{\partial C}{\partial t} + (\vec{q} \cdot \vec{\nabla}) C = D_M \nabla^2 C + D_T \nabla^2 T + \bar{K} (C_\infty - C) \quad (8.6)$$

Magnetic diffusion equation for small magnetic Reynolds number

$$\frac{\partial \vec{B}}{\partial t} = \eta \nabla^2 \vec{B} \quad (8.7)$$

Equation of state

$$\rho_\infty = \rho \left[1 + \beta (T - T_\infty) + \bar{\beta} (C - C_\infty) \right] \quad (8.8)$$

All the physical quantities are described in the list of symbols.

We, now consider a transient MHD free convective flow of a viscous incompressible electrically conducting optically thick non-Gray fluid past a semi-infinite vertical plate in presence of a uniform magnetic field applied in the transverse direction to the plate directed into the fluid region. Initially, the plate and the neighbouring fluid were at rest with uniform temperature T_∞ and concentration C_∞ at all points in the fluid. At time $\bar{t} > 0$, the plate is accelerated exponentially with velocity $U_o e^{a\bar{t}}$. The temperature of the plate is instantaneously

lifted to $T_\infty + (T_w - T_\infty) \frac{\bar{t}}{t_0}$, for $0 < \bar{t} \leq t_0$, and thereafter T_w when $\bar{t} > t_0$. The concentration is elevated to C_w and maintained thenceforth.

To idealize the mathematical design, the on-going analysis is confined to the following limitations-

- I. Apart from density variation in buoyancy force, all other fluid properties are assumed to be constant.
- II. Viscous dissipations of energy are neglected.
- III. The Magnetic Reynolds number is very small.
- IV. The plate is electrically insulating.
- V. Radiation heat flux present in the direction of the plate velocity is negligible in comparison to that in the normal direction.
- VI. Flow is parallel to the plate.
- VII. Polarization voltage is negligible as no external electric field is applied.
- VIII. The chemical reaction is of the first order and homogeneous.
- IX. Fluid temperature and concentration do not depend on the distance parallel to the surface.

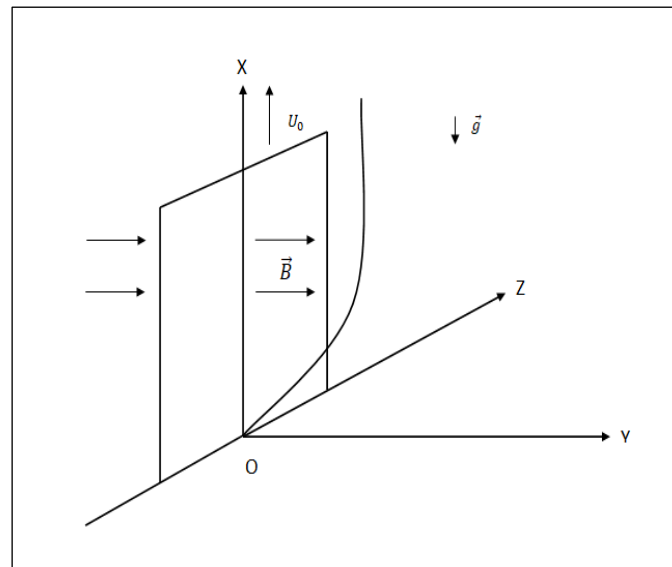


Figure 8.1: Flow diagram

We introduce a rectangular Cartesian co-ordinate system (x', y', z', t') with X axis vertically upwards, Y axis normal to the plate directed into the fluid region, Z axis along the

width of the plate. Let $\vec{q} = (u', 0, 0)$ be the fluid velocity, $\vec{B} = (B'_x, B_0, 0)$ be the magnetic induction vector and $\vec{q}_r = (0, q_r, 0)$ be the radiation heat flux at the point (x', y', z', t') in the fluid.

Equation (8.1) gives

$$\begin{aligned} \frac{\partial u'}{\partial x'} &= 0 \\ \text{i.e., } u' &= u'(y', t') \end{aligned} \quad (8.9)$$

Equation (8.2) gives

$$\begin{aligned} \frac{\partial B'_x}{\partial x'} &= 0 \\ \text{i.e., } B'_x &= B'_x(y', t') \end{aligned} \quad (8.10)$$

Equation (8.4) reduces to

$$\rho \left[\frac{\partial u'}{\partial t'} + \left(u' \frac{\partial}{\partial x'} \right) u' \hat{i} \right] = -\hat{i} \frac{\partial p}{\partial x'} - \hat{j} \frac{\partial p}{\partial y'} - \rho g \hat{i} + B_0 \eta \sigma \frac{\partial B'_x}{\partial y'} \hat{i} + \mu \left(\frac{\partial^2 u'}{\partial y'^2} \right) \hat{i} \quad (8.11)$$

Equation (8.11) gives

$$\rho \frac{\partial u'}{\partial t'} = -\frac{\partial p}{\partial x'} - \rho g + B_0 \eta \sigma \frac{\partial B'_x}{\partial y'} + \mu \frac{\partial^2 u'}{\partial y'^2} \quad (8.12)$$

and

$$0 = -\frac{\partial p}{\partial y'} \quad (8.13)$$

Equation (8.13) confirms that pressure near the plate and pressure far away from the plate is the same along the normal to the plate.

For fluid region far away from the plate, equation (8.12) takes the form

$$0 = -\frac{\partial p}{\partial x'} - \rho_\infty g \quad (8.14)$$

Eliminating $\frac{\partial p}{\partial x'}$ from (8.12) and (8.14), we get

$$\rho \frac{\partial u'}{\partial t} = (\rho_\infty - \rho)g + B_0 \eta \sigma \frac{\partial B'_x}{\partial y'} + \mu \frac{\partial^2 u'}{\partial y'^2} \quad (8.15)$$

Equation of state (8.8) gives

$$\rho_\infty - \rho = \rho \left[\beta(T - T_\infty) + \bar{\beta}(C - C_\infty) \right] \quad (8.16)$$

Putting value of (8.16) in (8.15)

$$\begin{aligned} \rho \frac{\partial u'}{\partial t} &= \rho \left[\beta(T - T_\infty) + \bar{\beta}(C - C_\infty) \right] g + B_0 \eta \sigma \frac{\partial B'_x}{\partial y'} + \mu \frac{\partial^2 u'}{\partial y'^2} \\ \text{i.e., } \frac{\partial u'}{\partial t'} &= g \beta(T - T_\infty) + g \bar{\beta}(C - C_\infty) + \frac{B_0 \eta \sigma}{\rho} \frac{\partial B'_x}{\partial y'} + \nu \frac{\partial^2 u'}{\partial y'^2} \end{aligned}$$

The radiation heat flux as per Rosseland approximation is given by

$$\vec{q}_r = -\frac{4\sigma^*}{3\kappa^*} \nabla T^4 \quad (8.17)$$

Using (8.17), Energy equation (8.5) reduces to

$$\rho C_p \frac{\partial T}{\partial t'} = \kappa \frac{\partial^2 T}{\partial y'^2} + \frac{16\sigma^* T_\infty^3}{3\kappa^*} \frac{\partial^2 T}{\partial y'^2} \quad (8.18)$$

Species continuity equation (8.6) reduces to

$$\frac{\partial C}{\partial t'} = D_M \frac{\partial^2 C}{\partial y'^2} + D_T \frac{\partial^2 T}{\partial y'^2} + \bar{K}(C_\infty - C) \quad (8.19)$$

Magnetic diffusion equation (8.7) becomes

$$\frac{\partial B'_x}{\partial t'} = \eta \frac{\partial^2 B'_x}{\partial y'^2} \quad (8.20)$$

The appropriate initial and boundary conditions are

$$\left. \begin{aligned}
u' &= 0, T = T_\infty, C = C_\infty, B_x' = 0 : \forall y' \geq 0; t' \leq 0 \\
u' &= U_0 e^{at'}, C = C_w, B_x' = H_0 : y' = 0, t' > 0 \\
T &= T_\infty + (T_w - T_\infty) \frac{t'}{t_0} : y' = 0; 0 < \bar{t} \leq t_0 \\
T &= T_w : y' = 0; t' > t_0 \\
u' &\rightarrow 0, T \rightarrow T_\infty, C \rightarrow C_\infty, B_x' \rightarrow 0 : y' \rightarrow \infty; t' > 0
\end{aligned} \right\} \quad (8.21)$$

For the sake of normalization of the mathematical model of the problem, we introduce the following non-dimensional quantities-

$$\begin{aligned}
Sr &= \frac{D_T (T_w - T_\infty)}{\nu (C_w - C_\infty)}, N = \frac{\kappa \kappa^*}{4 \sigma^* T_\infty^3}, u = \frac{u'}{U_0}, y = \frac{y' U_0}{\nu}, t = \frac{U_0^2 t'}{\nu}, Gr = \frac{\nu g \beta (T_w - T_\infty)}{U_0^3}, \\
Gm &= \frac{\nu g \bar{\beta} (C_w - C_\infty)}{U_0^3}, Pm = \frac{\nu}{\eta}, \theta = \frac{T - T_\infty}{T_w - T_\infty}, \phi = \frac{C - C_\infty}{C_w - C_\infty}, Pr = \frac{\mu C_p}{\kappa}, M = \frac{\sigma B_0^2 \nu}{\rho U_0^2}, Sc = \frac{\nu}{D_M} \\
K &= \frac{\bar{K} \nu}{U_0^2}, B_x = \frac{B_x'}{H_0}, \Pi = \frac{H_0}{B_0}, \Lambda = 1 + \frac{4}{3N}, t_1 = \frac{U_0^2 t_0}{\nu}
\end{aligned}$$

The non-dimensional non-dimensional governing equations are

$$Pm \frac{\partial B_x}{\partial t} = \frac{\partial^2 B_x}{\partial y^2} \quad (8.22)$$

$$Pr \frac{\partial \theta}{\partial t} = \Lambda \frac{\partial^2 \theta}{\partial y^2} \quad (8.23)$$

$$Sc \frac{\partial \phi}{\partial t} = \frac{\partial^2 \phi}{\partial y^2} + Sr Sc \frac{\partial^2 \theta}{\partial y^2} - Sc K \phi \quad (8.24)$$

$$Pm \frac{\partial u}{\partial t} = Pm Gr \theta + Pm Gm \phi + M \Pi \frac{\partial B_x}{\partial y} + Pm \frac{\partial^2 u}{\partial y^2} \quad (8.25)$$

The initial and boundary conditions becomes

$$\left. \begin{aligned}
u = 0, \theta = 0, \phi = 0, B_x = 0 : \forall y \geq 0; t \leq 0 \\
u = e^{at}, \phi = 1, B_x = 1 : y = 0, t > 0 \\
\theta = \frac{t}{t_1} : y = 0; 0 < t \leq t_1 \\
\theta = 1 : y = 0; t > t_1 \\
u \rightarrow 0, \theta \rightarrow 0, \phi \rightarrow 0, B_x \rightarrow 0 : y \rightarrow \infty; t > 0
\end{aligned} \right\} \quad (8.26)$$

8.3 Method of Solution

Taking Laplace transform of the equations from (8.22) to (8.25) and applying the conditions (26), we get the following governing equations-

$$\frac{d^2 \bar{B}_x}{dy^2} = Pm.s \bar{B}_x \quad (8.27)$$

$$\Lambda \frac{d^2 \bar{\theta}}{dy^2} = Pr.s \bar{\theta} \quad (8.28)$$

$$\frac{d^2 \bar{\phi}}{dy^2} - Sc(K+s) \bar{\phi} = -SrSc \frac{d^2 \bar{\theta}}{dy^2} \quad (8.29)$$

$$Pm \frac{d^2 \bar{u}}{dy^2} + PmGr \bar{\theta} + PmGm \bar{\phi} + M\Pi \frac{d \bar{B}_x}{dy} = Pm.s \bar{u} \quad (8.30)$$

subject to the initial and boundary conditions

$$\left. \begin{aligned}
y = 0 : \bar{\theta} = \frac{2}{s^2 t_1} (1 - e^{-st_1}), \bar{\phi} = \frac{1}{s}, \bar{u} = \frac{1}{s-a}, \bar{B}_x = \frac{1}{s} \\
y \rightarrow \infty : \bar{\theta} \rightarrow 0, \bar{\phi} \rightarrow 0, \bar{u} \rightarrow 0, \bar{B}_x \rightarrow 0
\end{aligned} \right\} \quad (8.31)$$

Solving the equations from (8.27) to (8.30) subject to the conditions (8.31) and taking inverse Laplace transform of the solutions, the expressions for the induced magnetic field B_x , temperature field θ , concentration field ϕ , and velocity field u are as follows-

$$B_x = E_1 \quad (8.32)$$

$$\theta = \frac{1}{t} \Delta \lambda_1 \quad (8.33)$$

$$\phi = \phi = \begin{cases} \phi_{1,1} + \phi_{1,2} - \phi_{1,3} : \Lambda Sc \neq Pr \\ \phi_{2,1} + \phi_{2,2} - \phi_{2,3} : \Lambda Sc = Pr \end{cases} \quad (8.34)$$

$$u = \begin{cases} u_{1,1} - u_{1,2} - u_{1,3} - u_{1,4} + u_{1,5} + u_{1,6}; Pm \neq 1, Sc \neq 1, Pr \neq \Lambda Sc \\ u_{2,1} - u_{2,2} - u_{2,3} - u_{2,4} + u_{2,5} + u_{2,6}; Pm = 1, Sc \neq 1, Pr \neq \Lambda Sc \\ u_{3,1} - u_{3,2} - u_{3,3} - u_{3,4} + u_{3,5} + u_{3,6}; Pm \neq 1, Sc = 1, Pr \neq \Lambda Sc \\ u_{4,1} - u_{4,2} - u_{4,3} - u_{4,4} + u_{4,5} + u_{4,6}; Pm \neq 1, Sc \neq 1, Pr = \Lambda Sc \\ u_{5,1} - u_{5,2} - u_{5,3} - u_{5,4} + u_{5,5} + u_{5,6}; Pm = 1, Sc = 1, Pr \neq \Lambda Sc \\ u_{6,1} - u_{6,2} - u_{6,3} - u_{6,4} + u_{6,5} + u_{6,6}; Pm = 1, Sc \neq 1, Pr = \Lambda Sc \\ u_{7,1} - u_{7,2} - u_{7,3} - u_{7,4} + u_{7,5} + u_{7,6}; Pm \neq 1, Sc = 1, Pr \neq \Lambda Sc \\ u_{8,1} - u_{8,2} - u_{8,3} - u_{8,4} + u_{8,5} + u_{8,6}; Pm = 1, Sc = 1, Pr = \Lambda Sc \end{cases} \quad (8.35)$$

8.4 Nusselt Number

The heat flux q^* at the plate $y' = 0$ is obtained by Fourier's law of conduction is given by

$$q^* = -\kappa_0^* \left. \frac{\partial T}{\partial y'} \right]_{y'=0} \quad (8.36)$$

Where $\kappa_0^* = \kappa + \frac{16\sigma^* T_\infty^3}{3\kappa^*}$ is the modified thermal conductivity.

Equation (8.36) yields

$$Nu = - \left. \frac{\partial \theta}{\partial y} \right]_{y=0} \quad (8.37)$$

Where $Nu = \frac{q^* \nu}{\kappa_0^* U_0 (T_w - T_\infty)} = \frac{q^* \nu}{\kappa \Lambda (T_w - T_\infty) U_0}$ is called the Nusselt number which is concerned with the rate of heat transfer at the plate.

Equation (8.37) gives,

$$Nu = - \frac{1}{t_1} \Delta \nu_1 \quad (8.38)$$

8.5 Sherwood Number

The mass flux M_w at the plate $y' = 0$ is specified by Fick's law of diffusion is given by

$$M_w = -D_M \left. \frac{\partial C}{\partial y'} \right]_{y'=0} \quad (8.39)$$

Equation (8.39) gives

$$Sh = - \left. \frac{\partial \phi}{\partial y} \right]_{y=0} \quad (8.40)$$

In (8.40), $Sh = \frac{\nu M_w}{D_M (C_w - C_\infty)}$ is called the Sherwood number which is associated with the rate of mass transfer at the plate.

Equation (8.40) yields

$$Sh = - \begin{cases} Sh_{1,1} + Sh_{1,2} - Sh_{1,3}; \text{Pr} \neq \Lambda Sc \\ Sh_{2,1} + Sh_{2,2} - Sh_{2,3}; \text{Pr} = \Lambda Sc \end{cases} \quad (8.41)$$

8.6 Skin Friction

The viscous drag at the plate $y' = 0$ is determined by Newton's law of viscosity is given by

$$\bar{\tau} = -\mu \left. \frac{\partial u}{\partial y'} \right]_{y'=0} \quad (8.42)$$

Equation (8.42) gives

$$\tau = - \left. \frac{\partial u}{\partial y} \right]_{y=0} \quad (8.43)$$

In (8.43), $\tau = \frac{\nu \bar{\tau}}{\mu U_0^2}$ is called the skin friction or coefficient of friction which is associated with the rate of momentum transfer at the plate.

Equation (8.43) yields,

$$\tau = - \begin{cases} \tau_{1,1} - \tau_{1,2} - \tau_{1,3} - \tau_{1,4} + \tau_{1,5} + \tau_{1,6}; Pm \neq 1, Sc \neq 1, Pr \neq \Lambda Sc \\ \tau_{2,1} - \tau_{2,2} - \tau_{2,3} - \tau_{2,4} + \tau_{2,5} + \tau_{2,6}; Pm = 1, Sc \neq 1, Pr \neq \Lambda Sc \\ \tau_{3,1} - \tau_{3,2} - \tau_{3,3} - \tau_{3,4} + \tau_{3,5} + \tau_{3,6}; Pm \neq 1, Sc = 1, Pr \neq \Lambda Sc \\ \tau_{4,1} - \tau_{4,2} - \tau_{4,3} - \tau_{4,4} + \tau_{4,5} + \tau_{4,6}; Pm \neq 1, Sc \neq 1, Pr = \Lambda Sc \\ \tau_{5,1} - \tau_{5,2} - \tau_{5,3} - \tau_{5,4} + \tau_{5,5} + \tau_{5,6}; Pm = 1, Sc = 1, Pr \neq \Lambda Sc \\ \tau_{6,1} - \tau_{6,2} - \tau_{6,3} - \tau_{6,4} + \tau_{6,5} + \tau_{6,6}; Pm = 1, Sc \neq 1, Pr = \Lambda Sc \\ \tau_{7,1} - \tau_{7,2} - \tau_{7,3} - \tau_{7,4} + \tau_{7,5} + \tau_{7,6}; Pm \neq 1, Sc = 1, Pr = \Lambda Sc \\ \tau_{8,1} - \tau_{8,2} - \tau_{8,3} - \tau_{8,4} + \tau_{8,5} + \tau_{8,6}; Pm = 1, Sc = 1, Pr = \Lambda Sc \end{cases} \quad (8.44)$$

8.7 Results and Discussion

The effects of various flow parameters on flow and transport characteristics are analysed by assigning some specific values.

Figures 8.2 and 8.3 display the variation of induced magnetic field versus normal coordinate y . Figure 8.2 shows that induced magnetic field hikes with time. Ascending values of magnetic Prandtl number lowers induced magnetic field as noticed in Figure 8.3. Increasing magnetic Prandtl number is equivalent to decreasing magnetic diffusivity and as a result strength of magnetic field becomes weak.

Figures 8.4 and 8.5 demonstrate the variation of temperature field versus normal coordinate y . Figure 8.4 suggests that the temperature field falls with increasing radiation parameter. It establishes the fact that radiation has a tendency to decline fluid temperature. Temperature field declines with an uplift in Prandtl number as displayed in Figure 8.5. Thus, higher thermal diffusivity declines fluid temperature.

Figures 8.6 to 8.9 illustrate the variation of concentration field versus normal coordinate y . Figure 8.6 reveals that fluid concentration declines as chemical reaction parameter hikes. High chemical reaction consumes chemical stuff present in the fluid rapidly and hence fluid concentration lowers. Figure 8.7 shows that fluid concentration rises in a thin layer adjacent to the plate but its behaviour reverses outside the layer with growing values of Prandtl number. This implies that higher thermal diffusivity leads to a decrease in the fluid concentration in a slim layer adjoining the plate but its nature takes a reverse turn outside the layer. With increasing Schmidt number, fluid concentration reduces as displayed in Figure 8.8. This agrees with the fact that greater mass diffusivity hikes fluid concentration. There is a comprehensive rise in fluid concentration with a growing Soret number as depicted in

Figure 8.9. In Soret effect, the concentration of the fluid is affected by temperature gradient. So physically, a higher Soret number corresponds to a higher temperature gradient which produces higher convective flow. As a result, fluid concentration gets enhanced.

Figures 8.10 to 8.19 demonstrate the variation of velocity field versus normal coordinate y . Figure 8.10 reveals that enhancement in chemical reaction parameter decelerate fluid velocity. Increasing chemical reaction parameter suggests that collision between fluid molecules is also increasing. As a result, Kinetic energy is lost and velocity declines. Velocity declines considerably with ascending values of Prandtl number as shown in Figure 8.11. This result agrees with the fact that velocity gets enhanced for high thermal diffusivity. Figure 8.12 admits that velocity decreases in a small layer adjacent to the plate but its behaviour reverses outside the layer with increasing Schmidt number. Thus the phenomena of mass diffusivity first increase velocity in a slim layer along the plate but its nature takes a reverse turn outside the layer. Figure 8.13 asserts that growing Soret number increases velocity in a thin layer but decreases outside the layer. Thus, temperature gradient enhances fluid velocity for a small layer only adjoining the plate. Increasing radiation lowers the thickness of the momentum boundary layer which eventually leads to a dip in velocity. Figure 8.14 suggests that radiation declines fluid velocity. Figure 8.15 displays that increasing magnetic Prandtl number upsurges the velocity field. As magnetic Prandtl number is the ratio of viscous diffusivity to magnetic diffusivity, so high magnetic diffusivity slows down fluid velocity. It is demonstrated in Figure 8.16 that ascending values of magnetic parameter reduce fluid velocity. The presence of a magnetic field in the transverse direction of flow produces a resistive force called Lorentz force which diminishes fluid velocity. As Π is the ratio of induced magnetic field strength to applied magnetic field strength, so if the strength of the applied magnetic field is higher than that of the induced magnetic field, then fluid velocity hikes considerably. This phenomenon is noticed in Figure 8.17 It is noticed from Figure 8.18 and Figure 8.19 that increment in both thermal Grashof number and solutal Grashof number hikes velocity field. Thus increasing thermal diffusivity and mass diffusivity both lead to a dip in the velocity field.

Figures 8.20 and 8.21 demonstrate the variation of Nusselt number versus time t . There is a comprehensive rise in the Nusselt number for increasing values of radiation parameter as observed in Figure 8.20. Thus, heat transfer from the plate to the fluid get enhances for high radiation. Figure 8.21 shows that increasing Prandtl number lifts Nusselt

number. This result establishes the fact that higher thermal diffusivity slows down the rate of heat transfer.

Figures 8.22 to 8.25 display the variation of Sherwood number versus time t . It is observed from Figure 8.22 that the uplifting radian parameter diminishes Sherwood number. This suggests that radiation decelerates the rate of mass transfer from the plate to the fluid. Figure 8.23 shows that Sherwood number hike with ascending values of chemical reaction parameter. This is because increasing chemical reaction parameter speed up the collision between the molecules and as a result mass transfer rate from the plate to the fluid accelerates. Increasing Prandtl number declines Sherwood number as noticed in Figure 8.24. This result agrees with the fact that high thermal diffusivity enhances the rate of mass transfer as time progresses. Figure 8.25 reveals that ascending values of Soret number diminish Sherwood number to a great extent. This means that a high temperature gradient uplifts the rate of mass transfer from the plate to the fluid.

Numerical values of Skin friction τ against different time radiation parameter N , Prandtl number Pr , Soret number Sr , Schmidt number Sc and radiation parameter K are illustrated in Table 8.1. It is observed that skin friction declines with an increment in radiation parameter. Thus, radiation slows down the process of momentum transfer from the plate to the fluid. Upsurge in both Prandtl number and Soret number diminishes skin friction. This asserts that high thermal diffusivity increases but a high temperature gradient declines the process of momentum transfer from the plate to the fluid. An opposite nature is observed for increasing chemical reaction parameter. Thus the high rate of collision between the molecules reduces the momentum transfer rate.

Numerical values of skin friction τ against different thermal Grashof number Gr , solutal Grashof number Gm , magnetic Prandtl number Pm and magnetic parameter M are analyzed in Table 8.2. It is observed that upsurge in both thermal Grashof number and solutal Grashof number declines skin friction. This means that both thermal buoyancy force and solutal buoyancy force slow down the process of momentum transfer from the plate to the fluid. Ascending values of magnetic Prandtl number diminishes skin friction. So, high magnetic diffusivity upsurses the momentum transfer rate. A reverse phenomenon is observed for the magnetic parameter, i.e., increasing magnetic parameter hikes skin friction. Lorentz force opposes the motion of flow by significantly exerting drag force. As a result coefficient of friction hikes.

8.8 Conclusion

The main motivation behind the present investigation is to study the effects of induced magnetic field and thermal diffusion in a chemically reacting, free convective, incompressible viscous and radiative, unsteady MHD flow past an exponentially accelerated moving vertical plate. The wall temperature is taken to be ramped. A set of non-dimensional variables and parameters is used to transform the governing equations to non-dimensional differential equations and they are solved with the help of Laplace transformation technique. The prominent outcomes of our investigation are:

- i. The induced magnetic field gets lowered with ascending values of magnetic Prandtl number.
- ii. The effect of chemical reaction declines both fluid velocity and concentration.
- iii. Thermal diffusion effect upsurges fluid concentration.
- iv. Radiation has a tendency to decline both temperature and velocity fields.
- v. Radiation hikes Nusselt number but lowers Sherwood number.
- vi. Increasing thermal diffusivity enhances both rate of momentum transfer and mass transfer but decline rate of heat transfer from the plate to the fluid.
- vii. Lorentz force hinders the rate of momentum transfer.

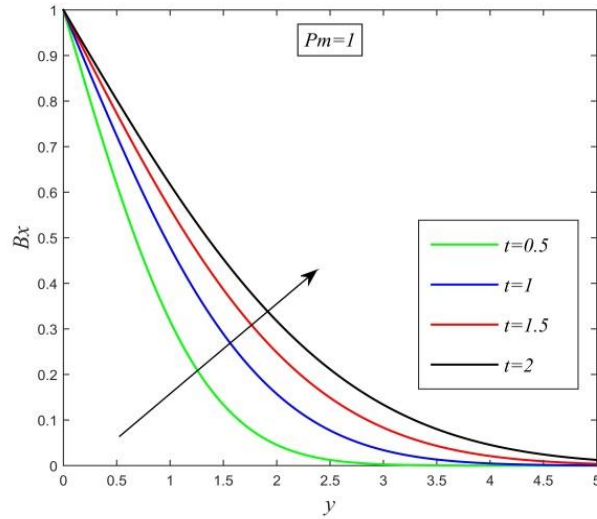


Figure 8.2: Induced magnetic field versus y for different t and $Pm=1$

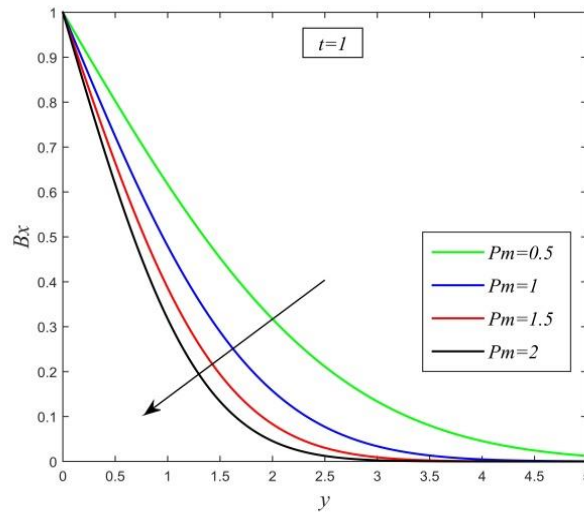


Figure 8.3: Induced magnetic field versus y for different Pm and $t=1$

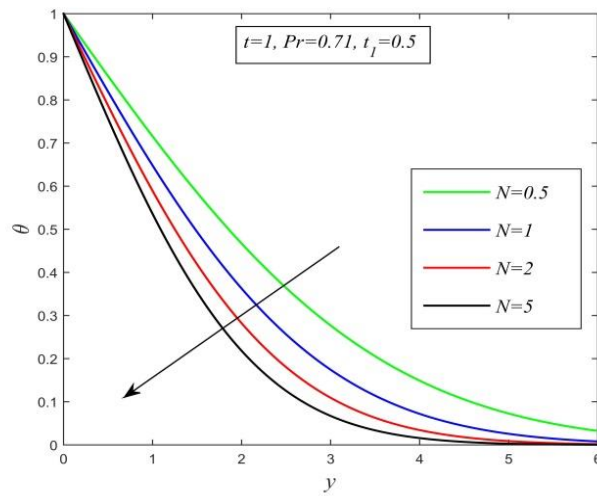


Figure 8.4: Temperature field versus y for different N and $t=1, Pr=0.71, t_I=0.5$

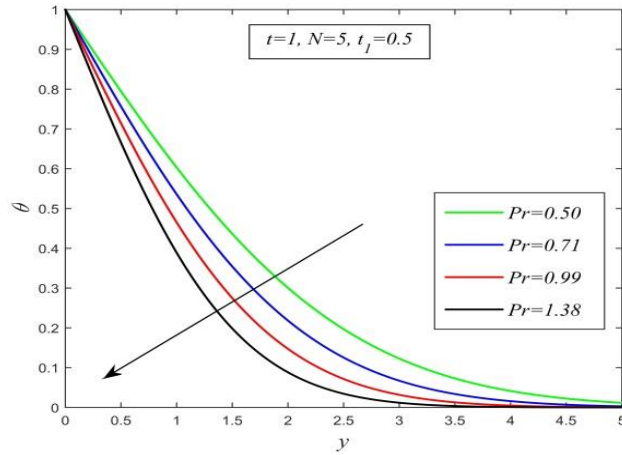


Figure 8.5: Temperature field versus y for different Pr and $t=1, N=5, t_1=0.5$

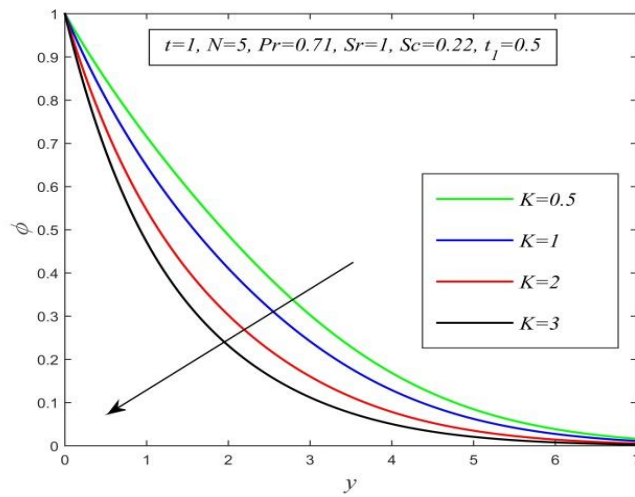


Figure 8.6: Concentration field versus y for different K and $t=1, N=5, Pr=0.71, Sr=1, Sc=0.22, t_1=0.5$

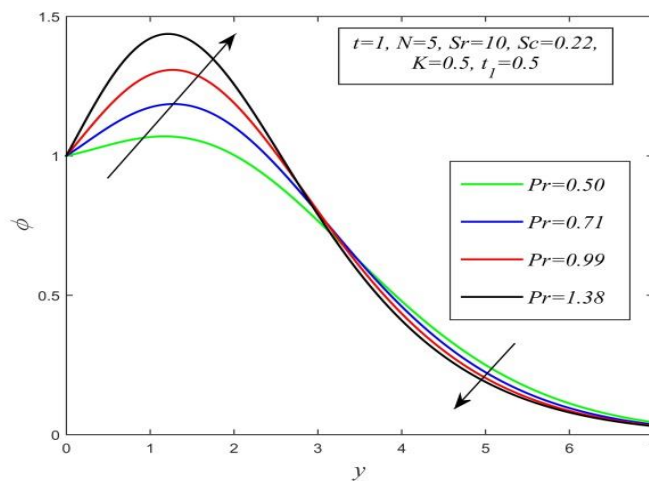


Figure 8.7: Concentration field versus y for different Pr and $t=1, N=5, Sr=10, Sc=0.22, K=0.5, t_1=0.5$

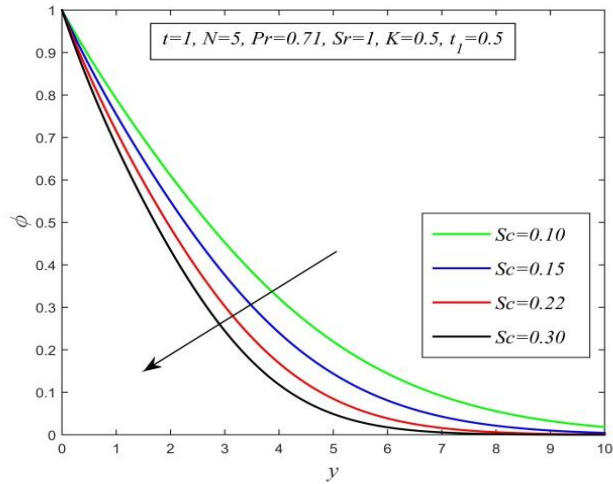


Figure 8.8: Concentration field versus y for different Sc and $t=1, N=5, Pr = 0.71, Sr=1, K=0.5, t_1=0.5$

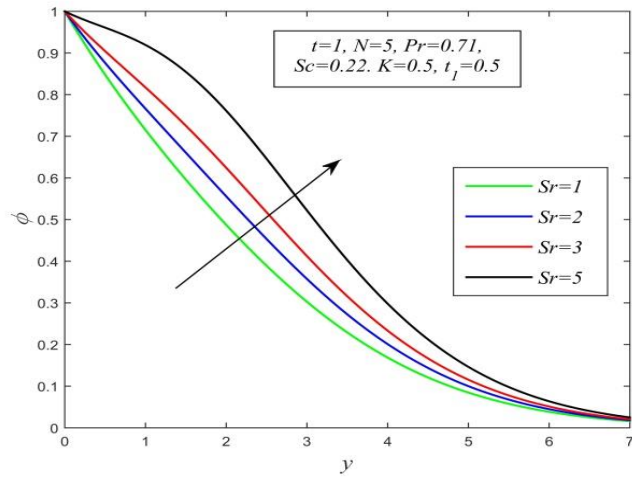


Figure 8.9: Concentration field versus y for different Sr and $t=1, N=5, Pr = 0.71, Sc=0.22, K=0.5, t_1=0.5$

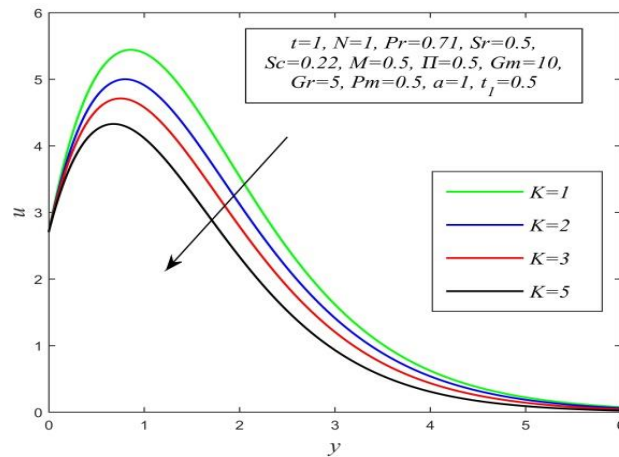


Figure 8.10: Velocity field versus y for different K and $t=1, N=1, Pr = 0.71, Sr=0.5, Sc=0.22, M=0.5, \Pi = 0.5, Gm=10, Gr=5, Pm=0.5, a=1, t_1=0.5$

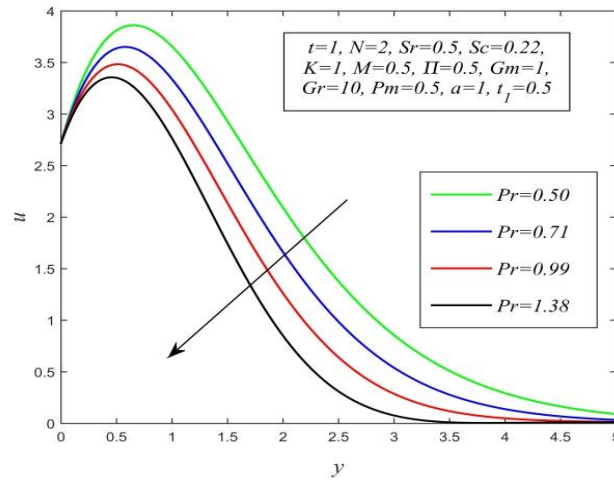


Figure 8.11: Velocity field versus y for different Pr and $t=1, N=2, Sr=0.5, Sc=0.22, K=1, M=0.5, \Pi = 0.5, Gm=1, Gr=10, Pm=0.5, a=1, t_1=0.5$

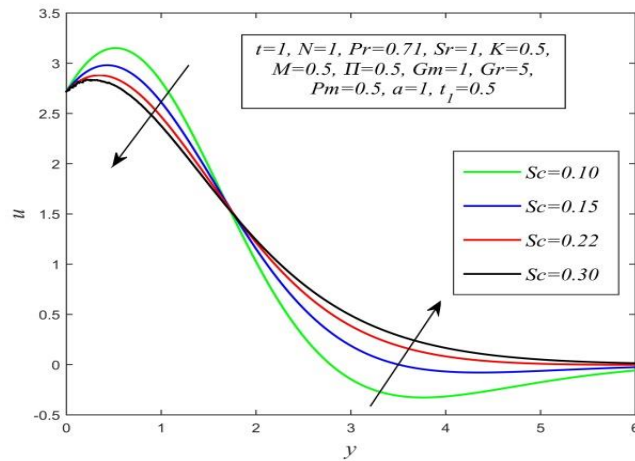


Figure 8.12: Velocity field versus y for different Sc and $t=1, N=1, Pr=0.71, Sr=1, K=0.5, M=0.5, \Pi = 0.5, Gm=1, Gr=5, Pm=0.5, a=1, t_1=0.5$

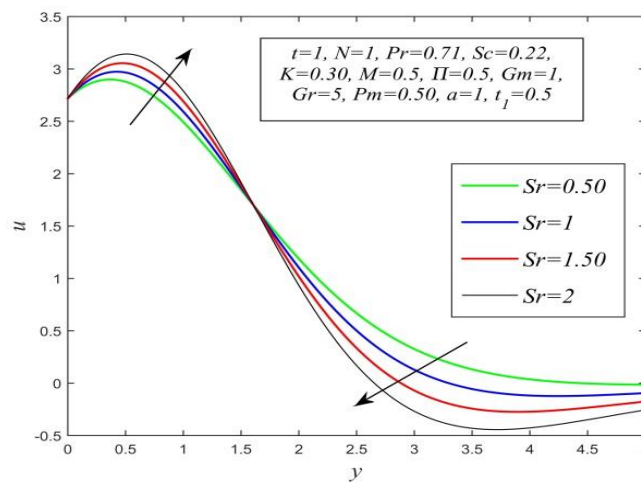


Figure 8.13: Velocity field versus y for different Sr and $t=1, N=1, Pr=0.71, Sc=0.22, K=0.3, M=0.5, \Pi = 0.5, Gm=1, Gr=5, Pm=0.5, a=1, t_1=0.5$

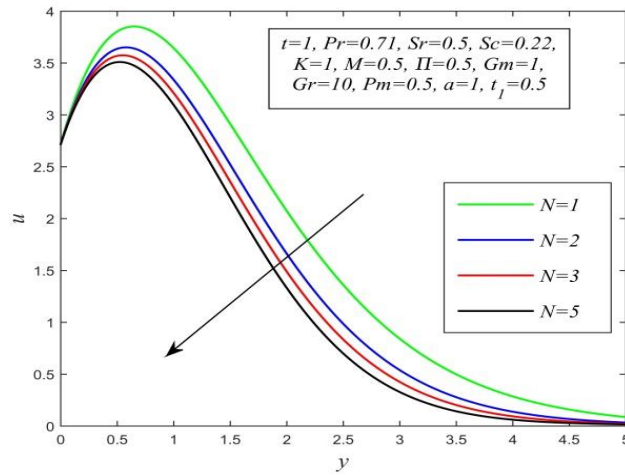


Figure 8.14: Velocity field versus y for different N and $t=1, Pr=0.71, Sr=0.5, Sc=0.22, K=1, M=0.5, \Pi = 0.5, Gm=1, Gr=10, Pm=0.5, a=1, t_1=0.5$

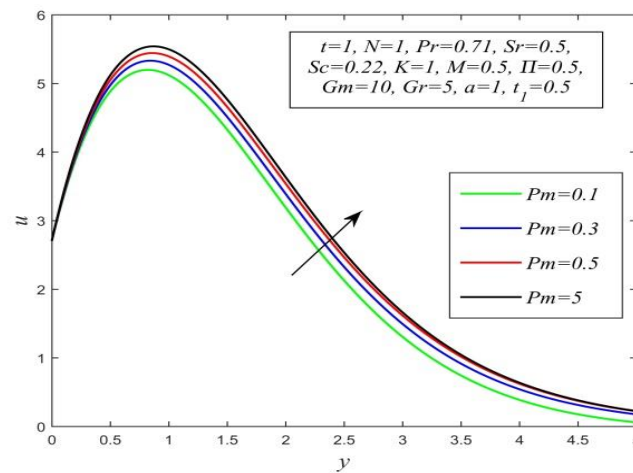


Figure 8.15: Velocity field versus y for different Pm and $t=1, N=1, Pr=0.71, Sr=0.5, Sc=0.22, K=1, M=0.5, \Pi = 0.5, Gm=10, Gr=5, a=1, t_1=0.5$

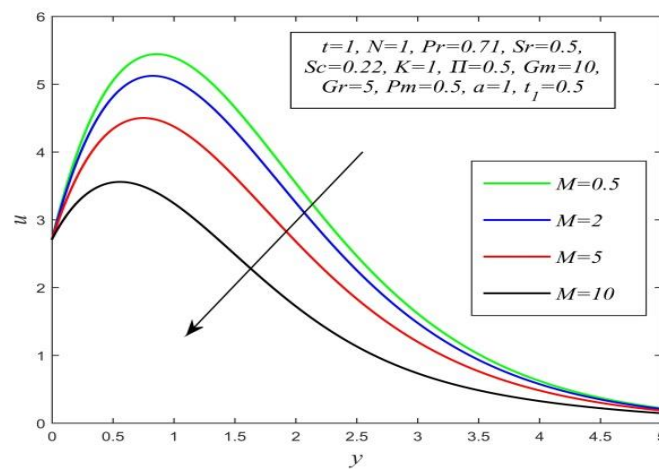


Figure 8.16: Velocity field versus y for different M and $t=1, N=1, Pr=0.71, Sr=0.5, Sc=0.22, K=1, \Pi = 0.5, Gm=10, Gr=5, Pm=0.5, a=1, t_1=0.5$

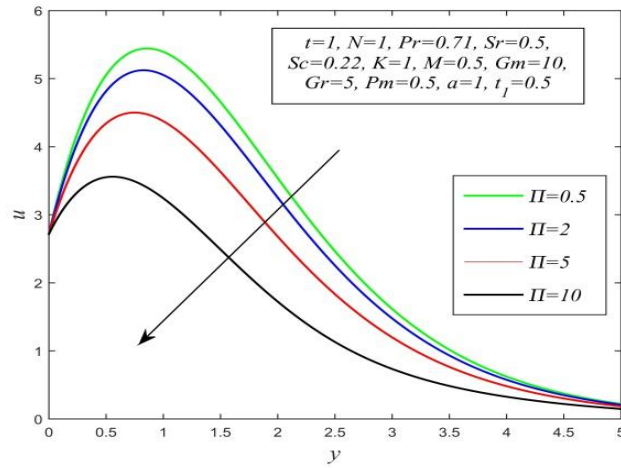


Figure 8.17: Velocity field versus y for different Π and $t=1, N=1, Pr=0.71, Sr=0.5, Sc=0.22, K=1, M=0.5, Gm=10, Gr=5, Pm=0.5, a=1, t_1=0.5$

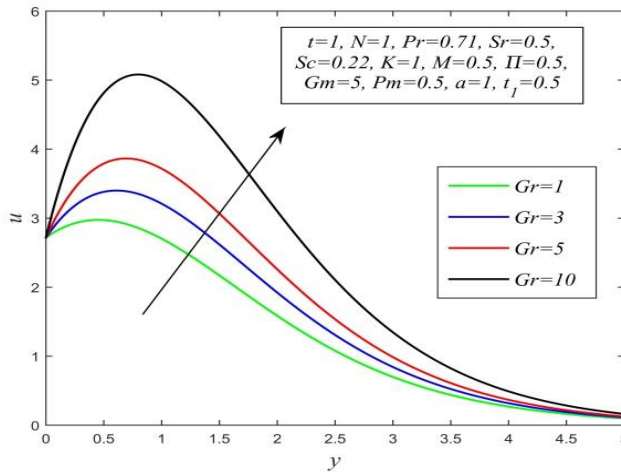


Figure 8.18: Velocity field versus y for different Gr and $t=1, N=1, Pr=0.71, Sr=0.5, Sc=0.22, K=1, M=0.5, \Pi = 0.5, Gm=5, Pm=0.5, a=1, t_1=0.5$

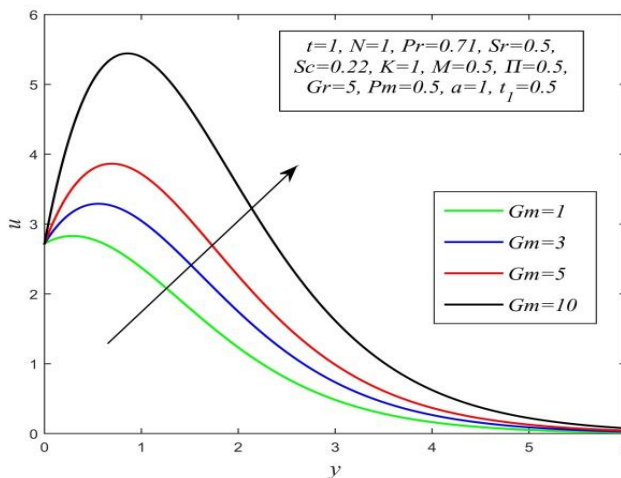


Figure 8.19: Velocity field versus y for different Gm and $t=1, N=1, Pr=0.71, Sr=0.5, Sc=0.22, K=1, M=0.5, \Pi = 0.5, Gr=5, Pm=0.5, a=1, t_1=0.5$

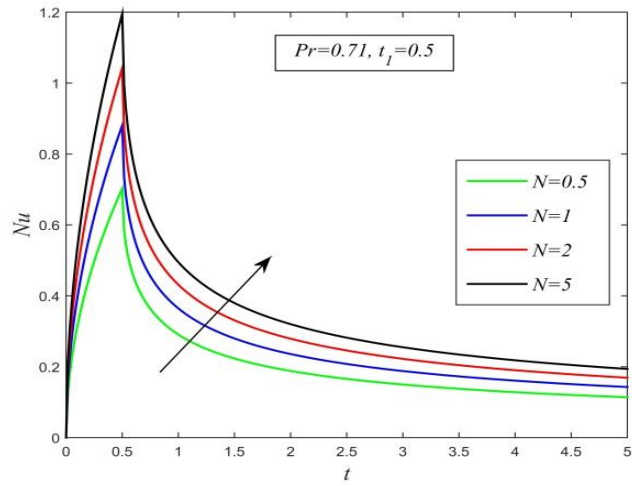


Figure 8.20: Nusselt Number versus t for different N and $Pr=0.71, t_1=0.5$

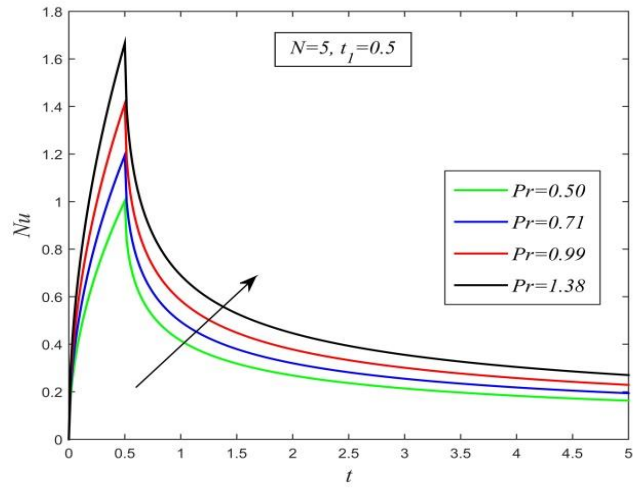


Figure 8.21: Nusselt Number versus t for different Pr and $N=5, t_1=0.5$

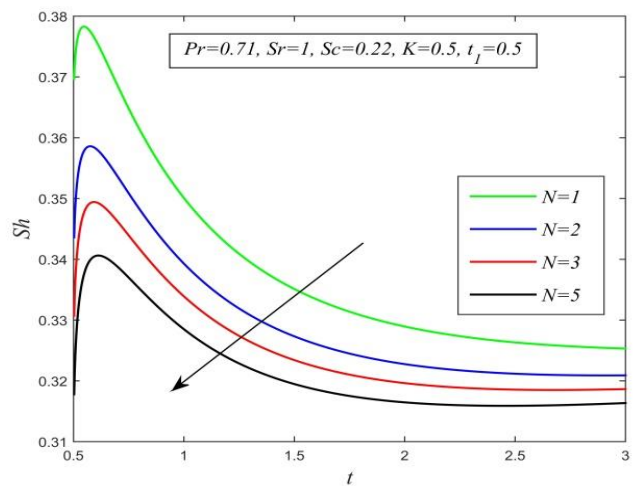


Figure 8.22: Sherwood Number versus t for different N and $Pr=0.71, Sr=1, Sc=0.22, K=0.5, t_1=0.5$

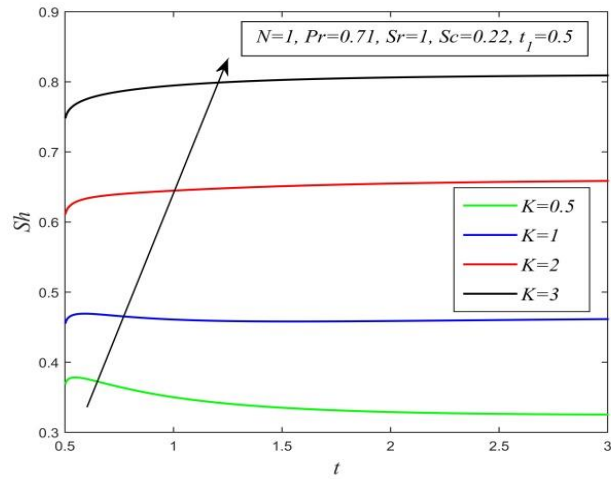


Figure 8.23: Sherwood Number versus t for different K and $N=1, Pr=0.71, Sr=1, Sc=0.22, t_1=0.5$

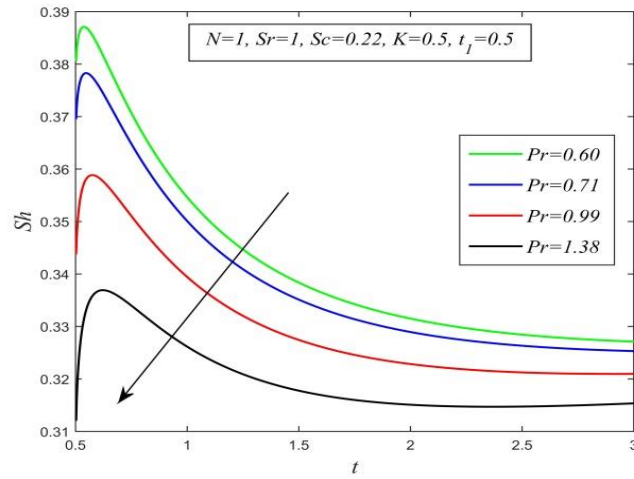


Figure 8.24: Sherwood Number versus t for different Pr and $N=1, Sr=1, Sc=0.22, K=0.5, t_1=0.5$

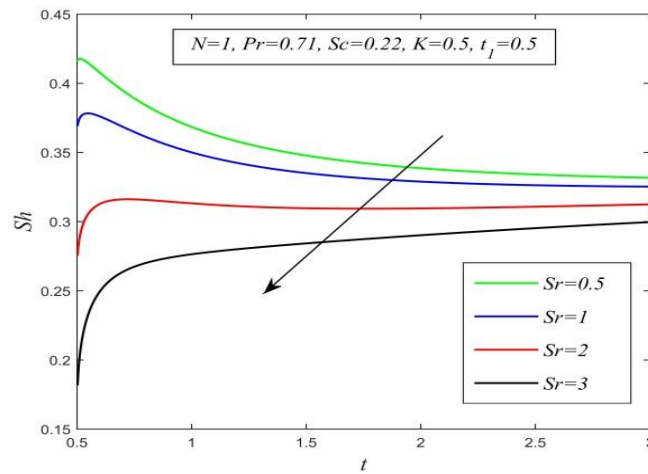


Figure 8.25: Sherwood Number versus t for different Sr and $N=1, Pr=0.71, Sc=0.22, K=0.5, t_1=0.5$

N	Pr	Sr	Sc	K	τ
1	0.71	1	0.22	1	1.6651
2					1.6113
3					1.5648
5					1.5033
1	0.60	1	0.22	1	1.6733
	0.71				1.6651
	0.99				1.6123
	1.38				1.4715
1	0.71	0.5	0.22	1	1.7012
		1			1.6651
		2			1.5929
		5			1.3763
1	0.71	1	0.10	1	1.4222
			0.15		1.5606
			0.22		1.6651
			0.25		1.6959
1	0.71	1	0.22	0.5	1.5113
				1	1.6651
				2	1.7542

Table 8.1: Computational values of skin friction for various N , Pr , Sr , Sc and K when $t=1$, $Gr=1$, $Gm=1$, $Pm=0.5$, $\Pi=0.5$, $M=0.5$, $a=1$, $t_1=0.5$

Gr	Gm	Pm	M	τ
0.5	1	0.5	0.5	1.9785
1				1.6651
2				1.0383
3				0.4115
1	0.5	0.5	0.5	2.0501
	1			1.6651
	2			0.8950
	3			0.1250
1	1	0.5	0.5	1.6651
		1.5		1.5498
		3		1.5108
		5		1.4925
1	1	0.5	0.5	1.6651
			1	1.8722
			3	2.7066
			5	3.5291

Table 8.2: Computational values of skin friction for various Gr , Gm , Pm and M when $t=1$, $N=1$, $Pr=0.71$, $\Pi=0.5$, $Sr=1$, $Sc=0.22$, $K=1$, $a=1$, $t_1=0.5$

Nomenclature

a : Surface acceleration parameter

a^* : Absorption coefficient

\vec{B} : Magnetic flux density

B_0 : Strength of the applied magnetic field

B'_x : Induced magnetic field

C : Molar species concentration

C_p : Specific heat at constant pressure

C_∞ : Concentration far away from the plate

C_w : Concentration at the plate

D_M : Mass diffusivity

D_T : Molar thermal diffusivity

H_0 : Induced magnetic field

\vec{J} : Current density vector

\vec{g} : Gravitation acceleration vector

g : Gravitational acceleration

Gr : Thermal Grashof number

Gm : Solutal Grashof number

\vec{J} : Current density vector

\bar{K} : Chemical reaction rate

K : Chemical reaction parameter

M : Magnetic parameter

N : Radiation parameter

p : Pressure

Pr : Prandtl number

Pm : Magnetic Prandtl number

\vec{q} : Fluid velocity vector

\vec{q}_r : Radiation heat flux vector

q_r : Radiation heat flux

Sc : Schmidt number

Sr : Soret number

\bar{t} : Time

t_0 : Critical time for rampedness

t_1 : Non- dimensional critical time for rampedness

T_w : Temperature at the plate

T_∞ : Undisturbed temperature

u' : X-component of fluid velocity

U_0 : Plate velocity

Greek Symbols:

η : Magnetic diffusivity

μ_e : Magnetic permeability

μ : Coefficient of viscosity

σ : Electrical conductivity

σ^* : Stefan-Boltzmann constant

ρ : Fluid density

ρ_∞ : Fluid density far away from the plate

κ : Thermal conductivity

κ^* : Mean absorption constant

β : Volumetric coefficient of thermal expansion

$\bar{\beta}$: Volumetric coefficient of solutal expansion

ν : Kinematic viscosity

Subscripts:

w : Refers to physical quantity at the plate

∞ : Refers to physical quantity far away from the plate

Appendix

$$\begin{aligned}
E_1 &= \operatorname{erfc}\left(\frac{y\sqrt{Pm}}{2\sqrt{t}}\right), a_1 = \frac{\operatorname{Pr}}{\Lambda}, \lambda_1 = \lambda(a_1, y, t), a_3 = \frac{Sc.K}{a_1 - Sc}, a_4 = \frac{SrSc.a_1}{t_1(a_1 - Sc)}, \phi_{1,1} = \psi_1, \\
\psi_1 &= \psi(Sc, K, y, t), \phi_{1,2} = a_4(A_1\Delta\psi_1 + A_2\Delta\psi_2), A_1 = -\frac{1}{a_3}, A_2 = -A_1, \psi_2 = \Psi(Sc, K, a_3, y, t), \\
\phi_{1,3} &= a_4(A_1\Delta E_2 + A_2\Delta\psi_3), E_2 = \operatorname{erfc}\left(\frac{y\sqrt{a_1}}{2\sqrt{t}}\right), \psi_3 = \Psi(a_1, 0, a_3, y, t), \phi_{2,1} = \phi_{1,1}, \phi_{2,2} = a_5\Delta\psi_1, \\
\phi_{2,2} &= a_5\Delta\psi_1, a_5 = -\frac{SrSc}{t_1K}, \phi_{2,3} = a_5\Delta E_2, a_6 = \frac{Gr}{t_1(a_1 - 1)}, a_7 = \frac{ScK}{Sc - 1}, a_8 = \frac{M\Pi}{(Pm - 1)\sqrt{Pm}}, \\
u_{1,1} &= u_{1,1,1} + u_{1,1,2} + u_{1,1,3} + u_{1,1,4} - u_{1,1,5} - u_{1,1,6}, u_{1,1,1} = h_2, h_2 = e^{at}h_1, h_1 = h(a, y, t), u_{1,1,2} = a_6\Delta G_1, \\
G_1 &= G(1, y, t), a_9 = \frac{Gm}{Sc - 1}, u_{1,1,3} = a_9(A_3E_3 + A_4h_4), E_3 = \operatorname{erfc}\left(\frac{y}{2\sqrt{t}}\right), h_3 = h(-a_7, y, t), h_4 = e^{-a_7t}h_3, \\
A_3 &= \frac{1}{a_7}, A_4 = -A_3, u_{1,1,4} = a_{10}(A_5\Delta E_3 + A_6\Delta h_6 + A_7\Delta h_4), A_5 = -\frac{1}{a_3a_7}, A_6 = \frac{1}{a_3(a_3 + a_7)}, \\
A_7 &= \frac{1}{a_7(a_3 + a_7)}, h_5 = h(a_3, y, t), h_6 = e^{a_3t}h_5, u_{1,1,5} = a_{11}(A_8\Delta E_2 + A_1\Delta F_1 + A_9\Delta h_6), a_{11} = \frac{Gma_4}{a_1 - 1}, \\
F_1 &= F(y, t), A_8 = -A_9, A_9 = \frac{1}{a_3}, u_{1,1,6} = a_8m_1, m_1 = m(y, t), u_{1,2} = a_6\Delta G_2, G_2 = G(a_1, y, t), \\
u_{1,3} &= a_9(A_3\psi_1 + A_4\psi_4), \psi_4 = \Psi(Sc, k, -a_7, y, t), u_{1,4} = a_{10}(A_5\Delta\psi_1 + A_6\Delta\psi_2 + A_7\Delta\psi_4), \\
u_{1,5} &= a_{11}(A_8\Delta E_2 + A_1\Delta\lambda_1 + A_9\Delta\psi_3), u_{1,6} = a_8m_2, m_2 = m(y\sqrt{Pm}, t), \\
u_{2,1} &= u_{2,1,1} + u_{2,1,2} + u_{2,1,3} + u_{2,1,4} - u_{2,1,5} - u_{2,1,6}, u_{2,1,1} = u_{1,1,1}, u_{2,1,2} = u_{1,1,2}, u_{2,1,3} = u_{1,1,3}, u_{2,1,4} = u_{1,1,4}, \\
u_{2,1,5} &= u_{1,1,5}, u_{2,1,6} = a_{12}E_3, a_{12} = \frac{M\Pi y}{2}, u_{2,2} = u_{1,2}, v = u_{2,3} = u_{1,3}, u_{2,4} = u_{1,4}, u_{2,5} = u_{1,5}, u_{2,6} = u_{2,1,6}, \\
u_{3,1} &= u_{3,1,1} + u_{3,1,2} + u_{3,1,3} + u_{3,1,4} - u_{3,1,5} - u_{3,1,6}, u_{3,1,1} = u_{1,1,1}, u_{3,1,2} = u_{1,1,2}, u_{3,1,3} = a_{13}E_3, a_{13} = \frac{Gm}{K}, \\
u_{3,1,4} &= a_{13}(A_1\Delta E_3 + A_2\Delta h_6), u_{3,1,5} = u_{1,1,5}, u_{3,1,6} = Km_1, u_{3,2} = u_{1,2}, u_{3,3} = a_{13}h_7, h_7 = h(K, y, t), \\
u_{3,4} &= a_{13}(A_1\Delta\psi_1 + A_2\Delta\psi_2), u_{3,5} = u_{1,5}, u_{3,6} = Km_2, u_{4,1} = u_{4,1,1} + u_{4,1,2} + u_{4,1,3} + u_{4,1,4} - u_{4,1,5} - u_{4,1,6}, \\
u_{4,1,1} &= u_{1,1,1}, u_{4,1,2} = u_{2,1,2}, u_{4,1,3} = u_{1,1,3}, u_{4,1,4} = a_{14}(A_3\Delta E_3 + A_4\Delta h_4), a_{14} = -\frac{GmSrSc}{(Sc - 1)K}, u_{4,1,5} = a_{15}\Delta F_1, \\
a_{15} &= \frac{GmSrSca_1}{t_1(a_1 - 1)}, u_{4,1,6} = u_{1,1,6}, u_{4,2} = u_{1,2}, u_{4,3} = u_{1,3}, u_{4,4} = a_{14}(A_3\Delta\psi_1 + A_6\Delta\psi_4), u_{4,5} = u_{4,1,5}, u_{4,6} = u_{1,6}, \\
u_{5,1} &= u_{5,1,1} + u_{5,1,2} + u_{5,1,3} + u_{5,1,4} - u_{5,1,5} - u_{5,1,6}, u_{5,1,1} = u_{1,1,1}, u_{5,1,2} = u_{1,1,2}, u_{5,1,3} = u_{3,1,3}, u_{5,1,4} = u_{3,1,4}, \\
u_{5,1,5} &= u_{1,1,5}, u_{5,1,6} = u_{2,1,6}, u_{5,2} = u_{1,2}, u_{5,3} = u_{3,3}, u_{5,4} = u_{3,4}, u_{5,5} = u_{1,5}, u_{5,6} = u_{2,6}, \\
u_{6,1} &= u_{6,1,1} + u_{6,1,2} + u_{6,1,3} + u_{6,1,4} - u_{6,1,5} - u_{6,1,6}, u_{6,1,1} = u_{1,1,1}, u_{6,1,2} = u_{4,1,2}, u_{6,1,3} = u_{1,1,3}, u_{6,1,4} = u_{4,1,4}, \\
u_{6,1,5} &= u_{4,1,5}, u_{6,1,6} = u_{2,1,6}, u_{6,2} = u_{4,2}, u_{6,3} = u_{1,3}, u_{6,4} = u_{4,4}, u_{6,5} = u_{4,5}, u_{6,6} = u_{2,6}, \\
u_{7,1} &= u_{7,1,1} + u_{7,1,2} + u_{7,1,3} + u_{7,1,4} - u_{7,1,5} - u_{7,1,6}, u_{7,1,1} = u_{1,1,1}, u_{7,1,2} = u_{4,1,2}, u_{7,1,3} = u_{3,1,3}, u_{7,1,4} = u_{3,1,4}, \\
u_{7,1,5} &= u_{4,1,5}, u_{7,1,6} = u_{1,1,6}, u_{7,2} = u_{4,2}, u_{7,3} = u_{4,3}, u_{7,4} = u_{3,4}, u_{7,5} = u_{4,5}, u_{7,6} = u_{1,6},
\end{aligned}$$

$$u_{8,1} = u_{8,1,1} + u_{8,1,2} + u_{8,1,3} + u_{8,1,4} - u_{8,1,5} - u_{8,1,6}, u_{8,1,1} = u_{1,1,1}, u_{8,1,2} = u_{5,1,2}, u_{8,1,3} = u_{3,1,3}, u_{8,1,4} = u_{7,1,4},$$

$$u_{8,1,5} = u_{3,1,5}, u_{8,1,6} = u_{2,1,6}, u_{8,2} = u_{5,2}, u_{8,3} = u_{3,3}, u_{8,4} = u_{7,4}, u_{8,5} = u_{3,5}, u_{8,6} = u_{2,6}$$

$$v_1 = v(a_1, t), Sh_{1,1} = \Omega_1, \Omega_1 = \Omega(Sc, K, t), Sh_{1,2} = a_4 (A_1 \Delta \Omega_1 + A_2 \Delta Z_1), Z_1 = Z(Sc, K, y, t),$$

$$Sh_{1,3} = a_4 (A_1 \Delta \alpha_2 + A_2 \Delta Z_2), \alpha_2 = \alpha \left(\frac{\sqrt{a_1}}{2\sqrt{t}} \right), Z_2 = Z(a_1, 0, a_3, t), Sh_{2,1} = Sh_{1,1},$$

$$Sh_{2,2} = a_5 \Delta \Omega_1, Sh_{2,3} = a_5 \Delta \alpha_2$$

$$\tau_{1,1} = \tau_{1,1,1} + \tau_{1,1,2} + \tau_{1,1,3} + \tau_{1,1,4} - \tau_{1,1,5} - \tau_{1,1,6}, \tau_{1,1,1} = N_2, N_2 = e^{at} N_1, N_1 = N(a, t), \tau_{1,1,2} = a_6 \Delta \zeta_1,$$

$$\zeta_1 = \zeta(1, t), \tau_{1,1,3} = a_9 (A_3 \alpha_3 + A_4 N_4), \alpha_3 = \alpha \left(\frac{1}{2\sqrt{t}} \right), N_4 = e^{-a_7 t} N_3, N_3 = N(-a_7, t),$$

$$\tau_{1,1,4} = a_{10} (A_5 \Delta \alpha_3 + A_6 \Delta N_6 + A_7 \Delta N_4), N_6 = e^{as t} N_5, N_5 = N(a_3, t), \tau_{1,1,5} = a_{11} (A_8 \Delta \alpha_2 + A_1 \Delta W_1 + A_9 \Delta N_6),$$

$$W_1 = W(t), \tau_{1,1,6} = a_8 R_1, R_1 = R(1, t), \tau_{1,2} = a_6 \Delta \zeta_2, \zeta_2 = \zeta(\sqrt{a_1}, t), \tau_{1,3} = a_9 (A_3 \Omega_1 + A_4 Z_3),$$

$$Z_3 = Z(Sc, K, -a_7, t), \tau_{1,4} = a_{10} (A_5 \Delta \Omega_1 + A_6 \Delta Z_1 + A_7 \Delta Z_3), \tau_{1,5} = a_{11} (A_8 \Delta \alpha_2 + A_1 \Delta v_1 + A_9 \Delta Z_2),$$

$$\tau_{1,6} = a_8 R_2, R_2 = R(\sqrt{Pm}, t), \tau_{2,1} = \tau_{2,1,1} + \tau_{2,1,2} + \tau_{2,1,3} + \tau_{2,1,4} - \tau_{2,1,5} - \tau_{2,1,6}, \tau_{2,1,1} = \tau_{1,1,1}, \tau_{2,1,2} = \tau_{1,1,2},$$

$$\tau_{2,1,3} = \tau_{1,1,3}, \tau_{2,1,4} = \tau_{1,1,4}, \tau_{2,1,5} = \tau_{1,1,5}, \tau_{2,1,6} = a_{12} \alpha_3, \tau_{2,2} = \tau_{1,2}, \tau_{2,3} = \tau_{1,3}, \tau_{2,4} = \tau_{1,4}, \tau_{2,5} = \tau_{1,5}, \tau_{2,6} = \tau_{2,1,6},$$

$$\tau_{3,1} = \tau_{3,1,1} + \tau_{3,1,2} + \tau_{3,1,3} + \tau_{3,1,4} - \tau_{3,1,5} - \tau_{3,1,6}, \tau_{3,1,1} = \tau_{1,1,1}, \tau_{3,1,2} = \tau_{1,1,2}, \tau_{3,1,3} = a_{13} \alpha_3,$$

$$\tau_{3,1,4} = a_{13} (A_1 \Delta \alpha_3 + A_2 \Delta N_6), \tau_{3,1,5} = \tau_{1,1,5}, \tau_{3,1,6} = KR_1, \tau_{3,2} = \tau_{1,2}, \tau_{3,3} = a_{13} N_7, N_7 = N(K, t),$$

$$\tau_{3,4} = a_{13} (A_1 \Delta \Omega_1 + A_2 \Delta Z_1), \tau_{3,5} = \tau_{1,5}, \tau_{3,6} = KR_2, \tau_{4,1} = \tau_{4,1,1} + \tau_{4,1,2} + \tau_{4,1,3} + \tau_{4,1,4} - \tau_{4,1,5} - \tau_{4,1,6},$$

$$\tau_{4,1,1} = \tau_{1,1,1}, \tau_{4,1,2} = \tau_{2,1,2}, \tau_{4,1,3} = \tau_{1,1,3}, \tau_{4,1,4} = a_{14} (A_3 \Delta \alpha_3 + A_4 \Delta N_4), \tau_{4,1,5} = a_{15} \Delta W_1, \tau_{4,1,6} = \tau_{1,1,6},$$

$$\tau_{4,2} = \tau_{1,2}, \tau_{4,3} = \tau_{1,3}, \tau_{4,4} = a_{14} (A_3 \Delta \Omega_1 + A_6 \Delta Z_3), \tau_{4,5} = \tau_{4,1,5}, \tau_{4,6} = \tau_{1,6},$$

$$\tau_{5,1} = \tau_{5,1,1} + \tau_{5,1,2} + \tau_{5,1,3} + \tau_{5,1,4} - \tau_{5,1,5} - \tau_{5,1,6}, \tau_{5,1,1} = \tau_{1,1,1}, \tau_{5,1,2} = \tau_{1,1,2}, \tau_{5,1,3} = \tau_{3,1,3}, \tau_{5,1,4} = \tau_{3,1,4},$$

$$\tau_{5,1,5} = \tau_{1,1,5}, \tau_{5,1,6} = \tau_{2,1,6}, \tau_{5,2} = \tau_{1,2}, \tau_{5,3} = \tau_{3,3}, \tau_{5,4} = \tau_{3,4}, \tau_{5,5} = \tau_{1,5}, \tau_{5,6} = \tau_{2,6},$$

$$\tau_{6,1} = \tau_{6,1,1} + \tau_{6,1,2} + \tau_{6,1,3} + \tau_{6,1,4} - \tau_{6,1,5} - \tau_{6,1,6}, \tau_{6,1,1} = \tau_{1,1,1}, \tau_{6,1,2} = \tau_{4,1,2}, \tau_{6,1,3} = \tau_{1,1,3}, \tau_{6,1,4} = \tau_{4,1,4},$$

$$\tau_{6,1,5} = \tau_{4,1,5}, \tau_{6,1,6} = \tau_{2,1,6}, \tau_{6,2} = \tau_{4,2}, \tau_{6,3} = \tau_{1,3}, \tau_{6,4} = \tau_{4,4}, \tau_{6,5} = \tau_{4,5}, \tau_{6,6} = \tau_{2,6},$$

$$\tau_{7,1} = \tau_{7,1,1} + \tau_{7,1,2} + \tau_{7,1,3} + \tau_{7,1,4} - \tau_{7,1,5} - \tau_{7,1,6}, \tau_{7,1,1} = \tau_{1,1,1}, \tau_{7,1,2} = \tau_{4,1,2}, \tau_{7,1,3} = \tau_{3,1,3}, \tau_{7,1,4} = \tau_{3,1,4},$$

$$\tau_{7,1,5} = \tau_{4,1,5}, \tau_{7,1,6} = \tau_{7,1,6}, \tau_{7,2} = \tau_{4,2}, \tau_{7,3} = \tau_{7,3}, \tau_{7,4} = \tau_{7,4}, \tau_{7,5} = \tau_{4,5}, \tau_{7,6} = \tau_{1,6},$$

$$\tau_{8,1} = \tau_{8,1,1} + \tau_{8,1,2} + \tau_{8,1,3} + \tau_{8,1,4} - \tau_{8,1,5} - \tau_{8,1,6}, \tau_{8,1,1} = \tau_{1,1,1}, \tau_{8,1,2} = \tau_{8,1,2}, \tau_{8,1,3} = \tau_{3,1,3}, \tau_{8,1,4} = \tau_{7,1,4},$$

$$\tau_{8,1,5} = \tau_{8,1,5}, \tau_{8,1,6} = \tau_{2,1,6}, \tau_{8,2} = \tau_{5,2}, \tau_{8,3} = \tau_{3,3}, \tau_{8,4} = \tau_{7,4}, \tau_{8,5} = \tau_{3,5}, \tau_{8,6} = \tau_{2,6}$$

(The functions are defined in **Chapter I**)

FUTURE SCOPE

The equations governing the flow problems of the proposed thesis are solved using Laplace transform technique. The problems are idealized by imposing some realistic constraints (e.g., viscous dissipation, Joule heating, effect of suction, etc. are neglected for mathematical simplicity). The problems may be re- investigated by removing or reducing number of constraints. In this context, some numerical and computational techniques like Runge- Kutta method, shooting method, Crank- Nicolson method etc. may be suggested.

REFERENCES

- [1] Abdullah, M. R., Alghazawi, O.K. and Al- Ayyad, M. (2019): Non- uniform heat source and radiation effect on a transient MHD flow past a vertical moving plate with inclined magnetic field and periodic heat flux, *Eng. Technol. Appl. Sci. Res.*, **9**(4), 4361-4366.
- [2] Abdullah, M.R. (2018): Transient free convection MHD flow past an accelerated vertical plate with periodic temperature, *Chem. Eng. Trans.*, **66**, 331-336.
- [3] Aboeldahab, E.M. and Azzam, G.E.D.A. (2006): Unsteady three-dimensional combined heat and mass transfer for convective flow over a stretching surface with time dependent chemical reaction, *Acta Mech*, **184**, 121–136.
- [4] Acharya, A.K., Dash, G.C., and Mishra, S.R. (2014): Free convective fluctuating MHD flow through porous media past a vertical porous plate with variable temperature and heat source, *Phys. Res. Int.*, Article ID 587367.
- [5] Acharya, M., Dash, G.C. and Singh, L.P. (2000): Magnetic field effects on the free convection and mass transfer flow through porous medium with constant suction and constant heat flux, *Indian J. Pure Appl. Math.*, 31,1-18.
- [6] Afify, A.A. (2009): Similarity solution in MHD: Effects of thermal diffusion and diffusion thermo on free convective heat and mass transfer over a stretching surface considering suction or injection, *Commun. Nonlinear Sci. Numer. Simul*, **14**(5), 2202-2214.
- [7] Afsana, S., Parvin, A., Nag, P., and Molla, M.M. (2021): Investigation of MHD free convection of power- law fluids in a sinusoidally heated enclosure using MRT- LBM, *Heat Transfer*, **51**(1), 355-376.
- [8] Afzal, N. (1972): Heat transfer in magnetohydrodynamic flow with aligned field on a flat plate at high Prandtl number, *Int. J. Heat. Mass Transfer*, **15**, 863-865.
- [9] Agrawal, A.K., Kishor, B., and Raptis, A. (1989): Effects of MHD free convection and mass transfer on the flow past a vibrating infinite vertical circular cylinder, *Heat Mass Transf.*, **23**, 243-250.
- [10] Ahmadi, G. and Manvi, R. (1971): Equation of motion for viscous flow through a rigid porous medium, *Indian J. Tech.*, **9**,441.
- [11] Ahmed, N. (2010): MHD convection with Soret and Dufour effects in a three dimensional flow past an infinite vertical porous plate, *Can. J. Phys.*, **28**, 663-674.

- [12] Ahmed, N. (2012): Soret and radiation effects on transient MHD free convection from an impulsively started infinite vertical plate, *J Heat Transfer*, **134**, 1-9.
- [13] Ahmed, N. (2023): MHD flow with diffusion- thermo and induced magnetic field. In: Tghermal and Solutal Convection in Some Hydromagnetic Flows, *Springer, Singapore*, 45-68.
- [14] Ahmed, N. and Dutta, M. (2014): Analytical analysis of magnetohydrodynamic transient flow past a suddenly started infinite vertical plate with thermal radiation and ramped wall temperature, *J. Heat Transfer (ASME)*, **136**(4), 041703–041711.
- [15] Ahmed, N. and Sarmah, H.K. (2009): Thermal radiation effect on a transient MHD flow with mass transfer past an impulsively fixed infinite vertical plate, *Int. J. of Appl. Math. Mech.*, **5**(5), 87–98.
- [16] Ahmed, N., and Sarma, S. (2021): Thermal diffusion effect on unsteady MHD free convective flow past an impulsively started but temporarily accelerated semi- infinite vertical plate with parabolic ramped conditions, *Heat Transfer*, **50**(4), 8656-8688.
- [17] Ahmed, N., and Sengupta, S. (2011): Thermo diffusion and diffusion thermo effects on a three dimensional MHD mixed convection flow past an infinite vertical porous plate with thermal radiation, *Magnetohydrodynamics*, **47**(1), 41-60.
- [18] Ahmed, N., Kalita, H. and Barua, D.P. (2010): Unsteady MHD free convective flow past a vertical porous plate immersed in a porous medium with Hall current, thermal diffusion and heat source, *Int. J. Eng. Sci. Tech.*, **2**(6), 59-74.
- [19] Ahmed, N., Sinha, S. and Talukdar, S. (2013): Dufour effect on a transient MHD flow past a uniformly porous plate with heat sink, *Adv. Appl. Fluid Mech.* , **13**(1), 1-24.
- [20] Alam, M.S. and Rahman M.M. (2005): Dufour and Soret effects on MHD free convective heat and mass transfer flow past a vertical porous flat plate embedded in a porous medium, *J. Nav. Archit. Mar. Eng.*, **1**, 55-65.
- [21] Alam, M.S., Rahman, M.M. and Sattar, M.A. (2006): MHD free convective heat and mass transfer flow past an inclined surface with heat generation, *Thammasat Int. J. Sc. Tech.*, **11**(4), 1-8.
- [22] Alfven, H. (1942): Discovery of Alfven Waves, *Nature*, **150**, 405-406.
- [23] Ali, A., Kanwal, T., Awais, M., Shah, Z., Kumam, P. and Thounthong, P. (2021): Impact of thermal radiation and non- uniform heat flux on MHD hybrid nanofluid along a stretching cylinder, *Sci. Rep.*, **11**, 20262.

- [24] Ali, M.M., Mamun, A.A., Maleque, M.A., and Azim, N.H.M.A. (2013): Radiation effects on MHD free convection flow along vertical flat plate in presence of Joule heating and heat generation, *Procedia Eng.*, **56**, 503-509.
- [25] Andersson, H.I., Hansen, O.R. and Holmedal, B. (1994): Diffusion of a chemically reactive species from a stretching sheet, *Int. J. Heat Mass Transf.*, **37**(4), 659-664.
- [26] Anil Kumar, M., Reddy, Y.D., Goud, B.S., and Rao, V.S. (2021): Effects of Soret, Dufour Hall current and rotation on MHD natural convective heat and mass transfer flow past an accelerated vertical plate through a porous medium, *Int. J. Thermofluids*, **9**, 1000061.
- [27] Anwar, T., Kumam, P., Watthayu, W., and Asifa (2020): Influence of ramped wall temperature and ramped wall velocity on unsteady magnetohydrodynamic convective Maxwell fluid flow, *Symmetry*, **12**(3), 392.
- [28] Apelblat, A. (1982): Mass transfer with chemical reaction of first order, effect of axial diffusion, *J. Chem. Eng.*, **23**(2), 193-203.
- [29] Arifuzzaman, S.M., Khan, M.S., Mehedi, M.F.U., Rana, B.M.J., and Ahmmed, S.F. (2018): Chemically reactive and naturally convective high speed MHD fluid flow through an oscillatory vertical porous plate with heat and radiation absorption effect, *Eng. Sci. Technol. an Int. J.*, **21**(2), 215-228.
- [30] Asimoni, N.R.M., Mohammad, N.F., Kasim, A.R.M., and Shafie, S. (2017): MHD free convective flow past a vertical plate, *J. Phys. Conf. Ser.*, **890**
- [31] Asogwa, K., Bilal, S., Animasaun, I., and Mebarek- Oudina, F. (2021): Insight into the significance of ramped wall temperature and ramped surface concentration: The case of Casson fluid flow on an inclined Riga plate with heat absorption and chemical reaction, *Nonlinear Eng.*, **10**(1), 213-230.
- [32] Babu, M.S., Kumar, J.G., and Reddy, T.S. (2013): Mass transfer effects on unsteady MHD convection flow of micropolar fluid past a vertical moving porous plate through porous medium with viscous dissipation, *International Journal of Applied Mathematics and Mechanics*, **9**(6), 48-67.
- [33] Baehr, H.D. and Stephan, K. (1998): Heat and mass transfer, *Springer, New York*.
- [34] Balla, C.K. and Naikoti, K. (2015): Radiation effects on unsteady MHD convective heat and mass transfer past a vertical plate with chemical reaction and viscous dissipation, *Alex. Eng. J.*, **15**(3), 661-671.

- [35] Basha, P.M.S. and Nagarathna, N. (2019): Heat and mass transport on MHD free convective flow through a porous medium past an infinite vertical plate, *Int. J. Appl. Eng. Res.*, **14**(21), 4067-4076.
- [36] Bear, J. (1972): Dynamics of Fluids in Porous Media, *Dover Publications, New York*.
- [37] Bejan, A. (1978). Natural convection in an infinite porous medium with a concentrated heat source, *J. Fluid Mech.*, **89**, 97–107.
- [38] Bird, R.B., Stewart, W.E. and Lightfoot, E.N. (1960): Transport Phenomena, *John Wiley & Sons, New York*.
- [39] Bird, R.B., Stewart, W.E. and Lightfoot, E.N.(1966): Transport Phenomena, *Wiley, New York*.
- [40] Boelter, L.M.K., Cherry, V.H., Johnson, H.A. and Martinelli, R.C. (1965): Heat Transfer Notes, *McGraw-Hill Book Co., New York*.
- [41] Brinkman, H.C. (1947b): On the permeability of media consisting of closely packed porous particles, *Appl. Sc. Res.*, **A1**, 81-86
- [42] Brinkman, H.C. (1947a): A Calculation of the Viscous Force exerted by a flowing fluid on a Dense Swarm of Particles, *Appl. Sc. Res.*, **A1**,27-34
- [43] Bulinda, V.M., Kang'ethe, G.P., and Kiogora, P.R. (2020) Magnetohydrodynamics free convection flow of incompressible fluids over corrugated vibrating bottom surface with Hall currents and heat and mass transfers, *J. Appl. Math.*, 2020, Article ID 2589760.
- [44] Camargo, R., Luna, E. and Trevine, C. (1996): Numerical study of natural convective cooling of a vertical plate, *Heat Mass Transf*, **32**, 89-95.
- [45] Chamkha, A.J. (2004): Unsteady MHD convective heat and mass transfer past a semi-infinite vertical permeable moving plate with heat absorption, *Int. J. Eng. Sci.*, **42**, 217–230.
- [46] Chandrakala, P. (2010): Thermal radiation effects on moving infinite vertical plate with uniform heat flux, *Int. J. Fluid Dyn.*, **6**(1), 49-55. (2010).
- [47] Chaudhary, R.C. and Jain, P. (2007): Combined heat and mass transfer effects on MHD free convection flow past an oscillating plate embedded in porous medium, *Romanian J. Phys.*, **52** (5-6), 471-490.
- [48] Chaudhury, R.C. and Sharma, B.K. (2006): Combined heat and mass transfer by laminar mixed convection flow from a vertical surface with induced magnetic field, *J. Appl. Phys.*, **99**, 034901-034910.

- [49] Cheng, C.Y. (2009): Soret and Dufour effects on natural convection heat and mass transfer from a vertical cone in a porous medium, *Int. Comm. Heat Mass Transf.*, **36**, 1020–1024.
- [50] Cheng, C.Y. (2011): Soret and Dufour effects on natural convection heat and mass transfer near a vertical wavy cone in a porous medium with constant wall temperature and concentration, *Int. Comm. Heat Mass Transfer*, **38**, 1056–1060.
- [51] Cheng, C.Y. (2012a): Soret and Dufour effects on double-diffusive free convection over a vertical truncated cone in porous media with variable wall heat flux and mass fluxes, *Transp. Porous Media*, **91**, 877–888.
- [52] Cheng, C.Y. (2012b): Soret and Dufour effects on free convection heat and mass transfer from an arbitrarily inclined plate in a porous medium with constant wall temperature and concentration, *Int. Comm. Heat Mass Transfer*, **39**, 72–77.
- [53] Cheng, C.Y. (2012c): Soret and Dufour effects on mixed convection heat and mass transfer from a vertical wedge in a porous medium with constant wall temperature and concentration, *Transp. Porous Media*, **94**, 123–132.
- [54] Choudhary, S., Singh, S. and Choudhary, S. (2015): Thermal radiation effects on MHD boundary layer flow over an exponentially stretching surface, *Appl. Math.*, **6**, 295-303.
- [55] Cowling, T.G. (1957): *Magnetohydrodynamics*, Wiley Interscience, New York.
- [56] Cramer, K.R. and Pai, S.I. (1973): *Magneto Fluid Dynamics for Engineers and Applied Physicist*, Mc Graw Hill Book Co., New York
- [57] Crank, J. (1957): *The Mathematics of Diffusion*, Oxford University Press, London.
- [58] Darcy, H.P.G. (1856): *Les Fontaines Publiques De La Ville De Dijon*, Victor Dalmont, Paris.
- [59] Das, K. (2011): Effect of chemical reaction and thermal radiation on heat and mass transfer flow of MHD micropolar fluid in a rotating frame of reference, *Int. J. Heat Mass Transfer*, **54**(15/16), 3505–3513.
- [60] Das, K. and Jana, S. (2010): Heat and mass transfer effects on unsteady MHD free convection flow near a moving vertical plate in porous medium, *Bull. Soc. Math. Banja Luka*, **17**, 15-32.
- [61] Das, M., Mahanta, G., and Shaw, S. (2020): Heat and mass transfer effect on an unsteady MHD radiative chemically reactive Casson fluid over a stretching sheet in porous medium, *Heat Transfer*, **49**(8), 4350-4369.

- [62] Das, S., Sarkar, B., and Jana, R. (2012): Radiation effects on free convection MHD Couette flow started exponentially with variable wall temperature in presence of heat generation, *Open J. Fluid Dyn.*, **2**(1), 14-27.
- [63] Das, S., Tarafdar, B., Jana, R.N., and Makinde, O.D. (2019): Influence of rotational buoyancy on magneto- radiation convection near a rotating vertical plate, *Eur. J. Mech. B/Fluids.*, **75**, 209-218.
- [64] Das, S.S., Tripathy, R.K., Sahoo, S.K. and Dash, B.K. (2008): Mass transfer effects on free convective MHD flow of a viscous fluid bounded by an oscillating porous plate in the slip flow regime with heat source, *Ultra Science*, **20** (1) M, 169-176.
- [65] Das, U.N. (1970): A small unsteady perturbation on the steady hydromagnetic boundary layer flow past a semi-infinite plate, *Proc. Camb. Phil. Soc.*, **68**, 509-528.
- [66] Das, U.N. and Ahmed, N. (1992): Free convective MHD flow and heat transfer in a viscous incompressible fluid confined between a long vertical wavy wall and a parallel flat wall, *Indian J. Pure Appl. Math.*, **23**(4), 295-304.
- [67] Davidson, P.A. (2001): An Introduction to Magnetohydrodynamics, *Cambridge University Press*.
- [68] Davies, T.V. (1963): The magnetohydrodynamic boundary layer in the two dimensional steady flow past a semi-infinite flat plate, *Proc. Roy. Soc. London*, **273** A, 496-508.
- [69] de Groot, S.R. (1951): Thermodynamics of Irreversible Processes, *North Holland Publishing Comp.*
- [70] Denno, K.I. and Fouad, A.A. (1972): Effects of induced magnetic field on the magnetohydrodynamic channel flow, *IEEE Trans Electron Devices*, **19**(3), 322-331.
- [71] Devi S.P.A. and Kandaswamy R. (2000): Effect of chemical reaction, heat transfer and mass transfer on MHD flow past a semi-infinite plate, *Z. Angew. Math. Mech.* **80**, 697-701.
- [72] Devi, C.D.S. and Nagaraj, M. (1984): Heat and mass transfer in unsteady magnetohydrodynamic flow over a semi-infinite flat plate, *Indian J. Pure Appl. Math.*, **15**(10), 1148-1161.
- [73] Devi, C.D.S., Takhar, H.S. and Nath, G. (1988): Unsteady laminar boundary layer forced flow over a moving wall with a magnetic field, *Indian J. Pure Appl. Math.*, **19**(8), 786-802.

- [74] Dormy, E. and Nunez, M. (2007): Special Issue: Magnetohydrodynamics in astrophysics and geophysics- Introduction, *Geophys. Astrophys. Fluid Dyn.*, **101**, 169-169.
- [75] Dwivedi, K., Khare, R.K. and Paul A. (2018): MHD flow through vertical channel with porous medium, *Int. J. Appl. Eng. Res.*, **13**(15), 11923- 11926.
- [76] Eckert, E.R.G. and Drake, R.M. (1972). Analysis of Heat and Mass Transfer, *McGraw -Hill, New York*.
- [77] Eid, M.R., and Makinde, O.D. (2018): Solar radiation effect on a magneto nanofluid flow in a porous medium with chemically reactive species, *Int. J. Chem. React. Eng.*, **16**(19), 20170212.
- [78] Elbasheshy, E.M.A (1997): Heat and mass transfer along a vertical plate with variable surface temperature and concentration in the presence of magnetic field, *Int. J. Eng. Sc.*, **34**, 515-522.
- [79] El-Kabeir, S.M.M. (2011): Soret and Dufour effects on heat and mass transfer due to a stretching cylinder saturated porous medium with chemically-reactive species, *Latin Amer. Appl. Res.*, **41**, 331–337.
- [80] El-Kabeir, S.M.M., Modather, M., and Rashad, A.M. (2015): Heat and mass transfer by unsteady natural convection over a moving vertical plate embedded in a saturated porous medium with chemical reaction, Soret and Dufour effects, *J. Appl. Fluid Mech.*, **8**(3), 453–463.
- [81] Eswaramoorthi, S., Bhuvaneswari, M., Sivasankaran, S. and Rajan, S. (2015): Effect of radiation on MHD convective flow and heat transfer of a viscoelastic fluid over a stretching surface, *Procedia Eng.*, **127**, 916-923.
- [82] Faraday, M. (1832): Experimental researches in electricity, *Phil. Trans. Roy. Soc. Lond.*, **122**, 125–162.
- [83] Faraday, M. (1832): Experimental researches in electricity, *Phil. Trans. Roy. Soc. Lond.*, **122**, 125–162.
- [84] Farrokhi, H., Otuya, D.O., Khimchenko, A. and Dong, J. (2019): Magnetohydrodynamics in biomedical applications, *Nanofluid Flow in Porous Media, Intech Open*, (2019).
- [85] Ferdows, M. and Chen, C.H. (2009): Heat and mass transfer on MHD free convection from a vertical plate in a porous medium with Dufour and Soret effects. *Int. J. Heat Tech.*, **27**, 33–38.

- [86] Ferdows, M., Tzirtzilakis, E., Kaino, K., and Chen, C.H. (2008). Soret and Dufour effects on natural convection heat and mass transfer flow in a porous medium, *Int. J. Appl. Math. Stat.*, **13**(8), 36–48.
- [87] Ferraro, V.C.A. and Plumpton, C. (1966): An Introduction to Magneto-Fluid Mechanics, *Clarendon Press, Oxford*.
- [88] Fick, A. (1855): Ueber Diffusion, *Ann. Physik*, **170**, 59-86.
- [89] Fourier, J.B. (1822): Theorie Analytique de la Chaleur, *Dover reprint, 1955, New York*.
- [90] Ganesan, P. and Rani, H.P. (2000): On diffusion of chemically reactive species in convective flow along a vertical cylinder, *Chem Eng Process*, **39**(2), 93-105.
- [91] Gebhart, B. (1971): Heat transfer, *McGraw Hill Book Company, New York*
- [92] Ghaly, A.Y. (2002): Radiation effects on a certain MHD free- convection flow, *Chaos, Solitons and Fractals*, **13**(9), 1843-1850.
- [93] Ghosh, S.K., Beg, O.A. and Zueco, J. (2010): Hydromagnetic free convection flow with induced magnetic field effects, *Meccanica*, **45**, 175- 185.
- [94] Glasstone, S., Laidler, K.J. and Eyring, H. (1941): The Theory of Rate Processes, *McGraw Hill Book Company, New York*.
- [95] Glauret, M.B. (1956): The laminar boundary layer on oscillating plates and cylinders, *J. Fluid Mech.*, **1**, 97-110
- [96] Goud, B.S., Kumar, P.P. and Malga, B.S. (2021): Induced magnetic field effect on MHD free convection flow in nonconducting and conducting vertical microchannel walls, *Heat Transfer*, **51**(2), 2201- 2218.
- [97] Goud, B.S., Kumar, P.P., and Malga, B.S. (2020): Effect of heat source on an unsteady MHD free convection flow of Casson fluid past a vertical oscillating plate in porous medium using finite element analysis, *Partial Differential Equations in Applied Mathematics* , **2**, 1-7.
- [98] Greenspan, H.P. and Carrier, G.F. (1959): The magnetohydrodynamic flow past a flat plate, *J. Fluid Mech.*, **6**, 77-96.
- [99] Grober, H., Erk, S. and Grigull, U. (1961): Fundamentals of Heat Transfer, *McGraw Hill, New York*.
- [100] Gulab, R. and Mishra, R. (1977): Unsteady flow through magnetohydrodynamic porous media, *Indian J. Pure Appl. Math.*, **8**, 637-642.

- [101] Gulle, N., and Kodi, R. (2022): Soret radiation and chemical reaction effect on MHD Jeffrey fluid flow past an inclined vertical plate embedded in porous medium, *Mater.Today: Proceedings*, **50**(5), 2218-2226.
- [102] Gundagani, M., Sheri, S., Paul, A. and Reddy, M.C.K. (2013): Radiation effects on an unsteady MHD convective flow past a semi-infinite vertical permeable moving plate embedded in a porous medium with viscous dissipation, *Walailak J Sci Technol*, **10**(5), 499–515.
- [103] Gurram, D., Rani, C.H.B., Vedavathi, N., Balamurugan, K.S. (2018): Heat and mass transfer on MHD fluid flow over a semi infinite flat plate with radiation absorption, heat source and diffusion thermo effect, *Front. Heat Mass Transf.*, **11**(6).
- [104] Harris, S.D. and Ingham, D.B. (1997): Free convection from a vertical plate in a porous medium subject to sudden change in surface heat flux., *Trans. Porous Media*, **26**, 207-226.
- [105] Hayat, T., Nazar, H., Imtiaz, M., and Alsaedi, A. (2017): On chemical reaction and porous medium effect in the MHD flow due to a rotating disk with variable thickness, *Eur. Phys. J. Plus*, **132**, 256.
- [106] Hazarika, N.J. and Ahmed, S. (2021): Thermo- diffusive flow of chemically reacting fluid in a saturated porous medium for radiative heat flux, *J. Sci. Res.*, **13**(2), 507-520.
- [107] Helmy, K.A. (1998): MHD unsteady free convection flow past a vertical porous plate, *J. Appl. Math. Mech.*, **78**(4), 255-270.
- [108] Hertz, H. (1884): On relation between Maxwell's fundamental equations of the opposing electromagnetics ,*Wiedemann's Annalen*, **23**, 84–103.
- [109] Hertz, H. (1888): On the finite velocity of propagation of electromagnetic action, (Sitzungsber. d. berl. akad. d. wiss.), *Wiedemann's Annalen*, **34**, 107-123.
- [110] Hertz, H. (1962): *Electric Waves*, *Dover Publication Inc., New York*.
- [111] Hirefelder, J.O., Curtiss, C.F. and Bird, R.B. (1954): *Molecular Theory of Gases and Liquids*, *Wiley, New York*.
- [112] Hosain, M.A. and Ahmed, M. (1990): MHD forced and free convection boundary layer flow near the leading edge, *Int. J. Heat Mass Transf.*, **33**(3), 571-575.
- [113] Hossain, M.M.T. and Khatun, M. (2012): Study of diffusion thermo effect on laminar mixed convection flow and heat transfer from a vertical surface with induced magnetic field, *International Journal of Applied Mathematics and Mechanics*, **8**(5), 40-60.

- [114] Hughes, W.F. and Young ,F. J. (1966): The Electrodynamics of Fluids, *John Wiley and Sons Inc., New York.*
- [115] Ibrahim F.S., Elaiw A.M., Bakr A.A. (2008): Effect of the chemical reaction and radiation absorption on the unsteady MHD free convective flow past a semi infinite vertical permeable moving plate with heat source and suction, *Commun Nonlinear Sci Numer Simul*, **13**(6), 1056-1066.
- [116] Ibrahim, S.M., Reddy, T.S., and Reddy, N.B. (2013): Thermal radiation effect on MHD free convection flow of a micropolar fluid past a stretching surface embedded in a Darcian porous medium., *Innovative Systems Design and Engineering*, **4**(13).
- [117] Incropera, F.P. and Dewitt, D.P. (1981): Fundamentals of Heat Transfer, *Wiley, New York.*
- [118] Ingham, D.B. (1978): Transient free convection on an isothermal vertical flat plate, *Int.J. of Heat and Mass Transfer*, **21**, 67–79.
- [119] Jain, N.C. and Gupta, P. (2005): Unsteady hydromagnetic thermal boundary layer flow past an infinite porous surface in the slip flow regime, *Gantia*, **56**(1), 15-25.
- [120] Jakob, M. (1949): Heat Transfer, *John Wiley and Sons, New York.*
- [121] Jaluria, Y. (1980): Natural Convection Heat and Mass Transfer, *Pergamon Press, New York.*
- [122] Jayakar, R., Kumar, B.R., and Makinde, O.D. (2018): Thermo diffusion effects on MHD chemically reacting fluid flow past an inclined porous plate in a slip flow regime, *Defect Diffus. Forum*, **387**, 587- 599.
- [123] Jha, B.K. and Aina, B. (2018): Impact of induced magnetic field on magnetohydrodynamic (MHD) natural convection flow in a vertical annular micro-channel in the presence of radial magnetic field, *Propuls. Power Res.*, **7**(2), 171- 181.
- [124] Jha, B.K. and Ajibade, A.O. (2011): Diffusion- thermo effects on free convective heat and mass transfer flow in a vertical channel with symmetric boundary conditions, *J Heat Transfer*, **133**(5), 1-8.
- [125] Jha, B.K., and Aina, B. (2016): Role of induced magnetic field on MHD natural convection flow in vertical microchannel formed by two electrically non- conducting infinite vertical parallel plates, *Alex. Eng. J.*, **55**(3), 2087-2097.
- [126] Jonnadula, M., Polarapu, P., Reddy, G., and Malapati, V. (2015): Influence of thermal radiation and chemical reaction on MHD flow, heat and mass transfer over a stretching surface, *Procedia Eng.*, **127**, 1315-1322.

- [127] Joshna, N., Rao, Y.V.S. and Saroja, S. (2022): An analytical study of chemical reaction effect on MHD flow in a vertical surface filled with porous medium, *Journal of Positive School Psychology*, 6(5), 1865- 1873.
- [128] Kafoussias, N.G. (1992): MHD thermal- diffusion effects on free- convective and mass- transfer flow over an infinite vertical moving plate, *Astrophys. Space Sci.*, **192**, 11-19.
- [129] Kafoussias, N.G. and Williams, E.M. (1995): Thermal diffusion and diffusionthermo effects on mixed free forced convection and mass transfer boundary flow with temperature dependent viscosity, *Int. J. Engg. Sci.*, **33**, 1369-1384.
- [130] Kandasamy, R., Periasamy, K. and Prabhu, K.K.S. (2005): Effects of chemical reaction, heat and mass transfer along a wedge with heat source and concentration in the presence of suction or injection, *Int. J. Heat Mass Transf.*, **48**(7), 1388-1394.
- [131] Kataria, H., and Patel, R.H. (2019): Effects of chemical reaction and heat generation/ absorption on magnetohydrodynamic (MHD) Casson fluid flow over an exponentially accelerated vertical plate embedded in porous medium with ramped wall temperature and ramped surface concentration, *Propuls. Power Res.*, **8**(1), 35-46.
- [132] Kaviany, M. (1995): Principles of Convective Heat Transfer, *Springer, New York*.
- [133] Kays, W.M. (1975): Convective Heat and Mass Transfer, *Tata McGraw-Hill, New Delhi*.
- [134] Khan U., Ahmed N. and , Mohyud-Din, S.T.(2016): Thermo-diffusion, diffusion-thermo and chemical reaction effects on MHD flow of viscous fluid in divergent and convergent channels, *Chem. Eng. Sci.*, **141**, 17-27.
- [135] Knudsen, J.D. and Katz, D.L. (1958): Fluid Dynamics and Heat Transfer, *McGraw Hill Book Co. New York*.
- [136] Kolar, A.K. and Sastri, V.M.K. (1988): Free convective transpiration over a vertical plate: a numerical study, *Heat Mass Transf.*, **23**(6), 327-336.
- [137] Kumar, A. and Singh, A.K. (2013): Unsteady MHD free convective flow past a semi- infinite vertical wall with induced magnetic field, *Appl. Math. Comput.*, **222**, 462-471.
- [138] Kumar, T.S. and Kumar B.R. (2017): A comparative study of thermal radiation effects on MHD flow of nanofluids and heat transfer over a stretching sheet, *Front. Heat Mass Transf.*, **9**(1), 1-7.

- [139] Kumaresan, E., Vijaya Kumar, A.G. and Prakash, J. (2018): Analytical investigations of diffusion thermo effects on unsteady free convection flow past an accelerated vertical plate, *Front. Heat Mass Transf.*, **10**.
- [140] Langlois, W.E. (1964): *Slow Viscous Flow*, Macmillan, New York.
- [141] Lavanya, B. (2020): Radiation and chemical reaction effects on MHD convective flow over a porous plate through a porous medium with heat generation, *Journal of Advanced Research in Fluid Mechanics and Thermal Sciences*, **68**(1), 11-21.
- [142] Lavanya, S., and Kesavaiah, D.C. (2014): Radiation and Soret effects to MHD flow in vertical surface with chemical reaction and heat generation through a porous medium, *Int. J. Comput. Eng. Res.*, **4**(7), 62- 73.
- [143] Lehnert, B.O. (1952): On the behavior of an electrically conductive liquid in magnetic field, *Ark. Fys.*, **15**, 69-90.
- [144] Li, Y., Zhang, B., Xiao, L., Wang, Y. and He, G. (2017): Applications and prospects of magnetohydrodynamics in aeronautical engineering, *Adv. Mech.*, **47**, 452- 502.
- [145] Lighthill, M. J. (1963): Introduction. Boundary Layer Theory, *Oxford University Press*, Oxford.
- [146] Lighthill, M.J. (1950): Contributions to the theory of heat transfer through a laminar boundary layer, *Proc. Roy. Soc. London A*, **202**, 359–377.
- [147] Lighthill, M.J. (1954): The response of laminar skin friction and heat transfer to fluctuations in the stream velocity, *Proc. Roy. Soc. London A*, **224**, 1–306.
- [148] Lorentz, H.A. (1952): *Theory of Electrons*, Dover, New York.
- [149] Luikov, A.V. and Mikhailov, Yu. A. (1965): *Theory of Energy and Mass Transfer*, Pergamon Press, London.
- [150] Mahapatra, N., Dash, G.C., Panda, S. and Acharya, M. (2010): Effects of chemical reaction on free convection flow through a porous medium bounded by a vertical surface, *J. Eng. Phys. Thermophys.*, **83**, 130-140.
- [151] Mahdy, A. and Ahmed, S.E. (2015): Thermo solutal marangoni boundary layer magnetohydrodynamic flow with the Soret and Dufour effects past a vertical flat plate, *Eng. Sci. Technol., Int. J.*, **18**(1), 24–31.
- [152] Makinde, O.D. (2005): Free convection flow with thermal radiation and mass transfer past a moving vertical porous plate, *Int. Commun. Heat Mass Transf.*, **32**(10), 1411-1419.

- [153] Makinde, O.D. (2011): On MHD mixed convection with Soret and Dufour effects past a vertical plate embedded in a porous medium, *Lat. Am. Appl. Res.*, **41**, 63–68.
- [154] Malathy, T., Srinivas,S., and Reddy, A.S. (2017): Chemical reaction and radiation effects on MHD Pulsatile flow of an Oldroyd-B fluid in a porous medium with slip and convective boundary conditions, *J. Porous Media*, **20**(4), 287-301.
- [155] Manh, T.D., Nam, N.D., Abdulrahman, G.K., Moradi, R. and Babazadeh, H. (2020): Impact of MHD on hybrid nanomaterial free convective flow within permeable region, *J. Therm. Anal. Calorim.*, **140**, 2865-2873.
- [156] Manivannan, K., Muthucumeraswamy, R. and Thangaraj, V. (2009): Radiation and chemical reaction effects on isothermal vertical oscillating plate with variable mass diffusion, *Thermal Science*, **13**(2), 155–162.
- [157] Martynenko, O.G., Berezovski, A. and Sokovishin, Y.A. (1984): Laminar free convection from a vertical plate, *Int. J. Heat Mass Transf.*, **27**(6), 869-881.
- [158] Maxwell, J.C. (1864): Treatise on Electricity and Magnetism, *Dover, New York*.
- [159] Mbeledogu, I.U., Amakiri, A.R.C. and Ogulu, A. (2007): Unsteady MHD free convection flow of a compressible fluid past a moving vertical plate in the presence of radiative heat transfer, *Int. J. Heat Mass Transf.*, **50**(9-10), 326-331.
- [160] McAdams, W.H. (1954): Heat Transmission, *McGraw Hill Book Company, New York*.
- [161] Meghad, A.A. (1984): Unsteady MHD flow through porous medium bounded by a porous plate, *Indian J. Pure Appl. Math.*, **15**(10), 1140-1147.
- [162] Meksyn, D. (1962): Magnetohydrodynamic flow past a semi infinite plate, *J. Aerospace Sci.*, **29**, 662-665.
- [163] Mills, A.F. (1999): Basic Heat and Mass Transfer, *Prentice-Hall, New Jersey*, 2nd Ed.
- [164] Mohamed, R.A., and Abo- Daheb, S.M. (2009): Influence of chemical reaction and thermal radiation on the heat and mass transfer in MHD micropolar flow over a vertical moving porous plate in a porous medium with heat generation, *Int. J. Therm. Sci.*, **48**(9), 1800-1813.
- [165] Mohanty, A., Rath, P.K., and Dash, G.C. (2014): Thermal diffusion and radiation effects on three dimensional MHD free convective flow with heat and mass transfer through a porous medium with periodic permeability and chemical reaction, *AMSE Journals*, **83**(1), 85-109.

- [166] Murthy, P.V.S.N. and Narayana, P.A.L. (2010). Soret and Dufour effects on free convective heat and mass transfer along a horizontal plate in non-Darcy porous medium, *Int. J. Fluid Mech. Res.*, **37**, 70–84.
- [167] Muthucumaraswamy, R. and Ganesar, P. (2001): Effect of chemical reaction and injection on flow characteristics in an unsteady upward motion of an isothermal plate, *J. Appl. Mech. Tech.*, 42(4), 665-671.
- [168] Muthucumaraswamy, R. and Kumar, G.S. (2004): Heat and mass transfer effects on moving vertical plate in presence of thermal radiation, *Theoret. App. Mech.*, **31**(1), 35–46.
- [169] Nandi, S. and Kumbhakar, B. (2020): Unsteady MHD free convective flow past a permeable vertical plate with periodic movement and slippage in the presence of Hall current and rotation, *Therm. Sci. Eng. Prog.*, **19**(1), 100561.
- [170] Nandkeolyar, R., and Das, M. (2014): Unsteady MHD free convection flow of a heat absorbing dusty fluid past a flat plate with ramped wall temperature, *Afr. Mat.*, **25**, 779-798.
- [171] Nandkeolyar, R., Das, M., and Sibanda, P. (2013): Exact solutions of unsteady MHD free convection in a heat absorbing fluid flow past a flat plate with ramped wall temperature, *Bound. Value Probl.*, 2013, 247.
- [172] Narahari, M., Tippa, S., Pendyala, R., and Fetecau, C. (2021): Soret, heat generation, radiation and porous effects on MHD free convection flow past an infinite plate with oscillating temperature, *J. Therm. Anal. Calorim.*, **143**, 2525-2543.
- [173] Narayana, P.V.S., Tarakaramu, N., and Babu, D.H. (2022): Influence of chemical reaction on MHD couple stress nanoliquid flow over a bidirectional stretched sheet, *Int. J. Ambient Energy*, **43**(1), 4928-4938.
- [174] Nayak, M. K., Dash, G.C. and Singh, L.P. (2014): Effect of chemical reaction on MHD flow of a visco- elastic fluid through porous medium, *J. Appl. Anal. Comput.*, **4**(4), 367- 381.
- [175] Nield, D.A. and Bejan, A. (2017): Convection in Porous Media, 5th Ed, *Springer, New York*.
- [176] Niranjana, H., Sivasankaran, S. and Bhuvaneshwari, M. (2017): Chemical reaction, Soret and Dufour effects on MHD mixed convection stagnation point flow with radiation and slip condition, *Sci. Iran.*, **24**(2), 698- 706.

- [177] Nusselt, W. (1915): Das grundgesetz des warmeurberganges, *Gesund. Ing.*, **38**, 872.
- [178] Nusselt, W. (1931): Der Wärmeaustausch Zwischen Wand an Wasser in Ruhr, *Forch Geb Ingenieurwes*, **2**, 309.
- [179] Olajuwon, B.I. and Oahimire, J.I. (2014): Effect of thermal diffusion and chemical reaction on heat and mass transfer in a MHD micropolar fluid with heat generation. *Afr. Mat.*, **25**, 911–931.
- [180] Olanrewaju , P.O. and Makinde, O.D. (2011): Effects of thermal diffusion and diffusion thermo on chemically reacting MHD boundary layer flow of heat and mass transfer past a moving vertical plate with suction/injection, *Arab. J. Sci. Eng.*, **36**, 1607–1619
- [181] Orhan, A. and Ahmet,K. (2008): Radiation effect on MHD mixed convection flow about a permeable vertical plate, *Heat Mass Transf.*, **45**,239-246.
- [182] Oyekunle, T.L. and Agunbiade, S.A. (2020): Diffusion- thermo and thermal-diffusion effects with inclined magnetic field on unsteady MHD slip flow over a permeable vertical plate, *J. Egypt. Math. Soc.*, **28**, 51 (2020).
- [183] Ozisik, M.N. (1977): Basic Heat Transfer, *McGraw Hill Book Co., New York*.
- [184] Pai, S.I. (1962): Magnetogasdynamics and Plasma Dynamics, *Prentice Hall International, Inc., London*.
- [185] Pal, D., and Mondal, H. (2012): Influence of chemical reaction and thermal radiation on mixed convection heat and mass transfer over a stretching sheet in Darcy porous medium with Soret and Dufour effects, *Energy Convers. Manag.*, **62**, 102-108.
- [186] Parida, S.K., Acharya, M.K., Dash, G.C., and Panda, S. (2011): MHD Heat and Mass Transfer in a Rotating System with Periodic Suction, *Arab J Sci Eng.*, **36**(6), 1139-1151.
- [187] Patankar, S.V. and Spalding, D.B. (1970): Heat and Mass Transfer in Boundary Layers, 2nd Ed., *International Text Book Co., London*
- [188] Patil, A.B., Patil, V.S., Humane, P.P., Patil, N.S., and Rajput, G.R. (2022): Thermally and chemically reacted MHD Maxwell nanofluid flow past an inclined permeable stretching surface, *Proc. Inst. Mech. Eng. E: J. Process Mech. Eng.*, **236**(3), 838-848.

- [189] Pattnaik, J.R., Dash G.C., and Singh, S. (2017): Radiation and mass transfer effects on MHD flow through porous medium past an exponentially accelerated inclined plate with variable temperature, *Ain Shams Eng. J.*, **8**(1), 67-75.
- [190] Pattnaik, P. and Biswal, T. (2015): Analytical solution of MHD free convective flow through porous media with time dependent temperature and concentration, *Walailak J. Sci. Technol.*, **12**, 749- 762.
- [191] Poddar, S., Islam, M.M., Ferdouse, J. and Alam,M.M. (2021): Characteristical analysis of MHD heat and mass transfer dissipative and radiating fluid flow with magnetic field induction and suction, *SN Appl. Sci.*, **3**, 470.
- [192] Pop I. and Ingham D.B. (1969a): Transport phenomena in porous media, *Pergamon Press, Oxford*.
- [193] Pop I. and Ingham D.B. (1969b): Transport phenomena in porous media II, *Pergamon Press, Oxford*.
- [194] Pop I. and Ingham D.B. (1969c): Transport phenomena in porous media III, *Elsevier Science and Technology* .
- [195] Pop, I. (1967): Hydromagnetic flow with variable suction in laminar periodic boundary layers, *Bull. Inst. Polytech., din Iasi*, **13**, 173-178.
- [196] Pop, I. (1969): Unsteady hydromagnetic free convection flow from a vertical infinite flat plate, *Z. Angew. Math. Mech.*, **49**.
- [197] Pop, I. and Ingham, D.B. (1969d): Convective heat transfer: Mathematical and computational modeling of viscous fluids and porous media, *Pergamon Press, Oxford*.
- [198] Postelnicu, A. (2004): Influence of a magnetic field on heat and mass transfer by natural convection from vertical surface in porous media considering Soret and Dufour effects, *Int. J. Heat Mass Transf.*, **47**, 1467-1472.
- [199] Prasad, N.R., Reddy, N.B. and Muthucumaraswamy, R. (2006): Transient radiative hydro-magnetic free convection flow past an impulsively started vertical plate with uniform heat and mass flux, *Theor. App. Mech.*, **33**(1), 31-63.
- [200] Prasad, V.R., Reddy, N.B. and Muthucumaraswamy, R.(2007): Radiation and mass transfer effects on two dimensional flow past an impulsively started infinite vertical plate, *Int. J. Therm. Sci.*, **46**(12), 1251-1258.
- [201] Qin, Y. and Kaloni, P.N. (1992): Steady convection in a porous medium based upon the Brinkman model, *IMA J. Appl. Math.*, **48**, 85–95.

- [202] Raghunath, K., Obulesu, M., and Sivaprasad, R. (2020): Heat and mass transfer on an unsteady MHD flow through porous medium between two porous vertical plates, *AIP Conf. Proc.*, **2220**.
- [203] Rajaiah, M., Sudhakaraiah, A., and Venkatalakshmi, P. (2015): Radiation and Soret effects on unsteady MHD flow past a parabolic started vertical plate in the presence of chemical reaction with magnetic dissipation through a porous medium, *Int. Journ. Sc. Res.*, **4**(3), 1608–1613.
- [204] Rajesh, V., and Chamkha, A. (2014): Effects of ramped wall temperature on unsteady two- dimensional flow past a vertical plate with thermal radiation and chemical reaction, *Communications in Numerical Analysis*, **2014**, 1-17.
- [205] Rajput, U.S., and Kanaujia, N. (2019): Effects of heat absorption and porosity of the medium on MHD flow past an oscillating vertical plate in the presence of Hall current, *Int. J. Sci. Res. Math. Stat. Sci.*, **6**(2), 359-365.
- [206] Rajput, U.S., and Kumar, G. (2017): Effect of heat absorption on MHD flow over a plate with variable wall temperature, *J. Appl. Sci. Eng.*, **20**(3), 277-282.
- [207] Raju, K.V.S., Reddy, T.S., Raju, M.C., Narayana, P.V.S. and Venkataramana, S. (2014): MHD convective flow through porous medium in a horizontal channel with insulated and impermeable bottom wall in the presence of viscous dissipation and Joule heating, *Ain Shams Eng. J.*, **5**(2), 543-551.
- [208] Raju, M.C. and Varma, S.V.K. (2011): Unsteady MHD Couette flow through a porous medium with periodic wall temperature, *i- manager's Journal on Future Engineering and Technology*, **6**(4), 7-11.
- [209] Raju, M.C., Chamkha, A.J., Philip, J., and Varma, S.V.K. (2017): Soret effect due to mixed convection on unsteady magnetohydrodynamic flow past a semi infinite vertical permeable moving plate in presence of thermal radiation, heat absorption and homogeneous chemical reaction, *Int. J. Comput. Math.*, **3**, 947-961.
- [210] Raju, M.C., Veeresh, C., Varma, S.V.K., and Vijayakumar, A.G. (2019): Effects of thermal diffusion and radiation on magnetohydrodynamic (MHD) chemically reacting fluid flow past a vertical plate in a slip flow regime, *J. Appl. Comput. Mech.*, **5**(2), 334-343.
- [211] Ramanaiah G. and Malarvizhi G. (1992): Unified treatment of free convection adjacent to a vertical plate with three thermal boundary conditions, *Heat Mass Transf.*, **27**(6), 393-396.

- [212] Raptis, A. (2017): Effects of thermal radiation on the MHD flow past a vertical plate, *J. Eng. Thermophys.*, **26**(1), 53–59.
- [213] Raptis, A. and Perdikis, C. (2006): Viscous flow over a non-linearly stretching sheet in the presence of a chemical reaction and magnetic field, *Int. J. Non. Linear. Mech.*, 41(4), 527-529.
- [214] Raptis, A. and Singh, A.K. (1983): MHD free convection flow past an accelerated vertical plane, *Int. Commun. Heat Mass Transf.*, **10**(4), 313-321.
- [215] Raptis, A., Perdikis, C. and Tzivanidis G. (1981a): Free convection flow through a porous medium bounded by an infinite vertical surface, *J.Phys. D. Appl. Phys.*, **14**(7), 99-102
- [216] Raptis, A., Tzivanidis, G. and Kafousias N.G. (1981b): Free convection and mass transfer flow through a porous medium bounded by an infinite vertical limiting surface with constant suction, *Lett. Heat Mass Transf.*, **8**, 417-424.
- [217] Rashidi, S., Esfahani, J. and Maskaniyan, M. (2017): Applications of magnetohydrodynamics in biological systems- a review on the numerical studies, *J. Magn. Magn. Mater.*, **439**, 358- 372.
- [218] Reddy, B.P. and Makinde, O.D. (2022): Newtonian heating effect on heat absorbing unsteady MHD radiating and chemically reacting free convection flow past an oscillating vertical porous plate, *Int. J. Appl. Mech. Eng.*, **27**(1), 168- 187.
- [219] Reddy, G.J., Raju, R.S., Manideep, P. and Rao, J.A. (2016): Thermal diffusion and diffusion thermo effects on unsteady MHD fluid flow past a moving vertical plate embedded in porous medium in the presence of Hall current and rotating system, *Trans. A. Razmadze Math. Inst.*, **170**(2), 243- 265.
- [220] Reddy, N.N., Rao, V.S., and Reddy, B.R. (2021): Chemical reaction impact on MHD natural convection flow through porous medium past an exponentially stretching sheet in presence of heat source/ sink and viscous dissipation, *Case Stud. Therm. Eng.*, **25**, 100879.
- [221] Reddy, S.H., Naidu, K.K., Babu, D.H., Narayana, P.V.S., and Raju M.C. (2020): Significance of chemical reaction on MHD near stagnation point flow towards a stretching sheet with radiation, *SN Appl. Sci.*, **2**, 1822.
- [222] Reddy, Y.D., Goud, B.S., Nisar, K.S., Alshahrani, B., Mahmoud, M. and Park, C. (2023): Heat absorption/ generation effect on MHD heat transfer fluid flow along a stretching cylinder with a porous medium, *Alex. Eng. J.*, **64**, 659- 666.

- [223] Reid, R.C. and Sherwood, T.K. (1966): *The Properties of Gases and Liquids*, McGraw-Hill Book Co., New York.
- [224] Revankar, S.T. (1983): Natural convection effects on MHD flow past an impulsively started permeable vertical plate, *Ind. J. Pure and Appl. Math.*, **14**(4), 530-539.
- [225] Roberts, P.H. (1967): *An Introduction to Magnetohydrodynamics*, American Elsevier Pub. Co., New York.
- [226] Rohsenow, W.M. and Choi, H.Y. (1961): *Heat, Mass and Momentum Transfer*, Prentice-Hall, New Jersey.
- [227] Romig, M.F. (1961): *Advances in heat transfer*, Academic Press, New York.
- [228] Rudraswamy, N.G., and Gireesha, B.J. (2014): Influence of chemical reaction and thermal radiation on MHD boundary layer flow and heat transfer of a nanofluid over an exponentially stretching sheet, *J. Appl. Math. Phys.*, **2**(2), 24-32.
- [229] Sahoo, S., Rout, P.K., and Dash, G.C. (2022): Unsteady MHD flow through porous media with temporal variation in temperature and concentration at the plate, *Int. J. Ambient Energy*, **43**(1), 7977- 7986.
- [230] Samad, M.A. and Rahman, M.M. (2006): Thermal radiation interaction with unsteady MHD flow past a vertical porous plate immersed in a porous medium, *J. Nav. Archit. Mar. Eng.*, **3**(1), 7-14.
- [231] Sarma, S. and Ahmed, N. (2022a): Thermal diffusion effect on unsteady MHD free convective flow past a semi- infinite exponentially accelerated vertical plate in a porous medium, *Can. J. Phys.*, **100**(10), 437- 451.
- [232] Sarma, S. and Ahmed, N. (2022b): Dufour effect on unsteady MHD flow past a vertical plate embedded in porous medium with ramped temperature, *Sci Rep*, **12**, 13343
- [233] Sarveshanand, and Singh, A.K., Magnetohydrodynamic free convection between vertical parallel porous plates in presence of induced magnetic field, *SpringerPlus*, **4**, 333, (2015).
- [234] Sattar, M.A. and Alam, M.M. (1994): Thermal diffusion as well as effects on MHD free convection and mass transfer flow past an accelerated vertical porous plate, *Indian J. Pure Appl. Math.*, **25**(6), 679-688.
- [235] Schlichting, H. (1968): *Boundary Layer Theory*, 6th Ed., McGraw-Hill, New York.
- [236] Schlichting, H. and Gersten, K. (2004): *Boundary Layer Theory*, 8th Ed. Springer.

- [237] Schlichting, H. and Gersten, K. (2004): Boundary Layer theory, *Springer (India) Private Limited*, 8th Ed.
- [238] Seddeek, M.A., Darwish, A.A., and Abdelmeguid, M.S. (2007): Effects of chemical reaction and variable viscosity on hydromagnetic mixed convection heat and mass transfer for Hiemenz flow through porous media with radiation, *Commun Nonlinear Sci Numer Simul*, **12**, 195–213.
- [239] Sehra, Haq, S.U., Shah, S.I.A., Nisar, K.S., Jan, S.U. and Khan, I. (2021): Convection heat mass transfer and MHD flow over a vertical plate with chemical reaction, arbitrary shear stress and exponential heating, *Sci. Rep.*, **11**, 4265.
- [240] Seth, G.S. and Sarkar, S. (2015): MHD natural convection heat and mass transfer flow past a time dependent moving vertical plate with ramped temperature in a rotating medium with Hall effects, radiation and chemical reaction, *J. Mech.*, **31**, 91–104.
- [241] Seth, G.S., Ansari, M.S., and Nandkeolyan, R. (2011): MHD natural convection flow with radiative heat transfer past an impulsively moving plate with ramped wall temperature, *Heat Mass Transf*, **47**, 551–561.
- [242] Seth, G.S., Hussain, S.M., and Sarkar, S. (2014): Hydromagnetic natural convection flow with radiative heat transfer past an accelerated moving vertical plate with ramped temperature through a porous medium, *J. Porous Media*, **17**(1), 67-79.
- [243] Seth, G.S., Kumbhakar B., and Sharma R. (2016a): Unsteady MHD free convection flow with Hall effect of a radiating and heat absorbing fluid past a moving vertical plate with variable ramped temperature, *J. Egypt. Math. Soc.*, **24**(3), 471-478.
- [244] Seth, G.S., Sarkar, S., Hussain, S.M., and Mahato, G.K. (2015): Effects of Hall current and rotating on hydromagnetic natural convection flow with heat and mass transfer of a heat absorbing fluid past an impulsively moving vertical plate with ramped temperature, *J. Appl. Fluid Mech*, **8**, 159–171.
- [245] Seth, G.S., Sharma, R., and Kumbhakar, B. (2016b): Heat and mass transfer effects on unsteady MHD natural convection flow of a chemically reactive and radiating fluid through a porous medium past a moving vertical plate with arbitrary ramped temperature, *J. Appl. Fluid Mech.*, **9**(1), 103-117.
- [246] Seth, G.S., Tripathi, R., Sharma, R. and Chamkha, A.J. (2017): MHD double diffusive natural convection flow over exponentially accelerated inclined plate, *J. Mech.*, **33**(1), 87-99.

- [247] Sharma, K. and Gupta, S. (2018): Radiation effects on MHD boundary layer flow and heat transfer along a stretching cylinder with variable thermal conductivity in a porous medium, *J. Porous Media*, **21**(8), 763-779.
- [248] Sharma, P.K. (2005): Simultaneous thermal and mass diffusion on three-dimensional mixed convection flow through a porous medium, *J Porous Media*, **8**(4), 409- 417.
- [249] Shateyi, S., Motsa, S.S. and Sibanda, P. (2010): The effects of thermal radiation, Hall currents, Soret, and Dufour on MHD flow by mixed convection over a vertical surface in porous media, *Math. Probl. Eng.*, **2010**, 1-20.
- [250] Sheikholeslami, M., Hayat, T. and Alsaedi, A. (2016): MHD free convection of Al_2O_3 - water nanofluid considering thermal radiation: A numerical study, *Int. J. Heat Mass Transf.*, **96**, 513-524.
- [251] Shercliff, J.A. (1965): A Text Book of Magnetohydrodynamics, *Pergamon Press, London*.
- [252] Sherman, F.S. (1990): Viscous Flow, *McGraw-Hill Publ. Comp., New York*.
- [253] Sherwood, T.K., Pigford, R.L. and Wilkie, C.R. (1975): Mass Transfer, *McGraw Hill Book Co., New York*.
- [254] Singh, K. and Chand, K. (2000): Unsteady free convective MHD flow past a vertical porous plate with variable temperature, *Proc. Nat. Acad. Sci., India*, **70**, 49–58.
- [255] Singh, K.D., Chand, K. and Rana, S.K. (1993): Heat transfer in three dimensional MHD flow past a porous plate, *Indian J.Pure Appl. Math.*, **24**(5), 327-335.
- [256] Singh, N.P. and Singh, A.K. (2000): MHD effects on heat and mass transfer in flow of a viscous fluid with induced magnetic field, *Indian J. Pure Appl. Phys.*, **38**, 182- 189.
- [257] Sinha, A., Ahmed, N. and Agarwalla, S. (2017): MHD free convective flow through a porous medium past a vertical plate with ramped wall temperature, *Appl. Math. Sci.*, **11**(20), 963- 974.
- [258] Sivaiah, S., Anitha, K., and Venkataramana, S. (2012): Effects of thermal diffusion and radiation on unsteady MHD free convection flow past an infinite heated vertical plate in a porous medium, *ISRN Thermodynamics*, **2012**, 1-8.
- [259] Siviah, S., Muraligoud, G., Murali, G., Reddy, M.C.K. and Raju S. (2012): Unsteady MHD mixed convection flow past a vertical porous plate in presence of radiation, *Int. J. Basic Appl. Sci.*, **1**(4), 651-666.

- [260] Skelland, A.H.P. (1974): Diffusion Mass Transfer, *John Wiley and Sons, New York*.
- [261] Soundalgekar, V.M. (1969): On MHD fluctuating flow past an infinite wall with variable suction, *Arch. Mech. Stos.*, **21**,281-293.
- [262] Soundalgekar, V.M. (1970): Unsteady MHD free convection flow past an infinite vertical flat plate with variable suction, *Ind. J. Pure and Appl. Math.*, **3**(3), 426-436
- [263] Soundalgekar, V.M. (1973): Free convection effects on the oscillatory flow past an infinite vertical porous plate with constant suction, *Proc. Roy. Soc. A*, **333**, 25-36.
- [264] Soundalgekar, V.M. (1975): Free convection effects on the oscillatory flow of an incompressible electrically conducting viscous fluid past an infinite vertical porous plate with constant suction and the transverse magnetic field, *ZAMM*, **55**,257-268.
- [265] Soundalgekar, V.M. (1979): Free convection effects on the flow past a vertical oscillating plate, *Astrophys. Space Sci.*, **64**, 165-172.
- [266] Spalding, D.B. (1963): Convective Mass Transfer, *Edward Arnold Publishers Ltd., London*
- [267] Sravan Kumar, T., Dinesh, P.A., and Makinde, O.D. (2020): Impact of Lorentz force and viscous dissipation on unsteady nanofluid convection flow over an exponentially moving vertical plate, *Math. Models Comput. Simul.*, **12**, 631- 646.
- [268] Srinivasa, A.H., and Eswara, A.T. (2016): Effect of internal heat generation or absorption on MHD free convection from an isothermal truncated cone, *Alex. Eng. J.*, **55**(2), 1367-1373.
- [269] Srinivasacharya, D., Mallikarjuna, B. and Bhuvanavijaya, R. (2015): Soret and Dufour effects on mixed convection along a vertical wavy surface in a porous medium with variable properties, *Ain Shams Eng. J.*, **6**(2), 553-564.
- [270] Streeter, V.L. and Wylie, E.B. and Bedford, K.W. (1998): Fluid Mechanics, *McGraw Hill Book Co., New York*.
- [271] Sumathi, K., Arunachalam, T., and Kavitha, R. (2017): Effect of thermal radiation and chemical reaction on three dimensional MHD fluid flow in porous medium- A numerical study, *Int. J. Control. Theory Appl.*, **10**(32), 9-19.
- [272] Suneetha, K., Ibrahim, S., Reddy, G. and Kumar, P. (2021): Analytical study of induced magnetic field and heat source on chemically radiative MHD convective flow from a vertical surface, *J. Comput. Appl. Res. Mech. Eng.*, **11**(1), 165- 176.

- [273] Suresh, P., Krishna, H., Rao, R.S., and Reddy, P.V.J. (2019): Effect of chemical reaction and radiation on MHD flow along a moving vertical porous plate with heat source and suction, *Int. J. Appl. Eng. Res.*, **14**(4), 869- 876.
- [274] Sutton, G.W. and Sherman, A. (1965): Engineering Magnetohydrodynamics, *McGraw Hill Book Co., New York*.
- [275] Swain, B.K., Senapati, N., Dash, M. (2017): Chemical reaction effect on MHD convective flow with heat and mass transfer past a semi infinite vertical porous plate, *J. Adv. Math.*, **8**, 30-37.
- [276] Swetha, R., Reddy, G. and Varma, S.V.K. (2015): Diffusion- thermo and radiation effects on MHD free convection flow of chemically reacting fluid past an oscillating plate embedded in porous medium, *Procedia Eng.*, **127**, 553-560.
- [277] Takhar, H.S., Chamkha, A.J. and Nath, G. (2000): Flow and mass transfer on a stretching sheet with a magnetic field and chemically reactive species, *Int. J. Eng. Sci. Technol.*, **38**(12), 1303-1314.
- [278] Takhar, H.S., Gorla, R.S. and Soundalgekar, V.M. (1996): Radiation effects on MHD free convection flow of a radiating gas past a semi – infinite vertical plate, *Int. J. Numer. Methods Heat Fluid Flow*, **6**(2), 77-83.
- [279] Tan, C.W. and Wang, C.T. (1968): Heat transfer in aligned field magnetohydrodynamic flow past a flat plate, *Int. J. Heat Mass Transfer*, **11**, 299-319
- [280] Terill, R.M. and Shrestha G.M. (1965a): Laminar flow in a uniformly porous channel with an applied transverse magnetic field, *Appl. Sci. Res.*, **B12**, 203.
- [281] Terill, R.M. and Shrestha G.M. (1965b): Laminar flow in a porous channel of different permeability, *Appl. Sci. Res.*, **11A**, 4.
- [282] Thomas, L.C. (1980): Fundamentals of heat transfer, *Prentice Hall, New Jersey*.
- [283] Tobbal, T. and Bennacer, R. (1998): Heat and mass transfer in anisotropic porous layer, *Trends in Heat, Mass and Momentum Transfer*, **3**, 129–137.
- [284] Treybal, R.E. (1968): Mass Transfer Operations, 2nd Ed., *McGraw-Hill Book Co. New York*.
- [285] Turkyilmazoglu, M. (2019): MHD natural convection in saturated porous media with heat generation/ absorption and thermal radiation: closed- form solutions, *Arch. Mech.*, **71**(1), 49- 64.
- [286] Turner, J.S. (1973): Buoyancy Effects in Fluids, *Cambridge University Press, Cambridge*.

- [287] Ullah, I., Khan, I. and Shafie, S. (2017): Soret and Dufour effects on unsteady mixed convection slip flow of Casson fluid over a nonlinearly stretching sheet with convective boundary condition, *Sci. Rep.*, **7**, 1-19.
- [288] Ullah, M.S., Tammim, A. and Uddin, M.J. (2021): A study of two dimensional unsteady MHD free convection flow over a vertical plate in the presence of radiation, *Open J. Fluid Dyn.*, **11**(1).
- [289] Vedavathi, N., Ramakrishna, K., and Jayarami Reddy, K. (2015): Radiation and mass transfer effects on unsteady MHD convective flow past an infinite vertical plate with Dufour and Soret effects, *Ain Shams Eng. J.*, **6**(1), 363–371.
- [290] Vedhanayagam, M., Altenkirch, R.A., Eichorn, R. (1980): A transformation of the boundary layer equation for free convection flow past a vertical flat plate with arbitrary blowing and wall temperature variation, *Int. J. Heat Mass Transfer*, **23**,1236-1288
- [291] Veldman, A.E.P. (1976): Boundary Layer Flow Past a Finite Flat Plate, *Rijksuniversiteit Groningen, Holland*.
- [292] Venkateswarlu, M., and Makinde, O.D. (2018): Unsteady MHD slip flow with radiative heat and mass transfer over an inclined plate embedded in a porous medium, *Defect Diffus. Forum*, **384**, 31-48.
- [293] Vijaya Kumar, A.G., Reddappa, B., Babu, K.R. and Vijaykumar Varma, S. (2013): Dufour and radiation effects on unsteady MHD free convective heat and mass transfer flow past an infinite vertical plate in the presence of a chemical reaction, *JP J. Heat Mass Transf.*, **8**(1), 1-24.
- [294] Welty, J.R. (1974): Engineering Heat Transfer, *Wiley, New York*.
- [295] Welty, J.R., Wicks, C.E. and Wilson R.E. (1969): Fundamentals of Momentum, Heat and Mass Transfer, *Wiley, New York*.
- [296] Wiedemann, J. and Gersten, K. (1984): Drag reduction due to boundary-layer control by combined blowing and suction, *In: AGARD-CP-365*, **14**, 1–10.
- [297] Wilkinson, D.S. (2000): Mass Transfer in Solids and Fluids, *Cambridge University Press, Cambridge*.
- [298] Wooding, R.A. (1957): Steady state free thermal convection of liquid in a saturated permeable medium, *J. Fluid Mech.*, **2**, 273-285.
- [299] Wu, Y. and Xu, J. (2022): Simplified analysis of MHD flow in a porous surrounding bounded by an oscillating vertical cylindrical surface, *Case Stud. Therm. Eng.*, **30**, 101737.

- [300] Xie, Y.Q., Simmons, C.T., Werner, A.D., and Diersch, H.J.G. (2012): Prediction and uncertainty of free convection phenomena in porous media, *Water Resour. Rec.*, **48**, 2535.
- [301] Xu, Y.S., Liu, Y., and Huang, G. (2005): Lattice-Boltzmann simulation of momentum and energy transfer in a porous medium, *Mod. Phys Lett.*, **19**, 1531–1534.
- [302] Yabo, I., Jha, B. and Lin, J. (2016): Combined effects of thermal diffusion and diffusion-thermo effects on transient MHD natural convection and mass transfer flow in a vertical channel with thermal radiation, *Appl. Math.*, **7**(18), 2354-2373.
- [303] Yamamoto, K. and Iwamura, N. (1976): Flow with convective acceleration through a porous medium, *J. Engg. Math.*, **10**, 41-54.
- [304] Young, A.D. (1989): *Boundary Layers*, *BSP Professional Books, Oxford*.
- [305] Zaib, A. and Shafie, S. (2014): Thermal diffusion and diffusion thermo effects on unsteady MHD free convection flow over a stretching surface considering Joule heating and viscous dissipation with thermal stratification, chemical reaction and Hall current, *J Franklin Inst.*, **351**(3), 1268- 1287.
- [306] Zhang, J., Wang, F., Tamoor, M., Kamran, M., Farooq, A., Rehman, S., Aljohani, A.S., Khan, I., Alkhatib, S., and Ahmad, H. (2022): Influence of chemical reaction on MHD Newtonian fluid flow on vertical plate in porous medium in conjunction with thermal radiation, *Open Phys.*, **20**(1), 302-312.
- [307] Zhao, J., Zheng, L., Zhang, X., and Liu, F. (2016): Convection heat and mass transfer of fractional MHD Maxwell fluid in a porous medium with Soret and Dufour effects, *Int. J. Heat Mass Transfer*, **103**, 203–210.
- [308] Zigta, B. (2019): Thermal radiation, chemical reaction and viscous dissipation effects on unsteady MHD flow of viscoelastic fluid embedded in a porous medium, *Bp. Int. Res. Exact Sci.*, **1**(3), 35-57.
- [309] Zueco (2008): Unsteady free-convection radiation flow over a vertical wall embedded in a porous medium, *Comm. Numer. Meth. Engng*, **24**, 1093–1105.



OPEN Dufour effect on unsteady MHD flow past a vertical plate embedded in porous medium with ramped temperature

Subhrajit Sarma[✉] & Nazibuddin Ahmed

The present investigation aims to find an exact solution to the problem of a free convective, viscous, radiating, chemically reacting, optically thick, non-gray, and incompressible MHD flow past an exponentially accelerated semi-infinite vertical plate in presence of a transverse magnetic field. The medium of flow is porous. Arbitrary ramped temperature and diffusion thermo effects are also considered. Rosseland approximation method is used to describe the flux that appears in the energy equation. The effects of different parameters on flow and transport characteristics are discussed with the help of suitable graphs. It is noticed that velocity field and concentration field decreases but temperature field increases with an upsurge in Schmidt number. Also, Nusselt number and skin friction rise with increasing chemical reaction parameter but lowers with increasing radiation parameter. Faster consumption of chemical substances decelerates both concentration and velocity but accelerates temperature of the fluid. An interesting outcome of our investigation is that both Dufour effect and arbitrary ramped temperature diminishes fluid velocity.

List of symbols

a_w	Surface acceleration parameter
\vec{B}	Magnetic flux density
B_0	Strength of the applied magnetic field $\left(\frac{Wb}{m}\right)$
C	Molar species concentration $\left(\frac{mol}{m^3}\right)$
C_p	Specific heat at constant pressure $\left(\frac{J}{kgK}\right)$
C_s	Concentration susceptibility
C_∞	Concentration far away from the plate $\left(\frac{mol}{m^3}\right)$
C_w	Concentration at the plate $\left(\frac{mol}{m^3}\right)$
D_M	Mass diffusivity $\left(\frac{m^2}{s}\right)$
Du	Dufour number
\vec{g}	Gravitation acceleration vector
g	Gravitational acceleration $\left(\frac{m}{s^2}\right)$
Gr	Thermal Grashof number
Gm	Solutal Grashof number
K_T	Thermal diffusion ratio
K^*	Porosity parameter
\vec{j}	Current density vector $\left(\frac{A}{m^2}\right)$
\vec{K}	Chemical reaction rate $\left(\frac{mol}{m^2s}\right)$
K	Chemical reaction parameter
M	Magnetic parameter
N	Radiation parameter
p	Pressure $\left(\frac{N}{m^2}\right)$

Department of Mathematics, Gauhati University, Guwahati, Assam 781014, India. ✉email: sarmasj021@gmail.com

Thermal diffusion effect on unsteady MHD free convective flow past an impulsively started but temporarily accelerated semi-infinite vertical plate with parabolic ramped conditions

Nazibuddin Ahmed | Subhrajit Sarma

Department of Mathematics, Gauhati University, Guwahati, Assam, India

Correspondence

Subhrajit Sarma, Department of Mathematics, Gauhati University, Guwahati 781014, Assam, India.
Email: sarmasj021@gmail.com

Abstract

The purpose of the present study is to analyze the problem of a free convective MHD flow of incompressible, electrically conducting, and viscous fluid past an impulsively started semi-infinite moving vertical plate. The fluid is considered to be non-gray and optically thick. The parabolic ramped temperature of the plate and thermodiffusion effect are also taken into account. A magnetic field having uniform strength is applied in the transverse direction to the fluid velocity. Solutions of dimensionless governing partial differential equations are attained on the adoption of the closed-form Laplace transformation technique. Effects of different flow parameters on the velocity field, temperature field, concentration field, Nusselt number, skin friction, and Sherwood Number are discussed graphically. It is noticed that fluid concentration, temperature, and velocity decline considerably for ascending values of Prandtl Number. Increasing Ramped parameter hikes the Nusselt number and Sherwood Number but declines skin friction.

KEYWORDS

free convection, MHD, non-gray fluid, optically thick, radiation, Rosseland approximation, Soret effect

Thermal diffusion effect on unsteady MHD free convective flow past a semi-infinite exponentially accelerated vertical plate in a porous medium

Subhrajit Sarma and Nazibuddin Ahmed

Department of Mathematics, Gauhati University, Guwahati 781014, Assam, India

Corresponding author: Subhrajit Sarma (email: sarmasj021@gmail.com)

Abstract

The objective of the present work was to obtain an exact solution to the problem of a free convective, radiative, viscous, chemically reacting, heat-absorbing, incompressible, and unsteady magnetohydrodynamic flow past an exponentially accelerated moving vertical plate embedded in a porous medium. The fluid was assumed to be optically thick and nongray. A magnetic field was applied in the transverse direction of the flow. Effects of arbitrary ramped temperature and thermal diffusion were also considered. The Rosseland approximation method was used to describe the radiative heat flux that appears in the energy equation. Analytical solutions of the nondimensional governing equations were obtained by adopting a closed form of the Laplace transformation technique. The influence of various physical parameters on flow and transport characteristics was analyzed with suitable graphs. From the investigation, it was observed that increasing the Soret number increased both the concentration and velocity fields. Increasing the radiation parameter caused an upsurge in the Nusselt number but reduced the Soret number.

Key words: chemical reaction, Rosseland approximation, optically thick, nongray fluid, thermal diffusion

Résumé

L'objectif de ce travail est l'obtention d'une solution exacte du problème d'un écoulement MHD, instable, incompressible, absorbant de la chaleur, réagissant chimiquement, visqueux, radiatif et en convection libre, passant une plaque verticale accélérée exponentiellement imbriquée dans un milieu poreux. Le fluide est présumé être optiquement épais et non gris. Un champ magnétique est appliqué en direction transverse au flot. Nous considérons aussi les effets d'une augmentation de température arbitraire et de la diffusion thermique. L'approximation de Rosseland est utilisée pour décrire le flot de chaleur qui apparaît dans l'équation pour l'énergie. Des solutions analytiques sont obtenues pour les équations directrices adimensionnelles en adoptant une forme fermée des transformations de Laplace. L'influence des différents paramètres physiques des caractéristique d'écoulement et de transport de l'écoulement est analysée à l'aide des graphiques pertinents. De cette étude, il ressort que l'augmentation du nombre de Soret accroît les champs de concentration et de vitesse. L'augmentation du paramètre de radiation accroît le nombre de Nusselt, mais fait décliner celui de Soret. [Traduit par la Rédaction]

Mots-clés : réaction chimique, approximation de Rosseland, optiquement épais, fluide non gris, diffusion thermique

1. Introduction

Magnetohydrodynamics (MHD) is the branch of physics associated with the interaction of electrically conducting fluids with a magnetic field. Plasmas, electrolytes, liquid metals, and salt water are some common examples of such fluids. Renowned Swiss scientist Hannes Alfvén [1] introduced the concept of MHD, for which he received the Nobel Prize in 1970. However, MHD is in its present form due to significant contributions from other authors such as Cowling [2], Shercliff [3], Ferraro and Plumpton [4], Roberts [5], Crammer and Pai [6], and Davidson [7]. Engineering applications of MHD include the motor, dynamo, MHD generator, plasma confine-

ment, cooling of liquid metals, and nuclear reactors, and applications of MHD in biological systems have been studied by Rashidi et al. [8]. Farrokhi et al. [9] investigated biomedical applications of MHD. Apart from these, MHD has vast applications in astrophysics, geophysics, chemical sciences, nanotechnology, etc.

In a fluid mixture, density variation takes place due to changes in both the species concentration and fluid temperature. This variation develops a buoyancy force, which acts on the fluid. The flow produced by this force is termed "natural convection" or "free convection". Asimoni et al. [10] studied free convective viscous MHD flow past a vertical plate. Bu-



**DIFFUSION THERMO EFFECT ON UNSTEADY MHD
FREE CONVECTIVE FLOW PAST AN IMPULSIVELY
STARTED SEMI-INFINITE MOVING VERTICAL
PLATE WITH UNIFORM HEAT AND MASS FLUX**

Subhrajit Sarma^{*}, Nazibuddin Ahmed and Bijoy Krishna Taid

Department of Mathematics

Gauhati University

Guwahati-781014, Assam, India

e-mail: sarmasj021@gmail.com

nazib@gauhati.ac.in

bijoytaid@gmail.com

Abstract

The present investigation aims to study analytically the problem of free convective, unsteady MHD flow of a viscous, incompressible, and electrically conducting fluid past a semi-infinite vertical plate with uniform heat and mass transfer in presence of diffusion thermo effect. Exact solutions of the dimensionless governing partial differential equations are obtained by adopting the closed-form Laplace transformation technique. Expressions of concentration field, temperature field, velocity field, plate concentration, plate temperature, Nusselt number, Sherwood number and skin friction are attained and the effects of various flow parameters on them are displayed graphically. The study reveals that Dufour effect accelerates both fluid temperature and plate temperature.

Received: July 15, 2021; Accepted: August 28, 2021

Keywords and phrases: MHD, heat and mass transfer, free convection, Dufour effect.

^{*}Corresponding author